

UNIVERSITÄT  
BAYREUTH

**Evaluation of biophysical factors driving temporal variations in  
carbon gain, water use and yield production in rice**

Dissertation

to attain the academic degree of Doctor of Natural Science (Dr. rer. nat.)

of the Bayreuth Graduate School of Mathematical and Natural Sciences (BayNAT)

of the University of Bayreuth

presented by

Wei Xue

born 16 July 1985

in Taian (China)

Bayreuth, October 2015



This doctoral thesis was prepared at the Department of Plant Ecology, University of Bayreuth between October, 2012 and October, 2015. It was supervised by Prof. Dr. John Tenhunen, Prof. Dr. Christiane Werner, and Prof. Dr. Jonghan Ko.

This is a full reprint of the dissertation submitted to obtain the academic degree of Doctor of Natural Science (Dr. rer. nat.) and approved by the Bayreuth Graduate School of Mathematical and Nature Science (BayNAT) of the University of Bayreuth.

Date of submission: 15.10.2015

Date of defense: 28.01.2016

Acting director: Prof. Dr. Stephan Kümmel

Doctoral Committee:

- (1) Prof. John Tenhunen, Ph.D (1st reviewer)
- (2) Prof. Christoph Thomas, Ph.D (2nd reviewer)
- (3) Prof. Angelika Mustroph, Ph.D (chairman)
- (4) Prof. Egbert Matzner, Ph.D





## **Abstract**

Future sustainable rice production systems must be capable of producing high yields but with use of minimal additions of fertilizer and with low water consumption. Current production systems are challenged by global change trends which predict increasing water scarcity in rice production regions, and by environmental concerns to limit fertilizer applications that may impact water quality and increase greenhouse gas emissions. In order to harvest high grain yields from this fast-growing crop, while at the same time accomplishing environmental protection, requires that management is based on sound fundamental knowledge with respect to plant growth, to physiological adaptive capacities with respect to changing habitat conditions and these in the context of anthropogenic interventions, e.g. crop management under natural field conditions. Biomass accumulation by plants is a direct result of photosynthesis which occurs in the light concurrently with water lost via soil evaporation and canopy transpiration. Disentangling biophysical mechanisms responsible for regulation of rice plant growth, and determining their effect on ecosystem carbon and water fluxes are still research areas with unanswered questions. In this thesis, I attempt to understand ecophysiological traits that relate to rice plant growth under different methods of cultivation, and to determine the factors upon which one must focus in promoting sustainable rice production systems.

Experimental studies on canopy structure and function were carried out throughout the growth season with paddy rice grown under three fertilization regimes providing different nitrogen application rates (0 kg N/ha additional was termed low fertilization, 115 kg N/ha as recommended by local agricultural agencies is termed normal fertilization, and 180 kg N/ha is termed high fertilization), and with the same rice cultivar grown at two contrasting soil water regimes (comparison of the flooded paddy rice with a rainfed cultivation, both under condition of 115 kg N/ha additional fertilizer) in the summer monsoon region of Gwangju, South Korea in 2013. In paddy rice with different nutrient treatments, canopy stratified structure and leaf inclination angle, light distribution profiles, leaf nitrogen content and leaf ecophysiological response at different depths in the canopy profile, and canopy reflectance as

well as yield production were periodically determined or observed. Similar field measurements together with additional determinations of water fluxes to the atmosphere (evaporative, transpirational, and evapotranspiration) were periodically conducted in the rainfed rice field.

The results of the comparison between paddy and rainfed rice showed an essentially identical correlation between net primary production (NPP, equivalent to plant stand assimilation rate) and leaf area index (LAI), indicating that seasonal canopy net carbon gain is primarily regulated by LAI and in a similar manner. More than half of diurnal variations in canopy CO<sub>2</sub> gas exchange rates in both rice systems could be explained by changes in the intensity of incident solar radiation. Besides solar radiation, rainfed rice without standing water was impacted by higher air temperatures and increased water vapor pressure deficits (VPD) which inhibited instantaneous carbon gain at solar noon and reduced growing season GPP.

Rainfed rice had lower photosynthetic N use efficiency in sunlit leaves due to a significantly greater proportion of nitrogen investment into non-photosynthetic components. Lower efficiency was offset by delayed grain-filling and longer retention of higher canopy leaf N which facilitated late season carbon gain as compared to senescent paddy rice. However, increased respiratory carbon loss in rainfed rice as compared to paddy rice reduced the facilitation effects brought by relatively high carbon gain capacity (gross primary production, GPP). At flowering and grain-filling, the two cultures had comparable NPP and green biomass accumulation. Nevertheless, grain yield in rainfed rice decreased by ca. 10% in rainfed rice, which was ascribed to greater demand for photoproducts to support the root system along with a high proportion of unfilled spikelets being produced during a prolonged non-rainfall period. Additionally, during the dry period, leaf stomatal limitations on gas exchange increased and leaf rolling occurred to an extent that reduced carbon gain capacity. Intrinsic water use efficiency ( $WUE_{ins}$ , assimilation rate against stomatal conductance) of sampled leaves was constant and similar in the two cropping cultures, but substantially increased under drying conditions in rainfed rice due to pronounced stomatal closure.

Photosynthetic sensitivity and water use efficiency were related to hydraulically constrained stomatal conductance.  $WUE_{ins}$  was closely related to water availability with a large change occurring at soil matric potential ( $\psi_s$ ) of ca. -75 kPa and plant hydraulic conductance ( $k$ ) of  $5 \text{ mmol m}^{-2} \text{ s}^{-1} \text{ MPa}^{-1}$  that decreased carbon gain capacity.

A discernible effect of lower yield production in rainfed rice on agronomic water use efficiency ( $WUE_{agro}$ , ratio of grain yield to evapotranspiration, yield/ET) was not found.  $WUE_{agro}$  and ecological water use efficiency ( $WUE_{eco}$ , growing season GPP divided by ET,  $GPP_{total}/ET$ ) were significantly higher in rainfed rice primarily due to decline in soil evaporation (E) versus transpiration (T) at vegetative stage. When ecosystem respiration ( $R_{eco}$ ) was subtracted from  $GPP_{total}$ , paddy and rainfed rice had similar net ecosystem water use efficiency (net ecosystem production divided by ET,  $NEE/ET$ ). It indicates that there is a major contribution of  $R_{eco}$  to ecosystem water use efficiency, which is an indispensable consideration for ecosystem carbon balance. High ecosystem water use efficiency was obtained in rainfed rice at the cost of increased respiratory carbon losses and decline in grain yield production.

Nitrogen availability in the soil is the other major factor that influences photosynthetic productivity in rice. In paddy rice across three nutrient treatments, all photosynthesis-related variables were linearly related to leaf nitrogen content ( $N_a$ ), so that differences in N allocation were responsible for observed differences in crop carbon gain. Early in the season, tillering stage leaves in the fertilized treatments had higher photosynthetic rates due to higher leaf N content, leading to larger amounts of rate-limiting photosynthetic proteins. Thus, fertilized plots had an early head start and boost in productivity and LAI, resulting in increases in canopy light absorption. Later during the growth season, differences in leaf  $N_a$  and photosynthetic characteristics between treatments were small. Enhanced LAI and light interception in fertilized plots throughout the growing season was related to greater leaf number and leaf area per hill and a larger leaf area in the upper canopy (LAUC). Fertilized treatments had a higher LAUC with high leaf nitrogen concentration and reduced mesophyll

diffusion limitation, but greater exposure to full sunlight that led to improved nitrogen use efficiency and efficient carbon gain.

It is clear that high yield production and carbon gain capacity with adequate nutrient addition and with adequate soil water supply are strongly determined by canopy leaf area development and to a lesser extent by leaf physiological properties. Thus, promoting an early increase in canopy leaf area development is a promising strategy to improve production, since greater canopy light interception significantly contributes to gross carbon gain before light use efficiency declines. Adoption of lowland rice planting in upland fields in the summer monsoon region can lead to significant advantages in water-saving, if it is possible to achieve a decline in soil evaporation. The growing season carbon losses via soil and plant respiration in rainfed plots are significantly greater than in paddy rice. However, from an ecological perspective of ecosystem carbon balance and carbon stocks in future climate scenarios which predict more cloudy/rainy days in the Korean Peninsula, rainfed rice systems may decrease in terms of their strength as a carbon sink but, nevertheless, offer potentials for additional rice production.

## **Zusammenfassung**

Die zukünftige nachhaltige Reiserzeugung muss im Stande sein einen höchstmöglichen Ertrag bei minimaler Düngung und geringen Wasserverbrauch zu gewährleisten. Derzeitige Anbaumethoden stehen durch den vorschreitenden globalen Klimawandel und der damit verbundenen Wasserknappheit in den Reis produzierenden Regionen unter Kritik, aber auch wachsende ökologische Bedenken fordern eine verringerte Ausbringung an Dünger, welcher einen großen Einfluss auf die Wasserqualität und die Freisetzung von Treibhausgasen hat. Um die größtmöglichen Erträge von schnell wachsenden Kulturpflanzen, bei gleichzeitigem Schutz der Umwelt zu gewährleisten, müssen zuverlässige Grundkenntnisse über das Pflanzenwachstum, wie physiologische Anpassungsfähigkeiten hinsichtlich der sich wandelnden Habitatsbedingungen und anthropogenen Eingriffe, wie zum Beispiel die verwendete Anbaumethode, gewonnen werden. Die Biomassenproduktion bei Pflanzen ist ein direktes Resultat der Photosynthese, welche im Licht bei gleichzeitigem Verlust von Wasser durch Evaporation des Bodens und Transpiration des Bestandes stattfindet. Biophysikalische Mechanismen welche das Wachstum von Reispflanzen beeinflussen und ökosystemare Kohlenstoff- und Wasserflüsse zu bestimmen, sind jedoch immer noch Forschungsgebiete mit ungelösten Fragen. In dieser Arbeit, werden ökophysiologische Merkmale die im Zusammenhang mit dem Wachstum der Nutzpflanze Reis unter verschiedenen Anbaumethoden untersucht und dabei Faktoren für eine nachhaltige Kultivierung von Reis bestimmt.

Es wurden experimentelle Versuche bei Nassreis während einer Wachstumsperiode durchgeführt und die Bestandesstruktur aufgenommen. Der Nassreis wurde unter Zugabe von 0, 115 und 180 kg/ha Stickstoff (N) in drei Düngestufen gruppiert, wobei 0 kgN/ha einer geringen Düngung, 115 kgN/ha der von den lokalen Landwirtschaftlichen Behörden empfohlenen Düngung und 180 kgN/ha einer erhöhten Düngung entsprachen. Die verwendete Kultursorte wurde in 2013 zudem unter zwei Bodenwassergehalten in der Sommermonsun Region Gwangju in Südkorea angebaut, dabei zum Einen als bewässerten Nassreis und zum Anderen als von den Niederschlägen gewässerten Trockenreis. Im Nassreis

wurden von allen Dünge­stufen der geschichtete Aufbau des Bestandes, die Blattausrich­tung, die Lichtverteilungsprofile, der Blattstickstoffgehalt, das ökophysiologische Verhalten der Blätter in verschiedenen Tiefen im Bestandesprofil, die Reflexion des Bestandes sowie die Biomasseproduktion regelmäßig überwacht und bestimmt. Gleichartige Feldmessungen mit zusätzlicher Bestimmung der Wasserabgabe zur Atmosphäre (durch Evaporation, Transpiration und Evapotranspiration) wurden ebenfalls periodisch im Trockenreisfeld durchgeführt.

Die Resultate des Vergleichs zwischen Nass- und Trockenreis zeigten identische Korrelationen zwischen der Netto-Primär-Produktion (NPP, entspricht der Assimilationsrate des Bestandes) und des Blattflächenindex (LAI), welches offenbart das die saisonale Netto-Kohlenstoff-Aufnahme hauptsächlich durch die Blattfläche reguliert wurde. Mehr als die Hälfte der Schwankungen des CO<sub>2</sub>-Gasaustausches im Tagesgang konnten für beide Anbaumethoden durch Änderungen in der Intensität der einfallenden Lichtstrahlung erklärt werden. Neben der Strahlung, war der Trockenreis ohne eine permanente Wasserschicht durch höhere Lufttemperaturen und erhöhte Wasserdampfdruckdefizite (VPD), welche unverzüglich die Kohlenstoffaufnahme um die Mittagszeit verringerten und die saisonale Bruttoprimärproduktion (GPP) erniedrigte, betroffen.

Trockenreis zeigte eine geringer photosynthetische Stickstoffnutzungseffizienz auf Grund einer signifikant höheren Einlagerung an Stickstoff in nicht photosynthetisch aktive Komponenten. Im Gegensatz zum Nassreis, wurde beim Trockenreis eine erniedrigte Effizienz durch eine verspätete Kornfüllung und einem verlängerten erhöhten Stickstoffgehalt im gesamten Bestand kompensiert, was vor allem die Kohlenstoffaufnahme zum Ende der Saison erleichterte. Dennoch war die respiratorische Kohlenstoffabgabe im Trockenreis im Vergleich zum Nassreis erhöht und minderte dadurch den Vorteil einer relativ höheren Kohlenstoffaufnahmekapazität (GPP). In den Wachstumsperioden Blüte und Kornfüllung, zeigten beide Anbaumethoden vergleichbare Raten der NPP und des Biomassezuwachses. Der Ertrag war im Trockenreisfeld jedoch um 10% niedriger, welches durch einen hohen

Anteil an nicht gefüllten Ährchen verursacht wurde. Der überwiegende Teil der ungefüllten Ährchen entstand dabei während einer ausgedehnten Phase ohne Niederschlägen. Zusätzlich wurde während diesem wasserarmen Zeitraum eine Limitierung der Stomatären- und der Mesophyllären- Leitfähigkeit festgestellt und verringerte somit den Blatt-Gaswechsels. Zudem erfolgte ein Einrollen der Blätter bis hin zu einer Intensität bis die Kohlenstoffaufnahmekapazität verringert wurde. Die momentane Wassernutzungseffizienz ( $WUE_{ins}$ , Assimilationsrate aufgetragen gegen die stomatäre Leitfähigkeit) war konstant und gleich für beide Anbaumethoden, aber erhöhte sich merklich bei zunehmender Austrocknung im Trockenreis, dies wurde verursacht durch ein schließen der Stomata. Die Empfindlichkeit der Photosynthese und die Wassernutzungseffizienz waren abhängig von der hydraulisch beschränkten Stomatären-Leitfähigkeit.  $WUE_{ins}$  war sehr eng verbunden mit der Wasserverfügbarkeit und die größten Veränderungen geschahen ab einem Bodenmatrixpotential ( $\psi_s$ ) von ca. 75 kPa und einer hydraulischen Leitfähigkeit der Pflanze ( $k$ ) von  $5 \text{ mmol m}^{-2} \text{ s}^{-1} \text{ MPa}^{-1}$  und führten so zu einer verringerten Kohlenstoffaufnahmekapazität.

Eine erkennbare Auswirkung des erniedrigten Betrags im Trockenreis auf der agronomischen Wassernutzungseffizienz ( $WUE_{agro}$ , Verhältnis von Ertrag zur Evapotranspiration, Ertrag/ET) wurde nicht gefunden.  $WUE_{agro}$  und die ökologische Wassernutzungseffizienz ( $WUE_{eco}$ , saisonaler GPP dividiert durch Evapotranspiration,  $GPP_{total}/ET$ ) war signifikant höher im Trockenreis und wurde durch eine verringerte Bodenevaporation im Verhältnis zur Transpiration (T) verursacht. Die Ökosystemrespiration ( $R_{eco}$ ) wurde von  $GPP_{total}$  subtrahiert und zeigte dann für den Nass- und Trockenreis eine gleiche Netto- Wassernutzungseffizienz des Ökosystems (Netto-Ökosystem-Produktion dividiert durch ET,  $NEE/ET$ ). Dies weist auf einen bedeutenden Beitrag der  $R_{eco}$  zur Wassernutzungseffizienz des Ökosystems hin und muss daher unabdingbar beim Ökosystem Kohlenstoff Kreislauf berücksichtigt werden. Eine hohe Wassernutzungseffizienz wird dabei beim Trockenreis auf Kosten erhöhter respiratorischer Kohlenstoffverluste und einer Verringerung des Ertrags erzielt.

Die Nährstoffverfügbarkeit Im Boden ist ein weiterer wichtiger Faktor welcher die Photosynthetische Leistung in Reis beeinflusst. Für Nassreis wurde in allen drei Dünge­stufen eine lineare Abhängigkeit der photosynthetisch relevanten Variablen zum Blattstickstoffgehalt ( $N_a$ ) festgestellt, somit war die N-Verlagerung im Bestand verantwortlich für die festgestellten Unterschiede in der Kohlenstoffaufnahme. Am Anfang der Saison, hatten die Ausläufer bei den gedüngten Behandlungen höhere Photosynthese Raten auf Grund von höheren Blattstickstoffgehalten, dies wurde verursacht durch eine erhöhte Mengen an geschwindigkeitsbestimmenden Proteinen. Somit hatten die gedüngten Flächen einen Vorsprung in der Entwicklung und eine verstärkte Produktivität als auch LAI, was folglich in einer erhöhte Lichtabsorption des Bestandes resultierte. Später in der Saison, waren die Unterschiede in  $N_a$  und den photosynthetischen Eigenschaften geringer. Ein erhöhter LAI und gesteigerte Lichtaufnahme der gedüngten Flächen während der gesamten Saison waren durch die größere Anzahl an Blättern, der gesteigerten Blattfläche pro Reisbündel und einer größeren Blattfläche im oberen Bereich des Bestandes (LAUC) verursacht. Die gedüngten Flächen hatten einen höheren LAUC mit einer erhöhten Blattstickstoffkonzentration und einer verringerten Limitierung der mesophyllären Diffusion, jedoch führte eine exponierte Lage der Blätter zum Sonnenlicht zu einer verbesserten Stickstoffnutzungseffizienz und erhöhten Kohlenstoffaufnahme.

Man kann schlussfolgern das ein erhöhter Ertrag und eine erhöhte Kohlenstoffaufnahmekapazität bei angemessener Nährstoffzugabe und hinreichender Bodenwasserversorgung hauptsächlich durch die Blattflächenentwicklung des Bestandes und zu einem kleineren Teil den Blattphysiologischen Eigenschaften zugeschrieben werden kann. Diese Untersuchung verdeutlicht daher, dass eine frühzeitige Entwicklung der Blattfläche eine vielversprechende Möglichkeit ist, die Produktivität zu erhöhen, da eine erhöhte Lichtnutzungseffizienz signifikant zur Brutto-Kohlenstoff-Aufnahme beiträgt bis die Lichtnutzungseffizienz am Ende vom Saison wieder sinkt. Die Anpflanzung von Nassreis auf Trockenfeldern während des Sommers in Monsunregionen kann zu signifikanten Vorteilen führen und somit Wasser sparen, wenn die Möglichkeit besteht die Bodenevaporation zu



senken. Zudem sind die Kohlenstoffverluste durch Boden- und Pflanzenrespiration während der Wachstumsperiode im Trockenreis signifikant höher als im Nassreis. Wenn man von einem ökologischen Standpunkt den Kohlenstoffkreislauf und die Kohlenstoffbestände betrachtet, wobei zukünftige Klimaszenarios mehr bewölkte und regnerische Tage auf der koreanischen Halbinsel voraus sagen, könnten die Trockenreisfelder ihre Fähigkeit der Kohlenstoffaufnahme verringern, bieten aber dennoch das Potential für eine zusätzliche Reisproduktion.

## **Acknowledgments**

At the completion of my doctoral studies at the Department of Plant Ecology at the University of Bayreuth, I am keen to express my thanks and deep gratitude to all members who directly or indirectly provided me with useful help, knowledge and support during the field work and motivation to continuously move ahead. I know that several words and sentences are not enough to express my feelings, since they are rather meager and quickly disappear. Nevertheless, I would like to try to put it in written language here in order to release my thoughts and emotions.

It was important to me to have the opportunity to study at the Department of Plant Ecology and to become involved in interesting topics that allowed me to achieve deep insight with respect to understanding in rice plant growth, biomass production, and the seasonal courses of carbon and water fluxes, as well as the underlying physiological mechanisms. Sincere thanks are given to my supervisor Prof. John Tenhunen, who provided this precious chance, good ideas and guidance for me to initiate and complete the study theme. Thanks to Prof. Christiane Werner, Prof. Jonghan Ko, Dr. Dennis Otieno and Prof. Bernd Huwe for their kind help in preparation of field experiments, data analyses and thesis writing. I sincerely acknowledge the help of Prof. Peter Harley, who came to Bayreuth in June from USA and guided the organization of many aspects of my work and shared his scientific experience and ideas. Thanks to Prof. Hiroyuki Muraoka for his enthusiastic help in revision of paper drafts and invitation to participate in the Tsukuba ecosystem carbon balance workshop.

During the past three years, many questions were raised, discussed and later answered with the help of Mr. Steve Lindner and Mr. Bhone Nay-Htoon. With your help, my life at Bayreuth has been very interesting and worthy for memory. I acknowledge further the help in the field provided by Mr. Seung Hyun Jo, Mr. Toncheng Fu, Mr. Fabian Fischer, Mr. Nikolas Lichtenwald and Mr. Yannic Ege. I also gratefully acknowledge the technical assistance of Ms. Margarete Wartinger and Ms. Ilse Thaufelder for all their support in the field and in laboratory analyses.

Many thanks are given to my mother Ms. Zhaomei Zhang who took care for me and my brother and sister all of the time, in spite of where I am. She is a kind and friendly woman, is also brave and wise. Without her help in life, I believe I could not find the right way to enjoy my life. My father Mr. Zhenliang Xue passed away several years ago, I still remember him in my mind with his sunshine smile and great character that instructed me to always work hard. My father-in-law Mr. Hanzhen Dong loves me so much that I will never forget him and his support has been very important to me. My wife Ms. Jinli Dong, my sweet heart, is full of positive attitude and has taken care of home affairs all of the time during which I have had to remain for study at Bayreuth. Thanks a lot, my heart.

Thanks to the financial support from project International Research Training Group TERRECO (GRK 1565/1) funded by the Deutsche Forschungsgemeinschaft (DFG) at the University of Bayreuth, Germany and the Korean Research Foundation (KRF) at Kangwon National University, Chuncheon, S. Korea, and the program of China Scholarships Council (CSC No. 201204910156).

## Table of contents

Abstract .....	I
Zusammenfassung.....	V
Acknowledgments.....	X
List of figures.....	XVI
List of tables.....	XXIII
List of abbreviations .....	XXV
List of symbols.....	XXVII

## Chapter 1 ..... 1

### 1. Synopsis..... 1

1.1. Introduction.....	1
1.1.1. Habitat factors influencing rice production and water use: Background for the research .....	1
1.1.2. Effects of habitat factors on rice production: a meta-analysis .....	5
1.1.3. Thesis concept.....	13
1.1.4. Research objectives and hypotheses .....	14
1.1.4.1. Seasonal variations in carbon gain and yield in paddy versus rainfed rice.....	14
1.1.4.2. Ecophysiological response and acclimation in rice with differing soil water availability .....	17
1.1.4.3. Agronomic and ecological water use efficiency in paddy and rainfed rice.....	19
1.1.4.4. Nutritional influences on carbon gain capacity and yield of paddy rice.....	22
1.2. Materials and methods .....	26
1.2.1. Research area and study sites.....	26
1.2.2. Analyses of canopy scale CO <sub>2</sub> gas exchange and productivity in paddy and rainfed rice .....	28
1.2.3. Analyses of factors influencing carbon gain, water use and yield in paddy and rainfed rice .....	31
1.2.4. Analyses of agronomic and ecological water use in paddy and rainfed rice ...	32
1.2.5. Analyses of nutritional influence on components of carbon gain capacity .....	33
1.3. Results and discussion .....	35
1.3.1. Analyses of canopy scale CO <sub>2</sub> gas exchange and productivity in paddy and rainfed rice .....	35
1.3.2. Analyses of factors influencing carbon gain, water use and yield in paddy and rainfed rice .....	37
1.3.3. Analyses of agronomic and ecological water use in paddy and rainfed rice ...	40
1.3.4. Analyses of nutritional influence in components of carbon gain capacity in paddy rice.....	42
1.4. Conclusion and recommendation.....	45

1.5. List of manuscripts and specification of individual contributions.....	49
1.6. References.....	52
<b>Chapter 2 .....</b>	<b>66</b>
<b>2. Canopy scale CO<sub>2</sub> exchange and productivity of transplanted paddy and direct seeded rainfed rice production system in S. Korea.....</b>	<b>66</b>
2.1. Abstract .....	66
2.2. Introduction.....	68
2.3. Materials and methods .....	70
2.3.1. Study site.....	70
2.3.2. Experimental design/Description of the experimental plots.....	70
2.3.3. Field management.....	71
2.3.4. Microclimate .....	72
2.3.5. Soil water content .....	72
2.3.6. CO <sub>2</sub> flux measurement with chambers .....	73
2.3.7. Empirical description of canopy responses.....	74
2.3.8. Calculation of net-primary-production (NPP) .....	74
2.3.9. Biomass sampling .....	75
2.3.10. Plant carbon and nitrogen determination .....	75
2.3.11. Statistical analyses .....	75
2.4. Results.....	76
2.4.1. Microclimate .....	76
2.4.2. Daily and seasonal patterns of ecosystem CO <sub>2</sub> uptake .....	78
2.4.3. Biomass, leaf area and leaf N content.....	82
2.4.4. Regulation of CO <sub>2</sub> uptake .....	84
2.5. Discussion .....	85
2.6. Conclusion .....	89
2.7. Acknowledgements .....	89
2.8. References.....	89
<b>Chapter 3 .....</b>	<b>94</b>
<b>3. Differentiation in paddy versus rainfed rice in factors influencing carbon gain, water use and grain yield under monsoon climate in South Korea .....</b>	<b>94</b>
3.1. Abstract .....	94
3.2. Introduction.....	96
3.3. Materials and methods .....	99
3.3.1. Study site.....	99
3.3.2. Measurement of meteorological factors and soil water content .....	99
3.3.3. Measurements of leaf level gas exchange.....	100
3.3.4. Measurements of canopy level gas exchange and estimation of NPP and R <sub>plant</sub> .....	101
3.3.5. Measurement of diurnal courses of leaf water potential and degree of leaf rolling.....	103
3.3.6. Characterization of leaf nitrogen content, leaf area, biomass, and yield .....	

components .....	103
3.3.7. Estimating effects of plant hydraulic conductance, stomatal conductance ( $g_{sc}$ ) and stomatal limitation in carbon gain .....	104
3.3.8. Statistic analyses .....	105
3.4. Results .....	106
3.4.1. Meteorological conditions and leaf and soil water status over the growth seasons .....	106
3.4.2. Phenology of development over the course of the growth season .....	108
3.4.3. Seasonal developments of canopy structure, carbon fluxes, and nitrogen content in paddy and rainfed rice .....	109
3.4.4. Seasonal changes in gas exchange properties in paddy and rainfed rice .....	112
3.4.5. Comparisons in diurnal courses of gas exchange between paddy and rainfed rice .....	115
3.4.6. Leaf level components of the rainfed rice plants regulating gas exchange response under changing soil water availability .....	117
3.4.7. Canopy level components regulating carbon gain and biomass production under changing soil water availability .....	121
3.4.8. Comparison of yield in rainfed and paddy rice .....	123
3.5. Discussion .....	124
3.5.1. Leaf area index and allocation of N to leaves regulate seasonal patterns in net carbon gain .....	125
3.5.2. Enhanced respiratory carbon loss in rainfed rice .....	127
3.5.3. Vulnerability of canopy carbon gain to soil water depletion as regulated by leaf structure and function .....	128
3.5.4. Biomass accumulation and grain yield production between paddy and rainfed rice .....	132
3.6. Conclusion .....	133
3.7. Acknowledgments .....	134
3.8. References .....	134
3.9. Appendices .....	140
<b>Chapter 4 .....</b>	<b>144</b>
<b>4. Flux partitioning reveals trade-off between water and carbon loss of paddy and rainfed rice (<i>Oryza sativa</i> L.) .....</b>	<b>144</b>
4.1. Abstract .....	144
4.2. Introduction .....	146
4.3. Materials and methods .....	147
4.3.1. Study Site .....	147
4.3.2. Environmental variables .....	148
4.3.3. Canopy carbon and water flux measurement .....	149
4.3.4. UAV remote sensing, modeling daily NDVI .....	150
4.3.5. Modeling and partitioning crop evapotranspiration .....	150
4.3.6. Calculation of $K_{cb}$ .....	152

4.3.7. Calculation of $K_e$ .....	153
4.3.8. Modeling and partitioning daily carbon fluxes.....	154
4.3.9. Statistical analysis.....	156
4.4. Results.....	156
4.4.1. Climate and rice growth.....	156
4.4.2. Carbon and water fluxes of paddy and rainfed rice.....	158
4.4.3. Tradeoff between evaporative and respiratory losses in paddy and rainfed rice.....	161
4.5. Discussion.....	164
4.6. Conclusion.....	168
4.7. Acknowledgments.....	168
4.8. References.....	169
4.9. Annex 1.....	178
4.10. Supplementary.....	181
<b>Chapter 5.....</b>	<b>185</b>
<b>5. Nutritional and developmental influences on components of rice crop light use efficiency.....</b>	<b>185</b>
5.1. Abstract.....	185
5.2. Introduction.....	187
5.3. Materials and methods.....	189
5.3.1. Study site.....	189
5.3.2. Field measurements of diurnal courses of canopy and leaf $CO_2$ exchange ...	190
5.3.3. Measurements of $CO_2$ response curves of net assimilation rate.....	191
5.3.4. Measurement of canopy reflectance.....	191
5.3.5. Characterization of leaf nitrogen content, leaf area, leaf angle, and biomass.....	192
5.3.6. Characterization of canopy light and nitrogen distribution profiles.....	193
5.3.7. Estimation of the mesophyll diffusion conductance ( $g_m$ ).....	196
5.4. Results.....	197
5.4.1. Seasonal changes in canopy reflectance, biomass production, canopy LUE, and leaf area in response to fertilizer treatments.....	197
5.4.2. Seasonal changes in leaf morphology and physiology in response to fertilizer treatments and canopy position.....	200
5.4.3. Seasonal changes in canopy structure in responses to nutrient additions and effects on canopy LUE.....	205
5.5. Discussion.....	208
5.5.1. The role of leaf photosynthetic capacity in determining $LUE_{inc}$ .....	211
5.5.2. Differences in seasonal canopy development between fertilization treatments.....	213
5.5.3. Promoted canopy leaf area by fertilization depends on leaf number per bundle and relates to nitrogen-facilitated photosynthesis occurring initially.....	218
5.6. Conclusion.....	219
5.7. Acknowledgments.....	220
5.8. References.....	220
5.9. Appendices.....	227

<b>Appendix.....</b>	<b>231</b>
List of other publications .....	231
<b>Declaration / Erklärung .....</b>	<b>232</b>

## List of figures

<b>Figure 1.1</b> Life history of the “120-day” Unkwang rice cultivar planted in the monsoon region near Gwangju, South Korea in 2013 and studied in this research under a transplantation puddle cultivation system. Plants during the reproductive stage continuously extend height and develop new leaves at new nodes. Hence, this stage is also referred to as the internode elongation stage (Yoshida, 1981).....	3
<b>Figure 1.2</b> Correlation between growing season total gross primary production ( $GPP_{total}$ ) and growth duration (GD) (a), and mean daily air temperature ( $T_{air}$ ) (b), and mean daily vapor pressure deficiency (VPD) (c), and mean daily solar radiation (SR) in paddy and rainfed rice systems. Error bars indicate standard deviation. Data achieve was listed in Table 1.1. ....	9
<b>Figure 1.3</b> Vertical overview study of location with indication of rice cropping area and nutrient treatment plots for paddy rice system: T1_0 kg N ha <sup>-1</sup> named as low group, T3_180 kg N ha <sup>-1</sup> as high group, T4_115 kg N ha <sup>-1</sup> as normal group.....	28
<b>Figure 1.4</b> Schematic configuration of transparent chamber established in flooded rice field .....	30
<b>Figure 2.1</b> Daily solar radiation measured at 2 m height and photosynthetic active radiation (PAR) measured at 50 cm height above the vegetation inside the transparent CO <sub>2</sub> flux chambers, respectively, b) mean air temperature at 2 m height outside and at 20 cm height inside the chambers, c) volumetric water content (SWC) within 30 cm soil profile and daily precipitation, and d) mean daily vapor pressure deficit (VPD) at 2 m height in the open location, at 1 m above the paddy rice (VPD paddy rice) and rainfed rice (VPD rainfed rice), respectively. ....	78
<b>Figure 2.2</b> Daily trends of NEE and $R_{eco}$ in paddy rice (left panel) and rainfed rice (right panel), with light intensities (PAR, black line) on selected days during the development	



period. Data points are means of respective fluxes measured on the four collar plots.....79

**Figure 2.3** Seasonal changes in a) daily gross primary production ( $GPP_{int}$ ), b) daily net ecosystem exchange ( $NEE_{int}$ ) and c) net primary production ( $NPP_{int}$ ) of paddy (black circles) and rainfed rice (grey circles) derived from  $\alpha$  and  $\beta$  of the hyperbolic light response curve (Table 2.2). .....80

**Figure 2.4** Response of  $CO_2$ -Assimilation to changing light intensities of paddy (black circles) and rainfed (grey circles) rice representing three distinct phenological stages (line a—initial growth season, line b—mid season, line c—maturity season) during the development of the rice crop. ....81

**Figure 2.5** Dry weight [ $g\ DM\ m^{-2}$ ] of leaves, culms, grains, tuber, and green leaf area (GLAI) of the  $CO_2$ -measurement chambers during crop development in a) paddy and b) rainfed rice. Harvest was done after the  $CO_2$  plot measurements. ....84

**Figure 2.6**  $GPP_{max}$  response to a) green leaf area index (GLAI) and b) light use efficiency ( $\alpha$ ), while c) describes the changes in  $\alpha$  in response to changing GLAI and d) the influence of leaf nitrogen (N) on light use efficiency ( $\alpha$ ) in the rainfed and paddy rice. ....85

**Figure 3.1** Seasonal variations in daily integrated solar radiation (a), precipitation (a), daily maximum and minimum air temperature ( $T_{air,max}$  and  $T_{air,min}$ ) (b), maximum water vapor deficit between leaf surface and leaf tissues ( $VPD_{max}$ ) during the daytime period (b), soil water content (SWC) at 10 and 30 cm depth in rainfed field (c), and minimum leaf water potential ( $\Psi_{l,min}$ ) measured during daily observation cycles (c). Shading bars indicated dry periods between 197 and 203 DOY and between 218 and 234 DOY when SWC at 10 cm depth in rainfed field was less than  $0.3\ m^3\ m^{-3}$ . ....108

**Figure 3.2** Seasonal development of daily integrated gross primary production ( $GPP_{int}$ ) (a), daily integrated plant respiration ( $R_{plant,int}$ ) (a), daily integrated net primary production ( $NPP_{int}$ ) (b), leaf area index (LAI) (b); daily maximum carbon gain capacity ( $NPP_{max}$ ) (c), and canopy nitrogen content ( $N_{total}$ ) (c) in paddy and rainfed rice ecosystems. Time periods during which paddy and rainfed rice grew at different agronomic stages: T + E for tillering and elongation stage; F for flowering stage, and M for grain-filling and maturation stage. Shading bars indicate the first dry and second dry periods that potentially impact canopy structure and

function. Dashed lines emphasize that observations were not continuous with respect to potential soil drying effects. Error bars indicated S.E., n = 3 to 6. .... 111

**Figure 3.3** Seasonal development in leaf photosynthetic traits in uppermost leaves at flooded and rainfed rice cropping systems: (a) leaf nitrogen content per leaf area ( $N_a$ ) and photosynthetic nitrogen content generated by leaf nitrogen content minus residual N content derived from  $V_{cmax,30} - N_a$  correlation (dashed lines); (b) photosynthetic capacity ( $A_{max}$ ) and stomatal conductance ( $g_{s,30}$ ) acquired at saturating PAR of  $1500 \mu\text{mol m}^{-2} \text{s}^{-1}$ , ambient  $\text{CO}_2$  of  $400 \mu\text{mol mol}^{-1}$  and leaf temperature  $30^\circ\text{C}$ ; (c) the maximum carboxylation rate per area at leaf temperature  $30^\circ\text{C}$  ( $V_{cmax,30}$ ), (d) the maximum electron transport rate per leaf area at leaf temperature  $30^\circ\text{C}$  ( $J_{max,30}$ ). Bars indicated S.E., n = 3 to 6. Black triangles and open circles respectively represent rainfed and paddy rice. .... 113

**Figure 3.4** Correlations for (a) sunlit leaf maximum carboxylation rate ( $V_{cmax,30}$ ) and  $N_a$ ; (b) leaf maximum electron transport rate ( $J_{max,30}$ ) and  $N_a$ ; (c) photosynthetic capacity ( $A_{max,30}$ ) and  $N_a$ , and (d) daily maximum net primary production ( $\text{NPP}_{max}$ ) and total leaf nitrogen content ( $N_{total}$ ) in paddy and rainfed rice. Open circles represented measured  $A_{max,30}$  in paddy rice grown at growth chamber. Each point was computed average from 3 to 6 replications. Black triangles and open circles respectively represent rainfed and paddy rice. .... 115

**Figure 3.5** Diurnal course of meteorological factors PAR, water vapor pressure deficit (VPD) and leaf temperature, and assimilation rate (A), transpiration rate (E), stomatal conductance for  $\text{CO}_2$  diffusion ( $g_{sc}$ ) and intercellular  $\text{CO}_2$  concentration ( $C_i$ ) on 177 (early season) and 221 (late season) DOY in paddy rice, and 181 (early season; minimum leaf water potential = -1.4 MPa) and 229 DOY (late season; minimum leaf water potential = -2.0 MPa) in rainfed rice. .... 117

**Figure 3.6** Correlations between transpiration rate (E) and leaf water potential ( $\Psi_l$ ) during wet versus dry period, in rainfed rice (a); hyperbolic relationship of photosynthetic capacity ( $A_{max}$ ) to plant hydraulic conductance ( $\kappa$ ) (b); relationship between maximum stomatal conductance ( $g_{s,max}$ ) and  $\kappa$  at elongation ( $g_{s,max} = a \cdot b \cdot \kappa / (1 + b \cdot \kappa) + c$ ,  $a = 475$ ,  $b = 0.3$ ,  $c = -82$ ,  $R^2 = 0.97$ ,  $p < 0.01$ ) and grain-filling ( $g_{s,max} = a \cdot b \cdot \kappa / (1 + b \cdot \kappa) + c$ ,  $a = 349$ ,  $b = 0.3$ ,  $c = -64$ ,  $R^2 = 0.83$ ,  $p < 0.01$ ) (c); relationship between intrinsic water use efficiency ( $\text{WUE}_{ins}$ , as

the ratio of  $A_{\max}$  to  $g_{sw,\max}$  to water vapor) and  $\kappa$  (d); correlation between  $\kappa$  and  $\Psi_s$  (e), and correlation for leaf rolling degree and leaf water potential ( $\Psi_l$ ) (f). Black triangles represent rainfed rice. Representations of other symbols are indicated in plots. .... 118

**Figure 3.7** Correlations (a) between plant hydraulic conductance ( $k$ ) and inherent water use efficiency (intWUE); (b) correlation between  $k$  and water vapor pressure deficit (VPD) in rainfed rice. .... 120

**Figure 3.8** Diurnal courses of stomatal limitations of photosynthesis in paddy rice on DOY 221 and in rainfed rice on DOY 202 (dry), 206 (wet), 233 (dry) and 237 (dry)..... 121

**Figure 3.9** Seasonal trend in aboveground biomass accumulation (a); correlations between leaf area index (LAI) and daily integrated net primary production ( $NPP_{\text{int}}$ ) (b); correlations for aboveground biomass accumulation and total leaf nitrogen content ( $N_{\text{total}}$ ) (c). Bars indicated S.E.,  $n = 3$  to 6. Filled triangles and open circles indicate paddy at senescence stage and rainfed rice during first soil drying period, respectively. The two clearly deviate points in dotted square frames of Figure 3.9b for  $NPP_{\text{int}}$  were measured during dry period SWD1 (DOY 202 in rainfed rice) at elongation and at maturation stage (DOY 240) in the case of paddy rice..... 122

**Figure 3.10.A1** Light-net primary production response curve in paddy rice over growth stages..... 141

**Figure 3.11.A2** Light-net primary production response curve in rainfed rice over growth stages..... 142

**Figure 3.12.B1** Dependence of light saturating point (LSP) on leaf water potential ( $\Psi_l$ ) (a); relationships between maximum photosynthetic capacity ( $A_{\max}$ ) and ( $\Psi_l$ ) (b), between maximum stomatal conductance ( $g_{\max}$ ) and ( $\Psi_l$ ) (c); and temperature response of  $A_{\max}$  in rainfed rice (d)..... 143

**Figure 4.1** Climate conditions and rice growth during the monsoon 2013. (a) Daily averages of windspeed ( $\text{m s}^{-1}$ ) and relative humidity (%); (b) daily averages of air temperature ( $^{\circ}\text{C}$ ) and radiation ( $\text{MJ m}^{-2} \text{s}^{-1}$ ); (c) daily total rainfall ( $\text{mm d}^{-1}$ ) and daily average volumetric soil water content at 5 cm depth ( $\text{m}^3 \text{m}^{-3}$ ); (d) daily LAI of paddy (solid line) and rainfed (dashed line); lines represent simulated LAI and circles represent measured LAI (Black circle = measured

LAI of paddy, white circle measured LAI of rainfed rice, n = 9, mean values  $\pm$  SD)..... 158

**Figure 4.2** Seasonal carbon and water fluxes of paddy and rainfed rice: daily carbon fluxes of (a) paddy rice; (b) rainfed rice (simulated gross primary production, black line; measured gross primary production, black circle; simulated ecosystem respiration, red dashed line; measured ecosystem respiration, red triangle; simulated net ecosystem exchange, black dotted line; chamber measured net ecosystem exchange, white circle); daily water fluxes of (c) paddy rice and (d) rainfed rice. Simulated daily evapotranspiration, black line; chamber measured evapotranspiration, blue triangle, simulated transpiration, green dashed line; evaporation, blue dotted line) (n = 3, mean value  $\pm$  SD for measured fluxes). ..... 160

**Figure 4.3** Effects of respiratory carbon loss and evaporative water loss over water use efficiency: (a) Yield/ET of rainfed rice (light yellow) was higher than paddy rice (dark green) ( $W = 36.00$ ,  $p \leq 0.05$ ) but NEE/ET were not significantly different, (b) Yield/T was not significantly different between paddy and rainfed rice ( $W = 23.00$ ,  $p = 0.48$ ), highlighting the higher evaporative loss in paddy rice; (c) Lower GPP/ET of paddy rice due to its higher evaporative water loss ( $W = 119.00$ ,  $p \leq 0.05$ ); and higher GPP/ET of rainfed rice due to its higher respiratory carbon loss ( $W = 126.00$ ,  $p \leq 0.05$ ). (Wilcoxon-Mann-Whitney Rank Sum test (a non-parametric ANOVA) was performed to access WUE differences between paddy and rainfed (n = 3 to 12, mean value  $\pm$  SD); different small letters denote significant differences among paddy and rainfed rice within each panel (a to f) while different capital letters denote significant differences among different water use efficiencies (A to G)). ..... 163

**Figure 4.4** Seasonal carbon and water balance of paddy and rainfed rice. Measured and simulated daily gross primary production (GPP), net ecosystem exchange (NEE), ecosystem respiration (Reco), evapotranspiration (ET), transpiration (T) and grain yields were used in this schematic representation. All flux data and grain yield are mean values (flux data: n = 3  $\pm$  SD; grain yield: n = 6  $\pm$  SD). Crop growing season was 120 days (sowing to harvest)..... 165

**Figure 4.5.A1** Relationship between T/ETo and LAI of (a) paddy and (b) rainfed rice. LAI was calculated as leaf area per ground area where Leaf area (LA) was determined with a Leaf Area Meter (LI-3000A, LI-COR, USA). T/ETo was calculated as the ratio of estimate daily transpiration of the LAI measurement date (equation 4.3 and 4.6) to estimated reference

evapotranspiration (equation 4.3). ..... 179

**Figure 4.6.A2** Relationship between NDVI and LAI of (a) paddy rice and (b) rainfed rice. LAI was calculated as leaf area per ground area where Leaf area (LA) was determined with a Leaf Area Meter (LI-3000A, LI-COR, USA). NDVI was measured by Cropscan (Cropscan Inc., USA). Damping coefficient  $k^*$  (relationship between NDVI and LAI) was derived from figure 4.6A2.  $k^*$  for both paddy and rainfed rice = 0.8. .... 179

**Figure 4.7.A3** Simulated daily crop growth of paddy and rainfed rice a) LAI, b) NDVI, c) Dual crop coefficient ( $K_{cb}$ ). Daily  $K_{cb}$  was simulated based on daily NDVI, after following Choudhury (1994). .... 180

**Figure 5.1** (a) Exponential correlation between normalized difference vegetation indices (NDVI) and fraction of incident PAR to absorbed PAR in cereal crops. Filled stars represent data in paddy rice from Inoue et al. (2008) and open stars in other cereal crops from Choudhury (1987). (b) Seasonal development of NDVI in paddy rice grown under three nutrient treatments: low (filled circles, 0 kg N ha<sup>-1</sup>), normal (open circles, 115 kg N ha<sup>-1</sup>) and high (cross symbols, 180 kg N ha<sup>-1</sup>). .... 195

**Figure 5.2** Seasonal courses for aboveground biomass production, observed maximum rates in gross primary production ( $GPP_{max}$ ) during daily measurement cycles, integral daytime GPP ( $GPP_{int}$ ), canopy light use efficiency ( $LUE_{inc}$ ), and leaf area index for paddy rice grown at three levels of fertilization. Low = no fertilizer addition; normal = 115 kg N ha<sup>-1</sup>; high = 180 kg N ha<sup>-1</sup> as described in the methods. Bars indicate S.E.; n = 2 to 12. .... 199

**Figure 5.3** Seasonal changes in sunlit mature leaves at top of canopy for leaf nitrogen content ( $N_a$ ), specific leaf area (SLA), photosynthesis capacity ( $A_{max,30}$ ), and maximum Rubisco carboxylation rate ( $V_{cmax,30}$ ), maximum electron transport rate ( $J_{max,30}$ ), stomatal conductance ( $g_{s,30}$ ), and mesophyll conductance ( $g_{m,30}$ ) under the same environmental conditions. Bars indicate S.E., n = 3 to 6. .... 200

**Figure 5.4** Dependence on leaf position in crop canopy of paddy rice for leaf nitrogen content  $N_a$  (a, b), photosynthetic capacity  $A_{max,30}$  (c, d), maximum Rubisco carboxylation rate  $V_{cmax,30}$  (e, f), maximum electron transport rate  $J_{max,30}$  (g, h), mesophyll conductance  $g_{m,30}$  (i, j), and stomatal conductance  $g_{s,30}$  (k, l) at elongation and grain-filling stages. Bars indicate

S.E., n = 3 to 6. ....203

**Figure 5.5** (a) Dependence of photosynthetic capacity ( $A_{\max,30}$ ) on leaf nitrogen content ( $N_a$ ); (b) relationship of maximum carboxylation rate ( $V_{\max,30}$ ) to  $N_a$  (b); (c) correlation between maximum electron transport rate ( $J_{\max,30}$ ) and  $N_a$ ; (d) correlation of mesophyll conductance ( $g_{m,30}$ ) and  $V_{\max,30}$ , (e) stomatal conductance ( $g_{s,30}$ ) and  $N_a$ , and (f)  $g_{m,30}$  and  $N_a$  pooling data from both sunlit and within-canopy leaves grown in the field and from growth chamber experiments (open triangle). Inset in plot c indicated correlation between  $J_{\max,30}$  and  $V_{\max,30}$ . ....203

**Figure 5.6** Photosynthetic limitation by mesophyll conductance ( $L_{gm}$ ) and by stomatal limitation ( $L_{gs}$ ) in canopy profiles against leaf nitrogen content ( $N_a$ ) at the low, normal and high fertilization treatments in sunlit leaves during elongation and grain-filling stages. ....204

**Figure 5.7** Correlation between canopy light use efficiency ( $LUE_{inc}$ ) and leaf area index (a), seasonal development of  $LUE_{abs}$  (b), proportion of stratified leaf area height > 45 cm to total canopy area (c and d). Instantaneous canopy light use efficiency ( $LUE_{ins}$ ) and expansion of upper canopy leaves (based on plot c and d) (e), and  $LUE_{inc}$  and expansion of upper canopy leaves (f) during elongation (solid line) and grain-filling stage (dot line). Bars indicated S.E., n = 3 to 6. ....207

**Figure 5.8** (a) Correlation between nitrogen use efficiency and leaf nitrogen content per leaf area, and (b) leaf inclination angle comparisons in canopy positions at elongation and grain-filling stages. (c) and (d) Changes of sunlit leaf area at canopy layers from sunrise to sunset during grain-filling stage for low and normal groups using actual measured vertical leaf distributions (black lines) or using reversed leaf distributions (grey lines). Bars indicate S.E., n = 3 to 6. ....208

**Figure 5.9.A1** (a) Relationship between quantum yield of PS II and efficiency of  $CO_2$  fixation under varying ambient  $CO_2$  concentration and light intensity with  $O_2$  approximately 1% in rice (open circle) and other herbaceous (black circle). (b)  $CO_2$  response curves at measuring light intensities of 500, 200, 100  $\mu mol\ m^{-2}\ s^{-1}$  and leaf temperature 30°C during tillering (filled symbols) and grain-filling stage (open symbols). n = 5 to 6. Linear fits to each data set were made to estimate the  $C_i$  value at which response curves intersect, indicative of

$\Gamma^*$ of $44.4 \pm 1.3 \mu\text{mol mol}^{-1}$ .....	229
---	-----

## List of tables

<b>Table 1.1</b> Comparison of growth duration (DG), maximum leaf area index ( $\text{LAI}_{\text{max}}$ ), maximum daily gross primary production ( $\text{GPP}_{\text{max}}$ ), maximum daily integrated GPP ( $\text{GPP}_{\text{int}}$ ), total growing season GPP ( $\text{GPP}_{\text{total}}$ ), mean daily solar radiation (Ave. SR), mean daily vapor pressure deficiency (Ave. VPD), and mean daily air temperature (Ave. $T_{\text{air}}$ ) over the growth season in different climate regimes and two planting cultures, flooded and rainfed rice in subspecies Japonica and Indica.....	10
<b>Table 1.2</b> Partitioning evapotranspiration of rainfed and paddy rice .....	21
<b>Table 2.1</b> Field management of the study site in 2013 in Gwangju. ....	72
<b>Table 2.2</b> Quantum yield ( $\alpha$ ), Potential maximum GPP and the coefficient of determination ( $R^2$ ) of the relation between NEE and PAR in A) paddy and B) rainfed rice in 2013. ....	82
<b>Table 2.3</b> Percentage of carbon allocated in the aboveground biomass for the respective crop organ and leaf nitrogen content in paddy and rainfed rice.....	83
<b>Table 3.1</b> Root biomass distribution in soil profiles in rainfed rice field and comparisons in rice crop yield components per square meter ground area (panicle number, spikelet number, proportion of filled ones, and thousand grain weight) collected on 246 DOY. Values in parentheses indicated S.E., $n = 3$ to 6. ....	123
<b>Table 3.2.A1</b> Parameter estimation for instantaneous NPP-light response curve: initial slope ( $\alpha$ ) of response curve, saturating level ( $\beta$ ) of NPP at extremely high PAR, and y-axis intercept ( $\gamma$ ) when PAR is close to 0 in paddy and rainfed rice on different measuring dates. ....	142
<b>Table 4.1.S1</b> Soil chemical and physical properties of study area, Chonnam National University research farm, Gwangju, S. Korea. ....	181
<b>Table 4.2.S2</b> Water and carbon fluxes, grain yield and water use efficiency of paddy and rainfed rice. Net Ecosystem Exchange (NEE, $-\text{NEE} = \text{GPP} + R_{\text{eco}}$ ) is the balance between photosynthetic uptake and release of carbon dioxide by autotrophic and heterotrophic respiration. Gross primary production (GPP) is photosynthetic uptake. Ecosystem respiration ( $R_{\text{eco}}$ ) is respiration from soil and plant. Ecosystem water use efficiency was calculated as the	

ratio of NEE to evapotranspiration (ET); the ratio of NEE to transpiration (T) and the ratio of GPP to T. Agronomic water use efficiency was calculated as the ratio of grain yield to ET. Differences between paddy and rainfed were tested by one way ANOVA: Carbon, water fluxes, Grain yield and water use efficiency were compared not only as crop seasonal sum but also as growth stage specific.....	182
<b>Table 4.3.S3</b> Correlation matrix of carbon and water fluxes and environmental variables of paddy rice.....	183
<b>Table 4.4.S4</b> Correlation matrix of carbon and water fluxes and environmental variables of rainfed rice .....	184
<b>Table 5.1</b> Time periods during which paddy rice cultivar Unkwang grew in different agronomic stages.....	189
<b>Table 5.2</b> Leaf dry mass per planted bundle (g) and mean leaf laminar area (cm <sup>2</sup> ) at different developmental stages and in different canopy layers in paddy rice grown at low (0 kg N ha <sup>-1</sup> ), normal (115 kg N ha <sup>-1</sup> ) and high (180 kg N ha <sup>-1</sup> ) fertilizer levels. S.E. is given in parentheses. ....	199
<b>Table 5.3</b> Comparisons among nutrient treatments in plant area index (PAI, m <sup>2</sup> m <sup>-2</sup> ), leaf area index (LAI, m <sup>2</sup> m <sup>-2</sup> ), daytime integral GPP (GPP <sub>int</sub> , g C d <sup>-1</sup> ), average overall CO <sub>2</sub> diffusive limitation (L <sub>total</sub> , %), stomatal limitation (L <sub>gs</sub> , %) and mesophyll limitation (L <sub>gm</sub> , %), canopy light attenuation coefficient (K <sub>l</sub> ), and canopy nitrogen attenuation coefficient at elongation (ca. 54) and grain-filling stages (ca. 73) at low (0 kg N ha <sup>-1</sup> ), normal (115 kg N ha <sup>-1</sup> ) and high (180 kg N ha <sup>-1</sup> ) fertilizer levels. Grain yields (g m <sup>-2</sup> ) in three groups is indicated. S.E. is given in parentheses, n = 3 to 6. ....	202



## List of abbreviations

Abbreviation	Meaning	Unit
APAR	Daily integrated PAR intercepted by canopy	$\text{MJ m}^{-2} \text{d}^{-1}$
CGC	Plant carbon gain capacity	$\text{g C m}^{-2}$
DAT	Day after transplanting	--
DOY	Day of year	--
ET	Crop evapotranspiration	$\text{mm d}^{-1}$
ETR	Electron transport rate	$\mu\text{mol electrons m}^{-2} \text{leaf s}^{-1}$
$\text{ET}_0$	Reference crop evapotranspiration	$\text{mm d}^{-1}$
FEW	Fraction of soil surface exposed and wetted	%
fPAR	Fraction of incident integrated PAR to absorbed PAR	%
GPP	Gross primary production	$\mu\text{mol CO}_2 \text{m}^{-2} \text{s}^{-1}$
$\text{GPP}_{\text{max}}$	Daily maximum GPP under saturating PAR	$\mu\text{mol CO}_2 \text{m}^{-2} \text{s}^{-1}$
$\text{GPP}_{\text{int}}$	Daily integrated GPP	$\text{g C m}^{-2} \text{d}^{-1}$
$\text{GPP}_{\text{total}}$	Growing season GPP	$\text{g C m}^{-2}$
LAI	Leaf area index	$\text{m}^2 \text{m}^{-2}$
LIA	Leaf inclination angle	degree
$\text{LUE}_{\text{ins}}$	Instantaneous canopy light use efficiency	$\mu\text{mol CO}_2 \mu\text{mol}^{-1} \text{photons}$
$\text{LUE}_{\text{int}}$	Daily mean light use efficiency based on canopy light interception	$\text{g C MJ}^{-1}$
$\text{LUE}_{\text{inc}}$	Daily mean light use efficiency based on incident PAR	$\text{g C MJ}^{-1}$
NEE	Net ecosystem exchange	$\mu\text{mol CO}_2 \text{m}^{-2} \text{s}^{-1}$
NPP	Net primary production equivalent to canopy net	$\mu\text{mol CO}_2 \text{m}^{-2} \text{s}^{-1}$

	assimilate rate	
$NPP_{\max}$	Maximum NPP under saturating PAR	$\mu\text{mol CO}_2 \text{ m}^{-2} \text{ s}^{-1}$
$NPP_{\text{int}}$	daily integrated NPP	$\text{g C m}^{-2} \text{ d}^{-1}$
NDVI	Normalized difference vegetation index	--
$NDVI_{\max}$	Maximum normalized difference vegetation index	--
$NDVI_{\min}$	Minimum normalized difference vegetation index	--
PAR	Photosynthetically active radiation	$\mu\text{mol photons m}^{-2} \text{ s}^{-1}$
REW	Readily evaporable water which is cumulative depth of depletion from surface soil layer	mm
SWC	Volumetric soil water content	$\text{m}^3 \text{ m}^{-3}$
TEW	Maximum water amount for evaporation	mm
VPD	Water vapor pressure difference between surrounding air and leaf intercellular sir space	kPa
intWUE	Leaf instantaneous water use efficiency	$\mu\text{mol CO}_2 \text{ mmol}^{-1} \text{ H}_2\text{O}$
$WUE_i$	Leaf intrinsic water use efficiency	$\mu\text{mol CO}_2 \text{ mmol}^{-1} \text{ H}_2\text{O}$
$WUE_{\text{agro}}$	Agronomic water use efficiency	$\text{kg grain mm}^{-1} \text{ H}_2\text{O}$
$WUE_{\text{eco}}$	Ecological water use efficiency	$\text{g C mm}^{-1} \text{ H}_2\text{O}$

## List of symbols

Symbol	Definition	Unit
A	Leaf assimilation rate	$\mu\text{mol CO}_2 \text{ m}^{-2} \text{ s}^{-1}$
$A_{\text{max}}$	Photosynthetic rate at normal $\text{CO}_2$ concentration and saturating PAR	$\mu\text{mol CO}_2 \text{ m}^{-2} \text{ s}^{-1}$
$C_i$	Intercellular $\text{CO}_2$ concentration	$\mu\text{mol CO}_2 \text{ mol}^{-1} \text{ air}$
$C_a$	Ambient $\text{CO}_2$ concentration	$\mu\text{mol CO}_2 \text{ mol}^{-1} \text{ air}$
$E_L$	Leaf transpiration rate	$\text{mmol H}_2\text{O m}^{-2} \text{ leaf s}^{-1}$
E	Soil evaporation	$\text{mm d}^{-1}$
$\Gamma^*$	Chloroplast $\text{CO}_2$ compensation point	$\mu\text{mol CO}_2 \text{ mmol}^{-1}$
G	Soil heat flux density	$\text{W m}^{-2}$
g	Acceleration due to gravity	$\text{m s}^{-2}$
$g_{\text{sw}}$	Stomatal conductance to water vapor	$\text{mmol H}_2\text{O m}^{-2} \text{ leaf s}^{-1}$
$g_s$	Stomatal conductance to $\text{CO}_2$	$\text{mmol CO}_2 \text{ m}^{-2} \text{ leaf s}^{-1}$
$g_m$	Mesophyll conductance to $\text{CO}_2$	$\text{mmol CO}_2 \text{ m}^{-2} \text{ leaf s}^{-1}$
$g_{s,\text{max}}$	Stomatal conductance under saturating light	$\text{mmol CO}_2 \text{ m}^{-2} \text{ leaf s}^{-1}$
h	Length over which the pressure drop is taking place	m
$J_{\text{max},30}$	Maximum electron transport rate at leaf temperature $30^\circ\text{C}$	$\mu\text{mol electrons m}^{-2} \text{ leaf s}^{-1}$
$J_p$	Electron transport rate that is used by $\text{CO}_2$ fixation process	$\mu\text{mol electrons m}^{-2} \text{ leaf s}^{-1}$
k	Plant hydraulic conductance	$\text{mmol H}_2\text{O m}^{-2} \text{ leaf s}^{-1} \text{ MPa}^{-1}$
$K_{\text{cb}}$	Transpiration coefficient	--
$K_e$	Evaporation coefficient	--
$K_{\text{cmax}}$	Upper limit of evaporation and transpiration from	--

	crop surface	
$K_r$	Soil evaporation reduction coefficient	--
$K_L$	Light attenuation efficiency	--
$K_N$	Nitrogen attenuation efficiency	--
$K_p$	Coefficiency controlling correlation between LAI and LAI	--
$K_{vi}$	Coefficiency controlling correlation between NDVI and LAI	--
$L_{gs}$	Percent limitation due to finite stomatal conductance	%
$L_{gm}$	Percent limitation due to finite mesophyll conductance	%
$L_{total}$	Percent limitation due to finite CO <sub>2</sub> diffusion conductance	%
$N_a$	Leaf nitrogen content per leaf area	g m <sup>-2</sup> leaf
$N_{total}$	Canopy nitrogen content per ground	g m <sup>-2</sup> ground
rh	Relative humidity	%
$R_{soil}$	Soil respiration rate	μmol CO <sub>2</sub> m <sup>-2</sup> ground s <sup>-1</sup>
$R_{plant}$	Plant respiration rate	μmol CO <sub>2</sub> m <sup>-2</sup> ground s <sup>-1</sup>
$R_{eco}$	Ecosystem respiration rate	μmol CO <sub>2</sub> m <sup>-2</sup> ground s <sup>-1</sup>
$R_{day}$	Non-photorespiratory CO <sub>2</sub> evolution	μmol CO <sub>2</sub> m <sup>-2</sup> leaf s <sup>-1</sup>
$R_n$	Net radiation	W m <sup>-2</sup>
$r_c$	Canopy resistance	s m <sup>-1</sup>
$r$	Psychrometric constant	kPa °C <sup>-1</sup>
$r_a$	Aerodynamic resistance	s m <sup>-1</sup>
$T_{air}$	Air temperature above plant canopy	°C

$T_{\text{soil}}$	Soil temperature at 10 cm depth	$^{\circ}\text{C}$
$T$	Canopy transpiration	$\text{mm d}^{-1}$
$u_2$	Wind speed	$\text{m s}^{-1}$
$V_{\text{cmax},30}$	Maximum carboxylation rate at leaf temperature $30^{\circ}\text{C}$	$\mu\text{mol CO}_2 \text{ m}^{-2} \text{ leaf s}^{-1}$
$Z_e$	Depth of surface soil layer	$\text{m}$
$\alpha$	Slope of assimilation-light response curve, equivalent to $\text{LUE}_{\text{ins}}$	$\mu\text{mol CO}_2 \mu\text{mol}^{-1} \text{ photons}$
$\beta$	Saturating value of light response curve under infinitely high PAR	$\mu\text{mol CO}_2 \text{ m}^{-2} \text{ ground s}^{-1}$
$\gamma$	y-intercept of light response curve	$\mu\text{mol CO}_2 \text{ m}^{-2} \text{ ground s}^{-1}$
$\Psi_s$	Soil matric potential	$\text{kPa}$
$\Psi_l$	Leaf water potential	$\text{MPa}$
$\theta_r$	Residual soil water content	$\text{m}^3 \text{ H}_2\text{O m}^{-3} \text{ soil}$
$\theta_s$	Saturating soil water content	$\text{m}^3 \text{ H}_2\text{O m}^{-3} \text{ soil}$
$\theta_{\text{FC}}$	Soil water content at field capacity	$\text{m}^3 \text{ H}_2\text{O m}^{-3} \text{ soil}$
$\theta_{\text{WP}}$	Soil water content at wilting point	$\text{m}^3 \text{ H}_2\text{O m}^{-3} \text{ soil}$
$\sigma$	The inverse of the air entry suction	$\text{cm}^{-1}$
$\rho$	Water density	$\text{kg m}^{-3}$
$\lambda$	Latent heat of vaporization of water vapor	$\text{J g}^{-1}$
$\Delta$	The slope of the saturation vapor pressure -- temperature relationship	--

## **Chapter 1 - Synopsis**

### **Chapter 1**

#### **1. Synopsis**

##### **1.1. Introduction**

###### **1.1.1. Habitat factors influencing rice production and water use: Background for the research**

Rice production is carried out in more than 114 countries with large variations in climate conditions, and it is the foremost cereal crop with respect to agricultural yield from a global perspective (FAO, 2013). There are more than 100 million ha under rice cultivation, with 89% distributed in Asia. About 45% of the planted rice area is rainfed, of which 25% is never flooded (upland) (Hijmans and Serraj, 2008). After the beginning of the green revolution, rice production on average has increased markedly by up to 140%, whereas, large variations exist among farming regions (Mohanty et al., 2013). Although the total rice production in recent years has continued to increase, the utilization level has increased in parallel with yield. Global rice consumption is projected to rise from 439 million tons (milled rice) in 2010 to 496 million tons in 2020 and to increase further to ca. 555 million tons in 2035 (Seck et al., 2012). To keep pace with population growth, an annual yield increment of 1.2–1.5% will be needed as compared to the current rate of increase of less than 1% (Mohanty et al., 2013). Rice production systems are vulnerable to changes in biotic and abiotic factors, of which nutrient deficiency, high temperature, drought, salinity and diseases individually or interactively threaten the staple food supply in many countries. Undoubtedly, sustainable rice production is important to world food security. Maintaining or even gaining higher yields per unit area requires not only innovative breeding of new cultivars but also attention to the details of effective and reasonable field management of fertilization, irrigation, and pest, disease, and weed control (Tilman et al., 2002).

Long-term variations in rice production occur due to the inherent characteristics of crop growth and development (which are tightly related to canopy carbon gain capacity and carbon allocation pattern) and because of the disturbances of extreme weather events and due

## Chapter 1 - Synopsis

to human intervention (Alberto et al., 2012; Fageria and Baligar, 1999; Gimenez et al., 1994; Sinclair, 1991; Tuong and Bouman, 2003). Rice as a domesticated annual crop has evolved over a long history with more than 40,000 varieties of cultivated rice (the grass species *Oryza sativa*) believed to exist worldwide ([www.riceassociation.org.uk](http://www.riceassociation.org.uk)). Most varieties exhibit non-uniform growth due to internal genetic controls and differentiation in response to climate conditions, whereas the completion of the rice life cycle from planting to harvest in agronomically promoted cultivars usually takes 100 to 140 days (Köhl, 2015; Tuong and Bouman, 2003; Yoshida, 1981). During this brief period for growth, dynamic changes occur in ecosystem carbon and water fluxes, cover extent, canopy structure and physiology as the crop shifts from one growth stage to the next (Campbell et al., 2001a, b; Gimenez et al., 1994; Lindner et al., 2015; Yoshida, 1981). For example, the vegetative phase begins with a large area of fields having a bare land surface, while flowering and grain-filling stages occur with dense coverage and large time dependent changes in leaf area index (Figure 1.1). Practical management as well as climate that modify nutrient and water availability will influence the phenology shown. In a landscape context, such changes in growth over the season, as well as crop selection and distribution in agricultural catchments and field management activities, determine regional controls on carbon and water balance as well as biogeochemical processes (Bhattacharyya et al., 2013b; Kwon et al., 2010; Lee, 2014; Lindner et al., 2015). With respect to field practical management that can achieve higher yields, the ability to modify and control soil nutrient and water availability are viewed as most promising for the future (FAO, 2014).

## Chapter 1 - Synopsis

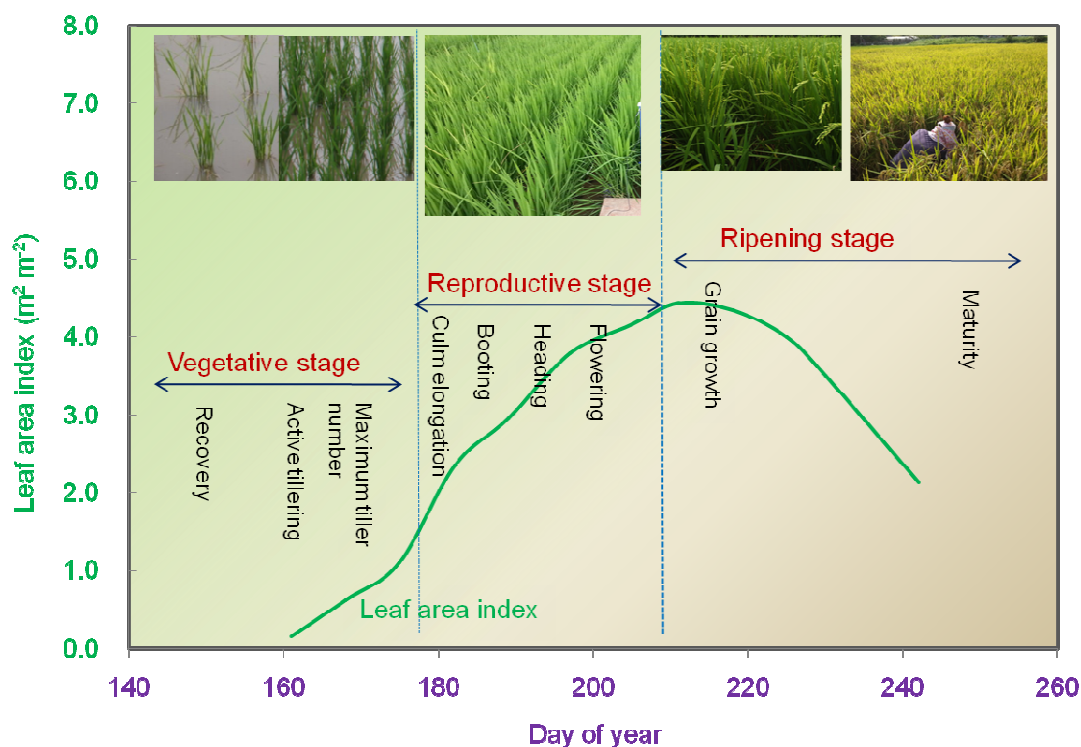


**Figure 1.1** Life history of the “120-day” Unkwang rice cultivar planted in the monsoon region near Gwangju, South Korea in 2013 and studied in this research under a transplantation puddle cultivation system. Plants during the reproductive stage continuously extend height and develop new leaves at new nodes. Hence, this stage is also referred to as the internode elongation stage (Yoshida, 1981).

The rice crop non-selectively utilizes nitrogen from mineralization and fertilizer applications (Koyama and Niamsrichand, 1973). After mineralized soil nitrogen is exhausted, the amount of added fertilizer nitrogen determines crop development and growth. With depletion of mineralized soil nitrogen, more fertilizer nitrogen leads to more nitrogen utilization by plants, at least up to a moderately high level, to greater biomass accumulation (Bandaogo et al., 2015; Gimenez et al., 1994; Janssen and Metzger, 1928; Koyama and Niamsrichand, 1973) and to increased grain yield (Dong et al., 2015; Ju et al., 2015; Koyama et al., 1972; Wyche, 1947; Amano et al., 1993). Intensive fertilizer use in agriculture in order to gain greater benefits and meet the needs of a continuously increasing population, especially in developing countries, is a global trend. The amount of nitrogen fertilizer used in 1977 versus 2005 increased rapidly from 7.07 to 26.21 million tons in China (Ju et al., 2009). Intensive land use with high levels of fertilization is also a common practice in mountainous landscapes in South Korea (Kettering et al., 2012). However, high fertilizer application rates that exceed plant



## Chapter 1 - Synopsis

requirements do not necessarily result in higher crop yield (Katsura et al., 2007; Yang et al., 2015) but may adversely result in environmental problems, such as decreased quality of fresh water and enhanced trace gas emissions, e.g., ammonia ( $\text{NH}_3$ ) volatilization and nitrous oxide ( $\text{N}_2\text{O}$ ) (Fillery et al., 1986; Nishimura et al., 2008; Reddy et al., 1984; Tian et al., 2012). In order to quantitatively analyze the effects of different levels of fertilization on rice production, field investigations examining characteristics of canopy structure and photosynthetic physiology that affect carbon assimilation at leaf and whole plant level are, therefore, required.

Increasing water scarcity due to climate change currently threatens the sustainability and productivity of traditional flooded rice culture systems (Tuong and Bouman, 2003), and may lead to a shift from flooded rice to rainfed cultivation (IRRI, 2002). Rainfed rice production systems can improve total water use efficiency by as much as 70% as compared to paddy rice (Tao et al., 2015). Average total water input for rainfed rice fields over the growing season has been reported to be 43 to 65% lower as compared to total water consumption for typical puddle transplanted rice (Alberto et al., 2013; Nie et al., 2012). Rice seed directly sown in upland fields with limited irrigation or no artificial water supply has emerged as a viable alternative for coping with excess labor costs and to avoid high water input (Hijmans and Serraj, 2008). Nevertheless, success has been limited in increasing productivity in rainfed rice (Nie et al., 2012). Rice yields in these ecosystems remain low at 1.0 to 2.5 t ha<sup>-1</sup>, and tend to vary due to erratic and unpredictable rainfall, even though there has been a constant release of new breeding lines with traits for drought-resistance and high water use efficiency, and for reduced plant mortality under water stress (Serraj et al., 2008). Among all abiotic factors, drought is the major constraint limiting sustainable productivity for rice in Asia and sub-Saharan Africa. At least 23 million hectares (20% of the rice planting area) are potentially impacted alone in Asia (Pandey and Bhandari, 2008). Frequent and serious droughts can directly cause enormous economic losses and can destabilize social development in resource-poor regions where drought impacts are not alleviated by other aid efforts. Even without dry spells occurring over the growth season, rice is still vulnerable to

## **Chapter 1 - Synopsis**

aerobic soil conditions (Kato and Okami, 2011; Okami et al., 2013). Thus, it is necessary to better understand temporal interactions and acclimation within the context of rice crop growth, especially in response to varying soil water content and the occurrence of non-rainfall periods.

Crop establishment and survival as well as achievement of high yield production with less water used in rainfed cultivation requires that water use efficiency (WUE) of plants should be improved (FAO, 2014). WUE may be defined as the amount of photosynthetic productivity per unit of water used. This term can be applied at different levels (crop, plant, canopy or leaf level) and at very different time scales, from months to minutes (Morison et al., 2008). Leaf intrinsic water use efficiency is the ratio of net carbon uptake to stomatal conductance (Fischer and Turner, 1978), and it is a factor of major importance in determining community productivity.  $WUE_i$  has mostly been used to characterize genetic effects and in selection of high-yielding varieties in crop breeding projects (Condon et al., 2004; Poni et al., 2009; Topbjerg et al., 2014) which often feature regulated deficit irrigation (Alberto et al., 2013; Bouman et al., 2005; Yang et al., 2002). Alternative concepts for water use efficiency in agronomic studies consider the ratio of yield to evapotranspiration (ET) or in recent ecosystem studies the ratio of gross primary production (GPP) to ET. Increasingly, studies have focused on evaluation of either yield/ET or GPP/ET in various systems (Adekoya et al., 2014; Hu et al., 2009; Huang et al., 2010; Suyker and Verma, 2008; Suzuki et al., 2014), although very few studies have compared rainfed and flooded rice (Alberto et al., 2013). Comparative studies using the same rice cultivar are lacking.

### **1.1.2. Effects of habitat factors on rice production: a meta-analysis**

As briefly stated above, individual field experiments in paddy and rainfed rice systems reported large variations in yield production. To gain an overview on the relative importance of different habitat factors for rice photosynthetic productivity, and to determine whether general correlations currently allow us to interpret fluctuations in carbon gain capacity, a meta-analysis of published investigations was conducted, compiling information on field

## Chapter 1 - Synopsis

management practices (fertilizer application rate and timing, and/or field irrigation), growth season duration (denoted as the time period from commencement of seed sowing or transplantation to grain harvest – GD), canopy development (maximum leaf area index – LAI), climate factors over the growth season (daily average solar radiation – SR, average vapor pressure deficit – VPD, and daily mean air temperature –  $T_{\text{air}}$ ), and measures of photosynthetic productivity ( $\text{GPP}_{\text{total}}$  and  $\text{GPP}_{\text{max}}$ ). The resulting information is presented in Table 1.1, and selected variables are plotted in Figure 1.1 in order to examine correlations between growth duration and climate factors with carbon gain ( $\text{GPP}_{\text{total}}$ ).

Recent studies aimed at selection of high-yielding cultivars have proposed that growth duration in rice genotypes is a critical factor influencing carbon gain potential and yield production when soil N supply is adequate (De Datta and Broadbent, 1988; Ju et al., 2015; Singh et al., 1998; Zhang et al., 2009). Accordingly, greater production should occur in medium-duration (ca. 119 days after seeding) genotypes and long-duration (ca. 130 days after seeding) ones. As expected, one does find a positive correlation between  $\text{GPP}_{\text{total}}$  and growth duration (GD) in flooded rice systems, with rapid increase in  $\text{GPP}_{\text{total}}$  from  $750 \text{ g m}^{-2}$  to  $1250 \text{ g m}^{-2}$  at long-duration genotypes ( $R^2 = 0.21$ ;  $p < 0.001$ ; Figure 1.2a). Extended presence of an active canopy continuously increases the amount of radiation intercepted and utilized, ensuring higher total GPP. While, there is an extremely large scatter in the  $\text{GPP}_{\text{total}}$ –GD correlation, it can be understood as occurring due to large genetic variation in the planted material and due to climatic differences and nutrient availability. For example, new hybrid rice genotypes are now produced which mature with only 100 days of growth but exhibit the highest grain yield (Tuong and Bouman, 2003; Köhl, 2015). In contrast to the flooded rice system, a negative correlation between total carbon gain and growth duration occurs with rainfed rice in the tabulated studies, meaning that extended growth may not be able to increase carbon gain. The lack of a discernable positive influence of growth duration on carbon gain in rainfed rice may be due to reduced photosynthetic productivity as a result of the occurrence of water stress periods.

## Chapter 1 - Synopsis

The evaluation shown in Figure 1.2b indicates a weakly negative correlation between daily mean air temperature and  $GPP_{total}$  in paddy ( $R^2 = 0.23$ ;  $p < 0.001$ ) and rainfed rice systems ( $R^2 = 0.36$ ;  $p < 0.001$ ) (Figure 1.2b). In general, high production is observed at moderate average  $T_{air}$  of 20°C but production decreases at ca. 27°C. No correlation between  $GPP_{total}$  and VPD was found with either paddy or rainfed rice systems (Figure 1.2c). The absence of ponded water in rainfed fields will cause microclimate deviations from those at paddy fields. Resulting higher air temperature and VPD in rainfed systems may be expected to impact photosynthetic activity (Xue et al., 2012) and constrain assimilation rate (Otieno et al., 2012), particularly via decreases in bulk stomatal conductance (Medlyn et al., 2002).

A clear positive correlation between mean daily solar radiation (SR) and  $GPP_{total}$  across various genotypes and research sites was found for paddy rice systems as shown by a high regression coefficient ( $R^2 = 0.69$ ;  $p < 0.001$ ; Figure 1.2d). The strong correlation found for paddy rice was not apparent for rainfed rice systems, although few studies were available. Short-time changes of  $CO_2$  uptake rate are driven by incident light intensity and air temperature (Bhattacharyya et al., 2013b; Miyata et al., 2000; Zhao et al., 2011). Aside from canopy structure which determines the seasonal course of GPP (Alberto et al., 2012; Campbell et al., 2001b; Lindner et al., 2015), fluctuations in daily incident PAR are suggested by this analysis to be an important factor controlling carbon uptake in paddy rice ecosystems and may determine whether carbon balance shifts between carbon sink and source. Surprisingly, although rainfed rice systems received lower average solar radiation in these studies, relatively high daily mean air temperature and VPD were evident. Based on this limited dataset, we can speculate that growing season GPP in rainfed rice system is to a larger extent affected by air temperature. Obviously, daily radiation is also one of the important factors driving diurnal GPP in rainfed cultures as highlighted by most of the literature.

Recommended application rates for nitrogen fertilization differ with specific soils and seasonal timing (potential phenological development) in paddy and rainfed rice grown at different sites by as much as a factor of 2 (from 68 to 115 kg N ha<sup>-1</sup>; Table 1.1). Relatively

## Chapter 1 - Synopsis

high nitrogen application or split applications seems to have little effect on plant development and growth (Fageria and Baligar, 1999; Rao et al., 1985). As highlighted above, the proportion of applied nitrogen used by plants for growth may only account for ca. 35% (Buresh et al., 1988; Fillery et al., 1986), most of the fertilizer being lost via ammonium volatilization and surface runoff. Indigenous soil N supply (Cui et al., 2008) and increasing annual N inputs via atmosphere deposition and irrigation water in north and south-east China contribute up to 89 kg N ha<sup>-1</sup> (Ju et al., 2009). Since all of these aspects of the N cycle are not documented in the studies in Table 1.1, it is not surprising that no relationship could be documented between photosynthetic productivity and observed N applications.

The meta-analysis implies that solar radiation plays the most important role in regulation of total gross primary production in both paddy and rainfed rice systems. Increasing average daily air temperature could exacerbate reductions in photosynthetic productivity in rice systems. Daily fluctuation of air temperature influence growing season carbon gain to a similar extent as does solar radiation. These factors should be considered simultaneously when attempting to assess the impact of climate change on rice photosynthetic productivity in both paddy and rainfed rice systems. Large error bars indicated in Figure 1.2 highlight the large changes in production that occur between research sites and climate regimes. Nevertheless, these studies do provide guidance, indicating that very integrated site- and cultivar-specific research should be implemented at field level to gain new insight on how seasonal change in climate factors affects rice growth and especially how this differs in paddy versus rainfed rice. The research in this thesis is aimed at providing such new insight, which will be helpful in considering potential consequences of climate change on rice production systems. The ecophysiological basis for response to climate variation and to changing the substrate from paddy to rainfed cultivation still requires clarification.

## Chapter 1 - Synopsis

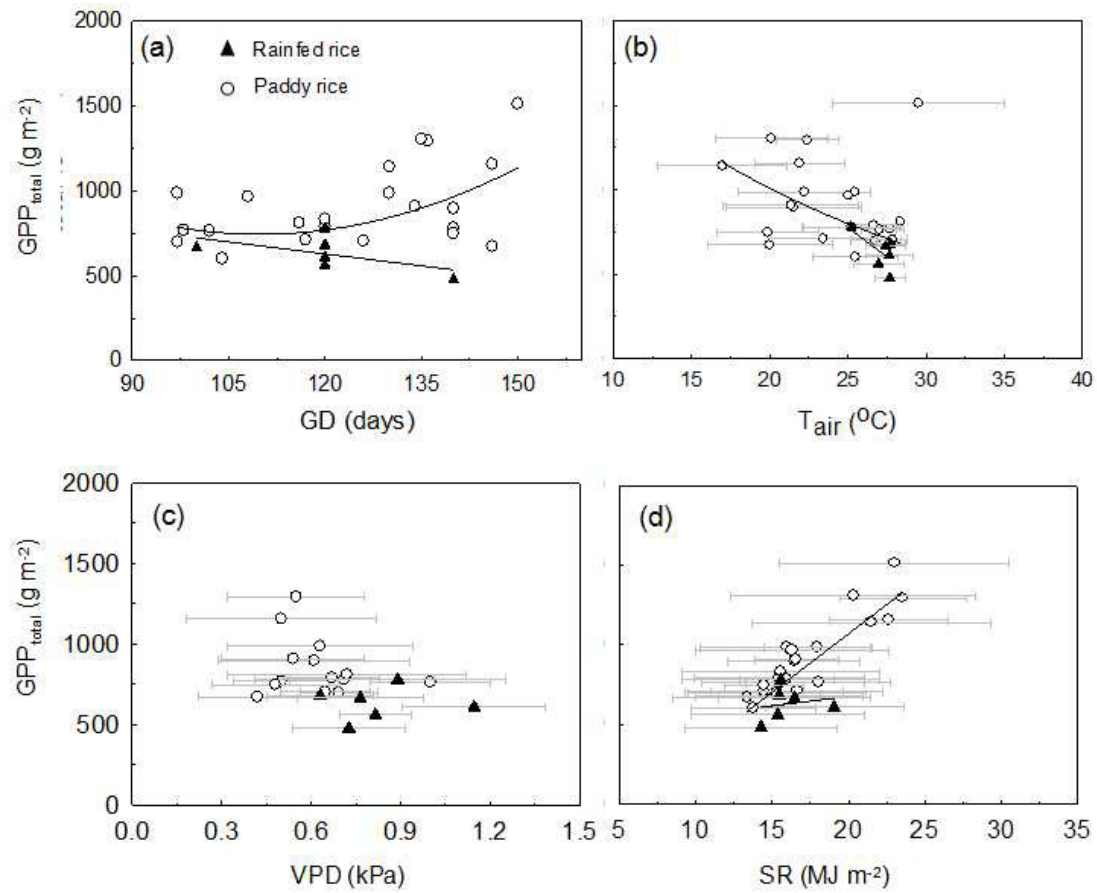


**Figure 1.2** Correlation between growing season total gross primary production ( $GPP_{total}$ ) and growth duration (GD) (a), and mean daily air temperature ( $T_{air}$ ) (b), and mean daily vapor pressure deficiency (VPD) (c), and mean daily solar radiation (SR) in paddy and rainfed rice systems. Error bars indicate standard deviation. Data achieve was listed in Table 1.1.

## Chapter 1 - Synopsis

**Table 1.1** Comparison of growth duration (DG), maximum leaf area index ( $LAI_{max}$ ), maximum daily gross primary production ( $GPP_{max}$ ), maximum daily integrated GPP ( $GPP_{int}$ ), total growing season GPP ( $GPP_{total}$ ), mean daily solar radiation (Ave. SR), mean daily vapor pressure deficiency (Ave. VPD), and mean daily air temperature (Ave.  $T_{air}$ ) over the growth season in different climate regimes and two planting cultures, flooded and rainfed rice in subspecies Japonica and Indica.

Authors	Imigation management	Rice cultivar	Research site	Fertilizer rate	GD <sup>1</sup> (d)	$LAI_{max}$ (m <sup>2</sup> m <sup>-2</sup> )	$GPP_{int}$ (g m <sup>-2</sup> d <sup>-1</sup> )	$GPP_{max}$ (μmol m <sup>-2</sup> s <sup>-1</sup> )	$GPP_{total}$ (g m <sup>-2</sup> )	Ave. SR (MJ m <sup>-2</sup> d <sup>-1</sup> )	Ave. VPD (kPa)	Ave. $T_{air}$ (°C)	Remark (year, fertilization timing)
Miyata et al. (2000)	Flooded field	lowland rice (Japonica)	Okayama Japan	77 kg N ha <sup>-1</sup>	~150	3.9	10.02	--	--	--	--	--	at the seeding
Lindner et al. (2015)	Flooded field	lowland rice (Japonica)	Haean, South Korea	98 kg NH <sub>4</sub> ha <sup>-1</sup>	149	5.4-6.3	--	21	--	--	--	--	as basal
Nishimura et al. (2008)	Flooded field	lowland rice (Japonica)	Tsukuba, Japan	90 kg N ha <sup>-1</sup>	130	--	10.9	--	--	--	--	--	as basal and top-dressing
Bhattacharyya et al. (2013)	Flooded field	upland rice (Indica)	Cuttack, India	80 kg N ha <sup>-1</sup>	116	5.5	8.99	25	--	--	--	--	as basal, tillering, and panicle initiation
Inoue et al. (2008)	Flooded field	lowland rice (Japonica)	Tsukuba, Japan	--	130	4.8	--	40	--	--	--	--	
This research	Flooded field				120	4.6	15.04	26.02	--	--	--	--	
		lowland rice (Japonica)	Gwangju, South Korea	115 kg N ha <sup>-1</sup>									as basal and tillering
	Rainfed field				120	3.8	14.32	24.72	--	--	--	--	

## Chapter 1 - Synopsis

Authors	Imigation management	Rice cultivar	Research site	Fertilizer rate	GD <sup>1</sup> (d)	LAI <sub>max</sub> (m <sup>2</sup> m <sup>-2</sup> )	GPP <sub>int</sub> (g m <sup>-2</sup> d <sup>-1</sup> )	GPP <sub>max</sub> (umol m <sup>-2</sup> s <sup>-1</sup> )	GPP <sub>total</sub> (g m <sup>-2</sup> )	Ave. SR (MJ m <sup>-2</sup> d <sup>-1</sup> )	Ave. VPD (kPa)	Ave. Tair (°C)	Remark (year, fertilization timing)
Alberto et al. (2012)	Flooded field	lowland rice (Indica)	Los Bãnos, Philippines	2 100 and 80 kg N ha <sup>-1</sup> in wet and dry season	97	6.4	15		699	15.32±5.84	0.692±0.13	26.76±1.59	2008DS
					98	6.2	12		768	15.71±5.32	0.5±0.16	27.67±0.9	2008WS
					120	6.9	14	--	790	15.48±5.53	0.67±0.16	26.66±1.64	2009DS
					126	6.1	16		705	14.45±5.17	0.648±0.15	27.86±0.95	2009WS
					102	7.9	12		764	18.04±4.72	1.0±0.2	27.02±1.11	2010DS
	Rainfed field	upland rice (Indica)			~120	4.9	8		561	15.41±5.68	0.815±0.12	26.96±1.61	2008DS
					~120	4.4	8		680	15.47±5.5	0.63±0.18	27.72±0.95	2008WS
					~100	6.4	11	--	665	16.49±4.99	0.764±0.21	27.41±1.23	2009DS
					~140	5.7	7.5		477	14.30±4.97	0.726±0.19	27.68±0.97	2009WS
					~120	6.4	8		609	19.08±4.52	1.146±0.24	27.65±1.54	2010DS
Alberto et al. (2013)	Rainfed field	lowland variety (Indica)	Los Bãnos, Philippines	150 kg N ha <sup>-1</sup>	119	4.8	17	35.5	1074	16.70±5.26	0.82±0.21	26.72±1.45	2011DS
					114	6.1	15.1	23.4	758	15.80±4.81	0.88±0.19	27.48±1.24	2012DS
Hossen et al. (2011)	Flooded field	lowland rice (Indica)	Bangladesh	110 kg N ha <sup>-1</sup> 185 kg N ha <sup>-1</sup>	117	6.2	--	--	711	16.63±5.64	--	23.40±3.48	2007DS
					104	5.1	--	--	601	13.77±4.08	--	25.47±2.73	2007WS as basal
Bhattacharyya et al. (2014)	Flooded field	lowland rice (Japonica)	Cuttack, India	--	121	--	12	--	642	--	--	27.05 <sup>3</sup>	2012WS
					125	--	15	--	287	--	--	27.9 <sup>3</sup>	2012-13DS
Lee (2014)	Flooded field	lowland rice (Japonica)	Haean, South Korea Haenam, South Korea Tsukuba, Japan	98 kg NH <sub>4</sub> ha <sup>-1</sup> -- --	146	5.8	13.28	--	672	13.34±4.79	0.42±0.20	20.46±3.61	as basal
					140	6.0	12.58	--	780	15.94±3.07	0.71±0.3	25.24±3.17	
					140	5.5	15.21	--	897	16.42±4.34	0.61±0.32	21.81±4.09	2002
					140	5.1	14.31	--	749	14.46±2.61	0.48±0.21	20.04±2.73	2003
					130	4.8	16.48	--	987	17.92±3.48	0.63±0.31	22.50±3.65	2004
					134	4.3	14.37	--	908	16.60±2.72	0.54±0.24	21.80±4.05	2005



## Chapter 1 - Synopsis

Authors	Irrigation management	Rice cultivar	Research site	Fertilizer rate	GD <sup>1</sup> (d)	LAI <sub>max</sub> (m <sup>2</sup> m <sup>-2</sup> )	GPP <sub>int</sub> (g m <sup>-2</sup> d <sup>-1</sup> )	GPP <sub>max</sub> (μmol m <sup>-2</sup> s <sup>-1</sup> )	GPP <sub>total</sub> (g m <sup>-2</sup> )	Ave. SR (MJ m <sup>-2</sup> d <sup>-1</sup> )	Ave. VPD (kPa)	Ave. Tair (°C)	Remark (year, fertilization timing)
Lee (2014)	Flooded field	lowland rice (Japonica)	El Saler, Spain	--	136	5.7	18.50	--	1294	23.56±4.16	0.55±0.23	22.41±1.95	2007
					146	6.1	18.04	--	1157	22.61±3.86	0.51±0.32	21.89±2.86	2008
Hatala et al. (2012)	Flooded field	lowland rice (Japonica)	Twitchell Island, USA	68 kg NH <sub>4</sub> ha <sup>-1</sup>	130	6.8	15.2	--	1141	21.49±7.8	--	16.98±4.1	2009 as basal
					135	7.1	15.1	--	1305	20.3±8.0	--	20.08±3.6	2010 as basal
Vote et al. (2015)	Flooded field	lowland rice (Japonica)	Griffith NWS, Australian	--	~150	--	18.2	--	1514	23.0±7.5	--	29.5±5.47	2010-2011
Chen et al. (2015)	Flooded field		Huaihe River basin, China	155 kg N ha <sup>-1</sup>	97	--	--	--	987	15.93±5.64	--	25.44	2008
					108	--	--	--	966	16.32±6.28	--	25.03	2009
Knox et al. (2015)	Flooded field	lowland rice (Japonica)	Twitchell Island, USA	135 kg NH <sub>4</sub> ha <sup>-1</sup>	150	4.1	12.95	--	1024	23.79±6.54	--	19.09±2.46	2012
Min et al. (2013)	Flooded field	lowland rice (Japonica)	Gimje, South Korea	110 kg N ha <sup>-1</sup>	122	--	12.5	--	710.3	10.58±2.6	0.51±0.24	22.1±3.61	2012
Takimoto et al. (2010)	Flooded field	lowland rice (Japonica)	Tamano, Japan	--	125	4.2	9.54	--	727	15.55±7.08	--	24.48±4.72	2008
This research	Flooded field	lowland rice (Japonica)	Gwangju, South Korea	115 kg N ha <sup>-1</sup>	120	4.6	15.04	26.02	832	15.55±6.44	--	--	2013 as basal and tillering
	Rainfed field				120	3.8	14.32	24.72	779	--	0.89±0.36	25.22±3.1	

<sup>1</sup> Growth duration of rainfed rice was accounted from date of seedling emergence to harvest

<sup>2</sup> Three split doses of 100 kg N ha<sup>-1</sup> (40–30–30) in the dry season and 80 kg N ha<sup>-1</sup> (25–30–25) in the wet season were applied at 10, 25 and 45 days after sowing (DAS) of the aerobic rice plants

<sup>3</sup> The mean highest and lowest temperatures were 30.3, 23.8°C and 32.7, 23.1°C, respectively during wet season 2012 and dry season 2012–2013

## Chapter 1 - Synopsis

### 1.1.3. Thesis concept

During the course of evolution, plants have developed sophisticated mechanisms allowing adaptation to their habitats, and they exhibit plasticity in their capacity to respond to the information they sense about the environment (Araus et al., 2008). Clarifying internal plant regulation affecting the performance and acclimation at different scales under specific climate conditions and in a shift with respect to soil water content is helpful in order to understand the effects of those shifts on ecosystem function and productivity. Nutrient stimulation, uncertainties with respect to climate change, and the need to extend rice production into new geographical regions emphasize the need to better understand in detail such eco-physiological response mechanisms, especially as related to field management and the transfer of rice genotypes from wetland to dryland growth conditions. Shifts in the “behavior” of rice, e.g., shifts in ecosystem function in terms of carbon and water fluxes that determine rice crop development and yields (Campbell et al., 2001b; Lindner et al., 2015; McMillan et al., 2007), must be viewed as a high research priority.

Questions exist as to how ecophysiological characteristics vary and limit biomass production and photosynthetic productivity. Considering those traits which are the most important in determination of crop development, we must determine whether or not they have a similar regulatory effect among rice cultivars grown under different field management practices, and how they could be linked to optimize carbon gain and reduce water use at field and landscape scales. In the first orientative study of this thesis, basic canopy level CO<sub>2</sub> gas exchange was observed in puddle transplanted versus direct-seeded rainfed rice over the course of the growth season in Gwanju, Korea, using the same cultivar or genotype in order to observe shifts in major flux process regulation (Chapter 2 ). In an extension of this study, I have then attempted to disentangle the multiple ecophysiological factors responsible for observed seasonal variations in carbon gain, water use and yield in Unkwang rice cultivated under these two extremely different situations with respect to water availability (Chapter 3). As discussed above, not only the yield potential of rice is an important concern when planning for the future, but also water use related to yield and ecosystem carbon sequestration are

## **Chapter 1 - Synopsis**

critical concerns for the sustainable development of rice agriculture. These have been evaluated via the simultaneous application of several innovative methodologies (Chapter 4). Finally, in order to gain new insight with respect to the balance that can be achieved between nutrient addition for higher production versus optimal environmental efficiency, a fourth study (Chapter 5) analyzes the detailed influence of variable fertilizer additions on canopy structure, light interception, light conversion, resource distribution, leaf physiology and CO<sub>2</sub> diffusion conductance for classical puddle transplanted rice. The following four sections (1.1.4.1 through 1.1.4.4) elaborate the state of knowledge upon which each study and its later interpretation have been based, and within this context, the objectives and hypotheses for each study are presented.

### **1.1.4. Research objectives and hypotheses**

#### **1.1.4.1. Seasonal variations in carbon gain and yield in paddy versus rainfed rice**

Biomass accumulation relates to canopy photosynthesis occurring during daytime and concurrent plant respiratory processes which consume photosynthetic products in maintenance and growth. In principle, increments in canopy assimilation rates that occur with development have a positive feedback, further increasing the amount of carbohydrates available for growth, and resulting in higher biomass production and subsequent yield (Monteith and Moss, 1977; Sheehy and Mitchell, 2013; Sinclair, 1991; Sinclair and Horie, 1989). When considering the shift of Unkwang rice from a paddy environment to rainfed cultivation, however, new demands on the production and use of available carbohydrates may be expected for several reasons. First, cropping methods seeding versus transplanting will modify the early stages of carbon gain and canopy development. Additionally, carbohydrate demand for development of the root system may be expected to increase.

Lowland rice planted in upland fields, on the other hand, has been shown to be capable of higher or comparable aboveground biomass production as compared to flooded systems in years with ample rainfall during the rice growing season (Katsura et al., 2010). Apparently this results due to high levels of N fertilization, which allows high leaf area index (LAI) and

## Chapter 1 - Synopsis

enhanced radiation use (Kato et al., 2006; Okami et al., 2013). Leaves with higher nitrogen content can enhance photosynthesis rate and light use efficiency may be promoted (Niinemets and Tenhunen, 1997). A hyperbolic relationship between leaf nitrogen content and the rate of biomass accumulation, and with light use efficiency have been reported for cereal crops, including paddy rice (Alberto et al., 2009; Campbell et al., 2001b; Sinclair and Horie, 1989). Interestingly, nitrogen uptake in lowland flooded rice differed from the same rice cultivar planted in upland fields (Kato and Katsura, 2014; Katsura et al., 2010), which could potentially lead to a shift in canopy carbon gain capacity and biomass production over the growth season. These comparisons of canopy and ecosystem gas exchange have been conducted with paddy and rainfed rice, but especially focusing on lowland versus upland-adapted cultivars (Alberto et al., 2012, 2011, 2009) and without analyzing the details of canopy physiology. Studies from the temperate monsoon region have rarely been reported.

### *Framework for study 1: Canopy scale CO<sub>2</sub> exchange and productivity of transplanted paddy and direct seeded rainfed rice in South Korea*

The first study included in this thesis compares canopy level gas exchange in paddy and rainfed rice planted in the temperate monsoon region in Gwangju, South Korea. The study provides an orientation for a single genotype with respect to the seasonal course (trend, strength, and frequency of variation) of carbon uptake capacity at important agronomic growth stages, i.e., during active tillering, elongation, panicle heading and grain-filling. Phenological development in rapid growing crops affects dry matter allocation among organs, eventually controlling seasonality of assimilatory capacity (Yoshida, 1981). Focusing on these important phenological stages, a comparison of canopy structure and functional traits between flooded and rainfed rice growing in a tropical region revealed influences due to land use change from flooded to rainfed cultivation conditions (Alberto et al., 2009). The only resource for re-charge of rainfed rice water supply is from precipitation. Persistent occurrence of water loss due to strong evaporative demands on sunny and clear days could trigger soil water content to decline close to the threshold level at which decreases in photosynthesis function occur. However, the past 30 years' records of monthly rainfall in Gwangju conform

## Chapter 1 - Synopsis

to typical characteristics of the East Asian monsoon climate where more than half (up to 70%) of total annual rainfall is distributed in summer season between June and September (<http://climatebase.ru/station/47156/?lang=en>) when growth and development of rainfed rice occurs.

Under global warming scenarios, the precipitation during the East Asian monsoon is expected to intensify and the duration of monsoon season should be extended in the Korean Peninsula (Yun et al., 2008). Changes in precipitation pattern will likely strengthen fluctuations of daily solar radiation, which could further alter the feedback in carbon exchange between rice agriculture systems and the atmosphere. During periods when the soil water store is frequently re-filled by intensive rainfall, short-term soil water depletion may not inhibit canopy carbon fixation in rainfed rice (Alberto et al., 2012, 2009). Under such conditions, relatively high yield production occurs in China, Philippines, and Japan (Nie et al., 2012; Okami et al., 2013). Thus, we initially hypothesize that rainfed rice in South Korea may exhibit comparable carbon gain capacity and biomass production to that observed with paddy rice. In this case, the diurnal course and seasonal development of carbon gain capacity will be primarily influenced by meteorological factors and internal growth mechanisms. Canopy CO<sub>2</sub> gas exchange, canopy leaf area development via destructive harvest method, and aboveground dry matter production and yield were measured in Unkwang rice cultivar grown under both rainfed and conventional paddy production systems to examine the following initial hypotheses:

- 1) Unkwang rice grown under rainfed conditions maintains similar rates of CO<sub>2</sub> uptake and light use efficiency to that observed under a paddy cultivation system, and
- 2) Growth of Unkwang rice under rainfed conditions does not alter C allocation patterns in comparison to the paddy condition. Under such circumstances we anticipate similarities in crop development and yield between rainfed and paddy rice.

## Chapter 1 - Synopsis

### 1.1.4.2. Ecophysiological response and acclimation in rice with differing soil water availability

Although study 1 hypothesizes that the performance of Unkwang rice planted under paddy and rainfed cultivation is essentially the same, since frequent rain occurs during the monsoon in summer, two unpredictable and relatively long periods without precipitation occurred during our field campaign. Due to the overall sampling design, chamber data analyzed in study 1 could not provide much information on canopy gas exchange regulation during these periods. However, parallel ecophysiological studies at leaf level were conducted in which the temporal resolution was adequate to support a more detailed examination of changes in carbon uptake and structuring of the rice plant canopy during periods with dry upper soil layers. This perspective is presented in the second study of the thesis. It provides an important view on adjustments that can occur in carbon and nitrogen allocation as they influence plant canopy function in carbon gain and water use.

The average yield production in rainfed systems in Asian countries has been reported to vary between 2,000 and 2,500 kg ha<sup>-1</sup>, far below the achievable yield potential during “normal precipitation” years (Hijmans and Serraj, 2008). Impacts of soil water shortage on crop production depend largely on the timing, duration and severity of drought. Production losses due to dry periods of milder intensity, although not alarming, can still be substantial. Despite irrigation management to ensure adequate soil water availability, a number of studies report that yield was far below the expected (Bouman et al., 2005; Westcott and Vines, 1986). Dry spells of relatively short duration can cause significant declines in photosynthetic productivity, especially if they occur during the flowering and grain-filling stages (Araus et al., 2008).

Allocation of nitrogen as well as carbon is important as plants adjust to modifications in the soil environment. It is well known that more than half of soluble proteins in leaves are involved in the photosynthetic apparatus, such as in light harvesting complex proteins and electron transport chains in photosystem I and II, and Rubisco and associated enzymes of the dark reaction. Above- and belowground environmental conditions substantially influence

## Chapter 1 - Synopsis

patterns in nitrogen allocation to the components of the photosynthetic apparatus, and regulate acclimation in photosynthetic performance (Niinemets, 2007; Niinemets and Valladares, 2004). Nitrogen use efficiency tightly correlates with photosynthetic productivity (Hirel et al., 2001; Ju et al., 2015; Ladha et al., 1998; Sinclair and Horie, 1989), and is one of important factors influencing plant survival and establishment (Feng, 2008; Niinemets, 2007). Nitrogen supplied in early growth probably stimulates an initial boost in carbon gain which subsequently influences total leaf area throughout the growth season (Sinclair and Horie, 1989), and causally affects seasonal canopy carbon gain capacity (Campbell et al., 2001a; Lindner et al., 2015). Decline of biomass production in rainfed rice has been partially attributed to weak canopy LAI development in the early growth stage (Okami et al., 2013). Additionally, the occurrence of intermittent dry periods inhibit leaf area expansion (Wopereis et al., 1996).

Relatively high transpiration rates at midday in rainfed rice have been reported (Bouman et al., 2005; Tanguilig et al., 1987; Yoshida, 1981). Therefore, limited soil water content periodically occurs in the top soil layer (0–20 cm) with rainfed rice, where soil water evaporates and is used in transpiration. More than half of the total root mass was found in this soil layer for several rice cultivars (Naklang et al., 1996), and under some climate regimes soil drying and stomatal closure during daytime have been reported to constrain photosynthetic activity. Rainfed rice must confront the dilemma of supplying adequate water to the canopy to support photosynthesis, which requires greater investment in roots to access deeper soil layers (Araus et al., 2008; Naklang et al., 1996). Despite the presence of deep roots accessing wet soil layers, decline in photosynthetic carbon gain and stomatal conductance may occur when plant xylem hydraulic conductance decreases to a threshold level (Bouman, 2001; Davatgar et al., 2009; Stiller et al., 2003). In conclusion, the differences in crop yield between paddy and rainfed rice that may occur are due to multiple causes, such as delayed establishment (Rang et al., 2011), reductions in photosynthetic productivity during dry periods, altered carbon allocation among plant organs (Niinemets, 2007), and their interactive influences.

## Chapter 1 - Synopsis

### *Framework for study 2: Differentiation in paddy versus rainfed rice in factors influencing carbon gain, water use and grain yield under monsoon climate in South Korea*

The second study in this thesis is an extension of the previous study (study 1) carried out in order to determine ecophysiological factors regulating seasonal and daily carbon gain and water use in flooded versus rainfed fields. Effects of soil water fluctuations on the instantaneous dynamics of canopy carbon fluxes from sunrise to sunset with high time resolution can not be captured with the canopy chamber methodologies applied in study 1. Intensive measurements of gas exchange at leaf level during important agronomic stages and during periods of soil drying were implemented, parallel with recording of soil water content and microclimate in both paddy and rainfed sites. Leaf water potential, as an index to examine potential drought impacts and recovery of plants after exposure to low soil water content (Jongdee et al., 2002), was determined at pre-dawn and over daily courses. The following hypotheses which are similar to those in study 1 were evaluated:

- 1) Rice crops growing under rainfed versus irrigated conditions in the monsoon climate region of South Korea develop similarly with respect to canopy structure and nitrogen use, as well as carbon gain and water use efficiencies at leaf level.
- 2) For the same genotype, leaf gas exchange regulation is unaffected by a change from paddy to rainfed field cultivation.
- 3) Similar nitrogen use, carbon gain and water use over the growth season under climate conditions in South Korea result because root systems and soil water storage are adequate to allow full daily recovery by rice plants during extended periods without rain.

#### **1.1.4.3. Agronomic and ecological water use efficiency in paddy and rainfed rice**

As an indispensable part of the overall goal set by this thesis, water flux research in study 3 helps to develop a new vision at crop level regarding the balances and trade-offs that occur in water use and carbon gain between paddy and rainfed rice cultivation systems. As has been discussed, not only the yield production per hectare is an important future concern but also



## Chapter 1 - Synopsis

water use efficiency of grain yield is an important question in rainfed rice production. An increasing number of field studies to evaluate agronomic water use (defined as ratio of grain yield to growing season total evapotranspiration,  $\text{yield}/\text{ET}$ ) and ecological water use ( $\text{GPP}$  integrated over some time to  $\text{ET}$  accumulated during the same period,  $\text{GPP}/\text{ET}$ ) have been carried out (Alberto et al., 2009; Bouman et al., 2005; Nishimura et al., 2008; Westcott and Vines, 1986). Seasonal and interannual variations in water use between flooded and rainfed rice systems and internal regulation mechanisms are a critical concern in order to maintain staple food supplies in many countries.

Transforming rice cultivation from the flooded paddy to rainfed model modifies microclimate conditions (Alberto et al., 2009; Stuerz et al., 2014) resulting in higher air temperature and VPD in rainfed fields and a larger proportion of energy partitioned to sensible heat flux (Alberto et al., 2011). These changes affect momentary photosynthetic activity and stomatal conductance as well as the transpiration rate (Alberto et al., 2012; Miyata et al., 2000), and also shift correlations among seasonal energy, carbon and water balances (Alberto et al., 2009; Bouman et al., 2005; Nishimura et al., 2008). Comparisons of agronomic water use efficiency between conventional flooding and water-saving dryland rice systems suggest that WUE of rainfed rice is higher (Alberto et al., 2009; Bouman et al., 2005) but at the expense of compromised yield production (Bouman et al., 2005).

Efforts to improve ecosystem or agronomic water use efficiency attempt to reduce the amount of water lost via evapotranspiration. Evapotranspiration constitutes two processes: 1) productive water lost by canopy transpiration ( $T$ ) which is linked to stomatal conductance and carbon assimilatory rate, and 2) soil evaporation ( $E$ ) as non-productive water lost. The fraction of  $T$  or  $E$  to  $\text{ET}$  changes significantly among species that are growing under comparable ecological conditions (Hu et al., 2009), and fluctuates over the course of the growth season (Allen et al., 1998; Huang et al., 2010; Scott et al., 2006). The relative importance of  $E$  in  $\text{ET}$  should be smaller with a dense canopy, since less radiation energy penetrates to the soil surface. Inversely, intensive  $E$  mainly occurs before canopy closure and

## Chapter 1 - Synopsis

is significantly greater than T (Suyker and Verma, 2008) but also depends on meteorological drivers such as the intensity of solar radiation and air temperature (Alberto et al., 2011). The growing season T/ET in paddy rice varied with difference being 2-fold larger in a report by Zhao (2014) at 0.38 in South Korea and 0.8 from Wei et al. (2015) in Japan (Table 1.2). The rest of literature records listed in table 1.2 fell within the span between Zhao (2014) and Wei et al. (2015). Accordingly, huge fluctuations in growing season E/ET among previous reports are expected. Whereas, growing season T/ET evaluations in rainfed rice without irrigation were non-existent, except one from Hossen et al. (2012) providing a ratio of 0.64. A second study in rainfed rice with flush irrigation via a sprinkler system reported T/ET at 0.56, lower by 12.5% than Hossen et al. (2012). These reports indicate that the amplitude of E and proportionality of E in ET is not only a function of growth stage, but also meteorological factors such as incident solar radiation and precipitation which vary over time and from site to site. We anticipate that soil water availability and canopy structure development in flooded vs. rainfed rice are the main factors influencing changes in E and ET as well as yield/ET and GPP/ET.

**Table 1.2** Partitioning evapotranspiration of rainfed and paddy rice

Authors	Irrigation management	Rice cultivar	Research site	GD (days)	Partitioning method			E/ET	T/ET	ET (mm d <sup>-1</sup> )	LAI <sub>max</sub> (m <sup>2</sup> m <sup>-2</sup> )
					ET	E	T				
Sakuratani and Horie (1985)	Flooded field	lowland rice (Indica)	Japan	130	M-lys	Pan	Pan	0.52	0.48	3.98	4.60
Maruyama and Kuwagata (2010)	Flooded field	lowland rice (Indica)	Japan	130	Two source model			0.57	0.43	3.78	4.60
	Flooded field			100				0.30	0.70	3.33	5.90
Hossen et al. (2012)	Rainfed rice (total rainfall 552.8 mm; no irrigation)	lowland rice (Indica)	Bangladesh	100	EC, empirical equation dependent on LAI			0.36	0.64	2.93	4.60
	Flooded field	lowland rice (Indica)		120				--	--	4.28	
Alberto et al. (2014; 2011)	Rainfed rice (sprinkler irrigation, 654.9 mm + 251.9 mm rainfall = 897.8 mm)		Philippines	120	EC and 56PM			0.44	0.56	3.81	4.65
Zhao (2014)	Flooded field	lowland rice (Japonica)	S. Korea	120	EC and , empirical equation dependent on LAI			0.62	0.38	2.0	5.80
Wei et al. (2015)	Flooded field	lowland rice (Japonica)	Japan	150	$\Delta^{18}\text{O}$			0.20	0.80	--	4.50

Remark: M-lys – micro lysimeter; Pan – Pan evaporation; EC – eddy covariance; 56PM – Penman–Monteith model modified by the FAO of the UN;  $\Delta^{18}\text{O}$  –  $\Delta^{18}\text{O}$  stable isotope partitioning; GD – growth duration

## Chapter 1 - Synopsis

### *Framework for study 3: Flux partitioning reveals trade-off between carbon gain and water use in rainfed and paddy rice*

Growing season total ET in rainfed rice had been shown to be lower than in paddy rice grown at the same research site, due to a decline in daily average ET (Alberto et al., 2014, 2011; Hossen et al., 2012). Lower daily ET in rainfed rice is influenced by the evaporative power of the atmosphere (which is similar to that for paddy rice), by the non-puddle soil environment and potentially by external water inputs. Climate factors, especially precipitation distribution and intensity, which affects soil water content in the top soil layer seems to be an important factor in determining daily ET in rainfed rice. Interestingly, growing season GPP from Table 1.1 in rainfed rice at  $700.4 \pm 180.6 \text{ g C m}^{-2}$  is close to paddy rice  $759.6 \pm 50.8 \text{ g C m}^{-2}$ . Small differences (although with large error bar) found in rainfed rice implies that rainfed rice which has always been viewed as a water saving cultivation method maintains an advantage in water use as compared to paddy rice. Partitioning ET in the two culture methods could aid to reveal seasonal courses of E and T and quantitative contributions to ET. In study 3, periodic measurements of gas flux by classic chamber methods and by applying the Penman-Monteith crop ET model (56PM), and combining this information with field measured basic leaf physiological parameters and remotely sensed NDVI data was conducted in paddy and rainfed rice to examine the following hypotheses:

- 1) Similar carbon gain capacity and yield production between paddy and rainfed rice in the monsoon climate region of South Korea are attainable
- 2) Comparative differences in agronomic/ecosystem water use efficiency between the two culture methods are due to significant alterations in ET processes where non-productive water loss via soil evaporation occurs during early growth season before canopy closure plays a dominant role.

#### **1.1.4.4. Nutritional influences on carbon gain capacity and yield of paddy rice**

Increased fertilizer additions can lead to increased productivity, but there is a threshold above

## Chapter 1 - Synopsis

which nutrients can no longer be used, but rather result in negative environmental effects. In order to gain insight with respect to the fertilization regimes recommended by agencies for rice farmers in South Korea, the detailed response of classical puddle transplanted paddy rice was studied with different fertilizer applications.

Increased fertilizer is expected to result in enhanced plant height, a greater number of tillers per hill at the harvest (Bandaogo et al., 2015; Koyama and Niamsrichand, 1973), earlier development of high leaf area index (Sinclair and Horie, 1989), an increased number of leaves per plant and larger leaf area per leaf mass (Gimenez et al., 1994), and a greater number of spikelets per panicle (Koyama et al., 1972). These traits are best observed when fertilizer was applied after full germination and before most rapid vegetative growth (Fageria and Baligar, 1999; Fujiwara and Ohira, 1951). The responses are independent of the number of split applications (Heenan and Thompson, 1984; Rao et al., 1985; Tao et al., 2015). Plant types that have short, stiff straw and erect leaves respond best (De Datta and Broadbent, 1988; Sheehy and Mitchell, 2013; Wells and Johnston, 1970), especially those genotypes with erect leaves in the upper canopy (Setter et al., 1995). Fertilization that led to accumulation of assimilated products in the culm and leaves, and was accompanied by efficient translocation before heading strongly influenced yield production (Ju et al., 2015; Amano et al., 1993). Early vigor in terms of canopy structure development in the vegetative stage depends on abundant soil available N which enhances photosynthetic capacity, produces more carbohydrate per ground area, and maximizes resource use efficiency.

Pioneering work by Monteith (1972) proposed that CO<sub>2</sub> uptake rate can be briefly expressed as a function of two variables: amount of light intercepted by canopy and light conversion efficiency by which absorbed light is converted into chemical energy (Eq. 1.1).

$$GPP = APAR \times LUE_{abs} \quad (1.1)$$

where, APAR is the amount of solar radiation intercepted and LUE<sub>abs</sub> is the efficiency of conversion.

## Chapter 1 - Synopsis

Previous studies suggested that capacity to assimilate carbon dioxide for a given crop species was almost constant over the course of the growth season (Kiniry et al., 1989). Nevertheless, radiation use efficiency can change with phenology of the crop species (Alberto et al., 2013; Gimenez et al., 1994) with the maximum during vegetative stage and lower values at early and late seasons (Hall et al., 1995).  $LUE_{abs}$  at post-anthesis of spikelets fluctuated in a range from 0.73 to 1.22 g C MJ<sup>-1</sup> and that during elongation growth fell between 1.52 and 2.1 g C MJ<sup>-1</sup> (Campbell et al., 2001b). A similar seasonal tendency was also reported in paddy rice (Inoue et al., 2008).  $LUE_{abs}$  declined as LAI increased, and a significant decline existed after anthesis. RUE of rice (biomass accumulation against APAR, equivalent to  $LUE_{abs}$ ) might change with LAI and stage of development, which relates to canopy leaf physiology (Sinclair and Horie, 1989). Decline in  $LUE_{abs}$  might explain GPP saturation at higher LAI.

Earlier studies assumed that the pattern of light attenuation is exponential and conforms to Beer's law in which the two key independent variables light attenuation efficiency ( $K_L$ ) and LAI play the major roles (Atwell et al., 1999; Kiniry et al., 1989). The purpose of fertilizer applications in rice is to boost the rapid development of the canopy crown in order to realize high light interception, so that relatively high photosynthetic activity can be maintained over the plant life cycle. The most significant effect introduced by fertilization on canopy structure development would thereby be canopy carbon gain capacity related to canopy light interception (Bennett et al., 1993; Gimenez et al., 1994; Okami et al., 2013). Hence, increments in the amount of photosynthetic production with nutrient additions may be ascribed to changes in the capacity for light interception rather than light conversion efficiency. Canopy light interception increases sharply with increases in LAI to about 95% once LAI exceeds roughly 4 m<sup>2</sup> m<sup>-2</sup>, and it approaches an asymptote at higher LAI (Atwell et al., 1999). Such a relationship seems to emphasize the importance of rapid LAI development during the early growth stage.

Potential photosynthesis capacity represented by daily maximum gross primary production ( $GPP_{max}$ ) showed weak correlation with observed maximum LAI, so did the relationship

## Chapter 1 - Synopsis

between maximum daily integrated GPP ( $GPP_{int}$ ) and LAI ( $R^2 = 0.01$ ;  $p > 0.05$ , Table 1.1).  $GPP_{max}$  curvilinearly related to LAI development (Atwell et al., 1999; Yoshida, 1981), saturating when LAI was higher than  $2 \text{ m}^2 \text{ m}^{-2}$  in several upland crops (Lindner et al., 2015). A saturation phenomenon was also found in maize and soybean, although shifted with respect to the value for saturating LAI (Gitelson and Gamon, 2015). Furthermore, meta-analyses in several crops documented that  $LUE_{abs}$  rapidly declines along with leaf nitrogen content (Campbell et al., 2001a; Sinclair and Horie, 1989). A saturation in the GPP–LAI correlation at higher LAI implies that canopy structure development is no longer the primarily limiting factor, since increasing canopy density commonly results in greater canopy light interception. Explanation of chronic saturation in GPP at higher LAI and optimal carbon gain may be better examined in terms of nitrogen resource availability in canopy profiles and leaf area distribution

To complete a dynamic picture of assimilation processes, leaf level studies are, nevertheless, essential (Sinclair and Horie, 1989; Niinemets and Tenhunen, 1997). Leaves are the small and basic units that make up the plant canopy volume and their function may change with development and changing habitat conditions. Photosynthetic activity of individual leaves for a given leaf nitrogen content and growth light regime may be characterized by maximum photosynthetic capacity and  $CO_2$  diffusion conductance from leaf surface to carboxylation site inside the chloroplasts. Changes in leaf nitrogen allocation within leaves which relate to maximum carboxylation rate ( $V_{cmax}$ ) and maximum electron transport rate ( $J_{max}$ ), and improve the  $CO_2$  diffusion conductance may have important implications, i.e. improve plant biomass production (Karaba et al., 2007; Wang et al., 2014), visa versa, may not affect biomass (Tanaka et al., 2013; Dow and Bergmann, 2014), and must be investigated along with canopy structure.

*Framework for study 4: Nutritional and developmental influences on components of rice crop light use efficiency*

In the fourth work of this thesis study, gas exchange and chlorophyll fluorescence

## Chapter 1 - Synopsis

measurements were made on leaves of rice to determine CO<sub>2</sub> uptake, transpiration, and CO<sub>2</sub> diffusion conductance. These measurements were carried out simultaneously with observations of crop development and canopy CO<sub>2</sub> exchange in experimental fields under three nutrient treatment levels. The extent to which increased nutrient supply leads to increases in canopy leaf area, altered nitrogen investments, as well as changes in leaf gas exchange and biomass production is examined. The following hypotheses were addressed:

- 1) Seasonal development of rice is characterized by a LUE optimization-oriented coordination in LAI, canopy N distribution, and leaf conductance limitations on carbon gain.
- 2) Increasing nutrient supply to the rice crop leads to an acceleration in the rate of canopy development (rate of increase in LAI) and overall carbon gain, but not to the basic way in which coordination of the process relevant to LUE occurs.
- 3) Variation in leaf function in rice grown with different nutrient supply and under varying light environments within the crop canopy is largely explained by variations in leaf nitrogen allocation and nitrogen-driven gas exchange.

### 1.2. Materials and methods

#### 1.2.1. Research area and study sites

The research studies were conducted at the agricultural experimental fields of Chonnam National University, Gwangju, South Korea (126°53'E, 35°10'N, altitude 33 m) (Figure 1.3). East Asian monsoon climate is prevailing in S. Korea, with an annual mean temperature of 13.8°C and an annual mean precipitation of between 1391 and 1520 mm/yr (1981–2010). More than half of precipitation events are distributed between June and October during which time rice plants complete their life cycle. Soil in the agricultural field is a gray lowland Fluvisol, with ratio of sand, silt and loam of 40: 37: 23, and total organic carbon of 12.3 g kg<sup>-1</sup>, total nitrogen of 1.0 g kg<sup>-1</sup>, available P (P<sub>2</sub>O<sub>5</sub>) of 13.1 g kg<sup>-1</sup>, soil pH in H<sub>2</sub>O of 5.5 (RDA, 2008) and an approximate bulk density of the top soil layer (0-12 cm) of 0.8 g cm<sup>-3</sup>. A new early maturity cultivar Unkwang (*Oryza sativa* L. cv. Unkwang) developed from the cross Sobibyeo and Cheolweon 54 (Kim et al., 2006) was selected as research material for

## Chapter 1 - Synopsis

our study. Seeds were sown in a nursery on April 22, 2013 (110 DOY) and seedlings of 10 cm height were transplanted into a pre-flooded field using an automatic rice planting machine on May 20, 2013 (140 DOY) with a row–line spacing of 12 × 30 cm. On average, 5 seedlings were planted in each hill. Three nitrogen application rates in paddy rice were adopted: 0 kg N ha<sup>-1</sup> (no supplemental fertilization as a control referred to as low; plot size ~511 m<sup>2</sup>), 115 kg N ha<sup>-1</sup> (the agricultural agency recommended amount, referred to as normal, plot size ~1387 m<sup>2</sup>) and 180 kg N ha<sup>-1</sup> (referred to as high, plot size ~511 m<sup>2</sup>) (Figure 1.3). Addition ratio of phosphate and that of potassium fertilizer were calculated based on mass ratio of N–P–K of 11:5:6. 80% of N fertilizer was applied two days before planting (May 18, 138 DOY), and the rest at the tillering stage 19 days after transplanting (157 DOY). Seeds of same rice variant were directly sown into the soil on April 22 (112 DOY) in a rainfed field spatially close to the paddy field (Figure 1.3), applying fertilizer at the same level of 115 kg N ha<sup>-1</sup> at two times: 80% of total N before seeding and the rest on 160 DOY. P fertilizer was applied as a 100% basal dosage. K fertilizer was applied as 65% basal dosage and 35% during tillering. During growth no artificial water supply was provided in the rainfed field. Paddy rice field was always flooded over whole growing season except water drainage for several days during the flowering stage. Soil was kept wet during the drainage period. All field managements reflected the practice of the farmers in the region.



## Chapter 1 - Synopsis

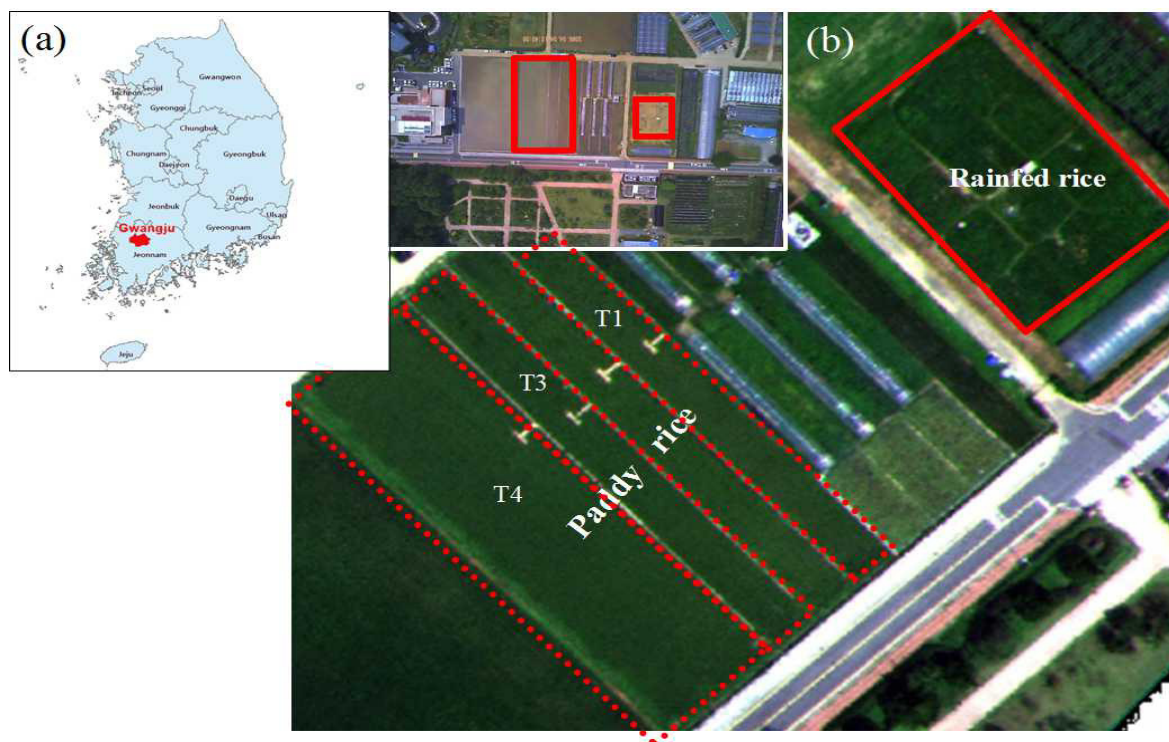


**Figure 1.3** Vertical overview study of location with indication of rice cropping area and nutrient treatment plots for paddy rice system: T1\_0 kg N ha<sup>-1</sup> named as low group, T3\_180 kg N ha<sup>-1</sup> as high group, T4\_115 kg N ha<sup>-1</sup> as normal group.

### 1.2.2. Analyses of canopy scale CO<sub>2</sub> gas exchange and productivity in paddy and rainfed rice

Meteorological factors such as solar radiation, air temperature, relative humidity, precipitation, and wind speed were continuously measured with 2 m high automatic weather stations installed at the margin of the rainfed field. Evaporation is expected to be higher in paddy rice due to the abundant evaporative source from the standing water layer as compared to non-puddled soil in the rainfed field, where more radiation energy is required for latent heat flux in evapotranspiration (Alberto et al., 2011; Stuerz et al., 2014) and air temperature in the canopy may be higher. Microclimate is tightly related to observed gas exchange which was measured with portable chambers (see below). Hence, discontinuous records of air temperature ( $T_{\text{air}}$ ) at 20 cm height inside and outside the chamber and soil temperature ( $T_{\text{soil}}$ ) at 10 cm depth within soil frames were recorded during CO<sub>2</sub> gas exchange measurements. Volumetric soil water content (SWC, m<sup>3</sup> m<sup>-3</sup>) at 10 cm depth in the paddy field and at 10 and 30 cm depth in the rainfed field were measured at several locations close to the collars

## Chapter 1 - Synopsis

installed for canopy gas exchange measurement using EC-5 (Decagon, WA, USA) soil moisture sensors. The sensors were installed during the initial growth stage and kept in the field throughout the season.

To acquire seasonal and diurnal courses of canopy CO<sub>2</sub> exchange rate in flooded and rainfed rice, chamber measurements were conducted periodically. In each nutrient treatment block of paddy rice, four white frames with sealing collar (L 38 × W 38 cm) were inserted in soil down to 10 cm depth in the middle part of each field several days after seedling transplanting. Edge effects were minimized as much as possible. Three of four frames were established with three hills of plants growing inside, and the fourth frame was without plants. A custom-built set of transparent chamber and one opaque chamber (L 39.5 × W 39.5 × H 50.5 cm) with flexible extensions to adjust chamber height to match height of the growing rice canopy during late season were placed on the white frames and tightened to avoid leakage with elastic shock cords (Figure 1.4). Air inside the chamber was mixed with three fans which provide wind speed of 1.5 m s<sup>-1</sup>. Thirty seconds after setting the chamber on the frame, the air outlet at the top side of the chamber was closed. CO<sub>2</sub> concentration change in the chamber was recorded every 15 seconds with a portable, battery operated infrared analyzer. Incident photosynthetically active radiation (PAR) at the top of the canopy was quantified with a light sensor (LI-190A, LI-COR, Nebraska USA). The difference between inside and outside air temperature was controlled within 1°C by dry ice packs mounted at the back of chamber, in order to avoid rapid increase in air temperature inside chamber especially during hot summer. More detailed information about chamber specification and pragmatic operation is described in Lindner et al. (2015) and Li et al. (2008). Net ecosystem exchange rate (NEE), ecosystem respiration rate (R<sub>eco</sub>), and soil respiration rate (R<sub>soil</sub>) were evaluated in 1) transparent chambers with plants, 2) dark chambers with plants and 3) dark chambers without plants, respectively, from sunrise to sunset. Intensive measurements were done at least every 2 weeks before harvest. Repeated measurements in rainfed rice were conducted on the days of year close to measuring dates in paddy rice. Chamber measurement campaigns in paddy (normal group\_115 kg N ha<sup>-1</sup>) and rainfed rice were carried out on 158, 166, 182, 197, 218,

## Chapter 1 - Synopsis

and 240 DOY and 157, 166, 181, 199, 221, and 239 DOY, respectively. Gross primary production (GPP) was calculated as:  $GPP = -NEE + R_{eco}$ .  $R_{eco}$  is the sum of plant respiration ( $R_{plant}$ ) and soil respiration, and plant net primary production (NPP) is denoted as net carbon gain per ground meter over given time after subtracting carbon loss by plant respiration from GPP during the same time period (Campbell et al., 2001a). Therefore, NPP could be expressed as:  $NPP = -NEE + R_{soil}$ .

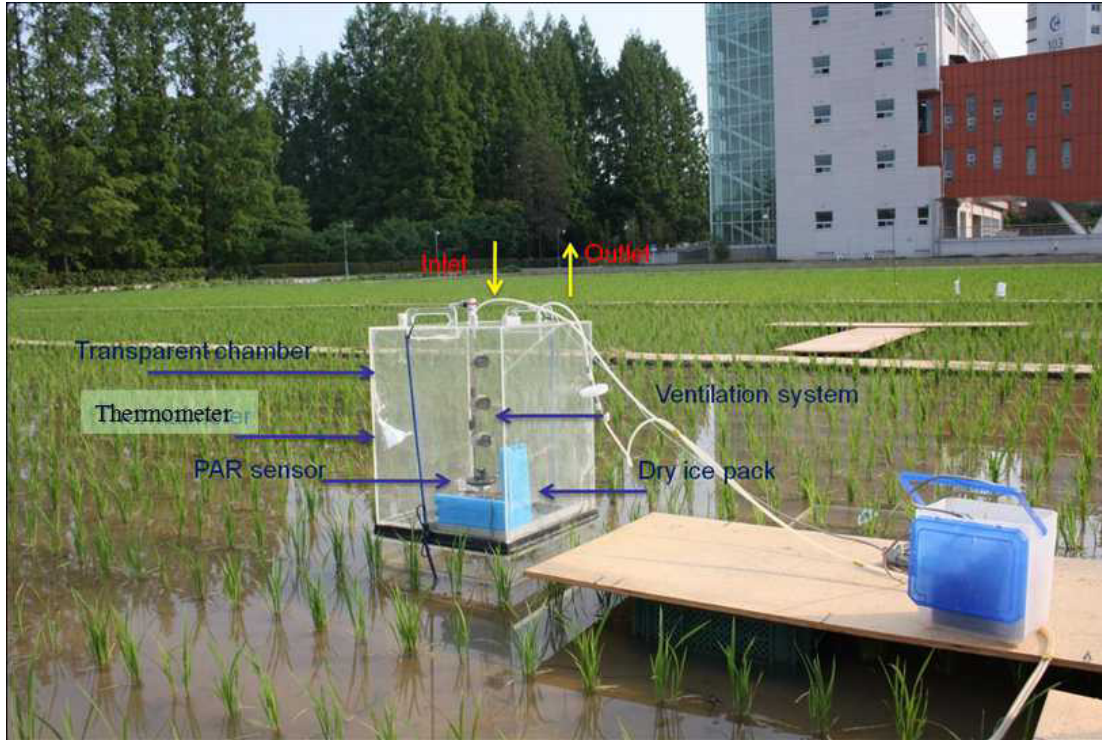


**Figure 1.4** Schematic configuration of transparent chamber established in flooded rice field

Linking measured meteorological factors and canopy carbon fluxes in a quantitative manner to extract ecophysiological parameters provides a pragmatic means for comparing carbon uptake capacity over the growth season and between flooded and rainfed rice. Rectangular hyperbolic light response curves were defined on each measurement day and for each frame that empirically depict responsive characteristics of ecosystem GPP or NEE or NPP to incident PAR dependent on two key parameters, i.e., the slope of the linear phase of the light curve ( $\alpha$ , also denoted as instantaneous light use efficiency,  $LUE_{ins}$ ) and the saturation value at infinitely high PAR ( $\beta$ ) (Li et al., 2008; Owen et al., 2007). Since the rectangular hyperbola may saturate very slowly in terms of light, we used the value calculated from

## Chapter 1 - Synopsis

$\alpha\beta \cdot \text{PAR} / (\alpha \cdot \text{PAR} + \beta)$  for high natural light intensity levels ( $\text{PAR} = 1500 \mu\text{mol m}^{-2} \text{s}^{-1}$ ) as indicative of the saturation value (Lindner et al., 2015). This value approximates the potential maximum GPP ( $\text{GPP}_{\text{max}}$ ) and can be thought of as the average maximum canopy uptake capacity during each observation period (noted here as  $(\beta + \gamma)_{1500}$ ). The parameters  $(\beta + \gamma)_{1500}$  (e.g. GPP at  $\text{PAR} = 1500 \mu\text{mol m}^{-2} \text{s}^{-1}$ ) and  $\gamma$  (residual respiration at zero PAR) were estimated for each day using NEE data from the four measurement plots per day (extended interpretation seen in study 1). Similar to definition of  $\text{GPP}_{\text{max}}$ , daily maximum NPP ( $\text{NPP}_{\text{max}}$ ) was generated from the average NPP values in the saturation portion of light response curves.

After conducting gas exchange measurements, sample leaves were cut and collected to estimate leaf blade area, dry mass and nitrogen content. To determine LAI, the green biomass overlying a half square meter of ground surface close to the chamber plots was harvested. Grain yield in the paddy and rainfed fields were measured in four sampling plots ( $0.5 \times 0.5 \text{ m}$ ) close to the chamber measurement plots at the end of the season (253 DOY), and yield components were evaluated based on recommendations from Yoshida et al. (1971). The seasonal development of LAI was additionally observed with a plant canopy analyzer.

### 1.2.3. Analyses of factors influencing carbon gain, water use and yield in paddy and rainfed rice

To gain insight with respect to ecophysiological adjustments that influence daily productivity during short-term non-rainfall periods, intensive measurements of diurnal courses of leaf assimilate rate (A), stomatal conductance and transpiration rate (E) were carried out in paddy and rainfed rice using a portable gas-exchange system (GFS-3000 and PAM Fluorometer 3050-F, Heinz Walz GmbH, Effeltrich, Germany) throughout the growth season (same procedures as described in section 1.2.5 below for comparisons with different fertilizer treatments). Measurements of leaf water potential ( $\psi_l$ ) were simultaneously conducted with a pressure chamber. Water flow from the soil matrix to leaves where water loss occurs via stomata is affected by the dynamic balance between water supply capacity and atmospheric demand (Davatgar et al., 2009; Wopereis et al., 1996). To evaluate changes in water flow

## Chapter 1 - Synopsis

along this pathway, soil water content was converted to soil matric potential ( $\psi_s$ ) using soil water retention curves from Van Genuchten (1980) and optimal estimation with Hydrus 1D model (Schaap et al., 1998) applying site-specific soil physical properties (ratio of sand, silt and loamy 40: 37: 23, approximation of soil density  $0.8 \text{ g cm}^{-3}$ ). The steady-state flow from soil matrix around the roots to the aboveground plant parts was described with Darcy's law (Franks, 2004; Otieno et al., 2012). As a result, the leaf-area-specific hydraulic conductance ( $k$ ,  $\text{mmol m}^{-2} \text{ s}^{-1} \text{ MPa}^{-1}$ ) was estimated. Effects of hydraulic conductance on variations in stomatal conductance occurring under saturating light environment were evaluated.

### 1.2.4. Analyses of agronomic and ecological water use in paddy and rainfed rice

Canopy  $\text{CO}_2$  and especially  $\text{H}_2\text{O}$  fluxes from rainfed rice fields were measured with a custom built open chamber constructed according to Pape et al. (2009) and successfully tested by Dubbert et al. (2013). Water vapor fluxes were measured by a cavity ring-down spectrometer and  $\text{CO}_2$  fluxes were measured by a portable infra-red gas analyzer. Both carbon and water fluxes were calculated as differential  $\text{CO}_2$  or  $\text{H}_2\text{O}$  concentration between the air samples taken from the chamber inlet and outlet. Air inlet to the chamber was stabilized by a buffer bottle (200 liter). Outlet air from the chamber was pumped to the analyzers via tubes heated to  $38^\circ\text{C}$  to avoid condensation.

An unmanned aerial vehicle (UAV) equipped with miniature multiple camera array (Mini MCA) with 6 bands spanning the visible and infrared regime (450, 550, 650, 800, 830, and 880 nm) and with a ground resolution of 10 cm at 300 m height was flown at noon of 172, 192, 206, 220 and 233 DOY. Three types of calibration panels (black, white and gray) were set up next to the paddy field for radiometric calibration of the MCA images. Concurrent measurements of canopy reflectance by a cropscan radiometer (MSR5, Cropscan Inc., MN, USA) horizontally positioned at 2 m above plant canopy were used to calibrate and evaluate the reflectance data obtained by the UAV system. Remote sensing images were analyzed by ENVI software (Exelis Visual Information Solutions, Inc., USA). Three sampling points for each treatment plot of both rainfed and paddy rice were used to calculate normalized

## Chapter 1 - Synopsis

difference vegetation index (NDVI). The GRAMI crop growth model (for details see Ko et al., 2006; Maas, 1993a; Maas, 1993b) that simulates daily crop growth based on growing degree-days, light use efficiency, daily carbohydrate production by crop canopy, conversion from carbohydrate to leaf development and the relationship between LAI and NDVI was calibrated via measured LAI (LAI 2000, LiCor, Lincoln, Nebraska) and measured NDVI from the crop scan instrument to generate daily LAI and NDVI values.

For daily crop ET modeling, daily reference crop evapotranspiration ( $ET_o$ ) was calculated based on the FAO 56 dual crop coefficient model which is a modified version of the Penman Monteith (1965) ET model (Allen et al., 1998), and daily transpiration coefficients ( $K_{cb}$ ) and daily evaporation coefficients ( $K_e$ ) were determined to produce daily ET:  $ET = (K_{cb} + K_e) * ET_o$ .  $ET_o$  is the reference crop evapotranspiration without a soil water deficit, which is computed from weather data and consideration of rice crop characteristics.  $K_{cb}$  is derived from the correlation between LAI and NDVI.  $K_e$  is maximal when the topsoil is wet or flooded and  $K_e$  tends to zero when the topsoil is dry, depending on the soil evaporation reduction coefficient ( $K_r$ ) and upper limit of evaporation and transpiration from the cropped surface (expanded explanation in Chapter 4). Estimation of GPP follows Eq. 1.1, with estimated APAR derived from daily NDVI.

### 1.2.5. Analyses of nutritional influence on components of carbon gain capacity

For assessment of nutritional influences on plant growth, biomass productivity and carbon gain capacity in paddy rice, measurements of canopy structure, light and nitrogen distribution, leaf physiology in canopy profiles and GPP were carried out at the low, normal and high nutrient groups. Diurnal courses of plant canopy gas exchange were measured on DOY 157, 167, 174, 200, 219. On each measuring day, chamber measurements rotated from one plot to the next until completion of one cycle in one group, and then was moved to the next nutrient group. Diurnal gas exchange and chlorophyll fluorescence measurements in the sunlit (uppermost), second, third and fourth mature leaves of the high fertilization group were conducted using a portable gas-exchange and chlorophyll fluorescence system (GFS-3000

## Chapter 1 - Synopsis

and PAM Fluorometer 3050–F, Heinz Walz GmbH, Effeltrich, Germany) on 57 (DOY 197) and 73 DAT (DOY 213) set to track ambient environmental conditions external to the leaf cuvette. The diurnal course of leaf gas exchange in the uppermost leaves was periodically measured in the low, normal and high fertilization groups.

Photosynthetic determinants  $V_{\text{cmax},30}$  and  $J_{\text{max},30}$  were derived from the linear phase and saturation phase of assimilation vs.  $\text{CO}_2$  response curve measured at leaf temperature  $30^\circ\text{C}$ , based on methods referred by Sharkey et al. (2007).  $\text{CO}_2$  curves were commenced according to the sequence of  $\text{CO}_2$  concentration 1500, 900, 600, 400, 200, 100 to  $50 \mu\text{mol mol}^{-1}$  after leaves had acclimated to the cuvette microenvironment ( $\text{CO}_2$  concentration of  $400 \mu\text{mol mol}^{-1}$  and saturating PAR of  $1500 \mu\text{mol m}^{-2} \text{s}^{-1}$ ). Relative humidity (rh) was controlled to ca. 60% and light intensity at  $1500 \mu\text{mol m}^{-2} \text{s}^{-1}$ . Assimilation rate, stomatal conductance and fluorescence signals were recorded after new steady-state readings were obtained. At least three replicated measurements of  $\text{CO}_2$  curve were conducted at tillering and grain-filling stage at the low and normal nutrient groups. The variable  $J_p$  method of Harley et al. (1992) for estimating mesophyll conductance was applied to data on the ETR-limited portions of  $\text{CO}_2$  response curves. Using values of  $V_{\text{cmax}}$  and  $J_{\text{max}}$  determined from  $\text{CO}_2$  response measurements, rates of net assimilation were predicted assuming different values of chloroplastic  $\text{CO}_2$  concentration ( $C_c$ ), the  $\text{CO}_2$  partial pressure at the site of fixation, which is jointly determined by fixation rate, stomatal and mesophyll conductances. The limitations on photosynthetic capacity resulting from finite stomatal and mesophyll conductance were evaluated by comparing measured  $A_{400}$  at  $C_a = 400$  with rates predicted assuming infinite stomatal and/or mesophyll conductance by method from Harley et al. (1986).

On 26, 33, 54, 72 and 86 DAT (corresponding to DOY 166, 173, 194, 212 and 226), three planted hills consisting of fifteen plants (five seedlings comprising one planted bundle) from each treatment were harvested, and total leaf area of each was determined with an LI-3100 leaf area meter. On 54 and 72 DAT the standing canopy in each fertilization treatment was stratified into vertical layers, each layer 15 cm in thickness. Leaf and stem area and biomass

## **Chapter 1 - Synopsis**

in each stratified layer were measured. On 43 DAT (DOY 183), three typical hills from each treatment were randomly selected to record individual leaf laminar area. Grain yield determinations were obtained at four sampling plots (0.5 × 0.5 m) at the end of the growing season at 113 DAT (DOY 253), and were weighed after air-drying.

Vertical profiles of incident light were determined either the day before or on the day of plant sampling (54 and 72 DAT) with light data loggers (HOBO, Onset Computer Corporation, Bourne, MA) mounted on thin rods with vertical spacing of 15 cm from base 0 cm to top of the canopy, and where multiple rods were placed along a transect diagonal to the planted rows. Data was logged every 15 min on two consecutive days when the measurements of stratified leaf area were made for nutrient groups. The HOBO logger light values were periodically compared to PAR measured with a LI-COR quantum sensor to develop a calibration curve and to estimate the PAR profiles. PAR was assumed to be attenuated through the canopy according to the Lambert-Beer law. Leaf nitrogen distribution in profiles was computed in similar way to that of light attenuation.

### **1.3. Results and discussion**

#### **1.3.1. Analyses of canopy scale CO<sub>2</sub> gas exchange and productivity in paddy and rainfed rice**

Study 1 canopy scale CO<sub>2</sub> gas exchange and productivity in paddy and rainfed rice yielded the following results. The seasonality in meteorological factors affecting paddy and rainfed rice was identical but difference in terms of air temperature and relative humidity (rh) microclimate during fair weather days between the two cultures were quite large. The magnitude of daily integrated solar radiation was not uniform over the growing season. It fluctuated largely depending on temporal pattern, and on distribution and timing of precipitation, with the maximum observed before commencement of the growth season and in July. Consecutive cloudless days in August when both paddy and rainfed rice started grain-filling had high incoming PAR, along with leaf temperature of rainfed rice up to 38°C, significantly higher than observed maximum level in paddy rice (36°C). During this period rh



## Chapter 1 - Synopsis

in paddy rice was 78%, significantly higher than 53% of rainfed rice. In general, high rh in flooded fields on days with high solar radiation was evident; as a result, mean daily VPD was significantly lower in paddy than rainfed rice. Warm microclimate in the canopy in rainfed rice without standing water layer resulted in a high Bowen ratio (see also Alberto et al., 2011) where more solar energy was partitioned to sensible heat flux and less for latent heat fluxes which appears to result in lower evapotranspiration rate (see discussion in part 1.3.3 of this section).

Daily integrated GPP ( $GPP_{int}$ ) increased during the growing period, achieving its maximum rates of  $11.1 \text{ g C m}^{-2} \text{ d}^{-1}$  in paddy rice and  $14.3 \text{ g C m}^{-2} \text{ d}^{-1}$  in rainfed rice based on chamber measurements, and coinciding with maximum leaf area index occurring in July and August. On clear and sunny days, the maximum NEE were registered between 10h-14h when PAR and temperature attained peak levels.  $R_{eco}$ , however, remained relatively constant during the day. Maximum daily integrated NPP ( $NPP_{int}$ ) were  $8.2$  and  $10.3 \text{ g C m}^{-2} \text{ d}^{-1}$  in paddy and rainfed rice, respectively. Although rainfed rice had significantly higher carbon gain capacity ( $GPP_{int}$ ) as compared to paddy rice, enhanced carbon loss due to plant respiration partially counteract ongoing benefits from greater carbon fixation for rainfed plants. In line with results previously reported in rice (Lindner et al., 2015; Zhao et al. 2011), more than 80% of daily fluctuations in GPP were explained by PAR. Estimated maximum GPP at saturating PAR were  $25.3$  and  $27.4 \text{ } \mu\text{mol m}^{-2} \text{ s}^{-1}$  in paddy and rainfed rice, while the respective maximum quantum yields were  $0.047$  and  $0.098 \text{ } \mu\text{mol m}^{-2} \text{ s}^{-1}$ . A close correlation between quantum yield and canopy nitrogen content was found. Higher quantum yield in rainfed rice was attributed to higher canopy leaf nitrogen content. Peak biomass in paddy field appeared in July, while it occurred one month later in rainfed rice.

Improved carbon gain capacity and light use efficiency occurring at peak season in rainfed rice and compatible biomass production between the two cropping cultures support the hypothesis that with abundant soil moisture supply, Unkang rice grown in a rainfed system maintains similar rates of  $\text{CO}_2$  uptake in the monsoon climate region of S. Korea. Higher

## Chapter 1 - Synopsis

rates of nitrogen accumulation in canopies during the reproductive stage help rainfed rice to improve light use efficiency and photosynthetic productivity. Lowland rice seeded in upland fields could be a promising alternative for the monsoon climate region having frequent summer rainfall to achieve relatively high photosynthetic production with water input only from precipitation. Rainfed rice recorded a relatively low grain yield, although the difference was not statistically significant with our sampling. One of underlining factors that leads to decline in grain yield is the carbon allocation pattern among plant organs (Yoshida, 1981). Other reasons such as yield components and short-term soil water depletion to some extent further constrain yield production (discussed below).

### **1.3.2. Analyses of factors influencing carbon gain, water use and yield in paddy and rainfed rice**

Analyses of factors influencing carbon gain, water use and yield in paddy and rainfed rice yielded the following results. Seasonality of carbon gain in rice canopies depends on canopy structure development and daily solar radiation as was documented when soil water limitation was not extreme (study 1). During the growing season in Gwangju, the observed monthly rainfall distribution in 2013 corresponded favorably to typical East Asia monsoon climate and was consistent with the past 30-year record. August 2013 had clearly higher precipitation of 312 mm as compared to the historical average of 276 mm, while the number of days with rainfall more than 0.1 mm in this month was only 6 days which only account for half of the past record that averaged 13.9 days. Temporal distribution of precipitation was not identical and two prolonged non-rainfall periods occurred with soil water decreasing to low values, especially in the 0-10 cm top soil layer. Impacts of soil water depletion on canopy structure and function in rainfed rice which were not covered by study 1 were further explored in this study.

SWC at 10 cm depth was more sensitive to temporal changes of precipitation as compared to 30 cm depth soil layer, declining to  $0.26 \text{ m}^3 \text{ m}^{-3}$  from 197 to 203 DOY (elongation stage) and again between 218 and 234 DOY (grain-filling stage). During the two periods, soil water

## Chapter 1 - Synopsis

depletion caused a decline of leaf water potential at noon ( $\psi_1$ ) to -2.0 MPa. Constraints on leaf and canopy gas exchange as well as modifications of leaf morphology during the two dry periods were substantial, but reversible without permanent drought injury, since predawn  $\psi_1$  remained close to zero together with visible appearance of guttation at leaf margins in the early morning.

Canopy net carbon gain (NPP) was vulnerable to decreases in SWC, exhibiting a short-term very large depression from an initial 7.02 (199 DOY) to 3.2 g C m<sup>-2</sup> d<sup>-1</sup> (202 DOY). Decline of canopy photosynthesis during the dry period was primarily caused by the vulnerable response of leaf morphology and physiology during the non-rainfall period, because leaf nitrogen and canopy nitrogen content did not change between the end of elongation and the beginning of grain-filling stages. Stomatal limitation of carbon gain was approximately 55% over most of the daytime, and was most severe at midday when PAR was saturating. Much stronger limitation due to stomatal closure existed in the rainfed plot during the dry period as compared to paddy rice and in the rainfed plot after rainfall. Lowering leaf water potential led to a dramatic decline of effective leaf area for photosynthesis by as much as 60% due to leaf rolling.

Under conditions of limiting soil water availability and high VPD during clear and sunny days, high evaporation demand in the atmosphere accelerated water loss. Avoidance of catastrophic damage by drought which threaten plant survival and continued growth could be achieved by internal functional regulation. Xylem hydraulic conductance ( $k$ ) has been considered as the main concern in plant growth regulation in response to environmental changes, especially in the case of water stress (Hacke, 2014; Stiller et al., 2003). A hyperbolic correlation was found between  $k$  and stomatal conductance, as well as  $k$  and assimilation rate, with both  $A$  and  $g_{sc}$  gradually saturating at high  $k$  and rapidly declining when  $k$  decreased below ca. 4.5 and 3.5 mmol m<sup>-2</sup> s<sup>-1</sup> MPa<sup>-1</sup> for stomatal conductance and assimilation rate, respectively, which is in line with previously reports for wetland grasses (Otieno et al., 2012) and rainfed rice (Stiller et al., 2003). A higher threshold value in the correlation between  $k$

## Chapter 1 - Synopsis

and stomatal conductance indicated that stomatal conductance was more sensitive to fluctuation of  $k$ . Insight with respect to the causal correlation between  $k$  and  $\psi_s$  could underpin understanding in soil-plant system associated with water transport and, thereafter, photosynthetic sensitivity under drought. The threshold for the correlation between  $k$  and  $\psi_s$  was  $-0.075$  MPa, conforming to  $k$  of  $5 \text{ mmol m}^{-2} \text{ s}^{-1} \text{ MPa}^{-1}$  at which value the rapid decline in stomatal conductance commenced. Our report of this threshold was in a range previously reported by Wopereis et al. (1996) and close to the threshold of the transpiration- $\psi_s$  correlation ( $-0.074$  MPa) in rainfed Japonica rice (Davatgar et al., 2009) and in upland Indica rice in the Philippines (Alberto et al., 2011). Intrinsic water use efficiency ( $\text{WUE}_i$ , assimilation rate to stomatal conductance) was constant in both cultures, irrespective of growth stages, but curvilinearly increased when  $k$  decreased to less than  $5 \text{ mmol m}^{-2} \text{ s}^{-1} \text{ MPa}^{-1}$ . This means that higher  $\text{WUE}$  of rice plants during soil water depletion occurred due to stomatal closure and response to plant hydraulic conductance, but at the expense of losses in carbon gain.

As yield production is the direct result of canopy photosynthesis, the decline in grain yield in rainfed rice appeared to be in part due to the response to drought events via large decreases in photosynthetic activity. The overall impact of drought depends on timing, extent and duration (Araus et al., 2008). For example, drought events occurring at an early growth stage stimulate leaf senescence and inhibit leaf expansion to a large extent, leading to smaller canopy size and lower photosynthetic productivity. When plants at flowering and at the beginning of the grain-filling stage encounter water stress, panicle development is inhibited, leading to kernel abortion and lower spikelet fertility. Yield component analyses indicated that spikelet sterility in rainfed rice in this study was significantly higher than paddy rice, which contributed to a 10% of decline in grain yield in rainfed rice.

Based on the observations in study 1 and 2, we conclude that Unkwang lowland rice planted in upland fields in monsoon climatic regions could produce compatible carbon gain capacity, leaf canopy size and biomass accumulation as compared to flooded paddy rice, which

## Chapter 1 - Synopsis

favorably supports the first hypothesis indicated in study 2. However, rainfed rice showed high respiratory carbon losses, which reduces the facilitation effects of high GPP. Photosynthetic nitrogen use efficiency at leaf and canopy levels was lower in rainfed rice than paddy rice and is attributable to increasing nitrogen investment in non-photosynthetic components within leaves. Significantly higher rates of nitrogen accumulation during the reproductive stage enhanced leaf and canopy carbon gain capacity of rainfed rice. Hence, the hypothesis 2 must be revised in the sense that leaf and canopy gas exchange regulation are altered by a change from paddy to rainfed field cultivation. Hypothesis 3 was not supported, because intermittent occurrence of prolonged non-rainfall periods strongly decreased photosynthetic productivity in rainfed rice, which results partially due to losses in plant hydraulic conductance.

### 1.3.3. Analyses of agronomic and ecological water use in paddy and rainfed rice

Analyses of agronomic and ecological water use in the paddy and rainfed rice systems yielded the following results. Rainfed and paddy rice systems exhibited similarity in terms of seasonal trends in overall water fluxes from the ecosystems, whereas, significant differences were found in the components of evapotranspiration (ET) which were related to the separate field water management practices. Evaporative water lost (E) was dominant in the early vegetative stage in both rice cultures. Transpiration (T) became dominant at the end of the active tillering stage when the canopy rapidly closed. Growing season total ET in paddy rice was 42.2% higher than that in the rainfed plot. E of paddy plots was significantly higher than in rainfed rice, especially at the vegetative stage when rice canopy coverage was low ( $LAI < 2 \text{ m}^2 \text{ m}^{-2}$ , 180 DOY) with substantial presence of bare soil surface area. Total ET during that period in paddy rice was ca. 93 mm, significantly higher than the estimated 40 mm in rainfed plots. Increase in ET by ca. 53 mm during the vegetative stage accounted for 55% of the difference in growing season total ET between the two cultures. T/ET of paddy rice steadily increased with increasing canopy density (LAI), while T/ET in rainfed rice fluctuated greatly in dependence on soil water content, since soil evaporation was determined by soil water content. The major contribution to total ET in rainfed rice was transpiration and a greater

## Chapter 1 - Synopsis

ratio of  $T/ET = 0.65$  was exhibited as compared to that of paddy rice at 0.42.

Growing season total gross production ( $GPP_{total}$ ) between paddy and rainfed rice were not significantly different. However, rainfed rice had significantly higher ecosystem respiration ( $R_{eco}$ ), hence net ecosystem exchange (NEE) was lower in rainfed rice. Growing season total respiratory carbon losses account for 48.7% of net carbon uptake in rainfed rice while respiratory carbon loss in paddy rice was only 33.8% of net fluxes. However, it is possible that some additional  $CO_2$  generated from root and soil respiration was loss in standing water of the paddy and could not be recorded by chamber gas analysis. Gas diffusion rate in the water column as compared to dry soil is 100 times lower, resulting in reduced gas exchange between root tissues and the atmosphere (Armstrong and Drew, 2002; Miyata et al., 2000).

Rainfed rice had higher agronomic water use ( $Yield/ET$ ) and ecosystem water use ( $GPP/ET$ ) relative to paddy rice, which conforms to previous studies (Adekoya et al., 2014; Alberto et al., 2009), but with a 10% reduction in grain yield. Surprisingly, comparison of  $Yield/T$  and  $GPP/T$  between the two rice systems provided a similar value without significant differences. These results reveal that large evaporation water loss in the paddy rice was the main reason leading to lower agronomic and ecosystem water use, rather than plant transpiration or grain yield. Net ecosystem exchange is directly indicative of ecosystem carbon balance between gross primary production and respiratory carbon consumption. When considering net ecosystem water use ( $NEE/ET$ ), paddy and rainfed rice had comparable  $NEE/ET$ , which highlights the important role of ecosystem respiration in determining the true efficiency of ecosystem water use.

The results indicate that agronomic water use and ecosystem water use in the rainfed rice system were improved primarily due to less water loss from soil evaporation rather than from extremely large differences in grain yield and ecosystem carbon gain capacity, which agrees with the proposed hypotheses. In certain situations, the observed reductions in grain yield may be acceptable and preferable to greater use of water. Greater ecosystem respiration in

## Chapter 1 - Synopsis

rainfed versus paddy rice emphasizes that ecosystem water use should not only be viewed in terms of the ratio of GPP to ET, and that the ecosystem internal regulation mechanisms for carbon and water fluxes should be also considered in calculation of  $WUE_{eco}$ . Increased water use efficiency in the rainfed system was accompanied by greater respiratory carbon loss (see also study 2 in chapter 3), which may eliminate the positive benefits of high carbon gain capacity (GPP), especially at other geographic sites when the climate becomes drier and water limitations increase. Viewed from a different perspective, sustainable high photosynthetic productivity and carbon sequestration in rainfed rice systems in fact require a means for mitigating this high proportion of fixed carbon lost to the atmosphere. One way is to flood the field as our results have documented, but this is accomplished only at the cost of increased evaporation of water.

### 1.3.4. Analyses of nutritional influence in components of carbon gain capacity in paddy rice

Analyses of the nutritional influence on components of carbon gain capacity in paddy rice yielded the following results. Aboveground biomass production in the normal and high fertilization groups was promoted significantly after the end of the active tillering stage at approximately 30 DAT, and achieved a peak level of ca.  $1.0 \text{ kg m}^{-2} \text{ s}^{-1}$ , greater by 60% in comparison with the unfertilized plot. Similar to biomass production, nitrogen addition plots had higher grain yield by ca. 62%. No significant difference was found with respect to yield production between normal ( $115 \text{ kg N ha}^{-1}$ ) and high ( $180 \text{ kg N ha}^{-1}$ ) nutrient treatments. The higher level of nitrogen application which exceeds the recommended rate of local agricultural agencies, could not further improve grain yield production (see also Dong et al., 2015; Fageria and Baligar, 1999). Canopy carbon gain potential indicated by daily integrated GPP ( $GPP_{int}$ ) in plots receiving ample fertilizer addition was highest at  $11.3 \text{ g C m}^{-2} \text{ s}^{-1}$  on 60 DAT, while only  $9.9 \text{ g C m}^{-2} \text{ s}^{-1}$  at that time was found in zero nutrient supplement plot. Maximum  $GPP_{int}$  in paddy rice systems managed under recommended nutrient addition conditions fluctuated from  $10.3$  to  $15.2 \text{ g C m}^{-2} \text{ d}^{-1}$  across climatic regions (Alberto et al., 2012; Lee, 2014; Miyata et al., 2000). To understand the biophysical mechanisms that result in enhanced

## Chapter 1 - Synopsis

carbon gain capacity and biomass production, two key components determining GPP must be separately assessed throughout growing season as in Eq. 1.1, e.g., canopy light interception and light conversion efficiency (Monteith, 1972). Structural traits such as leaf size and leaf angle development which determine canopy light interception and physiological traits such as nitrogen and leaf photosynthetic capacity as well as CO<sub>2</sub> diffusion conductance that relate to light conversion efficiency revealed coordinated adjustments of those factors in achievement of effective carbon gain in response to nutrient fertilization.

Leaf photosynthetic capacity ( $A_{\max}$ , photosynthetic rate at normal CO<sub>2</sub> concentration, saturating PAR of 1500  $\mu\text{mol m}^{-2} \text{s}^{-1}$  and leaf temperature 30°C) was linearly dependent on leaf nitrogen content ( $N_a$ ,  $\text{g m}^{-2}$ ), which conforms to previous reports (Campbell et al., 2001a; Niinemets, 2007; Yoshida, 1981). Furthermore, the key photosynthetic determinants  $V_{\text{cmax},30}$  and  $J_{\text{max},30}$  linearly scaled to  $N_a$  as often reported previously (Bernacchi et al., 2002; Wang et al., 2008; Xu and Baldocchi, 2003), which consequently results in a tight linearity existing between  $V_{\text{cmax},30}$  and  $J_{\text{max},30}$  with a slope of 1.3. The linear correlation between leaf nitrogen content and key photosynthetic determinants emphasized the important role of nitrogen availability in the soil matrix, and therefore in plants with a strong contribution to positive carbon gain. The other two important factors, stomatal and mesophyll conductance, which concurrently determine CO<sub>2</sub> concentration in the chloroplast stroma were also directly correlated with  $N_a$ , with stronger correlation found in the relationship between mesophyll conductance,  $g_m$ , and  $N_a$ . Hence, the relative importance of  $g_m$  in limiting photosynthetic capacity declined with increasing leaf N and stomatal limitation became increasing significant. Observed photosynthetic capacity of tillering plants was promoted in ample fertilization groups, apparently due to high nitrogen content. Significant differences in  $N_a$  among nutrient treatments decreased after the active tillering stage, and finally disappeared during the grain-filling phase. The current results from leaf physiology demonstrate that variations in canopy photosynthetic performance among nutrient treatments did not directly result from differences in leaf physiology.



## Chapter 1 - Synopsis

In agreement with previous reports concerning the stimulatory effects of nutrient additions on rice growth (Bandaogo et al., 2015; Gimenez et al., 1994; Koyama et al., 1972; Koyama and Niamsrichand, 1973), plants in fertilization groups achieved a head start and early burst in leaf canopy size at the end of vegetative stage (end of active tillering), and the significant momentum in increasing LAI was retained over the entire growing season. LAI development was promoted by multiple factors. At the end of active tillering, the leaf number per hill in the normal fertilization group was 101, almost two times greater than that of the low fertilization group (57), which is similar to results from earlier studies (Gimenez et al., 1994). They also reported enlarged individual leaf area in ample nutrient application plots. In partial conformation with their results, relatively larger leaf area was also found at the active tillering stage and internode elongation stage in the normal and high fertilization groups, but not at the grain-filling stage. In this research, the early rapid increase and consistently high LAI in fertilization groups significantly improved the canopy light interception ratio, which was 56% and 44% in ample fertilization versus low fertilization at the reproductive stage (internode elongation stage), and 93% and 86% in ample nutrient group versus low group at the grain-filling stage. The light attenuation coefficient ( $K_L$ ) that is one of two determinants of the canopy light interception ratio was similar between nutrient groups at both internode elongation and grain-filling stages. Light use efficiency ( $LUE_{abs}$ ) in each group had similar seasonal trends where it increased after seedlings were transplanted and peaked at active tillering stage, thereafter rapidly declining during the grain-filling stage. Nevertheless,  $LUE_{abs}$  values among nutrient treatments were quite similar without significant differences. These results indicate that enhanced carbon gain capacity in the fertilization groups mainly result due to greater canopy light interception and canopy size. The results compared well with previous research in several crops grown with different nutrient availability (Bennett et al., 1993; Gimenez et al., 1994; Setter et al., 1995).

In addition to partitioning more resources into leaf area development, plants in fertilized groups also developed a higher proportion of leaves in the upper layers of the canopy during both elongation and grain-filling stages. Positioning a higher percentage of leaves in the

## Chapter 1 - Synopsis

upper canopy with fertilization exposed greater leaf area to direct high sunlight, especially during midday. The advantage of vertical leaves in dense canopies is pronounced, since leaves in the upper part of the canopy commonly accumulate abundant nitrogen and effectively improve carbon acquisition via higher nitrogen use efficiency.

In conclusion, intensive fertilizer application in paddy rice up to the level of  $115 \text{ kg N ha}^{-1}$  significantly promoted biomass and grain yield production. No further benefits were obtained when more nitrogen was applied. A saturation in carbon gain capacity occurred after the vegetative stage due to decreases in  $\text{LUE}_{\text{abs}}$ , decreases in individual leaf N content, and increases in total  $\text{CO}_2$  diffusion limitation. Hence, hypothesis 1 that seasonal development of rice is characterized by an LUE optimization-oriented coordination in LAI, canopy N distribution, and leaf conductance limitations on carbon gain is not supported by these results. Observed enlargement of biomass production coincides with enhanced carbon gain capacity in the fertilization group mainly due to larger leaf canopy size which helps to increase the canopy light interception ratio rather than light conversion efficiency and leaf physiology, which is in agreement with hypothesis 2. The tight correlations between all photosynthetic parameters and leaf nitrogen content support hypothesis 3, i.e., that variations in leaf photosynthetic function in rice are largely explained by variations in leaf nitrogen allocation and nitrogen-driven gas exchange characteristics. The results highlight that developmental variations of carbon gain capacity of rice under conditions of different soil nutrient availability are highly coordinated with respect to leaf physiology and canopy structure.

### 1.4. Conclusion and recommendation

Rice can be grown under irrigated (lowland) or rainfed (upland or lowland) conditions. Paddy (flooded) rice accounts for about 55% of the global rice area and rainfed rice shares the rest which contributes approximately 25% of total rice production (Tuong and Bouman, 2003). One of serious environmental problems encountered in intensive paddy rice systems is downstream water pollution and emission of ammonium volatilization due to surplus organic nitrogen fertilizer application (Fillery et al., 1986; Ju et al., 2009). There is globally an

## Chapter 1 - Synopsis

increasing awareness of water scarcity spreading throughout the world, especially in Asian countries where irrigated rice systems prevail (Tuong and Bouman, 2003). Adoption of water-saving rice with the goal of high agricultural yield provision and reduced water requirements and improved water use efficiency could be a promising social–ecological intervention in some regions, where occurring or future water shortage make irrigation impossible. However, attempts to reduce water provision in rice production may result in yield reductions and threaten food security. To balance environmental sustainability, biomass production with high fertilizer application in paddy rice and efficient water use in rainfed rice systems requires a broad knowledge of crop growth and the developmental responses and adaptive capacities of field grown rice plants.

The studies in this thesis implemented a field experiment with contrasting field management, comparing continuous flooding and rainfed rice production systems, as well as varying nitrogen availability in paddy rice with zero, recommended and high nitrogen application rates. Multi-dimensional measurements in association with structural and physiological traits related to carbon and water fluxes and yield production were collected. The Unkwang lowland rice cultivar planted in rainfed upland fields under monsoon climate could have compatible canopy carbon gain capacity, leaf canopy size and biomass accumulation as compared to the flooded paddy cultivation. Notably, intermittent occurrence of prolonged non-rainfall periods will strongly inhibit photosynthetic productivity in the rainfed rice system. Sensitivities of carbon gain potential and water use efficiency relate to hydraulically constrained stomatal conductance. Decline of photosynthetic productivity results partially due to loss in plant hydraulic conductance. Agronomic water use efficiency and ecological water use efficiency in rainfed systems is higher than the flooded fields which results due to significantly higher evaporation in paddies. The rainfed rice system needs less water input. Nevertheless, high respiratory carbon loss through soil and plant respiration in rainfed fields will weaken the facilitation effects from enhanced carbon gain capacity and improved water use efficiency.

## Chapter 1 - Synopsis

Intensive fertilizer application in paddy rice up to an intermediate level of 115 kg N ha<sup>-1</sup> significantly promotes biomass and grain yield production. There is a slight difference in biomass and yield production between 115 and 180 kg N ha<sup>-1</sup> addition groups. No continuous benefits, however, occurred when more nitrogen above the recommended application level is applied. The fate of surplus nitrogen applied in paddied fields will most likely be transport in ground surface runoff to downstream locations and emission of greenhouse gases. Observed increases in biomass production coincide with enhanced carbon gain capacity in fertilization groups mainly due to larger leaf canopy size which helps to increase canopy light interception ratio rather than light conversion efficiency and leaf physiology. An early start and burst in canopy development stimulated by fertilization is a promising growth strategy to maximize growing season carbon gain potential and increments in biomass production. Importantly, nitrogen allocation in leaves at the early growth stage (vegetative stage with active tillering growth) provides an advantage, since more rate-limiting photosynthetic proteins of the photosynthetic apparatus promote photosynthetic productivity.

Rainfed rice produced relatively less grain, although the difference was not statistically significant with our sampling method. Grain yield production in the low fertilization group (0 kg N addition) was also significantly lower as compared to ample nutrient groups. Yield production per area ground surface depends on panicle number, spikelet number per panicle, filled percentage of spikelets and thousand grain weight. Nutrient availability may indirectly affect panicle number via effective tiller numbers that develop panicles (Gimenez et al., 1994), and may have highly significant effects on the filled percentage of spikelets (Fageria and Baligar, 1999). Microclimate conditions in the rainfed field largely differ from those in flooded plots, with higher air temperature and VPD. The differences increase especially on sunny and clear days. During the non-rainfall periods, leaf temperatures are slightly above the optimal growth temperature range for rainfed rice (ca. 33°C), which might be one of the factors causing spikelet sterility or abortion (Rang et al., 2011). Biomass and yield production is largely determined by the amount of starch in filled spikelets during the grain-filling stage. Daily carbon fluxes were largely affected by ambient meteorological drivers which fluctuate

## Chapter 1 - Synopsis

markedly during the monsoon season. Although our modeling of daily GPP in paddy and rainfed rice (only available in rice under  $115 \text{ kg N ha}^{-1}$ ) produce similar growing season GPP, overestimation in growing season GPP in rainfed rice is anticipated because assumptions are preset in the modelling calculation so that drought effects were not thoroughly considered. One important underlying factor that influences grain yield is carbon allocation pattern among plant organs (Yoshida, 1981), namely to the root system required to maintain water supply.

Development of environmental-friendly rainfed rice systems with high photosynthetic productivity and carbon sequestration will require that we reduce high ecosystem respiratory carbon losses which are an inhibiting factor for yield production, leading to lower net ecosystem exchange and carbon stocks. Flooding fields throughout the whole growth season is an effective measure to improve carbon gain, but unproductive water losses inevitably occur. Ongoing research must implement several technologies to reduce unproductive water losses in evapotranspiration by land coverage with mulch (Suzuki et al., 2014), preventing of seepage and percolation by increased soil resistance to water flow (Tuong and Bouman, 2003), and determining ways to maintain a saturating soil water environment (Bouman et al., 2005). Furthermore, growing season and annual ecosystem respiration and carbon budget under those modified conditions for the rice system should be further evaluated.

## Chapter 1 - Synopsis

### 1.5. List of manuscripts and specification of individual contributions

The four studies described in this thesis refer to four different manuscripts. Three manuscripts are in review for the *Journal of Agriculture and Forest Meteorology*. One is in review for the *Journal of Plant Research*. The following list specifies the contributions of the individual authors to each manuscript.

#### Manuscript 1

Authors	Steve Lindner, Wei Xue, Bhone Nay-Htoon, Jinsil Choi, Yannic Ege, Nikolas Lichtenwald, Fabian Fischer, Jonghan Ko, John Tenhunen, Dennis Otieno	
Title	Canopy scale CO <sub>2</sub> exchange and productivity of transplanted paddy and direct seeded rainfed rice production system in South Korea	
Journal	<i>Agriculture and Forest Meteorology</i>	
Status	Under review	
Contributions	S. Lindner	conceptualization, methods establishment, data collection, data analysis, modeling, manuscript preparation, corresponding author (50%)
	W. Xue	conceptualization, data collection, data analysis, discussion, manuscript editing (25%)
	B. Nay-Htoon	data collection, discussion (2%)
	J. Choi	data collection, discussion (2%)
	Y. Ege	data collection, discussion (2%)
	N. Lichtenwald	data collection, discussion (2%)
	F. Fischer	data collection, discussion (2%)
	J. Ko	conceptualization, discussion, manuscript editing (2%)
	J. Tenhunen	conceptualization, discussion, manuscript editing (3%)
	D. Otieno	conceptualization, discussion, manuscript editing (10%)

#### Manuscript 2

Authors	Wei Xue, Steve Lindner, Bhone Nay-Htoon, Peter Harley, Bernd Huwe, Jonghan Ko, Dennis Otieno, Hiroyuki Muraoka, Christiane Werner, John Tenhunen	
Title	Differentiation in paddy versus rainfed rice in factors influencing carbon gain, water use and grain yield under monsoon climate in South Korea	

## Chapter 1 - Synopsis

Journal	<i>Journal of Plant Research</i>	
Status	Under review	
Contributions	W. Xue	conceptualization, methods establishment, data collection, data analysis, modeling, manuscript preparation, corresponding author (50%)
	S. Lindner	data collection, data analysis, discussion, manuscript editing (25%)
	B. Nay-Htoon	data collection, discussion, manuscript editing (2%)
	P. Harley	data analyses, discussion, manuscript editing (3%)
	B. Huwe	soil data analysis recommendations (2%)
	J. Ko	discussion, manuscript editing (2%)
	D. Otieno	discussion, manuscript editing (2%)
	H. Muraoka	discussion, manuscript editing (2%)
	C. Werner	discussion (2%)
	J. Tenhunen	conceptualization, discussion, manuscript editing (10%)

## Manuscript 3

Authors	Bhone Nay-Htoon, Wei Xue, Steve Lindner, Matthias Cuntz, Jonghan Ko, John Tenhunen, Maren Dubbert, Christiane Werner	
Title	Flux partitioning reveals trade-off between water and carbon loss of paddy and rainfed rice ( <i>Oryza sativa</i> L.)	
Journal	<i>Agriculture and Forest Meteorology</i>	
Status	Under review	
Contributions	B. Nay-Htoon	conceptualization, methods development, data collection, data analysis, modeling, manuscript preparation, corresponding author (50%)
	W. Xue	Conceptualization, data collection, data analysis, discussion, manuscript editing (20%)
	S. Lindner	discussion, manuscript editing (2%)
	M. Cuntz	data analyses, discussion (2%)
	J. Ko	discussion, manuscript editing (2%)
	J. Tenhunen	discussion, manuscript editing (2%)
	M. Dubbert	conceptualization, data analysis, discussion, manuscript editing (12%)
	C. Werner	conceptualization, discussion, manuscript editing (10%)

## Chapter 1 - Synopsis

### Manuscript 4

Authors	Wei Xue, Steve Lindner, Bhone Nay-Htoon, Maren Dubbert, Dennis Otieno, Jonghan Ko, Hiroyuki Muraoka, Christiane Werner, John Tenhunen, Peter Harley	
Title	Nutritional and developmental influences on components of rice crop light use efficiency	
Journal	<i>Agriculture and Forest Meteorology</i>	
Status	Under review	
Contributions	W. Xue	conceptualization, methods implementation, data collection, data analysis, modeling, manuscript preparation, corresponding author (50%)
	S. Lindner	data analysis, discussion, manuscript editing (20%)
	B. Nay-Htoon	data collection, data analysis, discussion, manuscript editing (2%)
	M. Dubbert	discussion, manuscript editing (2%)
	D. Otieno	discussion, manuscript editing (2%)
	J. Ko	discussion, manuscript editing (2%)
	H. Muraoka	discussion, manuscript editing (2%)
	C. Werner	discussion, manuscript editing (2%)
	J. Tenhunen	conceptualization, discussion, manuscript editing (8%)
	P. Harley	conceptualization, data analyses, discussion, manuscript editing (10%)



## Chapter 1 - Synopsis

### 1.6. References

- Adekoya, M.A., Liu, Z., Vered, E., Zhou, L., Kong, D., Qin, J., Ma, R., Yu, X., Liu, G. and Chen, L. 2014. Agronomic and ecological evaluation on growing water-saving and drought-resistant rice (*Oryza sativa* L.) through drip irrigation. *Journal of Agricultural Science*, 6, pp. 110.
- Amano, T., Zhu Q., Wang Y., Inoue N. and Tanaka, H. 1993. Case studies on high yields of paddy rice in Jiangsu Province, China. I. Characteristics of grain production. *Japanese Journal of Crop Science*, 62, 267–274.
- Alberto, M.C.R., Buresh, R.J., Hirano, T., Miyata, A., Wassmann, R., Quilty, J.R., Correa, T.Q. and Sandro, J. 2013. Carbon uptake and water productivity for dry-seeded rice and hybrid maize grown with overhead sprinkler irrigation. *Field Crops Research*, 146, 51-65.
- Alberto, M.C.R., Hirano, T., Miyata, A., Wassmann, R., Kumar, A., Padre, A. and Amante, M. 2012. Influence of climate variability on seasonal and interannual variations of ecosystem CO<sub>2</sub> exchange in flooded and non-flooded rice fields in the Philippines. *Field Crops Research*, 134, 80–94.
- Alberto, M.C.R., Quilty, J.R., Buresh, R.J., Wassmann, R., Haidar, S., Correa, T.Q. and Sandro, J.M. 2014. Actual evapotranspiration and dual crop coefficients for dry-seeded rice and hybrid maize grown with overhead sprinkler irrigation. *Agricultural Water Management*, 136, 1–12.
- Alberto, M.C.R., Wassmann, R., Hirano, T., Miyata, A., Hatano, R., Kumar, A., Padre, A. and Amante, M. 2011. Comparisons of energy balance and evapotranspiration between flooded and aerobic rice fields in the Philippines. *Agricultural Water Management*, 98, 1417–1430.
- Alberto, M.C.R., Wassmann, R., Hirano, T., Miyata, A., Kumar, A., Padre, A. and Amante, M. 2009. CO<sub>2</sub>/heat fluxes in rice fields: Comparative assessment of flooded and non-flooded fields in the Philippines. *Agricultural and Forest Meteorology*, 149, 1737–1750.
- Allen, R.G., Pereira, L.S., Raes, D. and Smith, M. 1998. Crop evapotranspiration–Guidelines for computing crop water requirements–FAO Irrigation and drainage paper 56. FAO, Rome, 300, D05109.

## Chapter 1 - Synopsis

- Araus, J.L., Slafer, G.A., Royo, C. and Serret, M.D. 2008. Breeding for yield potential and stress adaptation in cereals. *Critical Reviews in Plant Science*, 27, 377–412.
- Armstrong, W. and Drew, M. 2002. Root growth and metabolism under oxygen deficiency. In: Waisel, Y., Eshel, A. and Kafkafi, U. (eds.), *Plant roots: the hidden half*, Marcel Dekker, New York, pp. 729–761.
- Atwell, B.J., Kriedemann, P.E. and Turnbull, C.G., 1999. *Plants in action: adaptation in nature, performance in cultivation*. Macmillan Education, South Yarra, Australia, pp. 613.
- Bandaogo, A., Bidjokazo, F., Youl, S., Safo, E., Abaidoo, R. and Andrews, O. 2015. Effect of fertilizer deep placement with urea supergranule on nitrogen use efficiency of irrigated rice in Sourou Valley (*Burkina Faso*). *Nutrient Cycling in Agroecosystems*, 102, 79–89.
- Bennett, J., Sinclair, T., Ma, L. and Boote, K. 1993. Single leaf carbon exchange and canopy radiation use efficiency of four peanut cultivars. *Peanut Science*, 20, 1–5.
- Bernacchi, C.J., Portis, A.R., Nakano, H., von Caemmerer, S. and Long, S.P. 2002. Temperature response of mesophyll conductance. Implications for the determination of Rubisco enzyme kinetics and for limitations to photosynthesis in vivo. *Plant Physiology*, 130, 1992–1998.
- Bhattacharyya, P., Neogi, S., Roy, K., Dash, P., Tripathi, R. and Rao, K. 2013. Net ecosystem CO<sub>2</sub> exchange and carbon cycling in tropical lowland flooded rice ecosystem. *Nutrient Cycling in Agroecosystems*, 95, 133–144.
- Bhattacharyya, P., Neogi, S., Roy, K.S., Dash, P.K., Nayak, A.K. and Mohapatra, T. 2014. Tropical low land rice ecosystem is a net carbon sink. *Agriculture, Ecosystems & Environment*, 189, 127–135.
- Bouman, B., Kropff, M.J., Tuong, T.P., Wopereis, M.C.S., ten Berge, H.F.M and van Laar, H.H. 2001. *ORYZA2000: modeling lowland rice*. Los Banos: International Rice Research Institute, and Wageningen: Wageningen University and Research Center. pp. 235.
- Bouman, B., Peng, S., Castaneda, A. and Visperas, R. 2005. Yield and water use of irrigated tropical aerobic rice systems. *Agricultural Water Management*, 74, 87–105.
- Buresh, R., De Datta, S., Padilla, J. and Chua, T. 1988. Potential of inhibitors for increasing response of lowland rice to urea fertilization. *Agronomy Journal*, 80, 947–952.

## Chapter 1 - Synopsis

- Campbell, C.S., Heilman, J.L., McInnes, K.J., Wilson, L.T., Medley, J.C., Wu, G. and Cobos, D.R. 2001a. Diel and seasonal variation in CO<sub>2</sub> flux of irrigated rice. *Agricultural and Forest Meteorology*, 108, 15–27.
- Campbell, C.S., Heilman, J.L., McInnes, K.J., Wilson, L.T., Medley, J.C., Wu, G. and Cobos, D.R. 2001b. Seasonal variation in radiation use efficiency of irrigated rice. *Agricultural and Forest Meteorology*, 110, 45–54.
- Chen, C., Li, D., Gao, Z., Tang, J., Guo, X., Wang, L. and Wan, B. 2015. Seasonal and interannual variations of carbon exchange over a rice–wheat rotation system on the north China Plain. *Advances in Atmospheric Sciences*, 32, 1365–1380.
- Cui, Z., Zhang, F., Chen, X., Miao, Y., Li, J., Shi, L., Xu, J., Ye, Y., Liu, C. and Yang, Z. 2008. On–farm evaluation of an in–season nitrogen management strategy based on soil N min test. *Field Crops Research*, 105, 48–55.
- Davatgar, N., Neishabouri, M., Sepaskhah, A. and Soltani, A. 2009. Physiological and morphological responses of rice (*Oryza sativa* L.) to varying water stress management strategies. *Intertional Journal of Plant Production*, 3, 19–32.
- De Datta, S. and Broadbent, F. 1988. Methodology for evaluating nitrogen utilization efficiency by rice genotypes. *Agronomy Journal*, 80, 793–798.
- Dong, Z.Z., Wu, L.H., Chai, J., Zhu, Y.H., Chen, Y.L. and Zhu, Y.Z. 2015. Effects of nitrogen application rates on rice grain yield, nitrogen–use efficiency, and water quality in paddy field. *Communications in Soil Science and Plant Analysis*, 46, 1579–1594.
- Dow, G.J. and Bergmann, D.C. .2014. Patterning and processes: how stomatal development defines physiological potential. *Current opinion in plant biology*, 21, 67–74.
- Dubbert, M., Cuntz, M., Piayda, A., Maguás, C. and Werner, C. 2013. Partitioning evapotranspiration–testing the Craig and Gordon model with field measurements of oxygen isotope ratios of evaporative fluxes. *Journal of Hydrology*, 496, 142–153.
- Fageria, N. and Baligar, V. 1999. Yield and yield components of lowland rice as influenced by timing of nitrogen fertilization. *Journal of Plant Nutrition*, 22, 23–32.
- FAO STAT online database. January 2013. <http://faostat3.fao.org/home/E>.
- FAO, 2014. Building a common vision for sustainable food and agriculture: principles and

## Chapter 1 - Synopsis

- approaches. [www.fao.org/3/a-i3940e.pdf](http://www.fao.org/3/a-i3940e.pdf).
- Feng, Y.L. 2008. Nitrogen allocation and partitioning in invasive and native *Eupatorium* species. *Physiologia Plantarum*, 132, 350–358.
- Fillery, I., Simpson, J. and De Datta, S. 1986. Contribution of ammonia volatilization to total nitrogen loss after applications of urea to wetland rice fields. *Fertilizer Research*, 8, 193–202.
- Fischer, R. and Turner, N.C. 1978. Plant productivity in the arid and semiarid zones. *Annual Review of Plant Physiology*, 29, 277–317.
- Franks, P.J. 2004. Stomatal control and hydraulic conductance, with special reference to tall trees. *Tree Physiology*, 24, 865–878.
- Fujiwara, A., and Ohira, K. 1951. Studies on the nitrogen nutrition of the rice plant. *Tohoku Journal of Agricultural Research*, 2, 141–152. *Abstracts in Soils and Fertilizer*. 15, 349.
- Gimenez, C., Connor, D. and Rueda, F. 1994. Canopy development, photosynthesis and radiation–use efficiency in sunflower in response to nitrogen. *Field Crops Research*, 38, 15–27.
- Gitelson, A.A. and Gamon, J.A. 2015. The need for a common basis for defining light–use efficiency: Implications for productivity estimation. *Remote Sensing of Environment*, 156, 196–201.
- Hacke, U.G. 2014. Variable plant hydraulic conductance. *Tree Physiology*, 34, 105–108.
- Hall, A., Connor, D. and Sadras, V. 1995. Radiation–use efficiency of sunflower crops: effects of specific leaf nitrogen and ontogeny. *Field Crops Research*, 41, 65–77.
- Harley, P., Tenhunen, J. and Lange, O. 1986. Use of an analytical model to study limitations on net photosynthesis in *Arbutus unedo* under field conditions. *Oecologia*, 70, 393–401.
- Harley, P.C., Loreto, F., Di Marco, G. and Sharkey, T.D. 1992. Theoretical considerations when estimating the mesophyll conductance to CO<sub>2</sub> flux by analysis of the response of photosynthesis to CO<sub>2</sub>. *Plant Physiology*, 98, 1429–1436.
- Hatala, J.A., Detto, M., Sonnentag, O., Deverel, S.J., Verfaillie, J. and Baldocchi, D.D. 2012. Greenhouse gas (CO<sub>2</sub>, CH<sub>4</sub>, H<sub>2</sub>O) fluxes from drained and flooded agricultural peatlands in the Sacramento–San Joaquin Delta. *Agriculture, Ecosystems & Environment*, 150,

## Chapter 1 - Synopsis

1–18.

- Heenan, D. and Thompson, J. 1984. Growth, grain yield and water use of rice grown under restricted water supply in New South Wales. *Animal Production Science*, 24, 104–109.
- Hirel, B., Bertin, P., Quilleré, I., Bourdoncle, W., Attagnant, C., Dellay, C., Gouy, A., Cadiou, S., Retailliau, C. and Falque, M. 2001. Towards a better understanding of the genetic and physiological basis for nitrogen use efficiency in maize. *Plant Physiology*, 125, 1258–1270.
- Hijmans R.J. and Serraj J. 2008. Modeling spatial and temporal variation of drought in rice production. In: *Drought frontiers in rice: crop improvement for increased rainfed production*. World Scientific Publishing, Singapore, pp. 19–31.
- Hirasawa, T. 1999. Physiological characterization of the rice plant for tolerance of water deficit. In: Ito, O., O'Toole, J.C. and Hardy, B. (eds.), *Genetic improvement of rice for water-limited environments*. International Rice Research Institute, Los Baños, Philippines, pp. 89–98.
- Hossen, M., Mano, M., Miyata, A., Baten, M. and Hiyama, T. 2011. Seasonality of ecosystem respiration in a double-cropping paddy field in Bangladesh. *Biogeosciences Discussions*, 8, 8693–8721.
- Hossen, M., Mano, M., Miyata, A., Baten, M. and Hiyama, T. 2012. Surface energy partitioning and evapotranspiration over a double cropping paddy field in Bangladesh. *Hydrological Processes*, 26, 1311–1320.
- Hu, Z., Yu, G., Zhou, Y., Sun, X., Li, Y., Shi, P., Wang, Y., Song, X., Zheng, Z., Zhang, L. and Li, S. 2009. Partitioning of evapotranspiration and its controls in four grassland ecosystems: Application of a two-source model. *Agricultural and Forest Meteorology*, 149, 1410–1420.
- Huang, X., Hao, Y., Wang, Y., Cui, X., Mo, X. and Zhou, X. 2010. Partitioning of evapotranspiration and its relation to carbon dioxide fluxes in Inner Mongolia steppe. *Journal of Arid Environments*, 74, 1616–1623.
- Inoue, Y., Peñuelas, J., Miyata, A. and Mano, M. 2008. Normalized difference spectral indices for estimating photosynthetic efficiency and capacity at a canopy scale derived

## Chapter 1 - Synopsis

- from hyperspectral and CO<sub>2</sub> flux measurements in rice. *Remote Sensing of Environment*, 112, 156–172.
- International Rice Research Institute [IRRI], 2002. Water-wise rice production. Proceedings of the International Workshop on Water-wise Rice Production, 8–11 April 2002. International Rice Research Institute [IRRI], Los Baños, Philippines, pp. 356.
- Jongdee, B., Fukai, S. and Cooper, M. 2002. Leaf water potential and osmotic adjustment as physiological traits to improve drought tolerance in rice. *Field Crops Research*, 76, 153–163.
- Ju, C.X., Buresh, R.J., Wang, Z.Q., Zhang, H., Liu, L.J., Yang, J.C. and Zhang, J.H. 2015. Root and shoot traits for rice varieties with higher grain yield and higher nitrogen use efficiency at lower nitrogen rates application. *Field Crops Research*, 175, 47–55.
- Ju, X.T., Xing, G.X., Chen, X.P., Zhang, S.L., Zhang, L.J., Liu, X.J., Cui, Z.L., Yin, B., Christie, P. and Zhu, Z.L. 2009. Reducing environmental risk by improving N management in intensive Chinese agricultural systems. *Proceedings of the National Academy of Sciences, USA*, 106, 3041–3046.
- Kato, Y., Kamoshita, A., Yamagishi, J. and Abe, J. 2006. Growth of three rice (*Oryza sativa* L.) cultivars under upland conditions with different levels of water supply: 1. Nitrogen content and dry matter production. *Plant Production Science*, 9, 422–434.
- Kato, Y. and Katsura, K. 2014. Rice adaptation to aerobic soils: physiological considerations and implications for agronomy. *Plant Production Science*, 17, 1–12.
- Kato, Y. and Okami, M. 2011. Root morphology, hydraulic conductivity and plant water relations of high-yielding rice grown under aerobic conditions. *Annals of Botany*, 108, 575–583.
- Katsura, K., Okami, M., Mizunuma, H. and Kato, Y. 2010. Radiation use efficiency, N accumulation and biomass production of high-yielding rice in aerobic culture. *Field Crops Research*, 117, 81–89.
- Karaba, A., Dixit, S., Greco, R., Aharoni, A., Trijatmiko, K.R., Marsch-Martinez, N., Krishnan, A., Nataraja, K.N., Udayakumar, M. and Pereira, A. 2007. Improvement of water use efficiency in rice by expression of HARDY, an Arabidopsis drought and salt

## Chapter 1 - Synopsis

- tolerance gene. *Proceedings of the National Academy of Sciences*, 104, 15270–15275.
- Kettering, J., Park, J.H., Lindner, S., Lee, B., Tenhunen, J. and Kuzyakov, Y. 2012. N fluxes in an agricultural catchment under monsoon climate: a budget approach at different scales. *Agriculture, Ecosystems & Environment*, 161, 101–111.
- Kiniry, J., Jones, C., O'toole, J., Blanchet, R., Cabelguenne, M. and Spanel, D. 1989. Radiation–use efficiency in biomass accumulation prior to grain–filling for five grain–crop species. *Field Crops Research*, 20, 51–64.
- Kim, K.Y., Ha, K.Y., Ko, J.C., Choung, J.I., Lee, J.K., Ko, J.K., Kim, B.K., Nam, J.K., Shin, M.S., and Choi, Y.H. 2006. A new early maturity rice cultivar, "Unkwang" with high grain quality and cold tolerance. *Korean Journal of Breeding*, 38, 261–262.
- Knox, S.H., Sturtevant, C., Matthes, J.H., Koteen, L., Verfaillie, J. and Baldocchi, D. 2015. Agricultural peatland restoration: effects of land–use change on greenhouse gas (CO<sub>2</sub> and CH<sub>4</sub>) fluxes in the Sacramento–San Joaquin Delta. *Global Change Biology*, 21, 750–765.
- Ko, J., Maas, S.J., Mauget, S., Piccinni, G. and Wanjura, D. 2006. Modeling water–stressed cotton growth using within–season remote sensing data. *Agronomy Journal*, 98, 1600–1609.
- Köhl, K. 2015. Growing rice in controlled environments. *Annals of Applied Biology*, 167, 157–177.
- Koyama, T., Chammek, C. and Niamsrichand, N. 1972. Soil–plant nutrition studies on tropical rice V. Yield components as affected by the timing of top–dressing of nitrogen in the Bangkhen paddy field. *Soil Science and Plant Nutrition*, 18, 233–245.
- Koyama, T. and Niamsrichand, N. 1973. Soil–plant nutrition studies on tropical rice VI. The effect of different levels of nitrogenous fertilizer application on plant growth, grain yield, and nitrogen utilization by rice plants. *Soil Science and Plant Nutrition*, 19, 265–274.
- Ladha, J., Kirk, G., Bennett, J., Peng, S., Reddy, C., Reddy, P. and Singh, U. 1998. Opportunities for increased nitrogen–use efficiency from improved lowland rice germplasm. *Field Crops Research*, 56, 41–71.
- Lee, B., 2014. Remote sensing–based assessment of gross primary production in agricultural ecosystems, Ph.D Thesis, University of Bayreuth, pp. 134.

## Chapter 1 - Synopsis

- Li, Y.L., Tenhunen, J., Owen, K., Schmitt, M., Bahn, M., Droesler, M., Otieno, D., Schmidt, M., Gruenwald, T. and Hussain, M. 2008. Patterns in CO<sub>2</sub> gas exchange capacity of grassland ecosystems in the Alps. *Agricultural and Forest Meteorology*, 148, 51–68.
- Lindner, S., Otieno, D., Lee, B., Xue, W., Arnhold, S., Kwon, H., Huwe, B. and Tenhunen, J. 2015. Carbon dioxide exchange and its regulation in the main agro–ecosystems of Haeen catchment in South Korea. *Agriculture, Ecosystems & Environment*, 199, 132–145.
- Limpus, S. 2009. Isohydric and anisohydric characterisation of vegetable crops. The classification of vegetables by their physiological responses to water stress. Project Report. The Department of Primary Industries and Fisheries. Queensland, pp. 11.
- Maas, S.J. 1993a. Parameterized model of gramineous crop growth: I. Leaf area and dry mass simulation. *Agronomy Journal*, 85, 348–353.
- Maas, S.J. 1993b. Parameterized model of gramineous crop growth: II. Within–season simulation calibration. *Agronomy Journal*, 85, 354–358.
- Maruyama, A. and Kuwagata, T. 2010. Coupling land surface and crop growth models to estimate the effects of changes in the growing season on energy balance and water use of rice paddies. *Agricultural and Forest Meteorology*, 150, 919–930.
- Medlyn, B., Dreyer, E., Ellsworth, D., Forstreuter, M., Harley, P., Kirschbaum, M., Le Roux, X., Montpied, P., Strassmeyer, J. and Walcroft, A. 2002. Temperature response of parameters of a biochemically based model of photosynthesis. II. A review of experimental data. *Plant, Cell & Environment*, 25, 1167–1179.
- Min, S., Shim, K., Kim, Y., Jung, M., Kim, S. and So, K. 2013. Seasonal variation of carbon dioxide and energy fluxes during the rice cropping season at rice–barley double cropping paddy field of Gimje. *Korean Journal of Agricultural and Forest Meteorology*, 15, 273–281.
- Miyata, A., Leuning, R., Denmead, O.T., Kim, J. and Harazono, Y. 2000. Carbon dioxide and methane fluxes from an intermittently flooded paddy field. *Agricultural and Forest Meteorology*, 102, 287–303.
- Mohanty, S., Wassmann, R., Nelson, A., Moya, P. and Jagadish, S. 2013. Rice and climate change: significance for food security and vulnerability. Discussion Paper Series No. 49,



## Chapter 1 - Synopsis

- International Rice Research Institute Los Baños, Philippines, pp. 14.
- Monteith, J. 1972. Solar radiation and productivity in tropical ecosystems. *Journal of Applied Ecology*, 747–766.
- Monteith, J.L. and Moss, C. 1977. Climate and the efficiency of crop production in Britain [and discussion]. *Philosophical Transactions of the Royal Society B: Biological Sciences*, 281, 277–294.
- Morison, J.I., Baker, N.R., Mullineaux, P.M. and Davies, W.J. 2008. Improving water use in crop production. *Philosophical Transactions of the Royal Society B: Biological Sciences*, 363, 639–658.
- Naklang, K., Shu, F. and Nathabut, K. 1996. Growth of rice cultivars by direct seeding and transplanting under upland and lowland conditions. *Field Crops Research*, 48, 115–123.
- Nie, L., Peng, S., Chen, M., Shah, F., Huang, J., Cui, K. and Xiang, J. 2012. Aerobic rice for water-saving agriculture. A review. *Agronomy for Sustainable Development*, 32, 411–418.
- Niinemets, U. 2007. Photosynthesis and resource distribution through plant canopies. *Plant, Cell & Environment*, 30, 1052–1071.
- Niinemets, Ü. and Tenhunen, J. 1997. A model separating leaf structural and physiological effects on carbon gain along light gradients for the shade-tolerant species *Acer saccharum*. *Plant, Cell & Environment*, 20, 845–866.
- Niinemets, Ü. and Valladares, F. 2004. Photosynthetic acclimation to simultaneous and interacting environmental stresses along natural light gradients: optimality and constraints. *Plant Biology*, 6, 254–268.
- Nishimura, S., Yonemura, S., Sawamoto, T., Shirato, Y., Akiyama, H., Sudo, S. and Yagi, K. 2008. Effect of land use change from paddy rice cultivation to upland crop cultivation on soil carbon budget of a cropland in Japan. *Agriculture, Ecosystems & Environment*, 125, 9–20.
- Okami, M., Kato, Y. and Yamagishi, J. 2013. Grain yield and leaf area growth of direct-seeded rice on flooded and aerobic soils in Japan. *Plant Production Science*, 16, 276–279.

## Chapter 1 - Synopsis

- Otieno, D., Lindner, S., Muhr, J. and Borken, W. 2012. Sensitivity of peatland herbaceous vegetation to vapor pressure deficit influences net ecosystem CO<sub>2</sub> exchange. *Wetlands*, 32, 895–905.
- Owen, K.E., Tenhunen, J., Reichstein, M., Wang, Q., Falge, E., Geyer, R., Xiao, X., Stoy, P., Ammann, C. and Arain, A. 2007. Linking flux network measurements to continental scale simulations: Ecosystem carbon dioxide exchange capacity under non–water–stressed conditions. *Global Change Biology*, 13, 734–760.
- Pape, L., Ammann, C., Nyfeler–Brunner, A., Spirig, C., Hens, K. and Meixner, F. 2009. An automated dynamic chamber system for surface exchange measurement of non–reactive and reactive trace gases of grassland ecosystems. *Biogeosciences*, 6, 405–429.
- Pandey S. and Bhandari H. 2008. Drought: economic costs and research implications. In: *Drought frontiers in rice: crop improvement for increased rainfed production*, World Scientific Publishing, Singapore, pp. 3–15.
- Rang, Z., Jagadish, S., Zhou, Q., Craufurd, P. and Heuer, S. 2011. Effect of high temperature and water stress on pollen germination and spikelet fertility in rice. *Environmental and Experimental Botany*, 70, 58–65.
- Rao, M., Reddy, B., Ghosh, B. and Panda, M. 1985. Nitrogen management in direct sown intermediate deep water rice (15–50 cm). *Plant and Soil*, 83, 243–253.
- RDA, Rural Development Administration. 2008. Taxonomical classification of Korean soils. NIAST (National Institute of Agricultural Science and Technology), Suwon, Korea, pp. 4.
- Sakuratani, T., and Horie, T. 1985. Studies on Evapotranspiration from crops: (1) on seasonal changes, varietal differences and the simplified methods of estimate in evapotranspiration of paddy rice. *Journal of Agricultural Meteorology*, 41, 45–55.
- Schaap, M.G., Leij, F.J. and van Genuchten, M.T. 1998. Neural network analysis for hierarchical prediction of soil hydraulic properties. *Soil Science Society of America Journal*, 62, 847–855.
- Scott, R.L., Huxman, T.E., Cable, W.L. and Emmerich, W.E. 2006. Partitioning of evapotranspiration and its relation to carbon dioxide exchange in a Chihuahuan Desert shrubland. *Hydrological Processes* 2006, 20, 3227–3243.

## Chapter 1 - Synopsis

- Seck, P.A., Diagne, A., Mohanty, S. and Wopereis, M.C. 2012. Crops that feed the world 7: rice. *Food Security*, 4, 7–24.
- Setter, T., Conocono, E., Egdane, J. and Kropff, M. 1995. Possibility of Increasing Yield Potential of Rice by Reducing Panicle Height in the Canopy. I. Effects of Panicles on Light Interception and Canopy Photosynthesis. *Functional Plant Biology*, 22, 441–451.
- Serraj J, Bennett J, Hardy B, editors. 2008. Drought frontiers in rice: crop improvement for increased rainfed production. Singapore: World Scientific Publishing and Los Banos (Philippines): International Rice Research Institute. 400 p.
- Sharkey, T.D., Bernacchi, C.J., Farquhar, G.D. and Singsaas, E.L. 2007. Fitting photosynthetic carbon dioxide response curves for C<sub>3</sub> leaves. *Plant, Cell & Environment*, 30, 1035–1040.
- Sheehy, J.E. and Mitchell, P., 2013. Designing rice for the 21st century: the three laws of maximum yield, IRRI Discussion Paper 48, International Rice Research Institute, Los Banos, Philippines, pp. 19.
- Sinclair, T. 1991. Canopy carbon assimilation and crop radiation–use efficiency dependence on leaf nitrogen content. In: Boote, K.J. and Loomis, R.S., (eds.), *Modeling crop photosynthesis—from biochemistry to canopy*. CSSA special publication 19. Madison, WI, USA: American Society of Agronomy: Crop Science Society of America, pp. 95–107.
- Sinclair, T. and Horie, T. 1989. Leaf nitrogen, photosynthesis, and crop radiation use efficiency: a review. *Crop Science*, 29, 90–98.
- Stiller, V., Lafitte, H.R. and Sperry, J.S. 2003. Hydraulic properties of rice and the response of gas exchange to water stress. *Plant Physiology*, 132, 1698–1706.
- Stuerz, S., Sow, A., Muller, B., Manneh, B. and Asch, F. 2014. Canopy microclimate and gas–exchange in response to irrigation system in lowland rice in the Sahel. *Field Crops Research*, 163, 64–73.
- Suyker, A.E. and Verma, S.B. 2008. Interannual water vapor and energy exchange in an irrigated maize–based agroecosystem. *Agricultural and Forest Meteorology*, 148, 417–427.
- Suzuki, T., Ohta, T., Hiyama, T., Izumi, Y., Mwandemele, O. and Iijima, M. 2014. Effects of

## Chapter 1 - Synopsis

- the introduction of rice on evapotranspiration in seasonal wetlands. *Hydrological Processes*, 28, 4780–4794.
- Takimoto, T., Iwata, T., Yamamoto, S. and Miura, T. 2010. Characteristics of CO<sub>2</sub> and CH<sub>4</sub> flux at barley–rice double cropping field in southern part of Okayama. *Journal of Agricultural Meteorology*, 66, 181–191.
- Tanguilig, V., Yambao, E., O'toole, J. and De Datta, S. 1987. Water stress effects on leaf elongation, leaf water potential, transpiration, and nutrient uptake of rice, maize, and soybean. *Plant and Soil*, 103, 155–168.
- Tao, Y.Y., Zhang, Y.N., Jin, X.X., Saiz, G., Jing, R.Y., Guo, L., Liu, M.J., Shi, J.C., Zuo, Q., Tao, H.B., Butterbach–Bahl, K., Dittert, K. and Lin, S. 2015. More rice with less water – evaluation of yield and resource use efficiency in ground cover rice production system with transplanting. *European Journal of Agronomy*, 68, 13–21.
- Tanaka, Y., Sugano, S.S., Shimada, T. and Hara–Nishimura, I. 2013. Enhancement of leaf photosynthetic capacity through increased stomatal density in *Arabidopsis*. *New Phytologist*, 198, 757–764.
- Tilman, D., Cassman, K.G., Matson, P.A., Naylor, R. and Polasky, S. 2002. Agricultural sustainability and intensive production practices. *Nature*, 418, 671–677.
- Tuong, T. and Bouman, B. 2003. Rice production in water scarce environments. In: Kijne, J.W., Barker, R., Molden, D. (eds.), *Water productivity in agriculture: limits and opportunities for improvement*. CAB International, Wallingford, UK, pp. 13–42.
- Van Genuchten, M.T. 1980. A closed–form equation for predicting the hydraulic conductivity of unsaturated soils. *Soil Science Society of America Journal*, 44, 892–898.
- Vote, C., Hall, A. and Charlton, P. 2015. Carbon dioxide, water and energy fluxes of irrigated broad–acre crops in an Australian semi–arid climate zone. *Environmental Earth Sciences*, 73, 449–465.
- Wang, Q., Iio, A., Tenhunen, J. and Kakubari, Y. 2008. Annual and seasonal variations in photosynthetic capacity of *Fagus crenata* along an elevation gradient in the Naeba Mountains, Japan. *Tree Physiology*, 28, 277–285.
- Wang, Y., Noguchi, K., Ono, N., Inoue, S., Terashima, I., Kinoshita, T. 2014. Overexpression

## Chapter 1 - Synopsis

- of plasma membrane H<sup>+</sup>-ATPase in guard cells promotes light-induced stomatal opening and enhances plant growth. *Proceedings of the National Academy of Sciences*, 111, 533–538.
- Wei, Z., Yoshimura, K., Okazaki, A., Kim, W., Liu, Z. and Yokoi, M. 2015. Partitioning of evapotranspiration using high frequency water vapor isotopic measurement over a rice paddy field. *Water Resources Research*, 51, 3716–3729.
- Wells, B. and Johnston, T. 1970. Differential response of rice varieties to timing of mid-season nitrogen applications. *Agronomy Journal*, 62, 608–612.
- Westcott, M. and Vines, K. 1986. A comparison of sprinkler and flood irrigation for rice. *Agronomy Journal*, 78, 637–640.
- Wopereis, M., Kropff, M., Maligaya, A. and Tuong, T. 1996. Drought-stress responses of two lowland rice cultivars to soil water status. *Field Crops Research*, 46, 21–39.
- Xu, L. and Baldocchi, D.D. 2003. Seasonal trends in photosynthetic parameters and stomatal conductance of blue oak (*Quercus douglasii*) under prolonged summer drought and high temperature. *Tree Physiology*, 23, 865–877.
- Xue, W., Li, X., Zhu, J. and Lin, L. 2012. Effects of temperature and irradiance on photosystem activity during *Alhagi sparsifolia* leaf senescence. *Biologia Plantarum*, 56, 785–788.
- Yoshida, S., 1981. Fundamentals of rice crop science. International Rice Research Institute, Los Banos, Philippines, pp. 269.
- Yoshida, S., Forno, D.A. and Cock, J.H. 1971. Laboratory manual for physiological studies of rice. International Rice Research Institute, Los Banos, Philippines, pp. 83.
- Yun, K.S., Shin, S.H., Ha, K.J., Kitoh, A. and Kusunoki, S. 2008. East Asian precipitation change in the global warming climate simulated by a 20-km mesh AGCM. *Asia-Pacific Journal of Atmospheric Sciences*, 44, 233–247.
- Zhao, P., 2014. Ecosystem-atmosphere exchange of carbon dioxide and water vapour in typical East-Asian croplands. Ph.D Thesis, University of Bayreuth, pp. 119.
- Zhao, P., Lüers, J., Kim, J.C., Seo, B., Lindner, S., Tenhunen, J. and Foken, T. 2011. Energy and Net Ecosystem CO<sub>2</sub> exchange between agro-ecosystems and the atmosphere over a

## **Chapter 1 - Synopsis**

complex terrain in Korea. TERRECO Science Conference, October 2–7, 2011, Karlsruhe Institute of Technology, Garmisch–Partenkirchen, Germany, pp. 95–102.

### Chapter 2

#### 2. Canopy scale CO<sub>2</sub> exchange and productivity of transplanted paddy and direct seeded rainfed rice production system in S. Korea

Steve Lindner<sup>1</sup>; Wei Xue<sup>1</sup>; Bhone Nay-Htoon<sup>2</sup>; Jinsil Choi<sup>3</sup>; Yannic Ege<sup>1</sup>; Nikolas Lichtenwald<sup>1</sup>; Fabian Fischer<sup>1</sup>; Jonghan Ko<sup>3</sup>; John Tenhunen<sup>1</sup>, Dennis Otieno<sup>1</sup>

<sup>1</sup>Department of Plant Ecology, BayCEER, University of Bayreuth, Universitätsstraße 30, 95447 Bayreuth, Germany.

<sup>2</sup>Department of Agro-ecosystem Research, BayCEER, University of Bayreuth, Universitätsstraße 30, 95447 Bayreuth, Germany.

<sup>3</sup>Division of Plant Biotechnology, Chonnam National University, 300 Youngbong-dong, Buk-gu, Gwangju, 500-757, Republic of Korea.

#### 2.1. Abstract

Rice (*Oryza sativa* L.) is a primary food crop which supports more than half the world population. Paddy rice accounts for more than 75% of the total global rice but requires large amounts of water for irrigation. Increasing water scarcity, however, raises concerns regarding the sustainability of paddy rice production and highlights the need for alternative approaches. Improved rice varieties that require less water, are drought tolerant and which can be directly seeded offer promising alternatives. In this study, we evaluated the performance of an improved rice variety (*Oryza sativa* L. cv. Unkwang) grown under direct seeding and rainfed cultivation. Aboveground biomass and leaf area development were measured every month by destructive harvesting. Canopy net ecosystem CO<sub>2</sub> exchange (NEE) and ecosystem respiration (R<sub>eco</sub>) were measured using chambers. Gross primary production (GPP) was calculated from NEE and R<sub>eco</sub>. The maximum green leaf area index (GLAI) attained under rainfed agriculture was  $4.9 \pm 0.5 \text{ m}^2 \text{ m}^{-2}$  compared to  $5.4 \pm 1.1 \text{ m}^2 \text{ m}^{-2}$  in the conventional paddy rice production. The respective peak total aboveground biomasses were  $2.16 \pm 0.28$  and  $1.85 \pm 0.27 \text{ kg m}^{-2}$  while the corresponding grain weights were  $1.16 \pm 0.09$  and

## Chapter 2 - Canopy carbon fluxes in paddy and rainfed rice

$1.19 \pm 0.10 \text{ kg m}^{-2} \text{ kg m}^{-2}$ , amounting to total yields of  $6.61 \pm 0.22$  and  $5.99 \pm 0.68 \text{ t/ha}^{-1}$  for paddy and rainfed rice, respectively. The maximum daily cumulative GPP were 11.1 and 14.3  $\text{gC m}^{-2} \text{ d}^{-1}$ , respectively, occurring at peak season, corresponding to maximum photosynthetic active radiation (PAR) and GLAI. On a daily basis, PAR explained  $> 82\%$  of the daily fluctuations in GPP while  $> 90\%$  of the seasonal changes in GPP were due to changes in GLAI and light use efficiency ( $\alpha$ ). Higher  $\alpha$  in RF was attributed to higher leaf nitrogen (N) content. With adequate soil moisture supply, the Unkwang variety demonstrated the potential to grow under rainfed agriculture with, comparatively good amount of yield. Since direct seeding, as in rainfed agriculture, eliminates the need for prior flooding of plots, it maximizes the use of early rainfall, which could be a water saving strategy and a reason to promote the introduction of Unkwang variety in the paddy rice-dominated Asian farming system.

**Keywords:** Agricultural crop, Biomass development, Closed-chamber technique, Crop productivity, Ecosystem  $\text{CO}_2$  exchange, Gross primary production



## Chapter 2 - Canopy carbon fluxes in paddy and rainfed rice

### 2.2. Introduction

Rice (*Oryza sativa* L.) is a primary food crop supporting more than half the world's population and covers about 150 million hectares of land (Bouman, 2007). Worldwide, most rice production is done through flooding or paddy (Barker et al., 1999). Increasing water scarcity due to droughts and competing demands for water resources (IPCC, 2008) from growing domestic and industrial uses however, threaten the current production practices, raising the need for alternative production approaches. In this regard, the development of improved varieties that require less water or are more drought tolerant has been promoted (Barker et al., 1999). The culture of direct-seeded rice grown in unsaturated soils is another promising way to reduce irrigation requirements by more than half, compared to the conventional paddy rice (IRRI, 2002; Kato et al., 2006a; Okami et al., 2013).

In paddy rice fields, the amount of water that directly supports production is the transpired water since it is directly linked to CO<sub>2</sub> uptake, plant growth and yield. The bulk of the water in the flooded field is not directly related to production and is either re-directed back to the streams, percolated or evaporated. Thus, production systems that only supply the evapotranspiration demands could be a big saving on water resources and are environmentally friendlier (Toung and Bouman, 2003). Dry-seeded, rainfed rice offers an alternative to rice farmers, especially in Asia, where flooded rice production is more or less cultural and does not accommodate alternative crops as a means of ensuring food security. Rainfed rice production is already being experimented in some parts of Asia as an alternative to the traditional paddy rice (Kato et al., 2006a). Although most results from these trials show yield losses of between 20 – 30% caused by drought (Okami et al., 2013), there are indications that yields of up to 8 – 11 t ha<sup>-1</sup> (as in the case of paddy rice) are tenable with proper management (Okami et al., 2013). The dry-seeded rainfed rice technology thus, may offer an opportunity for rice production through efficient use of ambient rainfall.

The main challenge to rainfed rice production however, is to supply adequate water that replaces daily evapo-transpiration and ensuring that photosynthesis proceeds uninterrupted.

## Chapter 2 - Canopy carbon fluxes in paddy and rainfed rice

High transpirational water demand that occurs almost on a daily basis during midday, when vapor pressure deficit (VPD) is high, potentially lowers production, since plants close their stomata in order to check runaway cavitation at the expense of CO<sub>2</sub> fixation (Sperry, 2000). On an annual basis, this could lead to a significant reduction in yield. Rainfed rice may improve water uptake through increased root biomass, or physiological adjustments by re-directing assimilates to the roots to increase the root osmoticum (Munns, 1988; Kato et al., 2007; Wada et al., 2014). In such cases however, resources that could be used in grain production are re-directed in order to increase the plant's water uptake capacity, and hence lowering yield.

While paddy rice may be spared such a reduction in productivity because it stands in saturated soil, it faces a different challenge that may effectively reduce shoot water supply and result in water stress during the day too. Flooding of paddy fields limits oxygen diffusion into the soil, creating an anoxic soil substrate. Plant roots must, therefore, rely on oxygen supply from the surface, transported by the aerenchyma to the root apex (Moog and Brüggemann, 1998; Busch, 2001; McDonald et al., 2002; Colmer et al., 2003). To minimize radial oxygen losses during transport, large sections of the roots are often suberized (i.e. deposition of suberin, a hydrophobic plant polymer, on the cell walls and in the intercellular space), effectively blocking water flow through the apoplast, such that the roots can no longer take part in water uptake. In this case, water uptake is restricted to the short, narrow portions near the root apex of the deep roots, which remain unsuberized (Ranathunge et al., 2004; Kotula et al., 2009). This must effectively lower the efficiency of water uptake in paddy rice and could result in transient water stress and stomatal closure during midday, when light conditions and temperature are most conducive for plant production. In this case, flooding may not offer any advantage to paddy rice, unless through the dampening the VPD above the canopy. Incorporating cultivars with efficient water and nutrient uptake and transport into the rainfed rice production offers an opportunity to respond to the challenges associated with rice production (Kato et al., 2006a).

## Chapter 2 - Canopy carbon fluxes in paddy and rainfed rice

In this study, we experimented on a new rice cultivar (*Oryza sativa* L. cv. Unkwang) that has been developed from a high yielding, cold tolerant and early maturing variety to accommodate the demands of the northern plains and mountainous areas of South Korea (Kim et al., 2006). The Unkwang rice variety was grown under both the rainfed and conventional paddy production systems for comparison. Our hypotheses were that under adequate soil moisture supply, the Unkwang rice grown in a rainfed system:

- 1) maintains similar rates of CO<sub>2</sub> uptake and light use efficiencies compared to that in a paddy system, and
- 2) does not alter C allocation patterns in comparison to the paddy condition. Under such circumstances we anticipated similarities in crop development and yield between rainfed and paddy rice.

### 2.3. Materials and methods

#### 2.3.1. Study site

The study was conducted during the growing period of 2013 at the Chonnam National University's research farm (35°10' N, 126°53' E, alt. 33m) in Gwangju, Chonnam province, South Korea. Chonnam province is one of the major rice growing regions of S. Korea, with a typical East Asian monsoon climate, a mean annual temperature of 13.8°C and precipitation of between 1391 and 1520 mm/yr (1981–2010). More than 60% of precipitation occurs during the summer monsoon season (July to August). The top soil layer (0–30 cm) is categorized as loam (Sand 388 g kg<sup>-1</sup>, Silt 378 g kg<sup>-1</sup>, Clay 234 g kg<sup>-1</sup>), with a pH 6.5, C<sub>org</sub> 12.3 C g kg<sup>-1</sup>, available P 13.1 mg P<sub>2</sub>O<sub>5</sub> kg<sup>-1</sup>, CEC 14.4 c mol kg<sup>-1</sup>, and total N before fertilization of 1.0 g N kg<sup>-1</sup>.

#### 2.3.2. Experimental design/Description of the experimental plots

An improved rice variety, *Oryza sativa* subsp. Japonica cv. Unkwang (Iksan 435 x Cheolweon 54) was cultivated as flooded paddy crop and as rainfed crop in two adjacent (separated by 100 m) experimental rice fields. Paddy rice was planted in 3 replicate blocks

## **Chapter 2 - Canopy carbon fluxes in paddy and rainfed rice**

measuring 73.0 m x 19.5 m, with a perimeter cement wall. Sampling was confined to the 8 m by 8 m sub-plots at the center of the blocks to minimize edge effects. In the rainfed rice field, we demarcated 3 replicate plots measuring 37.5 m x 28.0 m for our measurements. These plots were randomly selected, but at the middle of the field to avoid edge effects too. In both paddy and rainfed systems, the sample plots were accessed using footbridges to minimize disturbances of the soil and canopy.

### **2.3.3. Field management**

Measurements were conducted during the 2013 growing season. The rice seedlings were grown for 4 weeks as seedling mats in the greenhouse, before being transplanted into the paddy rice field, whereas in rainfed field the rice was directly seeded. Management practices and planting dates, including rice transplanting and the harvesting days are summarized in Table 2.1. Fertilization rate of 115 kg N/ha (80% as basal dosage and 20% during the tillering stage) for paddy rice and rainfed rice were done before transplanting and at seeding stages, respectively, at a ratio of 11 : 6 : 5 (N : P : K), following the recommendations of the Korean Ministry of Agriculture, Food and Rural Affairs (MAFRA). Rice in paddy field and rainfed field were planted at a distance of 10 cm and a line spacing of 30 cm at a seed-density of 50.48 kg/ha. The paddy field was kept flooded from 5 days before transplanting until the heading stage (late July). Irrigation water in paddy rice was applied when the water level decreased below 5 cm above the soil surface. The rainfed field was never irrigated and relied entirely on the ambient rainfall. Weed and insects were controlled with pesticides and insecticides, respectively.

## Chapter 2 - Canopy carbon fluxes in paddy and rainfed rice

**Table 2.1** Field management of the study site in 2013 in Gwangju.

Event	Date Paddy Rice	Date Rainfed Rice
Plowing	10.05.13	17.04.13
Flooding	14.05.13	—
Herbicides application	16.05.13	—
Basal fertilization	19.05.13	22.04.13
Transplanting / Planting	20.05.13	22.04.13
Pesticides application	20.05.13	26.04.13
Herbicides application	—	06.05.13
Manual weeding	—	22.05.13
Herbicides application	—	25.05.13
Manual weeding	—	20.06.13
Supplemental fertilization	07.06.13	09.06.13
Harvest	07.10.13	10.10.13

### 2.3.4. Microclimate

Meteorological variables, including air temperature, humidity, precipitation and global radiation were continuously measured with a 2 m high automatic weather station (AWS, WS-GP1, Delta-T Devices Ltd., UK). Data were recorded every 5 minutes, averaged and logged half-hourly. Additionally discontinuous records of photosynthetic photon flux density (PPFD, LI-190, LI-COR, USA) within the transparent CO<sub>2</sub> measurement chambers (approx. 50 cm above ground surface), air temperature ( $T_{\text{air}}$ ) at 20 cm height inside and outside the CO<sub>2</sub> chambers (Digital thermometer, Conrad, Hirschau, Germany) and soil temperature ( $T_{\text{soil}}$ ) at 10 cm soil depth (Soil thermometer, Conrad, Hirschau, Germany) within the soil frames were taken during the CO<sub>2</sub> flux measurements. Data were recorded every 15 s alongside CO<sub>2</sub> fluxes. This allowed closer monitoring of the internal chamber microclimate, in order to relate the CO<sub>2</sub> fluxes to the actual conditions within the chambers during measurements.

### 2.3.5. Soil water content

Volumetric soil water content at – 30 cm depth was measured at several locations close to the collars using EC-5 soil moisture sensors (Decagon, WA, USA). The sensors were installed 1

## Chapter 2 - Canopy carbon fluxes in paddy and rainfed rice

week before the onset of CO<sub>2</sub> flux measurements and kept in the field throughout the season. Data were logged every 30 min using EM50 data-logger (Decagon, WA, USA).

### 2.3.6. CO<sub>2</sub> flux measurement with chambers

In each treatment block, 4 soil frames (collars) enclosing healthy, representative crops (crop plots) and 3 bare plots (soil plots) were established in June 2013, several days before the commencement of CO<sub>2</sub> flux measurements. Each collar enclosed an area measuring 39.5 cm by 39.5 cm, providing a base for the CO<sub>2</sub> chambers. Repeated measurements were conducted on the same collars on selected days during the growing season (Table 2.2). Measurements were carried out between 06–18h (12 cycles per day), at least once every 2 weeks between June and September 2013. Most CO<sub>2</sub> flux measurements were performed on sunny days, when peak (midday) light intensity was >1300  $\mu\text{mol m}^{-2} \text{s}^{-1}$ . Net ecosystem CO<sub>2</sub> exchange (NEE), ecosystem respiration ( $R_{eco}$ ) and soil respiration ( $R_{soil}$ ) were sequentially observed with a systematic rotation over all plots using climate-controlled, manually operated, transparent and translucent chambers, respectively as described by Otieno et al. (2012), Lindner et al. (2014). The chambers measured 40 x 40 x 54 cm<sup>3</sup>. Change in chamber CO<sub>2</sub> concentration over time was assessed with a portable, battery operated infrared gas analyzer (LI-820, LI-COR, USA).

CO<sub>2</sub> fluxes were calculated from a linear regression describing the time dependent change in CO<sub>2</sub> concentration within the chamber. Influence of the CO<sub>2</sub> concentration change on plant physiological response was ignored. Internal chamber temperature during the measurements was maintained within 1 °C relative to ambient, using dry ice packs mounted at the back of the chamber.

Gross primary production (GPP) was determined as:

$$GPP = -NEE + R_{eco} \quad (2.1)$$

where  $R_{eco}$  is Ecosystem respiration = the sum of plant respiration ( $R_{plant}$ ) and soil respiration ( $R_{soil}$ ).

### 2.3.7. Empirical description of canopy responses

Empirical description of the measured NEE was performed with a non-linear least squares fit of the data to a hyperbolic light response model using Equation 2, also known as the Michaelis-Menten or rectangular hyperbola model (Owen et al., 2007)

$$NEE = \frac{\beta \cdot \alpha \cdot PAR}{\beta + \alpha \cdot PAR} - \gamma \quad (2.2)$$

where  $\alpha$  is the initial slope of the curve and an approximation of the canopy light utilization efficiency ( $\text{CO}_2/\text{photon}$ ),  $\beta$  is the maximum NEE of the canopy ( $\mu\text{mol CO}_2 \text{ m}^{-2} \text{ s}^{-1}$ ),  $PAR$  is photosynthetic photon flux density ( $\mu\text{mol photon m}^{-2} \text{ s}^{-1}$ ),  $\gamma$  is an estimate of the average ecosystem respiration occurring during the observation period ( $\mu\text{mol CO}_2 \text{ m}^{-2} \text{ s}^{-1}$ ). Since the rectangular hyperbola may saturate very slowly in terms of light, we used the value calculated from  $\alpha\beta*PAR/(\alpha*PAR+\beta)$  for high light intensity levels ( $PAR = 1500 \mu\text{mol m}^{-2} \text{ s}^{-1}$ ) in this study. This value approximates the potential maximum GPP and can be thought of as the average maximum canopy uptake capacity during each observation period (noted here as  $(\beta + \gamma)_{1500}$ ). The parameters  $(\beta + \gamma)_{1500}$  (e.g. NEE at  $PAR = 1500 \mu\text{mol m}^{-2} \text{ s}^{-1}$ ) and  $\alpha$  were estimated for each day using NEE data from the four measurement plots per day.

Statistical analysis and best fits for light and curves were performed using Sigma Plot version 11.0.

### 2.3.8. Calculation of net-primary-production (NPP)

Net primary production equivalent to canopy net assimilation rate (NPP) is defined as:

$$NPP = GPP - R_{plant} \quad (2.3)$$

Replacing GPP with Eq. 2.1 leads to Eq. 2.4:

$$NPP = -NEE + R_{eco} - R_{plant} \quad (2.4)$$

I.e.,

$$NPP = NEE + R_{soil} \quad (2.5)$$

## Chapter 2 - Canopy carbon fluxes in paddy and rainfed rice

where soil respiration was described as being dependent on soil temperature ( $T_{\text{soil}}$ ) by the function of Lloyd and Taylor (Lloyd and Taylor, 1994), normalized to 15°C,

$$R_{\text{soil}} = R_{\text{soilref}} e^{E_0 \left( \frac{1}{T_{\text{ref}} - T_0} - \frac{1}{T_{\text{soil}} - T_0} \right)} \quad (2.6)$$

where  $T_{\text{ref}}$  and  $T_0$  are fixed to 15 and -46°C, respectively.  $E_0$  depicting increasing amplitude of  $T_{\text{soil}}$ -temperature curve was considered to be a free parameter and was fitted to each data set.  $R_{\text{soilref}}$  is reference soil respiration. Daily integrated NPP ( $\text{NPP}_{\text{int}}$ ) was interpolated based on the hourly measurements using the parameterized light curves and PAR data recorded at the automatic weather station.

### 2.3.9. Biomass sampling

After  $\text{CO}_2$  flux measurements, aboveground biomass enclosed by the 39.5 cm x 39.5 cm soil frame (for  $\text{CO}_2$  flux measurements) was harvested at 3 randomly chosen locations (representing 3 replicates) in rainfed and paddy rice. The aboveground biomass was sorted into leaves, grains, culms and dead material. Green leaf area (GLA) was determined with leaf area meter (LI-3000A, LI-COR, USA) from the sampled leaves. All the biomass was oven-dried to a constant weight at 85°C for at least 48 hours. Green leaf area index (GLAI) was determined from total GLA within the 39.5 cm by 39.5 cm ground area and expressed per unit square meter.

### 2.3.10. Plant carbon and nitrogen determination

Sub-samples from the dried biomass of the respective collars (for  $\text{CO}_2$  flux measurements) were ball-milled into fine powder, re-dried at 80°C and kept in a desiccator for further analysis. A small fraction of the dried samples (< 1 g) was analyzed for total carbon/ nitrogen (C/N) content (%) using C:N Analyzer 1500 (Carlo Erba Instruments, Milan, Italy).

### 2.3.11. Statistical analyses

Statistical analysis was performed using R (R Core Team, 2012). Significance level was set to



## Chapter 2 - Canopy carbon fluxes in paddy and rainfed rice

$P \leq 0.05$ . All variables were tested for normal distribution (Shapiro–Wilk–test) and homogeneity of variance (Levene–test). The sample sizes were same for both rainfed and paddy rice, hence we performed student t–test. Factor interactions were examined through regression analyses using the Pearson correlation test.

### 2.4. Results

#### 2.4.1. Microclimate

Weather conditions during the growing season are summarized in Figure 2.1. The daily mean maximum solar radiation during the measurement period occurred in July and was  $25 \pm 1$  MJ m<sup>-2</sup> d<sup>-1</sup> in July (Figure 2.1a). During NEE measurements using the transparent chambers, the light environments inside and outside the chambers were not significantly different. Inside the transparent chambers, the maximum PAR recorded during the measurements ranged between 1500 and 1800  $\mu\text{mol m}^{-2} \text{s}^{-1}$ . Air temperature increased steadily from 8°C in spring, to a maximum of 31°C in August (Figure 2.1b). Leaf temperatures were significantly different ( $p < 0.01$ ) between paddy and rainfed systems, but in each case the maximum temperatures of around 36°C in paddy field and 38°C in rainfed field, were attained in August. The total amount of rainfall between May and September was 1028 mm (Figure 2.1c). Most of the rainfall occurred during late June to July, associated with the summer monsoon and in September. VWC in the rainfed field ranged between 37.2 and 54.8% (Figure 2.1d), whereas the soils in the paddy were water-logged throughout the growing season. Relative humidity (rh) was significantly higher ( $p < 0.01$ ) in paddy rice than rainfed rice. The lowest rh occurred in August. Noon time average of rh was  $78 \pm 1.4\%$  in paddy rice and  $53 \pm 2.3\%$  in rainfed rice. Consequently, the mean daily vapor pressure deficit (VPD) was significantly lower ( $p < 0.01$ ) in paddy rice than rainfed field. The highest averaged day-time VPD values during our measurements occurred in July with  $1.62 \pm 0.58$  kPa for paddy rice and in August with  $2.83 \pm 0.93$  kPa for rainfed rice (Figure 2.1d).

Chapter 2 - Canopy carbon fluxes in paddy and rainfed rice

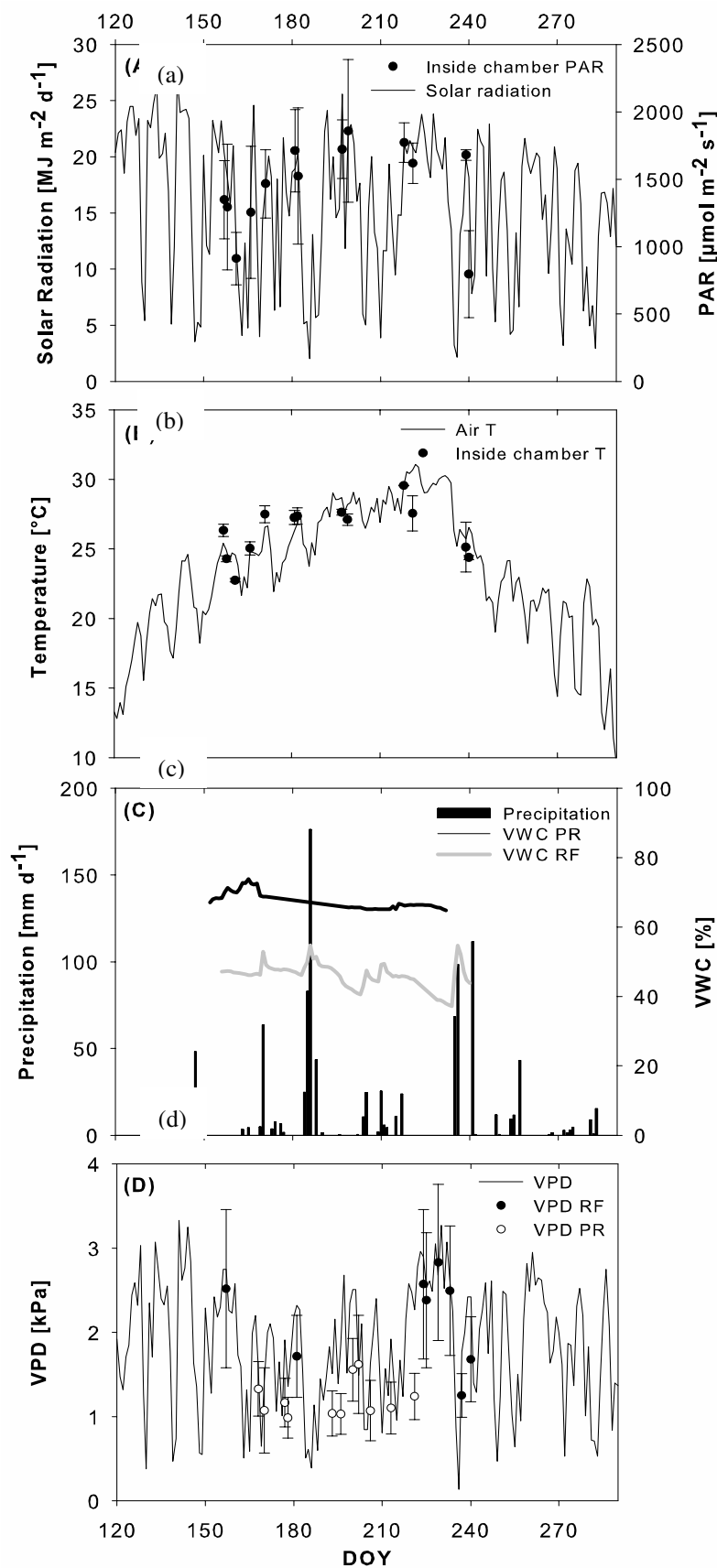


Figure 2.1

## Chapter 2 - Canopy carbon fluxes in paddy and rainfed rice

**Figure 2.1** Daily solar radiation measured at 2 m height and photosynthetic active radiation (PAR) measured at 50 cm height above the vegetation inside the transparent CO<sub>2</sub> flux chambers, respectively, b) mean air temperature at 2 m height outside and at 20 cm height inside the chambers, c) volumetric water content (SWC) within 30 cm soil profile and daily precipitation, and d) mean daily vapor pressure deficit (VPD) at 2 m height in the open location, at 1 m above the paddy rice (VPD paddy rice) and rainfed rice (VPD rainfed rice), respectively.

### 2.4.2. Daily and seasonal patterns of ecosystem CO<sub>2</sub> uptake

Examples of daily patterns of NEE and R<sub>eco</sub> for three selected days corresponding to early (DOY 182/181), mid (DOY 218/221) and mature (DOY 240/239) growth stages in paddy/rainfed rice, respectively, are shown in Figure 2.2. On clear, sunny days, the maximum NEE during the day were recorded between 10h–14h, with lower rates recorded during the earlier or later part of the day. R<sub>eco</sub>, however, remained relatively constant during the day.

The mean maximum NEE rates during the vegetative period were  $-19.9 \pm 0.1$  and  $15.0 \pm 3.2$   $\mu\text{mol m}^{-2} \text{s}^{-1}$  for paddy rice and rainfed rice, respectively (Figure 2.2), while the respective maximum R<sub>eco</sub> rates during the same period were  $5.9 \pm 0.1$  and  $28.6 \pm 0.8$   $\mu\text{mol m}^{-2} \text{s}^{-1}$ . In both treatments, the timing of the peak NEE and R<sub>eco</sub> coincided with the maximum green leaf area index (GLAI), occurring in July and August for the paddy and rainfed rice, respectively. The maximum integrated NEE (NEE<sub>int</sub>) were  $-8.0$  and  $-3.3$   $\text{g C m}^{-2} \text{d}^{-1}$  in the paddy and rainfed rice, respectively. NEE<sub>int</sub> was consistently, significantly higher in the paddy than in the rainfed (Figure 2.3b). The daily integrated GPP (GPP<sub>int</sub>) increased during the growing period, attaining its maximum rates of  $11.1$   $\text{g C m}^{-2} \text{d}^{-1}$  in the paddy and  $14.3$   $\text{g C m}^{-2} \text{d}^{-1}$  in the rainfed, in July and August, respectively (Figure 2.3a).

Unlike NEE, the NPP (a measure of net plant C exchange) of paddy plot and rainfed plot were not significantly different and the seasonal patterns were relatively, except for the one month delay in peak NPP in the rainfed rice compared to paddy rice (Figure 2.3c). The maximum integrated NPP (NPP<sub>int</sub>) were  $8.2$   $\text{g C m}^{-2} \text{d}^{-1}$  in paddy rice and  $10.3$   $\text{g C m}^{-2} \text{d}^{-1}$  in rainfed rice (Figure 2.3c).

## Chapter 2 - Canopy carbon fluxes in paddy and rainfed rice

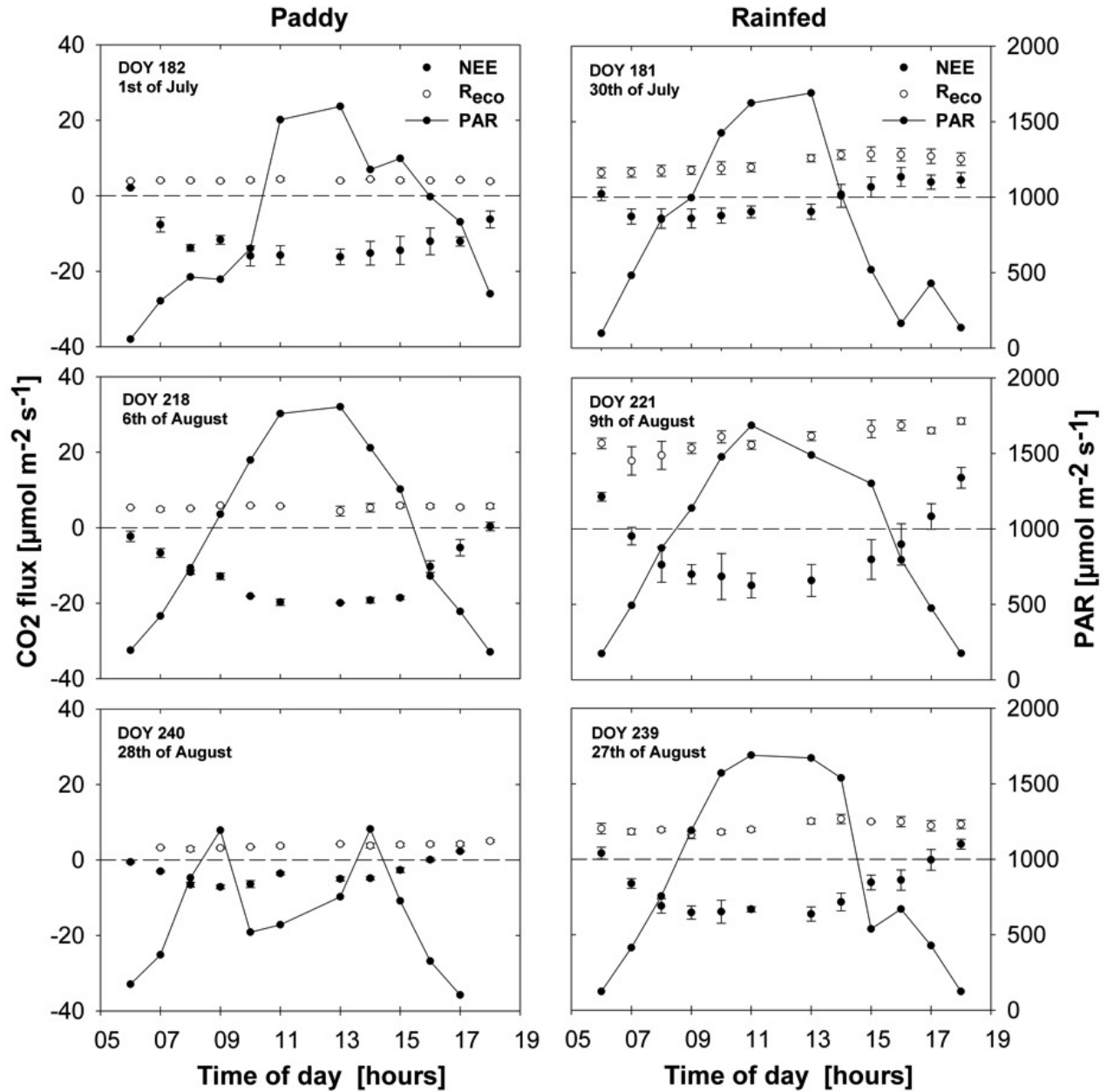


**Figure 2.2** Daily trends of NEE and  $R_{\text{eco}}$  in paddy rice (left panel) and rainfed rice (right panel), with light intensities (PAR, black line) on selected days during the development period. Data points are means of respective fluxes measured on the four collar plots.

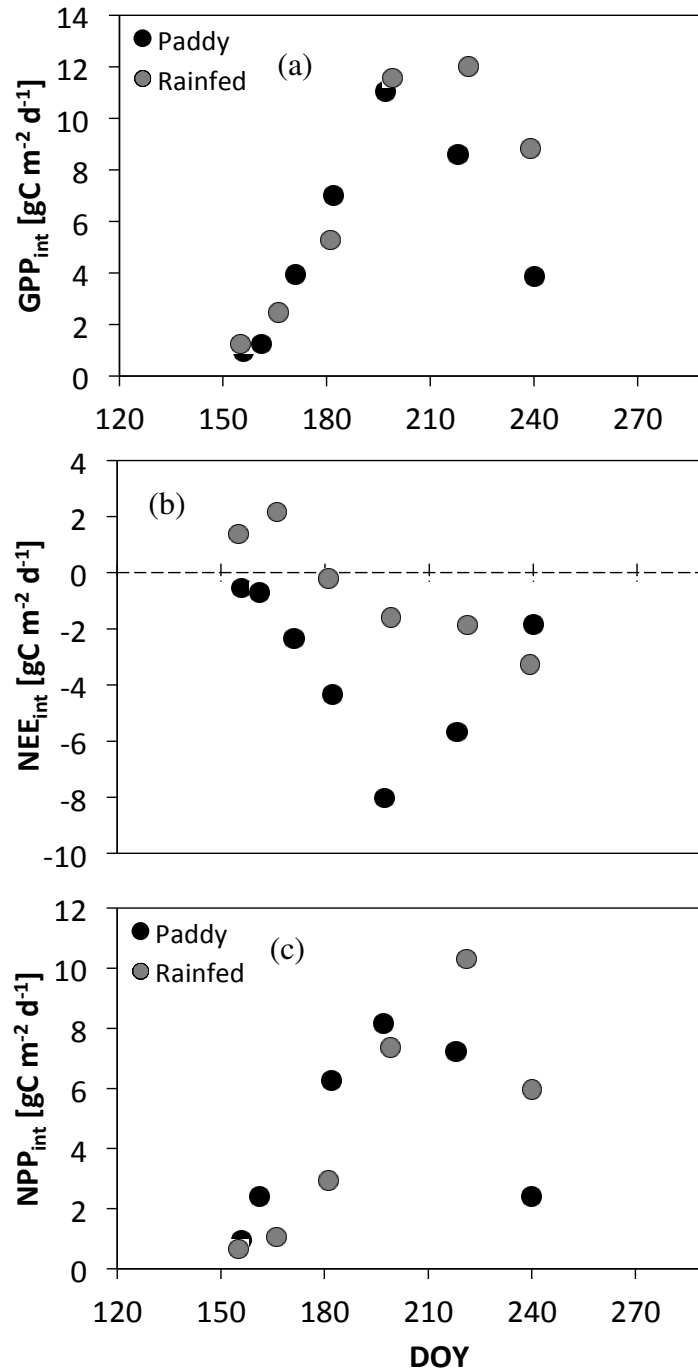


**Figure 2.3** Seasonal changes in a) daily gross primary production ( $GPP_{int}$ ), b) daily net ecosystem exchange ( $NEE_{int}$ ) and c) net primary production ( $NPP_{int}$ ) of paddy (black circles) and rainfed rice (grey circles) derived from  $\alpha$  and  $\beta$  of the hyperbolic light response curve (Table 2.2).

More than 80% of the daily fluctuations in GPP, both in the paddy and rainfed rice (Figure 2.4), were explained by PAR. The functional relationship between GPP and PAR was, therefore, used to derive canopy physiological parameters for describing canopy physiology

## Chapter 2 - Canopy carbon fluxes in paddy and rainfed rice

at different stages of crop developmental (Table 2.2). Simulated potential maximum canopy GPP at saturating PAR ( $= 1500 \mu\text{mol m}^{-2} \text{s}^{-1}$ ), i.e.  $((\beta+\gamma)_{1500})$  were 25.3 and 27.4  $\mu\text{mol m}^{-2} \text{s}^{-1}$  in paddy plot and rainfed plot, while the respective maximum quantum yields (or light use efficiency,  $\alpha$ ) were -0.047 and -0.098  $\mu\text{mol m}^{-2} \text{s}^{-1}$ .

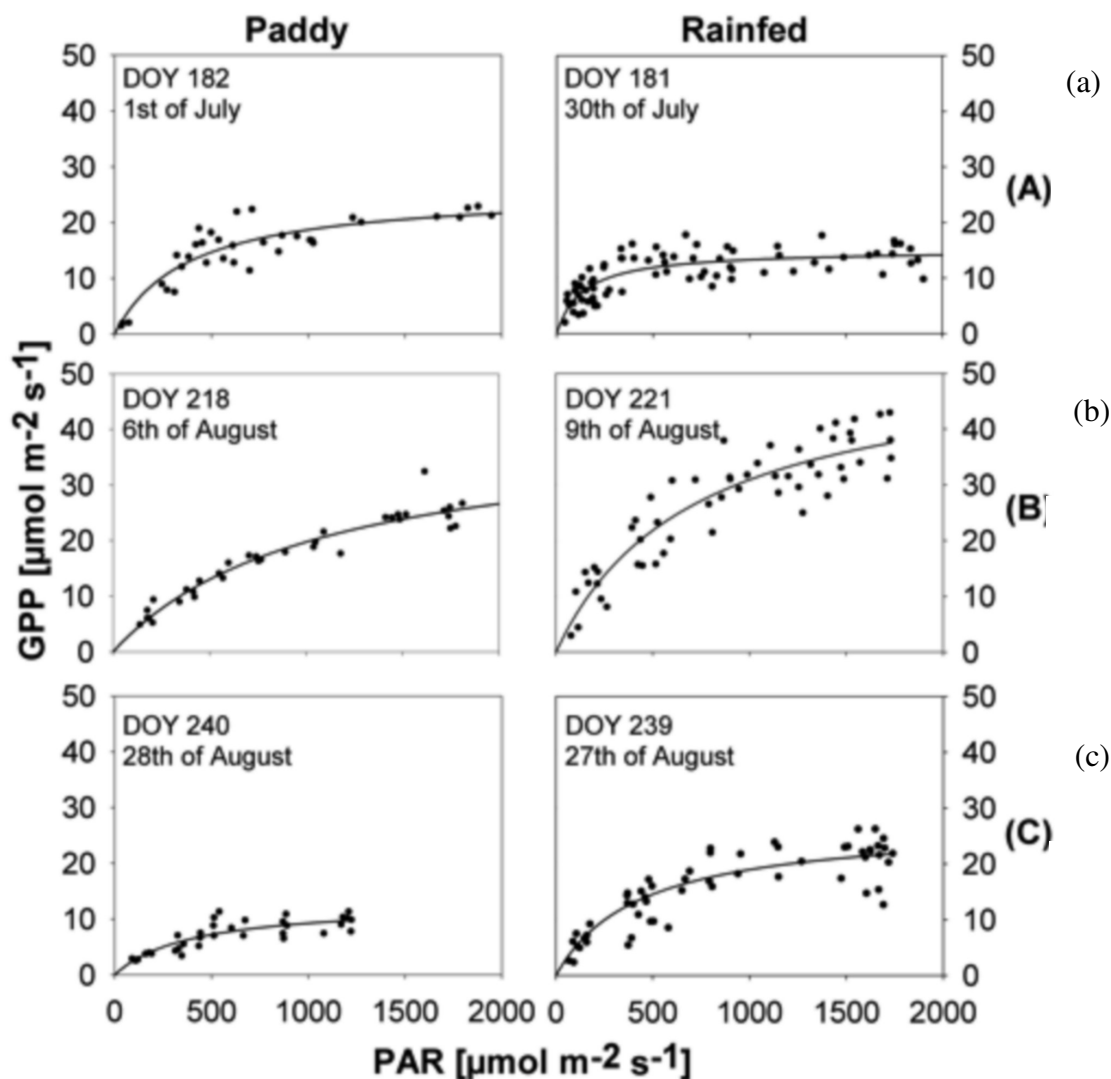


**Figure 2.4** Response of CO<sub>2</sub>-Assimilation to changing light intensities of paddy (black circles) and rainfed (grey circles) rice representing three distinct phenological stages (line a—initial growth season, line b—mid season, line c—maturity season) during the development of the rice crop.

## Chapter 2 - Canopy carbon fluxes in paddy and rainfed rice

**Table 2.2** Quantum yield ( $\alpha$ ), Potential maximum GPP and the coefficient of determination ( $R^2$ ) of the relation between NEE and PAR in A) paddy and B) rainfed rice in 2013.

DOY	$\gamma$	S. E.	$\alpha$	S. E.	$\beta$	S. E.	$R^2$	$(\beta+\gamma)_{1500}$
<b>A) PR</b> 158	0.66	0.04	-0.006	0.001	-3.51	0.22	0.96	2.56
161	0.83	0.04	-0.007	0.001	-8.71	1.32	0.89	4.70
171	2.45	0.26	-0.019	0.002	-18.32	6.53	0.96	11.17
182	4.15	0.28	-0.036	0.008	-25.27	1.16	0.97	17.20
197	4.70	0.40	-0.047	0.007	-39.59	3.43	0.95	25.31
218	4.50	0.23	-0.035	0.003	-39.50	2.74	0.97	22.40
240	3.15	0.23	-0.025	0.005	-13.53	1.90	0.85	9.95
<b>B) RF</b> 157	4.06	1.04	-0.009	0.010	-3.47	0.70	0.86	2.77
166	7.16	0.47	-0.011	0.002	-14.24	1.71	0.93	7.51
181	7.85	0.16	-0.047	0.005	-15.21	0.56	0.97	12.52
199	15.40	0.29	-0.098	0.012	-29.79	1.19	0.99	24.76
221	15.69	0.36	-0.090	0.012	-34.34	0.53	0.97	27.38
239	8.62	0.28	-0.055	0.006	-30.04	1.55	0.95	21.98

### 2.4.3. Biomass, leaf area and leaf N content

The total aboveground biomass (leaves, stems and grain) were  $1.85 \pm 0.27$  and  $2.16 \pm 0.28$  kg m<sup>-2</sup> of which  $0.24 \pm 0.06$  and  $0.31 \pm 0.05$  kg m<sup>-2</sup> were apportioned to the leaves in the paddy and the rainfed, respectively. Peak biomass was attained in July in the paddy fields, while it occurred a month later in the rainfed field, coinciding with the respective peak green leaf area index (GLAI) of  $5.4 \pm 1.1$  and  $4.9 \pm 0.5$  m<sup>2</sup> m<sup>-2</sup> (Figure 2.5a, b). Total crop yield (harvested grain) was  $1.19 \pm 0.10$  and  $1.16 \pm 0.09$  kg m<sup>-2</sup>, which was equivalent to  $6.61 \pm 0.22$  and  $5.99 \pm 0.68$  t ha<sup>-1</sup> in the paddy and rainfed rice, respectively. While rainfed fields had 0.62 t ha<sup>-1</sup> more yield than the paddy, the two were not significantly different. We however, observed significant differences between two cropping system in their C allocation patterns (i.e. allocation to the leaf, stem and grain) (see Table 2.3). During the early stages of growth, a large proportion of carbon was directed to leaf development both in two systems. At maturity, grains accounted for 64.4 and 53.9% of the total aboveground biomass in paddy and rainfed rice, respectively. Leaf N content was significantly higher in the rainfed than flooded rice and leaf N content declined with age (Table 2.3).

## Chapter 2 - Canopy carbon fluxes in paddy and rainfed rice

**Table 2.3** Percentage of carbon allocated in the aboveground biomass for the respective crop organ and leaf nitrogen content in paddy and rainfed rice.

	DOY	Leaf-C [%]	Culm-C [%]	Grain-C [%]	Leaf-N [%]
<b>A) Paddy Rice</b>	158	65.52	34.48		4.41
	161	59.96	40.04		4.64
	171	45.66	54.34		2.88
	182	48.94	51.06		3.12
	197	28.93	71.07		2.77
	218	15.28	39.39	45.33	2.58
	240	6.34	29.27	64.39	1.42
<b>B) Rainfed Rice</b>	157	62.50	37.50		5.24
	166	65.00	35.00		4.79
	181	32.54	67.46		4.39
	199	36.03	63.97		3.72
	221	22.07	58.20	19.74	3.58
	239	10.96	35.10	53.89	3.05



## Chapter 2 - Canopy carbon fluxes in paddy and rainfed rice

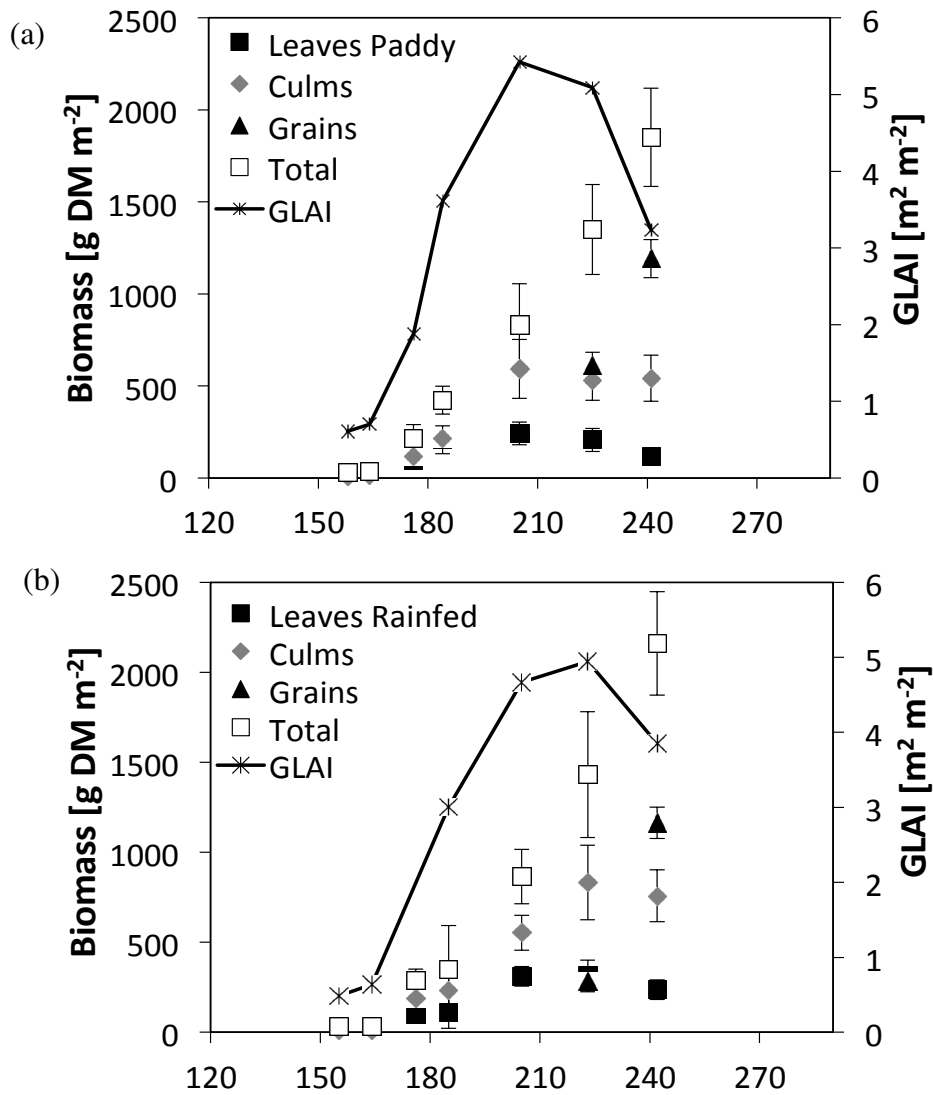


**Figure 2.5** Dry weight [g DM m<sup>-2</sup>] of leaves, culms, grains, tuber, and green leaf area (GLAI) of the CO<sub>2</sub>-measurement chambers during crop development in a) paddy and b) rainfed rice. Harvest was done after the CO<sub>2</sub> plot measurements.

### 2.4.4. Regulation of CO<sub>2</sub> uptake

At any time during the growing period, the maximum GPP rates ( $GPP_{max}$ ) on a clear sunny day were linearly correlated ( $R^2 = 0.87$  and  $0.98$ , for paddy and rainfed rice, respectively) with GLAI (Figure 2.6a) and  $\alpha$  ( $R^2 = 0.89$  and  $0.96$ ) (Figure 2.6b). Also,  $\alpha$  was positively correlated ( $R^2 = 0.93 - 0.94$ ) with GLAI (Figure 2.6c). Compared to flooded rice, rainfed rice demonstrated higher light use efficiency at higher GLAI. In both two cropping systems,  $\alpha$  was also sensitive to leaf N content and increased at higher leaf N content ( $R^2 = 0.86 - 0.99$ ,

Figure 2.6d).

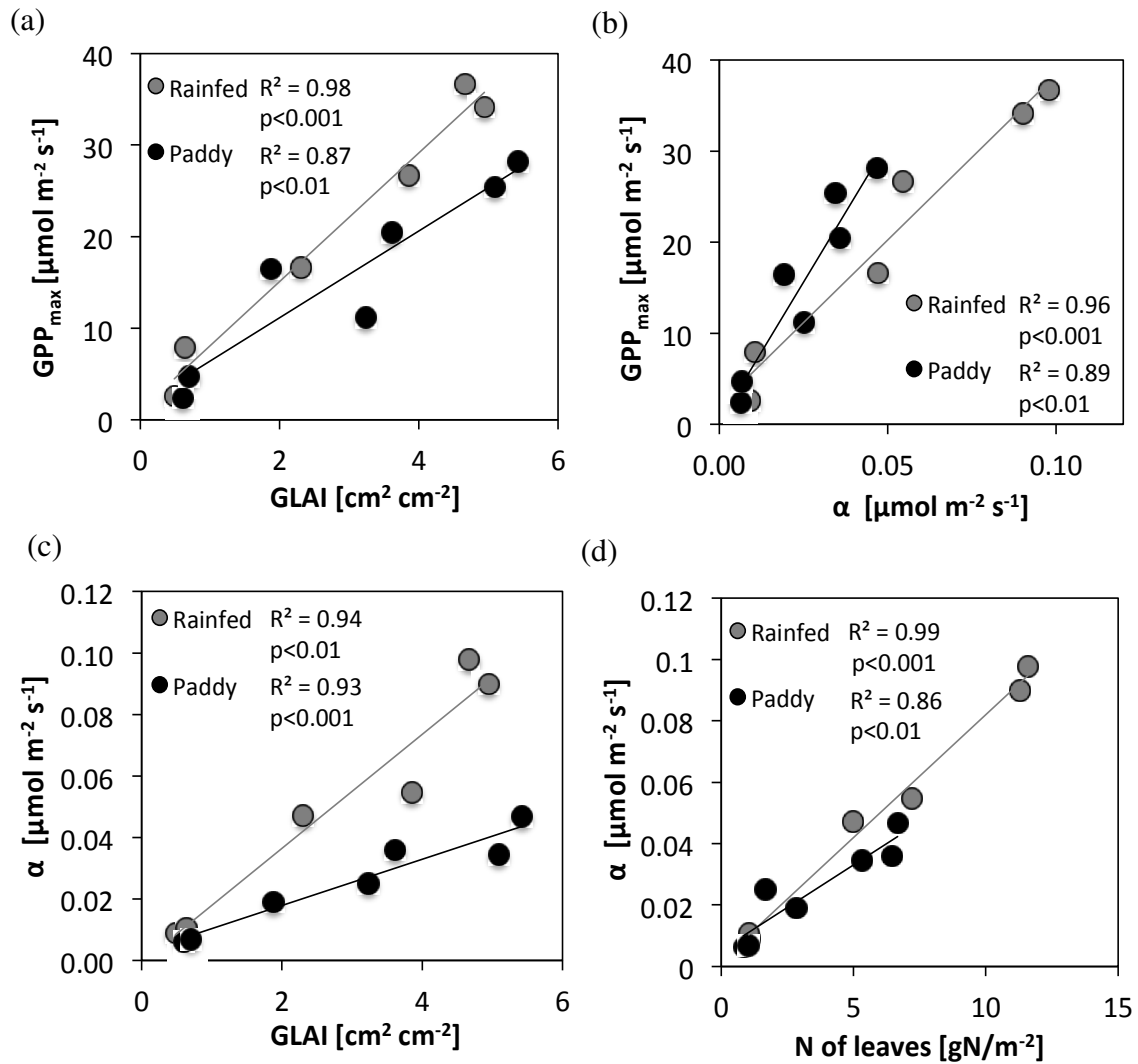


**Figure 2.6**  $GPP_{max}$  response to a) green leaf area index (GLAI) and b) light use efficiency ( $\alpha$ ), while c) describes the changes in  $\alpha$  in response to changing GLAI and d) the influence of leaf nitrogen (N) on light use efficiency ( $\alpha$ ) in the rainfed and paddy rice.

### 2.5. Discussion

In paddy rice production, the common practice is to raise seedlings in seedbeds before transplanting them into flooded fields, a process which requires 3 – 4 weeks (Cabangon et al., 2002). In the meantime, the prepared fields are flooded with water, awaiting seedling transplantation. Water loss through seepage and percolation during this period is estimated at 25 mm d<sup>-1</sup>, while evaporation accounts for 2 mm d<sup>-1</sup> (Tuong and Bouman, 2003). Direct

## Chapter 2 - Canopy carbon fluxes in paddy and rainfed rice

seeding as in rainfed field removes the need for irrigation and the idle period during land preparation (Bhuiyan et al., 1995), but the growing period is longer compared to the paddy rice (see Table 2.1). The amount of saved water, therefore, will depend on the balance between the reduction in water use caused by shortened land preparation and the increase in water use caused by the long vegetation period (Cabangon et al., 2002). Our study was, however, limited in capacity and could not provide these details. On the other hand, direct-seeded rice was planted earlier in the field compared to paddy rice. The amount of rainfall received between the two out-planting periods was 63.9 mm. Given an evapotranspiration rate of  $1.2 \text{ mm d}^{-1}$  for a young rainfed field (Nay-Htoon et al., in prep.), we deduce that 52.6% of this rainwater was put to productive use. Early establishment of rice, therefore, promotes better use of early season rainfall, and maybe associated with improved yield and reliability.

A characteristic of paddy rice fields is the prevailing high humidity and low VPD above the rice canopy (Alberto et al., 2009), which supports full stomatal opening during midday, when radiation is at its peak. This ensures maximum  $\text{CO}_2$  assimilation and GPP rates at a time when transient water stress due to high VPD negatively affects  $\text{CO}_2$  uptake by the vegetation as a result of stomatal closure in most terrestrial plants (Wopereis et al., 1996; Alberto et al., 2009). The mean maximum VPD measured in the flooded field was 1.62 kPa compared to 2.83 kPa in the rainfed field. VPD differences between the two fields, however, had no significant influence on leaf photosynthesis and canopy GPP (Figure 2.2). Instead, canopy GPP (Figure 2.3a) in both two systems attained and sustained saturation rates during most of the bright sunny days. In both cases, more than 80% of the daily GPP fluctuations were explained by PAR (Figure 2.4). Thus, we can speculate that, despite growing on non-saturated soils, root water uptake by rainfed rice is potentially adequate to sustain the maximum photosynthesis, under the environmental conditions similar to ours. This is demonstrated by similar NPP between two systems during the growing period (Figure 2.3c). It is however not clear why development stops and maturity attained earlier in the rainfed crops.

## Chapter 2 - Canopy carbon fluxes in paddy and rainfed rice

While significant drop in SWC within the top 30 cm soil profile were recorded in rainfed rice (Figure 2.1c), the plants did not show signs of water stress. Possible reasons include 1) extensive rooting system that access stable soil moisture below 30 cm depth (Kato et al., 2006b; Kato et al., 2007), 2) large root biomass (Kato et al., 2006a) and 3) osmotic adjustment that facilitate effective water uptake from the drying soil (Munns, 1988). Such adjustments, which promote improved soil water uptake, however, shift C from the aboveground organs and were likely to lower yield in rainfed rice (Munns et al., 1988). Alberto et al. (2013) reported maximum GPP rates of  $30 \mu\text{mol m}^{-2} \text{s}^{-1}$  under moderate VPD, while GPP was not sensitive to declining SWC within the top 10 cm soil profile, as long as SWC in deeper soil layers ( $> 15 \text{ cm}$ ) was  $> 21\%$ . They attributed such responses to large root biomass located in the soil layers deeper than  $> 15 \text{ cm}$ . In our case, the maximum GPP recorded for paddy rice was  $26.7 \mu\text{mol m}^{-2} \text{s}^{-1}$  compared to  $43.1 \mu\text{mol m}^{-2} \text{s}^{-1}$  in rainfed rice (Figure 2.4). GPP rates reported previously for Asian paddy rice range between 10 and  $56 \mu\text{mol m}^{-2} \text{s}^{-1}$  (Miyata et al., 2000; Campbell, 2001; Saito et al., 2005), while the rates reported for rainfed rice in Asia range from  $4 - 40 \mu\text{mol m}^{-2} \text{s}^{-1}$  (Alberto et al., 2009, 2013; Centritto et al., 2009). Given that NPP were not significantly different between two cropping systems, lower GPP in the paddy rice compared to rainfed rice in our study was partly due to lower  $R_{\text{eco}}$  measured in the paddy rice field (ref. Eq. 2.1). It is likely that a significant amount of  $\text{CO}_2$  generated from root and soil respiration was lost in the water column and was not registered by the analyzer. Diffusion rate of gases in the flooded compared to dry soils is 100 times lower, leading to reduced gas exchange between root tissues and the atmosphere (Armstrong and Drew, 2002).

In paddy rice, GPP is positively correlated with the aboveground biomass until maturity (Campbell et al., 2001, Alberto et al., 2013). This implies that the bulk of the NPP is allocated in the aboveground biomass (Smith et al., 2010), unlike in the rainfed system, where root development is also critical. Surprisingly, the maximum aboveground biomass recorded in rainfed field was  $2400 \text{ g m}^{-2}$  compared to  $1800 \text{ g m}^{-2}$  in the flooded field (Figure 2.5). The

## Chapter 2 - Canopy carbon fluxes in paddy and rainfed rice

need for structural support in the rainfed rice could be one reason for higher C allocation to the culms compared to paddy rice, which partially relies on hydrostatic support of the standing water. Approximately 13% of the total aboveground biomass was allocated to the leaves in paddy rice compared to 29% in rainfed rice. The higher leaf mass in rainfed rice was predominantly due to increased leaf thickness as opposed to leaf area (higher specific leaf weight), since GLAI were not significantly different between them (Figure 2.5). This could be a strategy in rainfed rice to increase photosynthetic efficiency, while checking on run-away transpiration. Due to this high leaf biomass, rainfed rice potentially could perform higher productivity, contributing to the observed higher GPP. It is likely that a large portion of this productivity is invested in securing sufficient soil water uptake (Munns et al., 1988). Higher GPP in rainfed rice is supported by the higher specific leaf weight, higher leaf N content (Table 2.3) and higher quantum yield. That the total yield between two systems were not significantly different, despite significant differences in GPP was not surprising. We speculate that in addition to investing proportionately large amount of C in structural support of the erect stems, rainfed rice invested a significant amount of carbon in order to improve root water uptake through increased root biomass and osmotic adjustment. This needs further investigations and we recommend more studies along these lines.

The yield in rain fed rice currently stands at 2.3 t/ha (Toung and Bouman, 2003), but drought-resistant cultivars produced yield levels of 5 – 6 t ha<sup>-1</sup>. Bouman et al. (2007) calculated that the country-average paddy rice yields in Asia ranges between 3 and 9 t ha<sup>-1</sup>, with an overall average of about 5 t ha<sup>-1</sup>. Alberto et al. (2009), Frageria and Baligar (2001) reported an average grain yield of 5.2 – 6.3 t ha<sup>-1</sup> for paddy rice. Peng et al. (2006) found minor reduction in yields in rainfed rice compared to paddy rice, with 6.32 and 7.78 t ha<sup>-1</sup>, respectively, and no significant differences in yield (7.22 t ha<sup>-1</sup> for the rainfed and 7.84 t ha<sup>-1</sup> for the paddy) of a variety that was adapted to both flooded and aerobic conditions. These values are comparable to our results. The results demonstrate that under ample soil moisture supply both flooded rice and rainfed rice develop relatively similar canopies and comparable yield.

## **Chapter 2 - Canopy carbon fluxes in paddy and rainfed rice**

### **2.6. Conclusion**

We conclude that with adequate rainfall, the new hybrid Unkwang rice variety has the potential to grow as direct seeded, rainfed rice, attaining yields that are comparable to paddy conditions. When grown as rainfed rice, Unkwang exhibits higher GPP, but it is likely that a significant portion of this GPP is apportioned to the roots to ensure improved water uptake. Improved leaf N and higher specific leaf weight result into higher quantum yield, contributing to improved productivity in the paddy rice. On a daily basis, PAR determined the daily fluctuations in GPP while seasonal GPP differences were due to GLAI and  $\alpha$  differences. While direct seeding as in the rainfed field eliminates the need for irrigation, maximizes the use of early rain events and is likely to require less water, it extends the production period. This study demonstrates the potential of Unkwang as a high yielding variety suitable for promoting rice production under rainfed conditions without extended soil drying. We recommend further studies to determine the amount of water that can be saved through using Unkwang cropped under rainfed conditions.

### **2.7. Acknowledgements**

This study was carried out as part of the International Research Training Group TERRECO (GRK 1565/1) funded by the Deutsche Forschungsgemeinschaft (DFG) at the University of Bayreuth, Germany and the Korean Research Foundation (KRF) at Kangwon National University, Chuncheon, S. Korea. We gratefully acknowledge the technical assistance of Ms. Margarete Wartinger for all her support in the field and laboratory. We also thank Mr. Seung-Hyun Jo, Mr. Seung-taek Jeong, Mr. Toncheng Fu and Ms. Mi-jeong Kim who provided a lot of help during field measurements and sample processing.

### **2.8. References**

Alberto, M.C.R., Wassmann, R., Hirano, T., Miyata, A., Kumar, A., Padre, A. and Amante, M.  
2009. CO<sub>2</sub>/heat fluxes in rice fields: Comparative assessment of flooded and non-flooded

## Chapter 2 - Canopy carbon fluxes in paddy and rainfed rice

- fields in the Philippines. *Agriculture and Forest Meteorology*, 149, 1737–1750.
- Alberto, M.C.R., Buresh, R.J., Hirano, T., Miyata, A., Wassmann, R., Quilty, J.R., Correa, T.Q. and Sandro, J. 2013. Carbon uptake and water productivity for dry-seeded rice and hybrid maize grown with overhead sprinkler irrigation. *Field Crop Research*, 146, 51–65.
- Armstrong, W. and Drew, M.C. 2002. Root growth and metabolism under oxygen deficiency. In: Waisel, Y., Eshel, A., Kafkafi, U. (eds.), *Plant Roots: The Hidden Half*, 3rd ed. Marcel Dekker, New York, pp. 729–761.
- Barker, R., Dawe, D., Tuong, T.P., Bhuiyan, S.I. and Guerra, L.C. 1999. The outlook for water resources in the year 2020: challenges for research on water management in rice production. In: *Assessment and Orientation towards the 21st Century. Proceedings of 19th session of the International Rice Commission*, Cairo, Egypt, 7–9 September 1998. Rome, Italy: FAO. 96–109.
- Bouman, B.A.M., Lampayan, R.M. and Tuong, T.P. 2007. *Water management in irrigated rice: coping with water scarcity*. Los Baños (Philippines): International Rice Research Institute. 54 p.
- Busch, J. 2001. Characteristic values of key ecophysiological parameters in the genus *Carex*. *Flora*, 196, 405–430.
- Bhuiyan, S.I., Sattar, M.A. and Khan, M.A.K. 1995. Improving water use efficiency in rice irrigation through wet seeding. *Irrigation Science*, 16, 1–8.
- Cabangon, R.J., Tuong, T.P. and Abdullah N.B. 2002. Comparing water input and water productivity of transplanted and direct-seeded rice production systems. *Agriculture Water Management*, 57, 11–31.
- Campbell, C.S., Heilman, J.L., McInnesa, K.J., Wilson, L.T., Medley, J.C., Wu, G. and Cobos, D.R. 2001. Diel and seasonal variation in CO<sub>2</sub> flux of irrigated rice. *Agricultural and Forest Meteorology*, 108, 15–27.
- Centritto, M., Lauteri, M., Monteverdi, C.M. and Serraj, R. 2009. Leaf gas exchange, carbon isotope discrimination, and grain yield in contrasting rice genotypes subjected to water deficits during the reproductive stage. *Journal of Exponential Botany*, 60, 2325–2339.
- Colmer, T.D., Gibberd, M.R., Wiengweera, A. and Tinh, T.K. 2003. The barrier to radial

## Chapter 2 - Canopy carbon fluxes in paddy and rainfed rice

- oxygen loss from roots of rice (*Oryza sativa* L.) is induced by growth in stagnant solution. Journal of Exponential Botany, 49, 1431–1436.
- Fageria, N.K. and Baligar, V.C. 2001. Lowland rice response to nitrogen fertilization. Soil Science and Plant Analysis, 32, 1405–1429.
- IPCC, 2008. Appendix A to the Principles Governing IPCC Work. Geneva: Intergovernmental Panel on Climate Change, first edition 1999, last amended 2008 (<http://ipcc.ch/pdf/ipcc-principles/ipcc-principles-appendix-a.pdf>)
- IRRI, 2002. Progress toward developing resilient crops for drought-prone areas– Abstracts of the workshop May 27–30, 2002. Los Banos, Philippines <http://www.irri.org/publications/limited/pdfs/ResilientCrops.pdf>
- Kato, Y., Kamoshita, A., Yamagishi, J. and Abe, J. 2006a. Growth of three rice (*Oryza sativa* L.) cultivars under upland conditions with different levels of water supply. I. Nitrogen content and dry matter production. Plant Production Science, 9, 422–434.
- Kato, Y., Abe, J., Kamoshita, A. And Yamagishi, J. 2006b. Genotypic variation in root growth angle in rice (*Oryza sativa* L.) and its association with deep root development in upland fields with different water regimes. Plant and Soil, 287, 117–129.
- Kato, Y., Kamoshita, A., Yamagishi, J., Imoto, H. and Abe, J. 2007. Growth of Rice (*Oryza sativa* L.) Cultivars under upland conditions with different levels of water supply 3. Root system development, soil moisture change and plant water status. Plant Production Science, 10, 3–13.
- Kim, K.Y., Ha, K.Y., Ko, J.C., Choung, J.I., Lee, J.K., Ko, J.K., Kim, B.K., Nam, J.K., Shin, S.S., Choi, Y.H., Kim, Y.D., Oh, M.K., Kim, Y.K., Kim, C.K. and Jung, K.Y. 2006. A new early maturity rice cultivar, “Unkwang” with high grain quality and cold tolerance. Korean Journal of Breeding, 38, 261–262.
- Kotula, L., Ranathunge, K. and Steudle, E. 2009. Apoplastic barriers effectively block oxygen permeability across outer cell layers of rice roots under deoxygenated conditions: roles of apoplastic pores and of respiration. New Phytologist, 184, 909–917.
- Lindner, S., Otieno, D., Lee, B., Xue, W., Arnhold, S., Kwon, H., Huwe, B. and Tenhunen, J. 2014. Carbon dioxide exchange and its regulation in the main agro–ecosystems of Haeen



## Chapter 2 - Canopy carbon fluxes in paddy and rainfed rice

- catchment in South Korea. *Agriculture, Ecosystem and Environment*, 199, 132–145.
- Lloyd, J. and Taylor, J.A. 1994. On the temperature dependence of soil respiration. *Functional Ecology*, 8, 315–323.
- McDonald, M.P., Galwey, N.W. and Colmer, T.D. 2002. Similarity and diversity in adventitious root anatomy as related to root aeration among a range of wetland and dryland grass species. *Plant Cell and Environment*, 25, 441–451.
- Miyata, A., Leuning, R., Denmead, O.T., Kim, J. and Harazono, Y. 2000. Carbon dioxide and methane fluxes from an intermittently flooded paddy field. *Agricultural and Forest Meteorology*, 102, 287–303.
- Moog ,P.R. and Brüggemann, W. 1998. Flooding tolerance of *Carex* species. II. Root gas–exchange capacity. *Planta*, 207, 199–206.
- Munns, R. 1988. Why measure osmotic adjustment? *Australian Journal of Plant Physiology*, 15, 717–726.
- Nay–Htoon, B., Xue, W, Dubbert, M., Lindner, S., Jeong, S., Fu, T., Kim, M., Cuntz, M., Ko, J., Tenhunen, J., Werner, Ch., in prep. Water use efficiency of rainfed and paddy rice (*Oryza sativa* L.): Is flux partitioning crucial to understand water use efficiency?
- Okami, M., Kato, Y. and Yamagishi, J. 2013. Grain yield and leaf area growth of direct–seeded rice on flooded and aerobic soils in Japan. *Plant Production Science*, 16, 276–279.
- Otieno, D., Lindner, S., Muhr, J. and Borken, W. 2012. Sensitivity of peatland herbaceous vegetation to vapor pressure deficit influences net ecosystem CO<sub>2</sub> exchange. *Wetlands*, 32, 895–905.
- Owen, K.E., Tenhunen, J., Reichstein, M., Wang, Q., Falge, E., Geyer, R., Xiao, X., Stoy, P., Ammann, C., Arain, A., Aubinet, M., Aurela, M., Bernhofer, C., Chojnicki, B.H., Granier, A., Gruenwald, T., Hadley, J., Heinesch, B., Hollinger, D., Knohl, A., Kutsch, W., Lohila, A., Meyers, T., Moors, E., Moureaux, C., Pilegaard, K., Saigusa, N., Verma, S., Vesala, T. and Vogel, C. 2007. Linking flux network measurements to continental scale simulations: ecosystem carbon dioxide exchange capacity under non–water–stressed conditions. *Global Change Biology*, 13, 734–760.

## Chapter 2 - Canopy carbon fluxes in paddy and rainfed rice

- Peng, S., Bouman, B., Visperas, R.M., Castañeda, A., Nie, L. and Park, H.K. 2006. Comparison between aerobic and flooded rice in the tropics: Agronomic performance in an eight-season experiment. *Field Crops Research*, 96, 252–259.
- R Core Team, 2012. R: a language and environment for statistical computing. R Foundation for Statistical Computing, Vienna. URL <http://www.R-project.org/>. ISBN 3-900051-07-0.
- Ranathunge, K., Kotula, L., Steudle, E. and Lafitte, R. 2004. Water permeability and reflection coefficient of the outer part of young rice roots are differently affected by closure of water channels (aquaporins) or blockage of apoplastic pores. *Journal of Exponential Botany*, 55, 433–447.
- Saito, M., Miyata, A., Nagai, H. and Yamada, T. 2005. Seasonal variation of carbon dioxide exchange in rice paddy field in Japan. *Agriculture and Forest Meteorology*, 135, 93–109.
- Smith, P., Lanigan, G., Kutsch, W.L., Buchmann, N., Eugster, W., Aubinet, M., Ceschia, E., Béziat, P., Yeluripati, J.B., Osborne, B., Moors, E.J., Brut, A., Wattenbach, M., Saunders, M. and Jones, M. 2010. Measurements necessary for assessing the net ecosystem carbon budget of croplands. *Agriculture, Ecosystem and Environment*, 139, 302–315.
- Sperry, J.S. 2000. Hydraulic constraints on plant gas exchange. *Agriculture and Forest Meteorology*, 104, 13–23.
- Tuong, T.P. and Bouman, B.A.M., 2003. *Rice Production in Water-scarce Environments*. IRRI, Manila, Philippines. ISBN 0851996698
- Wada, H., Masumoto-Kubo, C., Gholipour, Y., Nonami, H., Tanaka, F., Erra-Balsells, R., Tsutsumi, K., Hiraoka, K. and Morita, S. 2014. Rice chalky ring formation caused by temporal reduction in starch biosynthesis during osmotic adjustment under foehn-induced dry wind. *PLoS One*, 9(10).
- Wopereis, M.C.S., Kropff, M.J., Maligaya, A.R. and Tuong, T.P. 1996. Drought-stress responses of two lowland rice cultivars to soil water status. *Field Crops Research*, 46, 21–39.

## Chapter 3 - Canopy gain, water use and yield in paddy and rainfed rice

### Chapter 3

#### 3. Differentiation in paddy versus rainfed rice in factors influencing carbon gain, water use and grain yield under monsoon climate in South Korea

Wei Xue<sup>1,2</sup>, Steve Lindner<sup>1</sup>, Bhone Nay–Htoon<sup>3</sup>, Peter Harley<sup>1</sup>, Bernd Huwe<sup>4</sup>, Jonghan Ko<sup>5</sup>, Dennis Otieno<sup>1</sup>, Hiroyuki Muraoka<sup>6</sup>, Christiane Werner<sup>3,7</sup>, John Tenhunen<sup>1</sup>

<sup>1</sup>Department of Plant Ecology, University of Bayreuth, 95447 Bayreuth, Germany

<sup>2</sup>State Key Laboratory of Desert and Oasis Ecology, Xinjiang Institute of Ecology and Geography, Chinese Academy of Sciences, 830011 Urumqi, China

<sup>3</sup>Department of Agroecosystem Research, University of Bayreuth, 95447 Bayreuth, Germany

<sup>4</sup>Department of Soil Physics, University of Bayreuth, 95447 Bayreuth, Germany

<sup>5</sup>Department of Applied Plant Science, Chonnam National University, 500757 Gwangju, South Korea

<sup>6</sup>River Basin Research Center, Gifu University, 1–1 Yanagido, Gifu, 501–1193 Japan

<sup>7</sup>Department of Ecosystem Physiology, University of Freiburg, 79085 Freiburg, Germany

#### 3.1. Abstract

Our research is intended to disentangle relationships in eco–physiological factors responsible for variations in carbon gain, water use and yield in rice agro–ecosystems in order to advance the practical application of water–saving rice agriculture. Comparisons in leaf and canopy gas exchange between flooded and water–saving (rainfed) rice were conducted in a monsoon region of South Korea in 2013. Correlation between net primary production (NPP) and leaf area index (LAI) in the two cropping systems was essentially the same. Rainfed rice had lower photosynthetic N use efficiency resulted by significantly high proportion of nitrogen investment into non–photosynthetic components while, delayed grain–filling retained clearly higher leaf N which facilitated carbon gain (gross primary production, GPP) as compared to senescent paddy rice. Rainfed plants had markedly higher respiratory carbon ( $R_{\text{plant}}$ ) lost, resulting in narrowed facilitation effects brought by enhanced GPP. At flowering and

### Chapter 3 - Canopy gain, water use and yield in paddy and rainfed rice

grain-filling, the two cultures had compatible NPP, green biomass accumulation. However, compromised grain yield production by 10.2% in rainfed rice was registered due to a high proportion of unfilled spikelets occurring during prolonged non-rainfall periods, which was accompanied by strengthened stomatal limitation and leaf rolling that reduced carbon gain capacity. Intrinsic water use efficiency ( $WUE_i$ ) was constant and similar in two cropping cultures, but substantially increased under drying conditions due to pronounced stomatal closure. Photosynthetic sensitivity and water use efficiency were related to hydraulically constrained stomatal conductance.  $WUE_i$  was closely related to water availability with a large change occurring at soil matric potential ( $\psi_s$ ) at ca. -75 kPa and plant hydraulic conductance ( $k$ ) of  $5 \text{ mmol m}^{-2} \text{ s}^{-1} \text{ MPa}^{-1}$  that decreased carbon gain capacity. We conclude that intermittent occurrence of prolonged non-rainfall periods during the monsoon season will strongly hamper photosynthetic productivity in rainfed rice, which results partially due to lost in plant hydraulic conductance.

**Keywords:** Carbon balance, Water use, Hydraulic conductance, Leaf rolling, Rice, Yield

## **Chapter 3 - Canopy gain, water use and yield in paddy and rainfed rice**

### **3.2. Introduction**

The increasing probability of water scarcity due to changing global precipitation pattern and intensive competing demands for fresh water resources from growing domestic and industrial withdrawals especially in developing Asian countries which provide over half of the world's rice production, call for the initiation of water saving agricultural systems (IPCC, 2013) such as rainfed, continuous soil saturation, and flash—irrigation management practice (Bouman et al., 2005). Rainfed rice systems have been proposed as the most efficient among these field managements, due to significant less amount of water input and high production (Thanawong et al., 2014). The establishment of new breeding lines that will allow sustainable crop production (Araus et al., 2008) under rainfed conditions is based on the assumption that long-term evolution has in fact included potentials into the genetic inheritance of rice to cope with marginal oscillations in water supply (Jearakongman et al., 1995). Lowland rice planted in rainfed fields over several years resulted in relatively high photosynthetic productivity without compromising yield in Japan and Philippines as compared to flooded systems (Alberto et al., 2012; Kato et al., 2006; Katsura et al., 2010). These results suggest a parallel carbon uptake and similar net ecosystem production in the two cropping cultures (Alberto et al., 2009; 2012; 2013). Nevertheless, large fluctuations in grain yield production have also been registered in rainfed rice system (Bouman et al., 2005).

Uncertainties with respect to climate change, especially in the occurrence of infrequent but prolonged non-rainfall periods, and the need to extend rice production in other geographical regions emphasize the need to better understand in detail the ecophysiological response mechanisms related to the transfer of rice genotypes from wetland to dryland growth conditions. Shifts in the “behavior” of rice, e.g., shifts in ecosystem function in terms of carbon and water fluxes that influence determining rice crop development and yields (Campbell et al., 2001a; Lindner et al., 2015; McMillan et al., 2007), must be viewed as a high research priority. The differences in crop yield between paddy and rainfed rice that may be expected are due to multiple causes such as establishment (Rang et al., 2011), photosynthetic productivity and carbon allocation among plant organs (Niinemets, 2007), and

### **Chapter 3 - Canopy gain, water use and yield in paddy and rainfed rice**

their interactive influences.

Photosynthetic productivity which determines amount of available carbohydrate for growth and biomass accumulation is a predominant component influencing yield. Nitrogen use efficiency positively correlates to photosynthetic productivity (Hirel et al., 2001; Ju et al., 2015; Ladha et al., 1998; Sinclair and Horie, 1989), and has been proposed as one of key factors determining plant survival and establishment (Niinemets and Tenhunen, 1997; Feng, 2008). Nitrogen supplied in early growth could stimulate a initial burst in photosynthesis which eventually influences total leaf area throughout growth seasons (Murchie et al., 2005; Sinclair and Horie, 1989), and causally affects seasonal development of canopy carbon gain capacity. However, biomass accumulation and yield are not only determined by developing canopy structure and the potential for carbon uptake at seasonal dimension, rather soil water availability dynamically modifies response and dominates daily variations in intensity of crop carbon and water exchange.

Thus, the transfer of rice from paddy to a rainfed growth conditions requires carbon allocation and physiological adjustments that best avoid impacts of drying conditions. We can expect greater biomass allocation to roots in order to access wet soil layers (Fukai and Cooper, 1995; Osmont et al., 2007). On daily scale, limited exposure of leaf area and decline of stomatal conductance adjust leaf water potential and avoid catastrophic drought damage (Davatgar et al., 2009; Wopereis et al., 1996; Yu et al., 1998). Stomatal conductance shows cycling or oscillation between the open and closed conditions (Tenhunen, 1987) to optimize the conflicting requirement of CO<sub>2</sub> uptake and control of water loss (Cowan, 1982; Niinemets and Valladares, 2004).

In rice under drying conditions, assimilation rate declined in synchrony with stomatal conductance (Yoshida, 1981), inferring that carbon gain capacity is governed by stomatal conductance. Nevertheless, relative high transpiration rates were commonly observed during soil water depletion (Bouman et al., 2005; Tanguilig et al., 1987; Yoshida, 1981), which

### **Chapter 3 - Canopy gain, water use and yield in paddy and rainfed rice**

might expose rice plants to risk of xylem cavitation and lower hydraulic conductance. An increasing number of studies up to date reported a dependence of photosynthetic sensitivity on stomatal conductance linked to xylem hydraulic conductance in woody species (Franks, 2004; Hacke, 2014; Martorell et al., 2014). This may also be the case in crops (Locke and Ort, 2015) and such adjustments may largely influence water use efficiency, although there are few reported for field-grown rainfed rice (Davatgar et al., 2009; Stiller et al., 2003). We anticipate a positive regulation via momentary stomata oscillations during daytime and effective water compensation by the rooting systems in rainfed rice that will help to minimize soil drying impacts and optimize carbon gain and water use efficiency.

Studies of crop ecophysiology over the entire growth cycle and in natural field environment are essentially indispensable in order to better understand and sort out the multiple responses that regulate carbon gain and yield production (Alberto et al., 2013; Bhattacharyya et al., 2013; Niinemets and Keenan, 2012; Okami et al., 2013). Furthermore, identification of response characteristics that dominate in rice systems will be beneficial, not only for irrigation decision-making, but also to provide clarity in assumptions related to climate change effects, and in soil environment and rice ecosystem function. In our study, a single rice genotype was planted in two contrasting water regimes, i.e., with flooded paddy and rainfed cropping cultures. Gas exchange behavior and crop development were evaluated over an entire growing season via application of chamber flux measurements at leaf and stand level, assessments of biomass and nitrogen distribution, monitoring of water status in plant and soil matrix, and estimation of grain yield component, in order to address the following hypotheses:

- 1) Rice crops growing under rainfed versus irrigated conditions in the monsoon climate region of South Korea develop similarly with respect to canopy structure and nitrogen use, carbon gain and water use efficiencies.
- 2) For the same genotype, gas exchange process regulation in rice is unaffected by a change from paddy to rainfed field cultivation.
- 3) Similar nitrogen use, carbon gain and water use over the growth season under climate

## Chapter 3 - Canopy gain, water use and yield in paddy and rainfed rice

conditions in South Korea result because root systems and soil water storage are adequate to allow full daily recovery by rice plants during extended periods without rain.

### 3.3. Materials and methods

#### 3.3.1. Study site

Field research site was conducted at the agricultural fields of Chonnam National University, Gwangju, South Korea (126°53' E, 35°10' N, altitude 33 m) where over 60% of precipitation events occur from May to October during the monsoon season with an annual mean temperature of 13.8°C and annual mean precipitation of ~1391 mm during the past 30 years (1981–2010). Both paddy and rainfed rice fields had similar soil properties (gray lowland soil (Fluvisols), ratio of sand, silt and loamy 40: 37: 23) with total organic carbon 12.3 g kg<sup>-1</sup>, total nitrogen 1.0 g kg<sup>-1</sup>, available P (P<sub>2</sub>O<sub>5</sub>) 13.1 g kg<sup>-1</sup>, soil pH in H<sub>2</sub>O was 5.5 and approximation of bulk density of topsoil (0-12 cm) 0.8 g cm<sup>-3</sup> (RDA 2008). Seeds of Unkwang (*Oryza sativa* L. cv. Unkwang) were sown in a nursery on April 22, 2013 (DOY 110) and seedlings in 10 cm height were transplanted into a flooded field using an automatic rice planting machine on May 20, 2013 (DOY 140), with a row–line spacing of 12 × 30 cm. On average, 5 seedlings were planted in each hill. Fertilizer with a mass ratio of N–P–K of 11:5:6 was used in paddy rice to achieve an addition of 115 kg N ha<sup>-1</sup>. 80% of N fertilizer was applied two days before planting (May 18, DOY 138), and the rest at the tillering stage 19 days after transplanting (DOY 157). Seeds of same rice variant were directly sown into the soil on April 22 (DOY 112) in a field adjacent to the paddy field, applying fertilizer at the same level of 115 kg N ha<sup>-1</sup> at two times: 80% of total N before seeding and the rest on DOY 160. During growth no artificial water supply was provided in the rainfed field. All field managements reflected the practice of the farmers in the region.

#### 3.3.2. Measurement of meteorological factors and soil water content

Air temperature, relative humidity, precipitation and global radiation were continuously measured at 2 m height with an automatic weather station (AWS, WS-GP1, Delta-T Devices



### Chapter 3 - Canopy gain, water use and yield in paddy and rainfed rice

Ltd., UK) installed at the margin of the rainfed field. Meteorological variables were recorded every 5 minutes, averaged and achieved on a half-hourly basis. Volumetric soil water content (SWC,  $\text{m}^3 \text{m}^{-3}$ ) at 10 cm depth in the paddy field and at 10 and 30 cm depth in the rainfed field were measured at several locations close to the collars installed for canopy gas exchange measurement using EC-5 soil moisture sensors (Decagon, WA, USA). The sensors were installed during the initial growth stage and kept in the field throughout the season. Data were logged every 30 min using EM50 data-logger (Decagon, WA, USA) and calibrated based on actual soil water measurements conducted in the laboratory with the same soil.

#### 3.3.3. Measurements of leaf level gas exchange

A portable gas-exchange system (GFS-3000, Heinz Walz GmbH, Effeltrich, Germany) was used to measure net assimilation  $\text{CO}_2$  response curves at different leaf temperatures.  $\text{CO}_2$  response curves of uppermost canopy leaves were measured twice for the paddy rice, at around DOY 168 and around 214, and three times in the rainfed rice at around DOY 158, 182, and 239.  $\text{CO}_2$  curves were commenced after leaves had acclimated to the cuvette microenvironment ( $\text{CO}_2$  concentration of  $400 \mu\text{mol mol}^{-1}$  and saturating PAR of  $1500 \mu\text{mol m}^{-2} \text{s}^{-1}$ ) after which  $\text{CO}_2$  concentration was changed progressively according to the sequence 1500, 900, 600, 400, 200, 100 to  $50 \mu\text{mol mol}^{-1}$ . Relative humidity was controlled to ca. 60%. Net photosynthetic rate ( $A$ ) and stomatal conductance to  $\text{CO}_2$  ( $g_s$ ) data were recorded after new steady-state readings were obtained. At least three replicate  $\text{CO}_2$  curves were obtained at each leaf temperature, which was varied in  $5^\circ\text{C}$  steps from 20 to  $35^\circ\text{C}$  at initial growth stage and from 25 to  $35^\circ\text{C}$  at the grain-filling stage. For each  $\text{CO}_2$  response curve, the protocol described by Sharkey et al. (2007) was used to estimate carboxylase capacity,  $V_{\text{cmax}}$  and RuBP regeneration capacity,  $J_{\text{max}}$ . Additionally, ambient photosynthesis rate at near optimal temperature ( $A_{\text{max}}$  at  $400 \mu\text{mol CO}_2 \text{mol}^{-1}$ , saturating PAR of  $1500 \mu\text{mol m}^{-2} \text{s}^{-1}$  and  $30^\circ\text{C}$  which is close to optimal temperature best for photosynthesis) was measured in leaves of paddy rice at DOY 230 and rainfed rice at DOY 206.

### **Chapter 3 - Canopy gain, water use and yield in paddy and rainfed rice**

Apart from seasonal changes in leaf  $A_{\max}$  qualified by above measurements, insights in response of leaf gas exchange to varying meteorological factors and soil water depletion, and their sensitivity to plant water status under those conditions could be achieved by diurnal gas exchange measurements. Diurnal gas exchange measurements in the sunlit (uppermost) expanded leaves were conducted using the GFS-3000 system on DOY 177, 196, 213, and 221 in the paddy rice field. The measurement dates of diurnal courses of the sunlit (uppermost) leaves in the rainfed rice were DOY 157, 181, 202, 206, 224, 225, 229, and 240. Middle sections of two or three intact and healthy leaves were enclosed horizontally in the measurement cuvette from sunrise to sunset. Incident light intensity, air and leaf temperature, air humidity, and  $\text{CO}_2$  concentration were recorded simultaneously with gas exchange rates.

#### **3.3.4. Measurements of canopy level gas exchange and estimation of NPP and $R_{\text{plant}}$**

The daily course of canopy  $\text{CO}_2$  gas exchange was measured with a custom-built set of one transparent and one opaque chamber ( $L\ 39.5 \times W\ 39.5 \times H\ 50.5\ \text{cm}$ ; detailed information on chamber construction and measurement protocols are given in Li et al. (2008) and Lindner et al. (2015)) in the rainfed rice on DOY 157, 166, 181, 199, 221, and 239 and in the paddy rice on DOY 158, 166, 182, 197, 218, and 240 DOY. On 202 only transparent chamber measurement was carried out in rainfed field. Four plots in each field were established. The plots were accessed by raised walkways in the paddy field and the growing plants remained undisturbed. Four white plastic frames ( $L\ 38\text{cm} \times W\ 38\text{cm}$ ) that provided a sealing collar for the chambers were inserted into the soil down to 10 cm depth just after transplanting of seedlings in the flooded field, and after seedling establishment in the rainfed field, and were only removed after harvest at the end of growth season. Three frames, each enclosing three bundles of healthy plants, and a fourth frame without plants were deployed. Diurnal gas exchange courses of net ecosystem  $\text{CO}_2$  exchange ( $\text{NEE}$  – with transparent chamber), soil respiration ( $R_{\text{soil}}$  – with opaque darkened chamber in frame without plants) and ecosystem respiration ( $R_{\text{eco}}$  – with opaque darkened chamber in frame with plants) per square meter ground surface were intensively monitored from sunrise to sunset. Incident PAR in the transparent chamber was measured with a quantum sensor (LI-190, LI-COR, Lincoln,

### Chapter 3 - Canopy gain, water use and yield in paddy and rainfed rice

Nebraska, USA) and CO<sub>2</sub> concentration with a portable infra-red gas analyzer (LI-820, LI-COR, Lincoln, Nebraska, USA). Soil temperature in the soil profile at 10 cm depth was monitored concurrently. GPP estimation was conducted as following:

$$GPP = -NEE + R_{eco} = -NEE + R_{plant} + R_{soil} \quad (3.1)$$

Net primary production equivalent to canopy net assimilation rate (NPP), difference between gross primary production (GPP) and plant respiration ( $R_{plant}$ ), in the paddy and rainfed rice was therefore estimated from measured NEE and  $R_{soil}$  (Campbell et al., 2001a),

$$NPP = NEE + R_{soil} \quad (3.2)$$

where soil respiration was determined from a regression with respect to soil temperature ( $T_{soil}$ ), using the function of Lloyd and Taylor (1994), normalized to 15°C,

$$R_{soil} = R_{soilref} e^{E_0 \left( \frac{1}{T_{ref} - T_0} - \frac{1}{T_{soil} - T_0} \right)} \quad (3.3)$$

where  $T_{ref}$  and  $T_0$  are fixed to 15 and -46°C, respectively. As an absence of soil respiration measurement on 202 DOY,  $R_{soil}$  was supposed to approximate to that of 200 DOY.

A classical hyperbolic light response model was fit via a non-linear least square algorithm to estimate NPP as a function of incident PAR,

$$NPP = \frac{\beta \cdot \alpha \cdot PAR}{\beta + \alpha \cdot PAR} - \gamma \quad (3.4)$$

where,  $\alpha$  is initial slope of the light response curve,  $\beta$  provides NPP at a saturating level of PAR, and  $\gamma$  is y-axis intercept when PAR is close to 0. Data gaps in NPP during hourly measurement cycles were interpolated, using the parameterized light response curves and PAR data recorded at the automatic weather station. Similar hyperbolic light response model was also fit to estimate gross primary production (GPP; sum of NEE and  $R_{eco}$ ) as a function of incident PAR, to generate daily integrated gross primary production ( $GPP_{int}$ ).

## **Chapter 3 - Canopy gain, water use and yield in paddy and rainfed rice**

### **3.3.5. Measurement of diurnal courses of leaf water potential and degree of leaf rolling**

On the same measuring times as leaf gas exchange in July and August, daily courses for leaf water potential in the rainfed rice were measured with a pressure chamber (PMS Instruments, Corvallis, OR). Measurements were conducted hourly from sunrise to sunset. Healthy and well-exposed leaves in plant canopies were enclosed in a plastic bag before cutting and rapidly transferred into a pressure chamber. Moist tissue papers were inserted inside the chamber to minimize transpiration water loss during measurements. Once a leaf was fixed in the chamber, the chamber was slowly pressurized until water bead exude at the opposite, clean, severed end of the leaf. A regression describing correlation of leaf water potential with VPD, leaf temperature and PAR was used to estimate leaf water potential values at the times when leaf gas exchange rates were registered.

Thirty individual leaves were cut and scanned by an LI-3100 leaf area meter (LI-COR Inc, Lincoln, Nebraska, USA) to obtain the leaf area. Leaf length and width at the middle of each leaf were measured to determine an empirical equation for area estimation. True leaf area was found to equal  $(\text{Length} * \text{Width} * 0.759)$ . 48 individual leaves close to plants sampled for gas exchange and leaf water potential measurements were observed hourly from sunrise to sunset on 202, 225, 229, 233 and 236 DOY to estimate changes in projected leaf area  $(\text{Length} * \text{Width} * 0.759)$ .

### **3.3.6. Characterization of leaf nitrogen content, leaf area, biomass, and yield components**

After conducting gas exchange measurements, each sampled individual leaf was cut and collected to estimate leaf blade area, dry mass and nitrogen content. To determine LAI, the green biomass overlying a half square meter of ground surface close to the chamber plots was harvested. All samples were dried at 60°C in a ventilated oven for at least 48 hours before determination of dry mass. Leaf nitrogen content was measured by C:N analyzer (Model 1500, Carlo Erba Instruments, Milan, Italy). Grain yield in paddy and rainfed field were measured in four sampling plots (0.5 × 0.5 m) close to chamber measurement plots at the end

### Chapter 3 - Canopy gain, water use and yield in paddy and rainfed rice

of the season (DOY 253), and yield components (panicle number, spikelet number, proportion of filled spikelets and 1000 grain weight) were evaluated based on recommendation from Yoshida et al. (1971).

The seasonal development of LAI was additionally observed with a plant canopy analyzer (LAI-2000, LI-COR, Lincoln, Nebraska, USA). Measurements were conducted along a transect across the rows using a cover view of 45° during early growth stages, and a view of 270° at later growth stages. LAI measurements were regularly made in the late afternoon or during periods of uniform cloudiness when there was no direct beam of sunlight.

#### 3.3.7. Estimating effects of plant hydraulic conductance, stomatal conductance ( $g_{sc}$ ) and stomatal limitation in carbon gain

The volumetric water content was converted to soil-water tension,  $\Psi_s$  (kPa) with standard soil-water retention curves of van Genuchten (1980),

$$\theta(\psi_s) = \theta_r + \frac{\theta_s - \theta_r}{[1 + \sigma(\psi_s)^n]^m} \quad (3.5)$$

where  $\theta(\Psi_s)$  is soil water content at matrix potential  $\Psi_s$ ;  $\theta_r$  and  $\theta_s$  represent residual and saturating soil water content ( $\text{m}^3 \text{ m}^{-3}$ ), and  $\sigma$  relates to the inverse of the air entry suction, which are optimally estimated by Hydrus 1D model (Ruidisch, 2013; Schaap et al., 1998) based on the local investigation of soil texture and soil water content observations:  $\theta_r = 0.12 \text{ m}^3 \text{ m}^{-3}$ ,  $\theta_s = 0.57 \text{ m}^3 \text{ m}^{-3}$ ,  $\sigma = 0.0096 \text{ cm}^{-1}$ ,  $n = 1.49$ , and where  $m$  is  $(1 - 1/n)$ .

The steady-state flow through rice plants was described by Darcy's law (Franks, 2004; Otieno et al., 2012; Stiller et al., 2003), substituting molar for mass units, which equates mmolar fluxes with the product of leaf-area-specific hydraulic conductance ( $k$ ,  $\text{mmol m}^{-2} \text{ s}^{-1} \text{ MPa}^{-1}$ ):

$$k = \frac{E}{\psi_s - \psi_l - \rho gh} \quad (3.6)$$

### Chapter 3 - Canopy gain, water use and yield in paddy and rainfed rice

where  $E$  is the transpiration rate ( $\text{mmol m}^{-2} \text{s}^{-1}$ );  $(\Psi_s - \Psi_l)$  is the total pressure drop (MPa);  $h$  is the length over which the pressure drop is taking place (m);  $\rho$  is the water density ( $\text{kg m}^{-3}$ );  $g$  is the acceleration due to gravity ( $\text{m s}^{-2}$ ).

To evaluate the effects of hydraulic conductance on variations in stomatal conductance occurring under saturating light environment, a hyperbolic equation was used,

$$g_{s,\max} = \frac{a \cdot b \cdot k}{1 + b \cdot k} + c \quad (3.7)$$

where  $g_{s,\max}$  is the stomatal conductance under saturating light;  $a$  is  $g_{s,\max}$  under infinite hydraulic conductance;  $b$  is the slope of the relationship between  $g_{s,\max}$  to  $k$ ; and  $c$  is the residual conductance.

To quantify the extent to which leaf photosynthesis is constrained by stomatal conductance before and after rainfall events, to the relationship of Harley et al. (1986) was used,

$$L_{gs} = 100 \frac{A_{\text{ci=ambient}} - A}{A} \quad (3.8)$$

where,  $A$  is the measured assimilation rate;  $A_{\text{ci=ambient}}$  is the assimilation rate under conditions of intercellular  $\text{CO}_2$  concentration equal to ambient  $\text{CO}_2$  concentration.

#### 3.3.8. Statistic analyses

Descriptive statistics was used to calculate averages and standard error of the data from each set of replications. Standard errors were shown in error bars. Two samples T test was used to analyze statistic difference for periodical measurement of canopy and leaf gas exchange data between paddy and rainfed rice. Missing data of leaf water potential when leaf gas exchange rate were recorded were filled in by multi-variable linear model constructing correlation between measured leaf water potential and respective meteorological factor and leaf temperature. All data analyses mentioned above were done by using SPSS software (SPSS Statistic 17.0, IBM Inc., NY, USA).

## Chapter 3 - Canopy gain, water use and yield in paddy and rainfed rice

### 3.4. Results

#### 3.4.1. Meteorological conditions and leaf and soil water status over the growth seasons

Meteorological factors recorded at 2 m height at the rainfed field margin, SWC at 10 and 30 cm depth, and minimum leaf water potential observed around noon in the rainfed rice are shown in Fig. 3.1. Total rainfall in 2013 was ca. 1330 mm. Rainfall was distributed among seasons with 7.0% (94 mm), 30.1% (401 mm), and 23.4% (312 mm) of total precipitation occurring in June, July and August, and with large events of 176 mm (13.2%) on DOY 186 (July 5) as well as 7.3% on DOY 236 (August 24). Scattered low-precipitation events happened between DOY 140 (May 20) and DOY 177 (June 26).

Frequent rainfall occurred in July and August. In general, the observed monthly precipitation distribution exhibited typical monsoon climate that was consistent with the past 30-year record. The number of days with at least 0.1 mm of precipitation during July was 13, while only 6 days of effective precipitation were registered in August. That was lower than the past history which averaged 13.9 days, but, August 2013 still had significantly higher rainfall amount of 312 mm as compared to historical record of 276 mm. The abnormal uneven distribution of precipitation in August resulted in decreases in soil water content that influenced rice growth and development.

Continuous standing water in paddy field resulted in SWC fluctuating around  $0.7 \text{ m}^3 \text{ m}^{-3}$ . In contrast, the soil matrix at 10 and 30 cm depth in the rainfed plots showed large variations, although SWC remained above  $0.4 \text{ m}^3 \text{ m}^{-3}$  during most of the growth season when intensive precipitation occurred (Fig. 3.1c). SWC at 10 cm depth was more sensitive to temporal changes in rainfall as compared to 30 cm depth, decreasing to  $0.26 \text{ m}^3 \text{ m}^{-3}$  between DOY 197 and 203 (first soil water deficit period, SWD1) and again between DOY 218 and 234 (second soil water deficit period, SWD2). Maximum water vapor pressure deficit between leaf surface and leaf tissues ( $\text{VPD}_{\text{max}}$ ) during these two dry periods were high as compared to other periods, increasing up to 3.5 kPa (Fig. 3.1b). Daily solar radiation was almost constant over growth seasons (Fig. 3.1a), except on the rainy and cloudy days. Daily maximum air

### Chapter 3 - Canopy gain, water use and yield in paddy and rainfed rice

temperature ( $T_{\text{air,max}}$ ) gradually increased to 32°C in June and July, and arrived at maximum of ca. 37°C during SWD2 (Fig. 3.1b), which was one of the prime factors influencing VPD and SWC.

Decreasing soil water content caused a decline in the minimum leaf water potential ( $\Psi_l$ ) reached at midday during the SWD1 and SWD2 periods, with the lowest  $\Psi_l$  falling to -2.0 MPa (Fig. 3.1c) when soil water content was reduced to 0.26 m<sup>3</sup> m<sup>-3</sup> (corresponding to soil matrix potential  $\Psi_s$  ca. -0.19 MPa). The horizontal dashed line in Fig. 3.1c indicates SWC of 0.3 m<sup>3</sup> m<sup>-3</sup> at 10 cm depth, which is the apparent threshold value below which soil drying induced down-regulation of leaf gas exchange rates (see below). Accordingly, minimum  $\Psi_l$  at roughly -1.0 MPa was observed at the time when SWC dropped lower than that value. According to those two threshold signatures, two growth periods, dry and wet, were defined. The minimum  $\Psi_l$  at -2.0 MPa was observed on DOY 233 before rainfall on DOY 235. Pre-dawn  $\Psi_l$ , measured before sunrise over the course of growth season, was close to zero, together with appearance of copious guttation at leaf margin in the early morning, demonstrating that rainfed rice was capable of complete recovery from short-term impacts induced by dry conditions at daytime via nocturnal water uptake by roots (i.e. no permanent damage occurred).



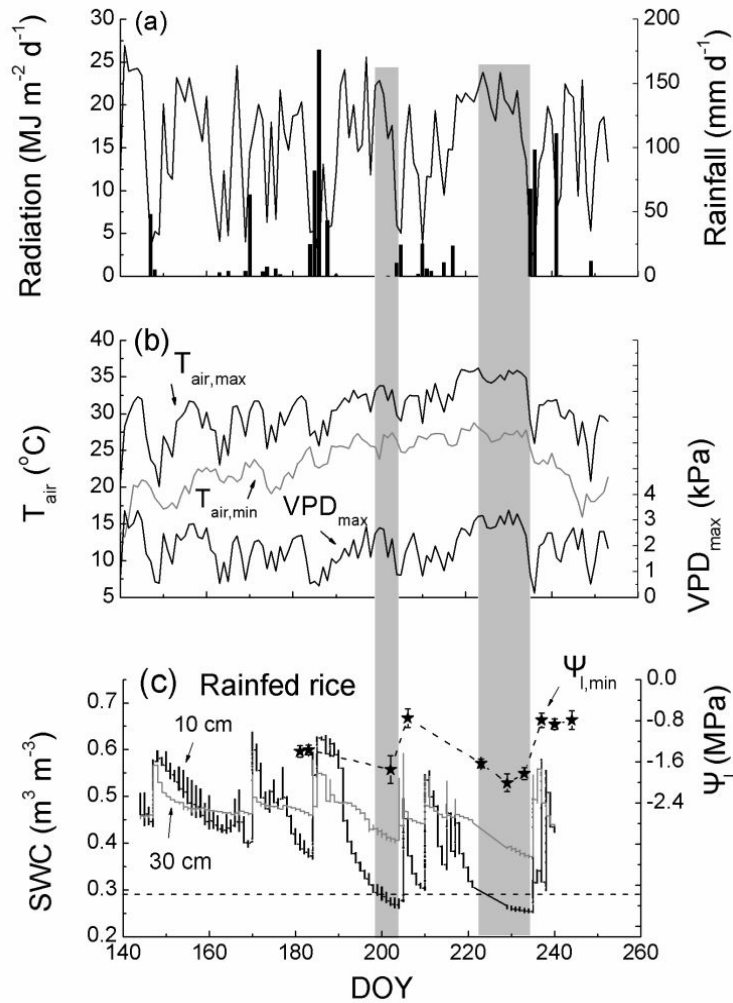


**Figure 3.1** Seasonal variations in daily integrated solar radiation (a), precipitation (a), daily maximum and minimum air temperature ( $T_{\text{air,max}}$  and  $T_{\text{air,min}}$ ) (b), maximum water vapor deficit between leaf surface and leaf tissues ( $\text{VPD}_{\text{max}}$ ) during the daytime period (b), soil water content (SWC) at 10 and 30 cm depth in rainfed field (c), and minimum leaf water potential ( $\Psi_{\text{l,min}}$ ) measured during daily observation cycles (c). Shading bars indicated dry periods between 197 and 203 DOY and between 218 and 234 DOY when SWC at 10 cm depth in rainfed field was less than  $0.3 \text{ m}^3 \text{m}^{-3}$ .

### 3.4.2. Phenology of development over the course of the growth season

Germination and seedling emergence through the ground surface in the rainfed field commenced around DOY 138, 26 days after sowing. On DOY 140 seedlings of 10 cm height cultivated in a nursery were transplanted into the paddy, resulting in a slightly advanced growth and development. Thus, the duration of vegetative crop growth (tillering and elongation) was shorter in the paddy field and the commencement of flowering (anthesis)

### Chapter 3 - Canopy gain, water use and yield in paddy and rainfed rice

occurred 9 days earlier than in rainfed rice (Figure 3.2). Nevertheless, the flowering stage lasted approximately 7 days in both situations. The delayed start of grain-filling in rainfed plots in mid-August was accompanied by a prolonged dry period, which clearly affected canopy structure and function (see below).

#### 3.4.3. Seasonal developments of canopy structure, carbon fluxes, and nitrogen content in paddy and rainfed rice

Daily integrated GPP ( $GPP_{int}$ ) linearly increased after beginning of growing season until the date ca. 200 DOY when  $GPP_{int}$  was at peak stage in paddy plot (Figure 3.2a). There was no clear difference in  $GPP_{int}$  on 157 DOY between paddy and rainfed plots, whereas, rapidly ascending in  $GPP_{int}$  in paddy rice promoted the differences to widen, for example  $GPP_{int}$  on 181 DOY ( $p = 0.036$ ). Large difference in  $GPP_{int}$  dismissed on 200 DOY. Maximum  $GPP_{int}$  in paddy rice ( $12.26 \text{ g C m}^{-2} \text{ d}^{-1}$ ) appeared earlier than that in rainfed rice ( $14.29 \text{ g C m}^{-2} \text{ d}^{-1}$ ). Significant discrepancy was not obtained but maximum  $GPP_{int}$  of rainfed rice was relatively high than paddy plot by 16.6%. Rainfed rice showed significantly higher  $GPP_{int}$  by 125% than paddy rice on 240 DOY. Seasonal trend in daily integrated plant respiration ( $R_{p\_int}$ ) was similar to  $GPP_{int}$  (Figure 3.2a). Maximum  $R_{p\_int}$  in paddy and rainfed plot were 3.4 and 4.3  $\text{g C m}^{-2} \text{ d}^{-1}$ , respectively. Ratio of  $R_{p\_int}$  to  $GPP_{int}$  in paddy plot on respective measuring day of year 158, 166, 197, 218, and 240 was 27.02%, 38.13%, 27.71%, 22.24% and 42.63%, respectively. The ratio in rainfed rice on respective measuring day of year 157, 166, 181, 199, 221, and 239 was 43.59%, 64.50%, 43.28%, 36.60%, 30.33% and 34.91%, respectively.

Hyperbolic response curves of momentary NPP to incident PAR in the paddy and rainfed rice measured on different days throughout the growth season are shown together with parameter values determined for equation 3 in Figure 3.10.A1 and Figure 3.11.A2. There was a tight correlation between NPP and PAR on each measuring date with significance at 0.05 level, correlation coefficient  $R^2 > 0.80$  (Table 3.2.A1). From the light responses of NPP, the daily integrated NPP ( $NPP_{int}$ ) was obtained from half-hourly estimations with measured PAR data. Daily  $NPP_{int}$  in the paddy and rainfed rice exhibited a rapid increase during the early growth

### Chapter 3 - Canopy gain, water use and yield in paddy and rainfed rice

season, reached the highest level of ca.  $8.2 \text{ g C m}^{-2} \text{ d}^{-1}$  in paddy rice between 200 and 220 DOY and ca.  $10.2 \text{ g C m}^{-2} \text{ d}^{-1}$  in rainfed rice at 220 DOY, and afterwards declined (Figure 3.2b). There was no significant difference in  $\text{NPP}_{\text{int}}$  between paddy and rainfed rice at initial stage before 170 DOY ( $p = 0.31$ ),  $\text{NPP}_{\text{int}}$  increased more rapidly in paddy rice by ca. 180 DOY ( $p = 0.001$ ). Difference in  $\text{NPP}_{\text{int}}$  between sites then narrowed between 200 and 220 DOY without statistical significance at 0.05 level. Following the maximum in daily  $\text{NPP}_{\text{int}}$ , rainfed rice had a markedly higher  $\text{NPP}_{\text{int}}$  than paddy rice at 240 DOY ( $p < 0.001$ ).

Seasonal patterns in LAI development are also shown in Figure 3.2b. Before 175 DOY, differences between paddy and rainfed rice were small, but rapid LAI development in paddy rice increased the differences after 180 DOY ( $p < 0.01$ ). Significant differences remained until 210 DOY ( $p = 0.06$ ). LAI rapidly declined in paddy rice after 220 DOY and, thus, LAI in rainfed rice was 28% higher by 240 DOY. Variations in the maximum NPP recorded at midday ( $\text{NPP}_{\text{max}}$ ) between paddy rice and rainfed rice were analogous to  $\text{NPP}_{\text{int}}$  changes over growth season (Figure 3.2c). Total canopy nitrogen content ( $\text{N}_{\text{total}}$ ,  $\text{g m}^{-2}$ ) was similar between the two cropping cultures before 185 DOY (Figure 3.2c), but then leveled off in the paddy rice, leading to significantly higher  $\text{N}_{\text{total}}$  in rainfed plots at 202, 223 and 240 DOY by ca. 50%, 120%, and 170%, respectively.

Two of the agronomic stages in the rice growth cycle, flowering and grain-filling, play vital roles in determining grain yield production. Rainfed rice had a longer growth period but showed similar duration for flowering and grain-filling as compared to paddy rice. Phenological development in rainfed plots lagged behind that of paddy rice throughout the season. Significant declines in both  $\text{NPP}_{\text{max}}$  rate and  $\text{NPP}_{\text{int}}$  was observed in rainfed rice during the first dry period SWD1 on 202 DOY (Figure 3.2b).  $\text{NPP}_{\text{max}}$  and  $\text{NPP}_{\text{int}}$  were only  $11.1 \mu\text{mol m}^{-2} \text{ s}^{-1}$  and  $3.3 \text{ g C m}^{-2} \text{ d}^{-1}$ , approximately 53.7% and 66.9% lower than maximum values. Although no measurements were made, similar or more severe decrease might be expected during the more prolonged dry period during grain-filling stage (DOY 218–234). The impacts during prolonged dry period occurring during grain-filling stage in the rainfed

### Chapter 3 - Canopy gain, water use and yield in paddy and rainfed rice

field were documented by carbon gain and water use at leaf level (discussed below).

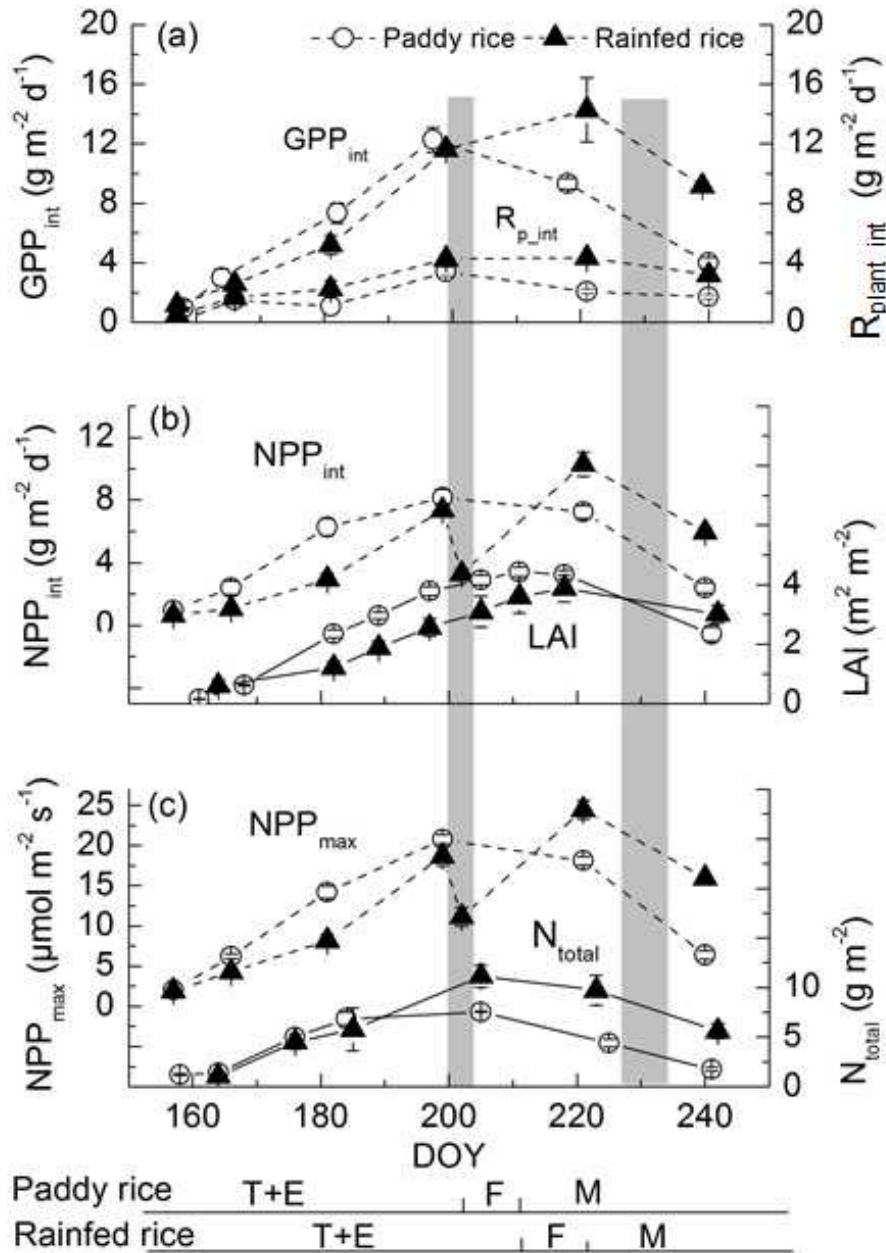


**Figure 3.2** Seasonal development of daily integrated gross primary production ( $GPP_{int}$ ) (a), daily integrated plant respiration ( $R_{plant\_int}$ ) (a), daily integrated net primary production ( $NPP_{int}$ ) (b), leaf area index (LAI) (b); daily maximum carbon gain capacity ( $NPP_{max}$ ) (c), and canopy nitrogen content ( $N_{total}$ ) (c) in paddy and rainfed rice ecosystems. Time periods during which paddy and rainfed rice grew at different agronomic stages: T + E for tillering and elongation stage; F for flowering stage, and M for grain-filling and maturation stage. Shading bars indicate the first dry and second dry periods that potentially impact canopy structure and function. Dashed lines emphasize that observations were not continuous with respect to potential soil drying effects. Error bars indicated S.E.,  $n = 3$  to 6.

### 3.4.4. Seasonal changes in gas exchange properties in paddy and rainfed rice

Leaf nitrogen content per leaf area ( $N_a$ ) of upper-canopy leaves rapidly declined in paddy rice leaves between 160 DOY and 193 DOY from 1.6 to 1.3 g m<sup>-2</sup>, remained relatively constant during flowering, and then decreased to 0.9 g m<sup>-2</sup> during grain-filling (Figure 3.3a). Leaf  $N_a$  in rainfed rice also declined over the course of the season, but much more gradually, from an initial 2.14 to 1.76 g m<sup>-2</sup> observed on 230 DOY. Thus,  $N_a$  in rainfed rice was significantly higher than that in paddy rice over the entire growth season ( $p < 0.01$ ) (Figure 3.3a). In parallel to the trends in  $N_a$ , the maximum carboxylation rate ( $V_{cmax,30}$ ) and electron transport rate ( $J_{max,30}$ ) both decreased over time, but were higher in rainfed rice compared to paddy rice (Figure 3.3c,d). Especially at 240 DOY, rainfed rice maintained a high  $V_{cmax,30}$  and  $J_{max,30}$  (approximately 45% greater than in paddy rice;  $p < 0.01$ ).

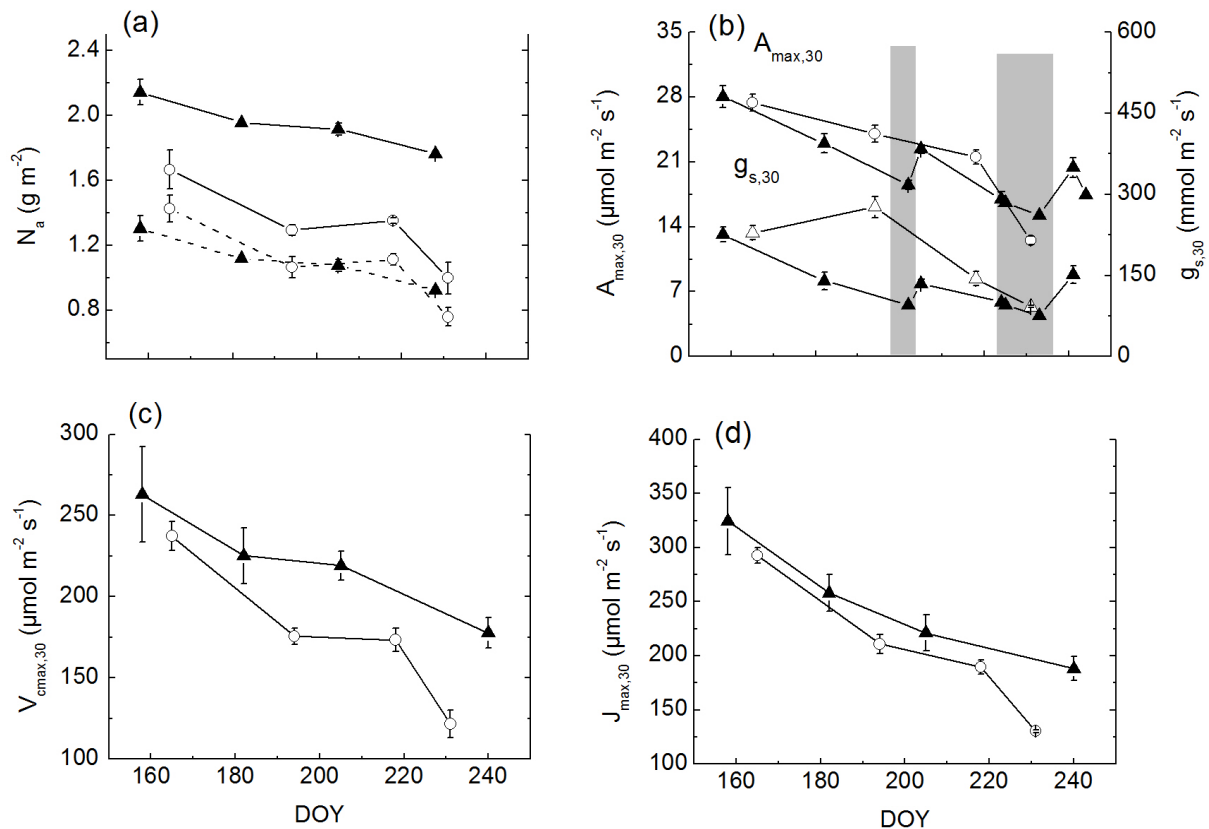


Figure 3.3

### Chapter 3 - Canopy gain, water use and yield in paddy and rainfed rice

**Figure 3.3** Seasonal development in leaf photosynthetic traits in uppermost leaves at flooded and rainfed rice cropping systems: (a) leaf nitrogen content per leaf area ( $N_a$ ) and photosynthetic nitrogen content generated by leaf nitrogen content minus residual N content derived from  $V_{cmax,30}-N_a$  correlation (dashed lines); (b) photosynthetic capacity ( $A_{max}$ ) and stomatal conductance ( $g_{s,30}$ ) acquired at saturating PAR of  $1500 \mu\text{mol m}^{-2} \text{s}^{-1}$ , ambient  $\text{CO}_2$  of  $400 \mu\text{mol mol}^{-1}$  and leaf temperature  $30^\circ\text{C}$ ; (c) the maximum carboxylation rate per area at leaf temperature  $30^\circ\text{C}$  ( $V_{cmax,30}$ ), (d) the maximum electron transport rate per leaf area at leaf temperature  $30^\circ\text{C}$  ( $J_{max,30}$ ). Bars indicated S.E.,  $n = 3$  to 6. Black triangles and open circles respectively represent rainfed and paddy rice.

Surprisingly, during the periods when soil was moist  $A_{max,30}$  was relatively lower in rainfed rice before 200 DOY but the difference was small ( $p = 0.31$ ). The seasonal decrease was less steep and only slightly decreased by 10.2% from 180 DOY till 240 DOY (Figure 3.3b). Significant difference in  $A_{max,30}$  between the two cropping cultures was observed on 240 DOY ( $p < 0.001$ ). The seasonal variations in  $A_{max,30}$  in rainfed rice could be interpreted by N use efficiency (defined as assimilate rate divided by N content) and changing  $g_s$ , or either of them. Although large discrepancy in leaf N between the two types of cultivation at each growth stage existed, there was still conservative correlations among photosynthetic characteristics and leaf N.  $V_{cmax,30}$  was linearly related to  $N_a$ , with similar slopes of 170.1 and 204.3 in paddy and rainfed rice, respectively (Figure 3.4a). However, there were distinct differences in residual  $N_a$  (the x-intercept), 0.26 and  $0.84 \text{ g m}^{-2}$  for paddy and rainfed plots, respectively. Similar performance as found in the  $V_{cmax,30}-N_a$  correlation occurred in the  $J_{max,30}-N_a$  correlation (Figure 3.4b), again showing similar slopes but higher residual  $N_a$  in rainfed rice at  $1.01 \text{ g m}^{-2}$ , compared to  $0.42 \text{ g m}^{-2}$  in leaves of paddy rice.  $A_{max,30}$  linearly scaled to  $N_a$  in paddy and rainfed rice, exhibited similar slopes of 20.3 and 22.5, respectively (Figure 3.4c). Clear discrepancies in y-intercept existed, with 0.32 and  $0.92 \text{ g m}^{-2}$  for paddy and rainfed rice, respectively. Residual N content invested in non-photosynthetic tissues in rainfed rice was as high as three times that of paddy rice. At the plot scale, the relationship between  $\text{NPP}_{max}$  and total nitrogen content ( $N_{total}$ ) (Figure 3.4d) was similar to that observed in  $A_{max,30}-N_a$  correlation, i.e., similar slopes but different intercepts. Thus, residual nitrogen values in the whole canopy data for paddy and rainfed plots were 0.5 and  $1.0 \text{ g m}^{-2}$  (ground), respectively, compared with 0.32 and  $0.92 \text{ g m}^{-2}$  (leaf) derived from the  $A_{max}-N_a$  in leaves of

### Chapter 3 - Canopy gain, water use and yield in paddy and rainfed rice

paddy and rainfed rice. Paddy rice had improved N use efficiency at given leaf N content due to lower non-productive N investment in leaves.

Contribution of photosynthetic N content to photosynthetic capacity was analyzed from the negative x-intercept (residual N content in  $A_{\max,30}-N_a$ ) with respect to leaf N content. Given that photosynthetic N content derived from  $V_{c\max,30}-N_a$  or  $A_{\max,30}-N_a$ , or  $J_{\max,30}-N_a$  relationship was roughly similar to the other, thus, productive N content from the side of  $A_{\max,30}-N_a$  correlation was displayed (dashed lines in Figure 3.3a). Photosynthetic N in rainfed rice at around 160 DOY and from 180 to 210 DOY was compatible to paddy rice but exceeded paddy rice from 230 DOY on by 22.6%. Difference in photosynthetic N between the two cultures widened, as delayed commencement of the grain-filling stage in rainfed rice resulted in a high volume of green leaves, while paddy rice had already senesced. Similar  $g_{s,30}$  occurred in paddy and rainfed rice during the initial growth stage, while a large discrepancy appeared at mid-season ( $p = 0.001$ ) when soil water content was abundant (Figure 3.3b).

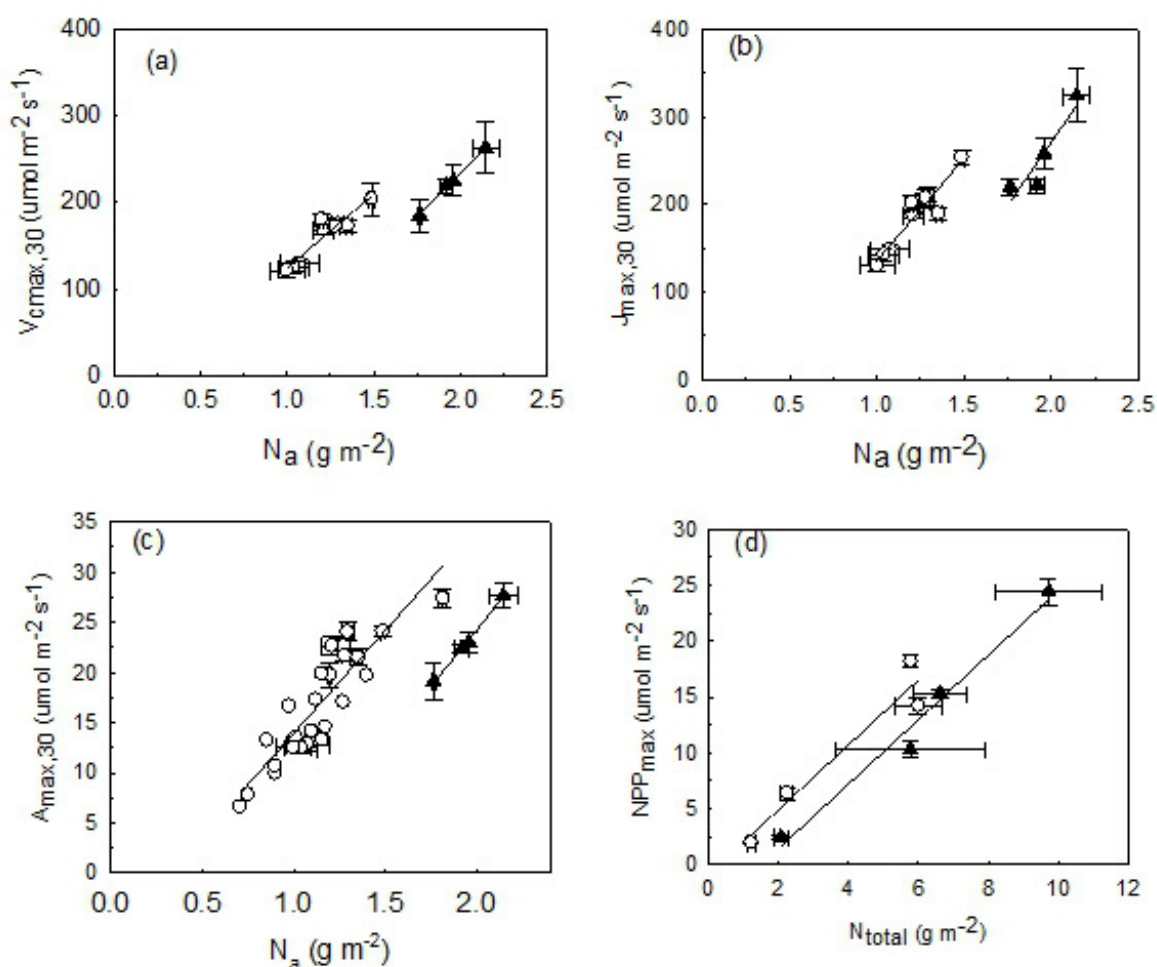


**Figure 3.4** Correlations for (a) sunlit leaf maximum carboxylation rate ( $V_{cmax,30}$ ) and  $N_a$ ; (b) leaf maximum electron transport rate ( $J_{max,30}$ ) and  $N_a$ ; (c) photosynthetic capacity ( $A_{max,30}$ ) and  $N_a$ , and (d) daily maximum net primary production ( $NPP_{max}$ ) and total leaf nitrogen content ( $N_{total}$ ) in paddy and rainfed rice. Open circles represented measured  $A_{max,30}$  in paddy rice grown at growth chamber. Each point was computed average from 3 to 6 replications. Black triangles and open circles respectively represent rainfed and paddy rice.

### 3.4.5. Comparisons in diurnal courses of gas exchange between paddy and rainfed rice

Decline of leaf  $N_a$  from 177 to 221 DOY in paddy rice was 24.1% accompanied by 21.4% of decline in  $A_{max,30}$  on average, whereas, 9.7% of decline in  $N_a$  in rainfed rice did not match the huge reduction of  $A_{max,30}$  by 42.3% on average (Figure 3.3b), which occurred simultaneously with lower  $g_{s,max}$ . To gain insight into the adjustments in regulatory mechanisms controlling leaf gas exchange fluxes in the rainfed plots during periods of adequate soil moisture versus during periods of drying, diurnal courses of gas exchange in the rainfed and paddy plots were



### Chapter 3 - Canopy gain, water use and yield in paddy and rainfed rice

compared (Figure 3.5). Days for comparison were chosen based on similar diurnal patterns of PAR (mostly clear sky and maximum midday irradiance of approximately 1600–1700  $\mu\text{mol m}^{-2} \text{s}^{-1}$ ) and leaf temperature. A perfect comparison was not possible, cf. 181 DOY when rainfed rice was measured, and where incident irradiation was influenced by intermittent clouds. When air temperatures in the two plots were similar, leaf temperatures in the rainfed rice were generally 2–3°C higher than in the paddy rice leaves, which leads to significantly higher water vapor pressure deficits (VPD) in the rainfed plots.

In the paddies (Figure 3.5a, c), where soil water content remained high throughout the season, the diurnal patterns for A, E and  $g_s$  were all “bell-shaped” with a maximum occurring near midday. During periods of adequate soil moisture in the rainfed plots ( $\text{SWC} > 0.3 \text{ m}^3 \text{ m}^{-3}$ ), such as 181 DOY (Figure 3.5b) a similar pattern was observed, although the pattern on 181 DOY was disrupted by periods of cloudiness. In the absence of soil water deficits, the maximum assimilation rates in the paddy (Figure 3.5a) and rainfed plots (Figure 3.5b) were relatively similar; however, stomatal conductance in the rainfed plots was substantially less than in the paddies (approximately 150  $\text{mmol m}^{-2} \text{s}^{-1}$  versus 230  $\text{mmol m}^{-2} \text{s}^{-1}$ ) as indicated above in Figure 3.3b. As a result, internal  $\text{CO}_2$  concentration ( $C_i$ ), averaging about 240  $\mu\text{mol mol}^{-1}$  in the paddies, was lower in the rainfed fields (maximum of approximately 200  $\mu\text{mol mol}^{-1}$ ).

During the second period of soil drying (SWD2 in Figure 3.1c) in the rainfed plots, differences between paddy (Figure 3.5c) and rainfed (Figure 3.5d) rice leaf gas exchange were amplified. On the one hand, maximum rates of assimilation in the paddy were significantly reduced compared to earlier in the season due to reduced leaf level nitrogen concentration, which had fallen from 1.78  $\text{g m}^{-2}$  on 177 DOY to 1.35  $\text{g m}^{-2}$  on 221 DOY. In addition, leaf temperatures were substantially higher, exceeding 36°C on 221 DOY, above the optimum for photosynthesis (ca. 33°C, Figure 3.12.B1d). Despite the fact that leaf nitrogen levels in rainfed rice (1.95  $\text{g m}^{-2}$ ) were substantially higher than in the paddy fields, maximum rates of assimilation were only approximately 15  $\mu\text{mol m}^{-2} \text{s}^{-1}$  on 229 DOY, a

### Chapter 3 - Canopy gain, water use and yield in paddy and rainfed rice

decline of 40% since 181 DOY. Stomatal conductance, driven by extremely high VPD and low soil moisture, decreased below  $80 \text{ mmol m}^{-2} \text{ s}^{-1}$ .  $C_i$  values which remained unchanged at ca.  $240 \text{ } \mu\text{mol mol}^{-1}$  in the paddy rice, fell to about  $140 \text{ } \mu\text{mol mol}^{-1}$  in rainfed leaves. Reduced stomatal aperture in the rainfed plants conserved water loss under extremely high VPD conditions and maximal transpiration rates were between 3 and  $4 \text{ mmol m}^{-2} \text{ s}^{-1}$ .

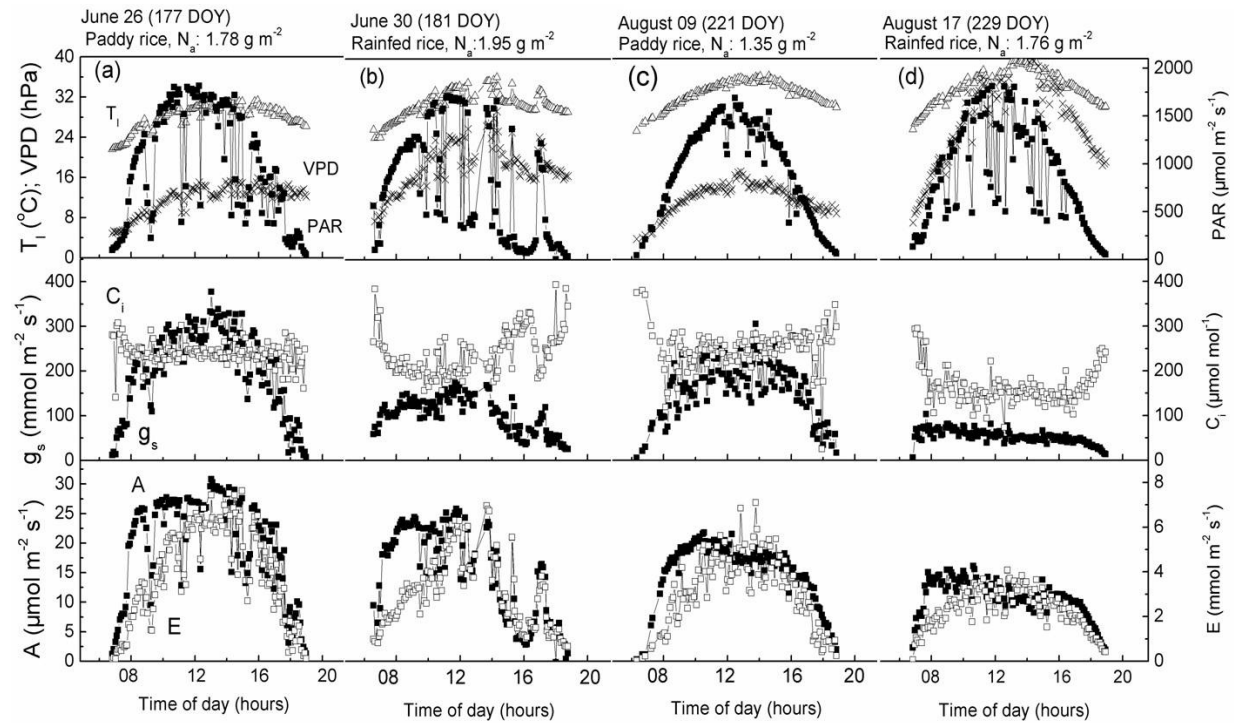


**Figure 3.5** Diurnal course of meteorological factors PAR, water vapor pressure deficit (VPD) and leaf temperature, and assimilation rate (A), transpiration rate (E), stomatal conductance for  $\text{CO}_2$  diffusion ( $g_{sc}$ ) and intercellular  $\text{CO}_2$  concentration ( $C_i$ ) on 177 (early season) and 221 (late season) DOY in paddy rice, and 181 (early season; minimum leaf water potential =  $-1.4 \text{ MPa}$ ) and 229 DOY (late season; minimum leaf water potential =  $-2.0 \text{ MPa}$ ) in rainfed rice.

#### 3.4.6. Leaf level components of the rainfed rice plants regulating gas exchange response under changing soil water availability

Regulation of instant stomatal conductance ( $g_s$ ) to reduce transpiration water loss was more pronounced during soil drying conditions, which is manifested by maximum E during dry period accounting for only half of that during wet period (Figure 3.6a). Nevertheless, leaf water potential ( $\Psi_l$ ) rapid declined to  $-2 \text{ MPa}$ , which means capacity of water compensation via water transport conduit to sustain relatively high leaf water content was constrained during daytime in the dry period.

### Chapter 3 - Canopy gain, water use and yield in paddy and rainfed rice

Photosynthetic saturating light (LSP), defined as the PAR value at which assimilation rate become light saturated, hyperbolically correlated to  $\Psi_l$  (Figure 3B1a). Rapid decrease in LSP initiated when  $\Psi_l$  declined beyond -1.0 MPa. Assimilate rate and stomatal conductance at saturating light around noon were extracted as instant maximum assimilation rate ( $A_{\max}$ ) and instant maximum stomatal conductance ( $g_{s,\max}$ ), to indicate the potential impacts of the soil water depletion on leaf gas exchange. Gas exchange behavior in rainfed rice during periods with high SWC and at drying time SWD1 and SWD2 is compared in Figure 3.6.

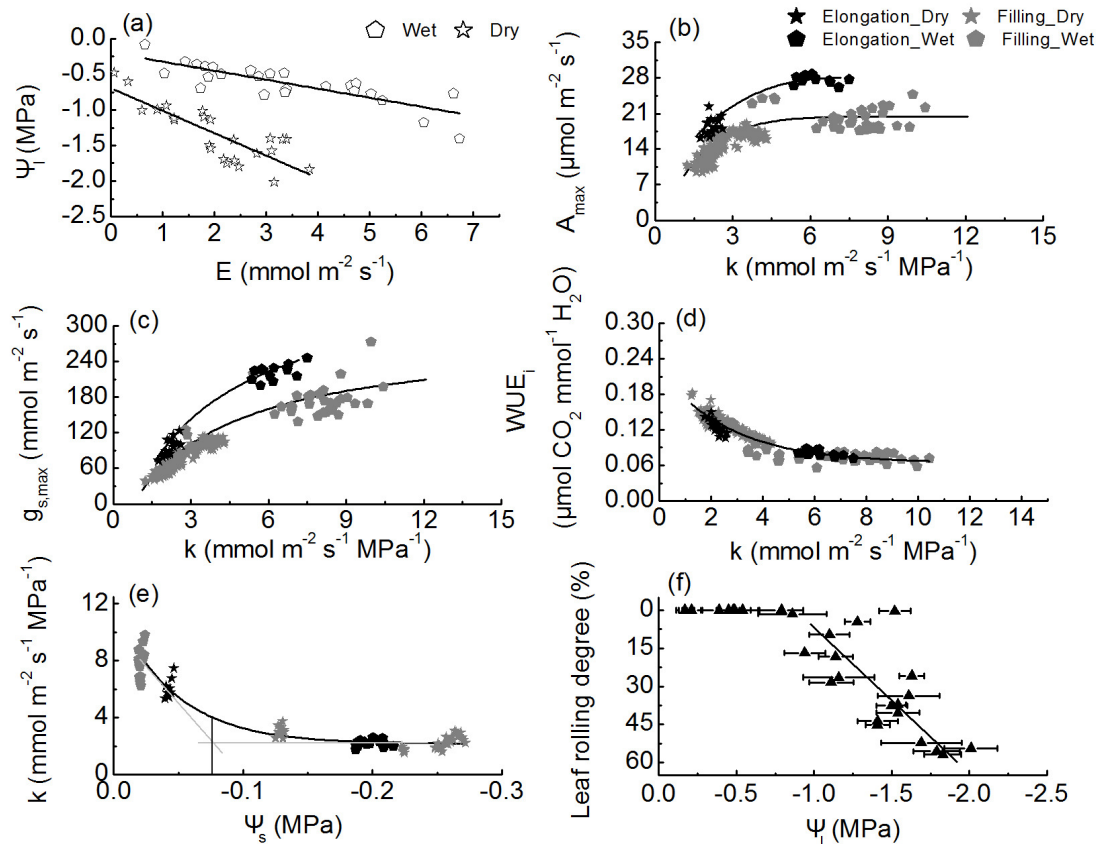


**Figure 3.6** Correlations between transpiration rate ( $E$ ) and leaf water potential ( $\Psi_l$ ) during wet versus dry period, in rainfed rice (a); hyperbolic relationship of photosynthetic capacity ( $A_{\max}$ ) to plant hydraulic conductance ( $\kappa$ ) (b); relationship between maximum stomatal conductance ( $g_{s,\max}$ ) and  $\kappa$  at elongation ( $g_{s,\max} = a \cdot b \cdot \kappa / (1 + b \cdot \kappa) + c$ ,  $a = 475$ ,  $b = 0.3$ ,  $c = -82$ ,  $R^2 = 0.97$ ,  $p < 0.01$ ) and grain-filling ( $g_{s,\max} = a \cdot b \cdot \kappa / (1 + b \cdot \kappa) + c$ ,  $a = 349$ ,  $b = 0.3$ ,  $c = -64$ ,  $R^2 = 0.83$ ,  $p < 0.01$ ) (c); relationship between intrinsic water use efficiency ( $WUE_{\text{ins}}$ , as the ratio of  $A_{\max}$  to  $g_{s,\max}$  to water vapor) and  $\kappa$  (d); correlation between  $\kappa$  and  $\Psi_s$  (e), and correlation for leaf rolling degree and leaf water potential ( $\Psi_l$ ) (f). Black triangles represent rainfed rice. Representations of other symbols are indicated in plots.

### Chapter 3 - Canopy gain, water use and yield in paddy and rainfed rice

During wet periods water potential gradients from soil matrix surrounding plants to leaves was relatively small less than 1 MPa, although transpiration rates at saturating light environment were ca.  $6 \text{ mmol m}^{-2} \text{ s}^{-1}$ . Hydraulic conductance ( $k$ ) of the soil-plant system was high. The reduced  $k$  was associated with strong shifts in leaf physiology, i.e.  $g_{s,\max}$  and  $A_{\max}$  appeared to have a hyperbolic correlation with respect to  $k$  (for  $g_{s,\max}$   $R^2 > 0.83$ ,  $p < 0.01$  and for  $A_{\max}$   $R^2 > 0.90$ ,  $p < 0.01$ ). The shape of the relationship seems independent of growth stage (Figure 3.6b, c) but the maximum rates for gas exchange and stomatal conductance change due to the seasonal trends in leaf nitrogen content. The threshold (cross point between extension of linear phase and extrapolation of saturating phase) which indicates sensitivity of  $A_{\max}$  to  $k$  decreased from the elongation stage to grain-filling stage from 3.5 to 4.1  $\text{mmol m}^{-2} \text{ s}^{-1} \text{ MPa}^{-1}$ , and in the case of  $g_{s,\max}$  from 4.5 to 5.3  $\text{mmol m}^{-2} \text{ s}^{-1} \text{ MPa}^{-1}$ . This suggests that stomatal conductance was more sensitive to fluctuations in hydraulic conductance.

To visualize the effects of soil drying on carbon gain and water use, intrinsic water use efficiency ( $WUE_i$  as the ratio of  $A_{\max}$  to  $g_{sw,\max}$ ) and inherent water use efficiency (intWUE, as assimilation rate to transpiration rate) were evaluated. As expected, at sufficient soil water conditions  $WUE_i$  in paddy and rainfed rice were similar over growth seasons without significant difference. But  $WUE_i$  steeply increased when  $k$  fell less than ca.  $5 \text{ mmol m}^{-2} \text{ s}^{-1} \text{ MPa}^{-1}$  (Figure 3.6d), which is in the range of aforementioned threshold in  $g_{s,\max}$ – $k$  relationship. Similar to the correlation between  $k$  and  $WUE_i$ ,  $k$  rapidly declined when  $\Psi_s$  dropped down to approximately -0.075 MPa, which corresponds to the threshold point of  $5 \text{ mmol m}^{-2} \text{ s}^{-1} \text{ MPa}^{-1}$  in  $WUE_i$ – $k$ .

In contrast to the uniform correlation between  $WUE_i$  and  $k$ , shape and amplitude of the correlation for intWUE to  $k$  under dry conditions differed from the wet (Figure 3.7a), although both two curves increased with decreasing  $k$ . As mentioned above, VPD dominated the direction and intensity in the diurnal pattern of  $E$  (Figure 3.5d). Increasing VPD promoted  $k$  when soil water content was abundant (Figure 3.7b). Surprising,  $k$  leveled off even though VPD increased to 4.5 kPa in a drying environment (Figure 3.7b).

### Chapter 3 - Canopy gain, water use and yield in paddy and rainfed rice

A two-segmented response curve for leaf rolling degree in response to  $\Psi_1$  was detected (Figure 3.6f). During the wet growth season that was featured by  $\Psi_1$  greater than -1 MPa, plants grew with fully expanded canopy crown, while initiation of a linear decline of canopy area exposure commenced after  $\Psi_1$  was reduced to less than -1 MPa, with maximum leaf rolling extent up to 60% when leaves completely rolled at  $\Psi_1$  of ca. -2 MPa.

Stomatal limitation ( $L_{gs}$ ) in both paddy and rainfed rice during grain-filling stages are illustrated in Figure 3.8. With wet soil,  $L_{gs}$  reached the maximum at midday, ranging between 20 to 30%. However, increased stomatal limitation occurred in rainfed rice during dry periods (DOY 202 and 233) with constraints up to 55% (80% greater than in paddy rice).

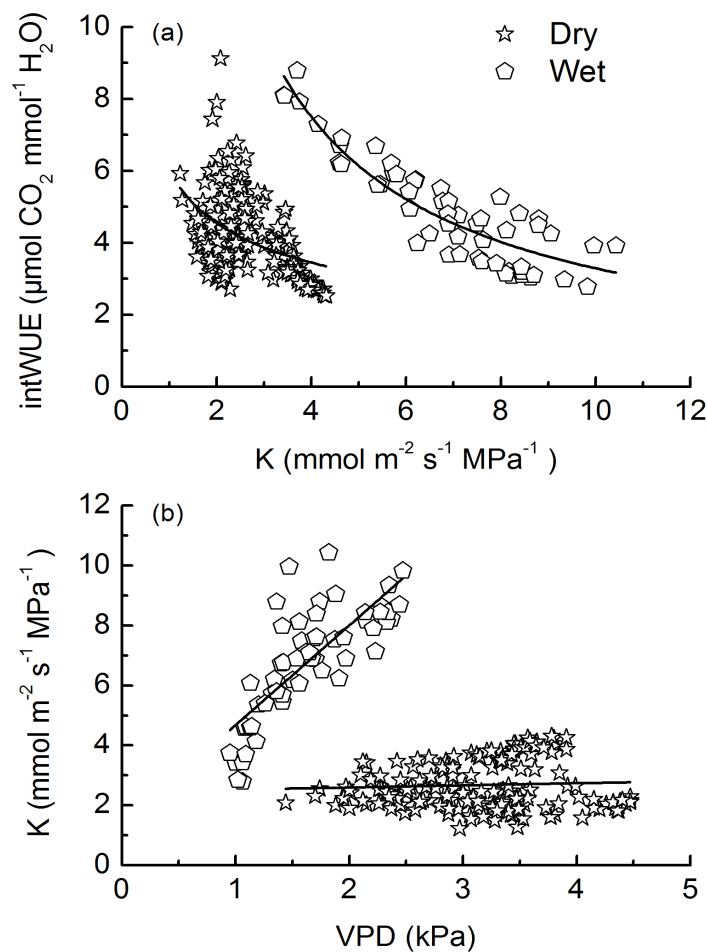


**Figure 3.7** Correlations (a) between plant hydraulic conductance ( $k$ ) and inherent water use efficiency (intWUE); (b) correlation between  $k$  and water vapor pressure deficit (VPD) in rainfed rice.

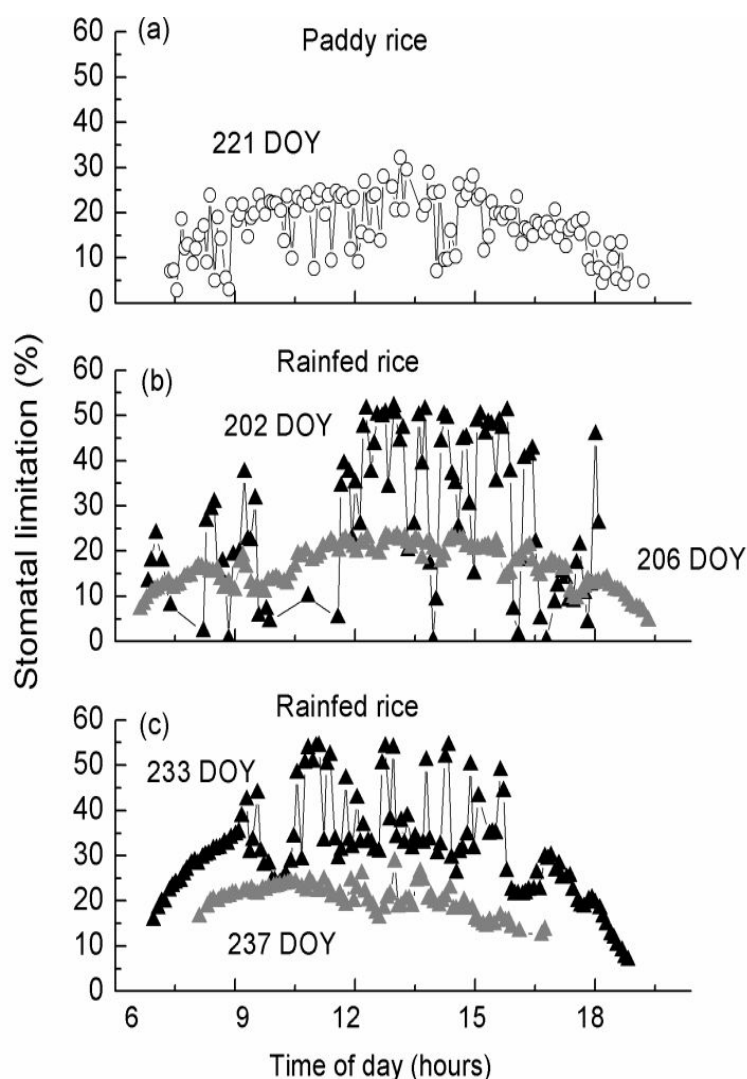


**Figure 3.8** Diurnal courses of stomatal limitations of photosynthesis in paddy rice on DOY 221 and in rainfed rice on DOY 202 (dry), 206 (wet), 233 (dry) and 237 (dry).

### 3.4.7. Canopy level components regulating carbon gain and biomass production under changing soil water availability

There was little accumulation of aboveground biomass in either paddy or rainfed rice until ca. DOY 170 (Figure 3.9a). Following DOY 170, biomass production accelerated in both, but the increase in paddy rice was more rapid. The difference in aboveground biomass continued to widen with maximum at ca. DOY 180 ( $p < 0.01$ ). Thereafter, the onset of senescence of paddy at ca. 205 DOY reduced the difference ( $p = 0.24$ ). By ca. DOY 220 until DOY 240, the aboveground biomass in rainfed plots exceeded that in the paddy rice by ca. 50%, which is in agreement with changes in NPP at the same agronomic stages (Figure 3.2b, c).

### Chapter 3 - Canopy gain, water use and yield in paddy and rainfed rice

Carbon gain as  $NPP_{int}$  directly related to aboveground biomass and LAI ( $R^2 = 0.91$ ,  $p < 0.01$ ) (Figure 3.9b). Exceptions in  $NPP_{int}$ -LAI correlation appeared at dry period SWD1 in rainfed rice when canopy carbon gain was strongly constrained by stomatal closure, and was observed further during ripening development in paddy rice DOY 240, presumably due to low leaf N and resulting decline in  $A_{max}$ . For those reasons, a scatter in the correlation between aboveground biomass and total leaf N content was observed for both paddy and rainfed rice ( $R^2 = 0.49$ ,  $p = 0.04$ ; Figure 3.9c).

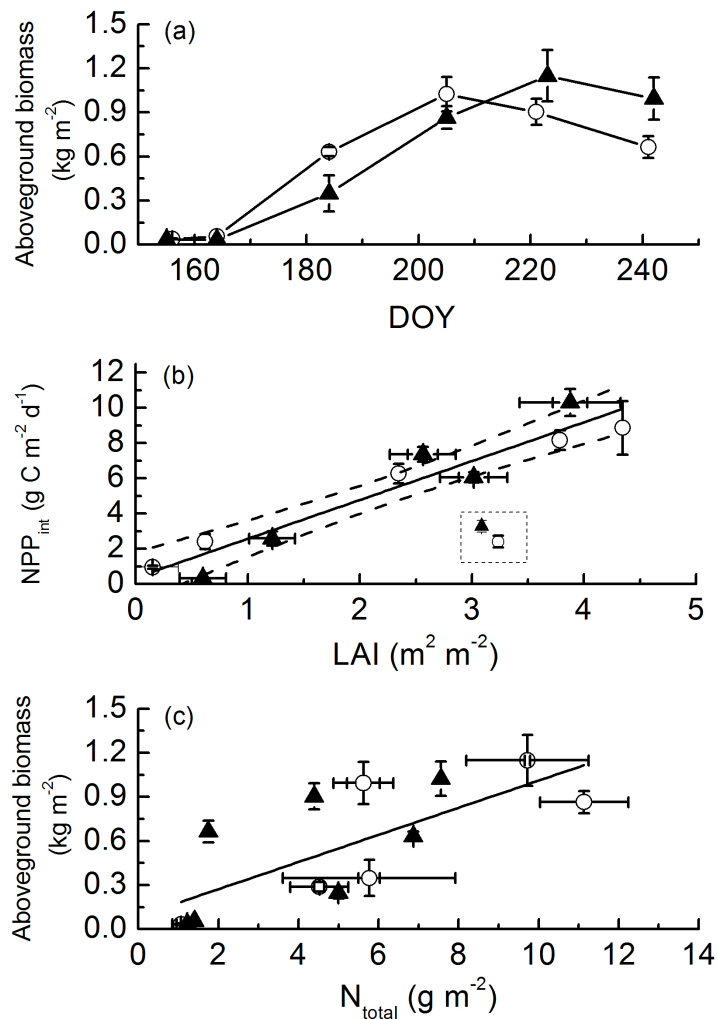


**Figure 3.9** Seasonal trend in aboveground biomass accumulation (a); correlations between leaf area index (LAI) and daily integrated net primary production ( $NPP_{int}$ ) (b); correlations for aboveground biomass accumulation and total leaf nitrogen content ( $N_{total}$ ) (c). Bars indicated S.E.,  $n = 3$  to 6. Filled triangles and open circles indicate paddy at senescence stage and rainfed rice during first soil drying period, respectively. The two clearly deviate points in dotted square frames of Figure 3.9b for  $NPP_{int}$  were measured during dry period SWD1 (DOY 202 in rainfed rice) at elongation and at maturation stage (DOY 240) in the case of paddy rice.

### 3.4.8. Comparison of yield in rainfed and paddy rice

Although aboveground biomass and LAI between paddy and rainfed rice were almost similar even with a slight time shift due to early establishment in paddy rice, and the relationship of NPP to LAI is essentially the same, grain yield production decreased by 10.2% in rainfed rice. We can conclude that this has multiple causes, the first being the reductions in carbon gain that occur during periods with relatively dry soil (cf. data shown in Figs. 3.2 through 3.6). A second probable cause is that more carbon must be invested in the root system (not systematically documented in the study). Root biomass measured in soil layers 0–5, 5–10, 10–20 and 20–30 cm depth in the rainfed rice at harvest was shown in Table 1. Even though the climate can be considered relatively moist, the rainfed rice used 25 to 30% of carbon gain to support the root system. Additional aboveground components (panicle number, spikelet number, proportion of filled ones, and thousand grain weight) that influence grain yield production is also indicated in Table 1. The proportion of filled spikelets 86.3% in rainfed rice as compared to flooded field of 93.5% decreased ( $p = 0.0001$ ). No significant differences in comparisons of other yield components were found ( $p > 0.05$ ). Grain yield was compromised due to constraints on filled spikelets, which occurred in parallel with decreases in carbon gain during the grain-filling stage (Figure 3.6d).

**Table 3.1** Root biomass distribution in soil profiles in rainfed rice field and comparisons in rice crop yield components per square meter ground area (panicle number, spikelet number, proportion of filled ones, and thousand grain weight) collected on 246 DOY. Values in parentheses indicated S.E.,  $n = 3$  to 6.

Rainfed rice						
Soil layer	5 cm	10 cm	20 cm	30 cm		
Root biomass	168.5 (15.5)	52.0 (6.6)	64.1 (37.5)	8.1 (0.55)		
Yield components	Panicle no./m <sup>2</sup>	Spikelet no./hill	% Filled spikelets	1000 grain weight (g)	Grain Ton/ha	
Paddy rice	221 (9)	108 (5)	93.5% (1.4%)	29.14 (0.62)	6.58 (0.32)	
Rainfed rice	225 (25)	105 (5)	86.27% (2.31%)	29.38 (0.75)	5.97 (0.32)	



## Chapter 3 - Canopy gain, water use and yield in paddy and rainfed rice

### 3.5. Discussion

In flooded rice field, rice seedlings with 4 true leaves were transplanted and five seedlings in average were grown in each hill. In rainfed field, 4 or 5 seeds were drilled into aerobic soil conditions. Crop establishment between two cropping cultures is totally different, which might lead to variations in crop growth and carbon gain over growth season. One recent study adopting direct-seeded rice under aerobic, unsaturated and flooded soil institutions at same cropping establishment claimed that rice was more vulnerable to varying soil water content rather than difference in planting methods (Okami et al., 2013). Congruent with their findings, LAI development in rainfed rice lagging behind that of paddy rice during vegetative stage but not at late stage was also observed in our research.

Impermeability of soils in paddy fields could influence rice plants by blocking oxygen diffusion and creating an anaerobic soil substrate. On the other hand, compensating mechanisms for delivery of oxygen to roots by aerenchyma and avoidance of radial oxygen loss by root suberization may limit effective water uptake and cause transient water stress, resulting in stomatal closure during midday (Kotula et al., 2009). In our field observations, however, there was no indication that paddy rice suffered from such water stress, since photosynthetic rate and stomatal conductance were simultaneously at maximum when PAR and leaf temperature reached a peak at midday (Figure 3.5) and similar behavior was observed throughout the season. Recorded daily maximum air temperature at 2 m height was between 30 and 36°C in July and August without large day to day changes. Leaf water potential on clear days in flooded paddy fields ranged between -0.5 and -0.2 MPa (Hirasawa, 1999). Based on the observed leaf response, the assumption made that flooded rice grew under non-water stress conditions seems be reasonable. Overall, the most important environmental factors influencing differentiation in biomass and grain yield production between the two contrasting cropping cultures are (1) soil water availability surrounding roots (Figure 3.1c) as it changes in the rainfed field over the course of the season and (2) differences in micrometeorological drivers such as air temperature just above canopy which determines water vapor pressure deficit (Figure 3.5). In response to these environment drivers,

## Chapter 3 - Canopy gain, water use and yield in paddy and rainfed rice

the observations revealed that rice plants modified several endogenous controls on carbon gain and water use.

### 3.5.1. Leaf area index and allocation of N to leaves regulate seasonal patterns in net carbon gain

Nitrogen is a key element of proteins required in photosynthesis such as Rubisco, enzymes of the dark reaction and components of the electron transport chains of the light reaction. Above- and belowground environment substantially modify patterns in nitrogen allocation to the components of the photosynthetic apparatus, and regulate acclimation in photosynthetic performance (Niinemets and Valladares, 2004; Niinemets, 2007). In line with previous reports (Adachi et al., 2013; Anten et al., 1995; Campbell et al., 2001b; Yoshida, 1981), we observed strong correlations between photosynthetic capacities and  $N_a$  for the rate-limiting photosynthetic parameters  $V_{cmax}$  and  $J_{max}$  (Figure 3.3 and 3.4).

Changes in leaf and canopy nitrogen allocation between paddy and rainfed rice could contribute to the observed variations in productivity. The similarity in slope of the linear correlation between the two planting systems indicated that increasing leaf nitrogen content results in the same degree of increase in photosynthetic capacity. Nevertheless, significant differences in residual N content at  $A_{max}$  of zero separates N use efficiency where rainfed rice exhibited lower N use efficiency as compared to flooded rice. Analogous changes in N use efficiency between non-flooded rice and flooded rice paddies have been reported in *Oryza sativa* cv. Araure 4 (Anten et al., 1995) and *Oryza sativa* cv. Takanari (Adachi et al., 2013). It appears that rice planted in rainfed field has a high “non-productive” N investment in leaves.

In our research, residual  $N_a$  in paddy and rainfed rice were 0.32 and 0.92 g m<sup>-2</sup>, a difference of 190% (Figure 3.4c). Rainfed rice also exhibited a high mass based leaf N (1.33% compared to 0.68% in paddy rice). Thus, crop growth in the modified soil environments shifts N allocation among photosynthetic components and non-photosynthetic components (Niinemets and Tenhunen, 1997). Plants growing in unsaturated soil substrates preferentially

### Chapter 3 - Canopy gain, water use and yield in paddy and rainfed rice

allocate more N into supporting tissues such as cell wall (Niinemets and Valladares 2004), which should allow enhanced drought-resistance manifested by higher leaf mass per leaf area (LMA, not shown).  $N_a$  is the product of  $N_m$  and LMA. Residual LMA derived by the ratio of residual  $N_a$  to residual  $N_m$  in paddy and rainfed rice leaves were 47 and 69.2 g m<sup>-2</sup> (47% difference), which alone does not account for the 190% difference in  $N_a$ . If the relationship of  $A_{max,30}$  to  $N_a$  is adjusted by eliminating residual N, the same tight dependence of photosynthetic capacity on varying N would exist. We conclude that adaption of rainfed rice to upland conditions was characterized by significant variations in leaf anatomy and consequently in N use efficiency.

Leaf area development is a key determinant of canopy level photosynthesis rate, where the canopy profile includes an aggregate of leaf response types that differ with respect to N investment, e.g., investments in biophysical response capacities (Niinemets, 2007). The linear correlation between  $NPP_{int}$  and LAI shown in Figure 3.8b documented that irrespective of cultivation, canopy photosynthesis over the course of the growth season in paddy and rainfed rice was regulated by canopy leaf area development in the same manner and amplitude. Lower NPP in rainfed rice in the initial growth stage was associated with lesser canopy leaf area (Figure 3.2b). The narrowed discrepancy in  $NPP_{int}$  and  $NPP_{max}$  at ca. 200 DOY between paddy and rainfed rice resulted from continuous enlargement of LAI but also from a gradual increase in leaf  $A_{max}$ . Contribution of leaf  $A_{max}$  to enlargement of NPP was amplified on DOY 240, where rainfed rice maintained  $A_{max}$  of 20.1  $\mu\text{mol m}^{-2} \text{s}^{-1}$  while paddy rice leaf rates declined to 10  $\mu\text{mol m}^{-2} \text{s}^{-1}$  (Figure 3.3b). Although paddy rice LAI was still relatively high LAI at 3.2 m<sup>2</sup> m<sup>-2</sup>,  $NPP_{int}$  declined to 2.4 g C m<sup>-2</sup> d<sup>-1</sup>.

The existing differences in the relationship to LAI existing before and after ripening most likely relate to translocation of leaf nitrogen to grain components and subsequent decreases in N available to support photosynthesis (Makino et al., 1984), which is in line with observations in soybean and maize (Gitelson and Gamon, 2015). Due to delayed grain-filling in rainfed rice, higher leaf N and total N significantly contribute to enlargement of carbon

### **Chapter 3 - Canopy gain, water use and yield in paddy and rainfed rice**

gain capacity at DOY 240 as compared to senescent paddy rice (Figure 3.2c; Figure 3.3b).

Regulatory mechanisms in seasonal gross primary production ( $GPP_{int}$ ) by canopy leaf size and nitrogen assemble to principle of NPP seasonality. Plant respiration rate plays a direct role in balance of net carbon gain by canopy. Linear correlation between LAI and  $NPP_{int}$  over growing season and two cropping cultures was evident, while, exponential relationship between LAI and GPP was generated when all data were integrated. It meant linear correlation between LAI and  $GPP_{int}$  is resulted by seasonal changes of plant respiration. Exponential correlation found between  $GPP_{int}$  and LAI is a result of multiple coordinated adjustments among canopy structure and leaf physiology, which is discussed by the other work not here.

#### **3.5.2. Enhanced respiratory carbon loss in rainfed rice**

Biomass accumulation is a direct result of canopy carbon fixation; therefore, carbon uptake capacity and carbon consummation by plant respiration both take a role. Higher proportion of plant respiration in seedling and late growth stages were found in two cultures, which favorably conform to previous report in rice (Alberto et al., 2012). Whereas, rainfed rice showed overall significantly higher ratio, meaning larger proportion of carbon gain was partitioned into plant respiration. Estimate of seasonal respiration as a fraction of photosynthesis in cereal crops ranged from 0.3 to 0.6 and the ratio varied depending growth conditions (Amthor, 2000). Plant respiration tightly related to GPP and accounted for approximately 40% of gross C assimilation until 2 weeks after flowering (Yoshida, 1981). Our values in rainfed rice fell in the reported range, while lower value in paddy rice were observed might due to low maintenance respiration in paddy plants to support growth. Respiration is a metabolic process in which carbohydrate substance produced by chloroplast is oxidized to intermediates along with generation of usable high energy matters ATP and NADPH. During oxidation process, several protein enzymes were involved. As a result, plant respiration depends on canopy temperature and leaf canopy size (Sinclair and Horie, 1989) and growth stage (Gimenez et al., 1994). Seasonal fluctuations in ratio of plant respiration to

### **Chapter 3 - Canopy gain, water use and yield in paddy and rainfed rice**

GPP are expected. Higher leaf thickness and supporting tissue which relates to improve drought resistance commonly have enhanced leaf respiration rate and leaf turn over rate (Niinemets and Valladares, 2004). Rice plants grown in unsaturated soil water environment had greater leaf thickness (data not shown) throughout growing season, which might promote enlargement of plant respiration. Enhanced ratio of plant respiration at end of growth season was greater in paddy by 22.1% than rainfed rice, due to early commencement of leaf age and senescence in paddy plot. GPP in rainfed rice relatively higher than paddy rice was accompanied by occurrence of enhanced plant respiration, leading to compatible net carbon gain between two cultures.

#### **3.5.3. Vulnerability of canopy carbon gain to soil water depletion as regulated by leaf structure and function**

CO<sub>2</sub> diffusion rate from the leaf surface to the carboxylation sites in the mesophyll is primarily regulated by stomatal and mesophyll conductance (Niinemets et al., 2009). Whether intermittent drying of soil during elongation and grain-filling stages impacted the aboveground green biomass production in rainfed rice could not be discerned from our data. On the other hand, canopy NPP were clearly vulnerable with respect to decreases in soil water availability, and high NPP in rainfed rice were severely depressed during SWD1 from initial 7.02 (199 DOY) to 3.2 g C m<sup>-2</sup> d<sup>-1</sup> (202 DOY) during the elongation stage (Figure 3.2b). Decline of canopy photosynthesis was affected by short-term responses in leaf morphology (display of leaf surface) and physiology, since total leaf nitrogen and individual leaf nitrogen content changed little between the end of elongation and the beginning of the grain-filling stage (Figure 3.3a).

With transfer of rice to a rainfed environment, both carbon gain capacity and water use efficiency are apparently important, and in general lower transpiration rates occur due to a decline in stomatal conductance. This regulation in leaves of rainfed rice led to lower C<sub>i</sub>, which reduced at times severely leaf assimilation rates. Stomatal limitation of carbon gain was approximately 55% during most of the daylight period, and was strongest at midday

### Chapter 3 - Canopy gain, water use and yield in paddy and rainfed rice

when PAR was saturating (Figure 3.7b, c). The limitation was much stronger in the rainfed environment during the short dry periods as compared to after rainfall and higher than in the flooded field. Leaf water potential at midday at 202 DOY was close to -2 MPa, resulting further in a dramatic decline of effective leaf area (by as much as almost 60%; Figure 3.6f). The observed declines in  $NPP_{max}$  by 116% during SWD1 reflected these superimposed impacts from down-regulation of stomatal conductance and a decline in leaf area exposure.

Leaf temperatures in rainfed rice on both 181 and 229 DOY were higher by 2 to 3 degree than observed in the flooded rice paddy, while VPD in the rainfed field was as high as 3.5 kPa on sunny days, two times higher relative to 1.5 kPa in the paddy (Figure 3.5). On the other hand, increases in radiation over the course of the day could promote stomatal opening in order to gain  $CO_2$ , water loss via transpiration with high VPD can lead to the opposite, namely strong stomatal closure (Niinemets and Valladares, 2004; Otieno et al., 2012). We found that although light intensity continuously increased in the morning and peaked around noon on both 181 and 229 DOY, assimilation rate in rainfed rice did follow in a same manner but rather decreased when PAR was over certain level (approximately  $900 \mu mol m^{-2} s^{-1}$ ; Figure 3.5d). Stomatal conductance could show cycling or oscillation between the open and closed conditions (Tenhunen, 1987), lasting short time in minutes to hours to optimize the conflicting requirement of  $CO_2$  uptake and control of water loss. Sensitive stomatal adjustments were not observed in rainfed rice during drying situations. Compatible transpiration rate in rainfed rice as compared to paddy rice led to increasing water lost and depress stomatal openness. Stomatal conductance was significantly lower by 120% in upper canopy leaves of rainfed rice and remained at a constant lower level around noon (Figure 3.5d). With development of dry conditions indicated by reduced soil water content from 0.35 to  $0.26 m^3 m^{-3}$  the minimum leaf water potential measured around noon significantly decreased to -2.0 MPa (Figure 3.1c), which resulted in an almost linear decline in both stomatal conductance and assimilation rate at both the elongation and grain-filling stages (Figure 3B1b, c). For example, leaf  $A_{max}$  declined from ca. 25 to ca.  $20 \mu mol m^{-2} s^{-1}$  when leaf water potential decreased to -2.0 MPa during the elongation stage. Relatively high

### Chapter 3 - Canopy gain, water use and yield in paddy and rainfed rice

assimilation rate at given leaf water potential at elongation than grain-filling stage resulted from relatively high leaf  $N_a$  (Figure 3.3a).

Adaptive adjustments in plants to reduce water lost may be achieved by modifying stomatal conductance and/or plant hydraulic conductance from the roots to the leaves. Several components of hydraulic conductance that respond to changes in soil water availability have been reported, such as altered stem hydraulic conductance, changes in characteristics of the soil–root interface (Stiller et al., 2003), and differences in leaf hydraulic conductance (Locke and Ort, 2015). However, xylem hydraulic conductance has been suggested as the main concern in plant growth regulation in response to environmental changes, especially in the case of water stress (Hacke, 2014). We found a hyperbolic correlations for plant hydraulic conductance  $k$  with stomatal conductance, and with assimilation rate (Figure 3.6b, c), both of them saturating at high  $k$  and rapidly declining when  $k$  dropped below ca.  $5.3 \text{ mmol m}^{-2} \text{ s}^{-1} \text{ MPa}^{-1}$ . The threshold point for stomatal conductance was in the range of 4.5 to  $5.3 \text{ mmol m}^{-2} \text{ s}^{-1} \text{ MPa}^{-1}$ , and for  $A_{\text{max}}$  in the range 3.5 to  $4.1 \text{ mmol m}^{-2} \text{ s}^{-1} \text{ MPa}^{-1}$ , which is approximately the same as previously reported for wetland grass species (Otieno et al., 2012) and in rainfed rice (Stiller et al., 2003). Stomatal conductance was more sensitive to fluctuations of  $k$ . We observed enhanced  $\text{WUE}_i$  during drought period (Figure 3.6d).

To underpin wide understanding in soil-plant system associated with water transport and thereafter impacts on photosynthetic physiology, it is useful to insight the internal correlation between  $\Psi_s$  and  $k$ . Threshold point in correlation between  $\Psi_s$  and  $k$  was close to  $-0.075 \text{ MPa}$ , corresponding to  $k$  of  $5 \text{ mmol m}^{-2} \text{ s}^{-1} \text{ MPa}^{-1}$  at which a rapid decline in stomatal conductance was initiated (Figure 3.6e). This threshold was in the range reported from other studies  $-0.05$  to  $-0.25 \text{ MPa}$  (Wopereis et al., 1996) and was close to a previous report for sensitivity of transpiration in rainfed Japonica rice ( $-0.074 \text{ MPa}$ ) (Davatgar et al., 2009) and in upland Indica rice cultivars in Asian tropic regions (Alberto et al., 2011; Davatgar et al., 2009). Although leaf level response regulated transpiration downwards and strengthened rolling extent in order to maintain high water content inside leaf to avoid irreversible impacts on

### Chapter 3 - Canopy gain, water use and yield in paddy and rainfed rice

photosynthetic processes during drought periods, decline of hydraulic conductance significantly constrained  $A_{\max}$ . Irrespective of growth stage,  $WUE_i$  was constant at  $0.075 \mu\text{mol mmol}^{-1}$ , but curvilinearly increased when  $\kappa$  decreased to less than  $5 \text{ mmol m}^{-2} \text{ s}^{-1} \text{ MPa}^{-1}$ . This indicates that the higher water use efficiency occurring during dry periods was at the cost of lowering intercellular  $\text{CO}_2$  concentration and carbon gain capacity.

Instantaneous water use efficiency (intWUE) increasing along with declining  $k$  at drying and wet soil environment was evident (Figure 3.7a), while the correlations between intWUE and  $k$  differentiated in the manners associated to responsive amplitude and tendency when soil water limitation was strong. As mentioned above, responsive correlation between  $WUE_{\text{ins}}$  ( $A/g_{\text{sw}}$ ) and  $k$  over growth season was essentially in the same manner (Figure 3.6d), while separated correlation between intWUE ( $A/E$ ,  $E = g_{\text{sw}} * \text{VPD}$ ) and  $k$  might attribute to correlation between  $k$  and VPD. VPD was direct driver that influences diurnal variations of transpiration (Figure 3.5d), but did not contribute to any changes in  $k$  during water stress periods, which in line with previously reported that blunt response of hydraulic conductance to increasing high temperature and VPD (Locke et al., 2013). It, likely explained soil water content dependent response curves of intWUE versus  $k$ . intWUE is largely affected by VPD and is a comprehensive surrogate that reflects influences caused from both meteorological and physiological processes.

In some plant species, particularly so-called “anisohydric water use plants”, high levels of stomatal conductance and photosynthesis are maintained even though hydraulic conductance and leaf water potential show very large decreases (Locke and Ort, 2015). One recent study claimed that rice plants are isohydric, which was supported by observations of a relatively stable leaf water potential at ca.  $-0.6 \text{ MPa}$  under mild-drying conditions and accompanying declines in stomatal conductance (Parent et al., 2010). In line with the report in rainfed rice (Stiller et al., 2003), stomatal conductance in our study was stabilized at high  $k$  but rapidly declined when  $k$  was less than ca.  $5 \text{ mmol m}^{-2} \text{ s}^{-1} \text{ MPa}^{-1}$ . In the field, leaf water potential during wet soil conditions varies in a range greater than  $-1 \text{ MPa}$ , but stomatal conductance as



### **Chapter 3 - Canopy gain, water use and yield in paddy and rainfed rice**

well as photosynthetic rates do not correlate to changes in  $k$  or leaf water potential. Our results support the idea that rainfed rice strongly regulates  $WUE_i$  in response to changing water availability at an identifiable level in soil water potential and level of  $k$ , and that this can be quite important for initiating irrigation to eliminate the potential impacts of drying soil on yield of rainfed rice. Demarcating response types for water use in plant species seems too simplistic and can lead to misunderstandings and mistakes for irrigation–decision making, since separation between isohydric and anisohydric could not be always successful in the field (Limpus, 2009).

#### **3.5.4. Biomass accumulation and grain yield production between paddy and rainfed rice**

High dry biomass production in certain studies has been related to the amount of N uptake in rainfed rice (Kato et al., 2006; Okami et al., 2013). In our research, total N content was only weakly correlated to aboveground biomass accumulation (Figure 3.9c) even though canopy leaf N could significantly contribute to carbon gain. A variety of factors additionally influence seasonal aboveground biomass production. Perhaps most important among these are seasonal development in canopy light interception, light conversion efficiency, and carbon allocation to different plant organs (Gitelson and Gamon, 2015; Niinemets, 2007). Although rainfed rice exhibited similar total leaf nitrogen content as compared to flooded rice at tillering and elongation stage, NPP and aboveground biomass production were still lower. One another factor interfering observed correlation between total nitrogen and biomass production might relate to proportion of carbon investment in root development. Although no data available to show seasonal development of root biomass in paddy and rainfed rice, there is general consensus that rainfed rice plants develop stronger and deeper root systems to reach moist soil layers (Fukai and Cooper, 1995). Thus, allocation to the root system may have played a role in reducing the rate of aboveground biomass accumulation.

Grain yield reduction in the field appeared to be influenced by the response to dry soil conditions. The overall impact of drought is controlled by multiple factors (Araus et al., 2008): 1) water stress accelerates leaf senescence and directly depresses photosynthesis

### Chapter 3 - Canopy gain, water use and yield in paddy and rainfed rice

during the growth cycle; 2) During grain-filling, panicle development is constrained, leading to barrenness and kernel abortion. Occurrence of soil water depletion during the grain-filling stage had a strong impact on the proportion of filled panicle, but not on panicle number and 1000 grain weight (Table 3.1), leading to a 10% of yield decline relative to paddy rice. During the drying periods, leaf temperatures are slightly above the optimal growth temperature range for rainfed rice (ca. 33°C, Figure 3.A3d), which might be one of factor causing spikelet sterility or abortion (Rang et al., 2011). Ultimately, grain yield is primarily determined by the amount of starch that filled spikelets have during the grain-filling stage (Yoshida, 1981). Concurrent down-regulation of photosynthesis and reduced effective photosynthetic area during grain-filling stage in rainfed rice may, therefore, be linked with kernel abortion.

#### 3.6. Conclusion

In our research, rainfed rice under wet conditions had similar maximum net primary production, leaf area index, and biomass accumulation as compared to paddy rice of the same genotype. Canopy structure and function in the rainfed rice was severely impacted by occurrence of drying soil conditions. Soil water depletion characterized by -75 kPa and plant hydraulic conductance  $5 \text{ mmol m}^{-2} \text{ s}^{-1} \text{ MPa}^{-1}$  initiated a rapid decline in carbon gain capacity, which directly resulted from lowering of intercellular  $\text{CO}_2$  concentration. A high proportion of spikelet abortion occurred during prolonged dry periods and also contributed to reducing the grain yield by 10.2% in rainfed rice. The results showed contrasting responsive correlation between plant hydraulic conductance and VPD under drying and wet conditions, which likely explains observed changes in  $\text{intWUE}$ .  $\text{intWUE}$  is more dependent on momentary environmental conditions, but  $\text{WUE}_i$  shifts are closely indicative of changes in photosynthetic physiology. Use of  $\text{WUE}_i$  and information on soil water potentials may be used to assess the impacts of water stress and to aid in irrigation-decision making.

The total farming area where rice is grown in rainfed fields is expected to increase in monsoon climate regions of Asia, as risks in water scarcity change in the next 50 years and

### **Chapter 3 - Canopy gain, water use and yield in paddy and rainfed rice**

along with uncertainties in the frequency and intensity of regional precipitation. The results of the study improves our understanding of canopy structural and functional adjustments which relate to carbon uptake and water use in rainfed rice as well as biomass and grain yield production. The information can contribute to improved insight of how variations in climate conditions will affect rice growth.

#### **3.7. Acknowledgments**

This study was carried out as part of the International Research Training Group TERRECO (GRK 1565/1) funded by the Deutsche Forschungsgemeinschaft (DFG) at the University of Bayreuth, Germany and the Korean Research Foundation (KRF) at Kangwon National University, Chuncheon, S. Korea. We thank the agricultural logistics group of Chonnam National University for field management and for the rice seedling cultivation in the nursery. Wei. Xue thanks the program of China Scholarships Council (CSC No. 201204910156) for financial support of this research. We acknowledge the helps in the field provided by Seung Hyun Jo, Toncheng Fu, Fabian Fischer, Nikolas Lichtenwald and Yannic Ege. We gratefully acknowledge the technical assistance of Ms. Margarete Wartinger for her support in the field and laboratory.

#### **3.8. References**

- Adachi, S., Nakae, T., Uchida, M., Soda, K., Takai, T., Oi, T., Yamamoto, T., Ookawa, T., Miyake, H. and Yano, M. 2013. The mesophyll anatomy enhancing CO<sub>2</sub> diffusion is a key trait for improving rice photosynthesis. *Journal of Experimental Botany*, 64, 1061–1072.
- Alberto, M.C.R., Buresh, R.J., Hirano, T., Miyata, A., Wassmann, R., Quilty, J.R., Correa, T.Q. and Sandro, J. 2013. Carbon uptake and water productivity for dry-seeded rice and hybrid maize grown with overhead sprinkler irrigation. *Field Crops Research*, 146, 51–65.
- Alberto, M.C.R., Hirano, T., Miyata, A., Wassmann, R., Kumar, A., Padre, A. and Amante, M. 2012. Influence of climate variability on seasonal and interannual variations of ecosystem CO<sub>2</sub> exchange in flooded and non-flooded rice fields in the Philippines. *Field Crops*

### Chapter 3 - Canopy gain, water use and yield in paddy and rainfed rice

- Research, 134, 80–94.
- Alberto, M.C.R., Wassmann, R., Hirano, T., Miyata, A., Hatano, R., Kumar, A., Padre, A. and Amante, M. 2011. Comparisons of energy balance and evapotranspiration between flooded and aerobic rice fields in the Philippines. *Agricultural Water Management*, 98, 1417–1430.
- Alberto, M.C.R., Wassmann, R., Hirano, T., Miyata, A., Kumar, A., Padre, A. and Amante, M. 2009. CO<sub>2</sub>/heat fluxes in rice fields: Comparative assessment of flooded and non-flooded fields in the Philippines. *Agricultural and Forest Meteorology*, 149, 1737–1750.
- Amthor, J.S. 2000. The McCree–de Wit–Penning de Vries–Thornley respiration paradigms: 30 years later. *Annual of Botany*, 86, 1–20.
- Amano, T., Zhu Q., Wang Y., Inoue N. and Tanaka, H. 1993. Case studies on high yields of paddy rice in Jiangsu Province, China. I. Characteristics of grain production. *Japanese Journal of Crop Science*, 62, 267–274.
- Anten, N., Schieving, F. and Werger, M. 1995. Patterns of light and nitrogen distribution in relation to whole canopy carbon gain in C<sub>3</sub> and C<sub>4</sub> mono- and dicotyledonous species. *Oecologia*, 101, 504–513.
- Araus, J.L., Slafer, G.A., Royo, C. and Dolores Serret, M. 2008. Breeding for yield potential and stress adaptation in cereals. *Critical Reviews in Plant Sciences*, 27, 377–412.
- Bhattacharyya, P., Neogi, S., Roy, K. and Rao, K. 2013. Gross primary production, ecosystem respiration and net ecosystem exchange in Asian rice paddy: an eddy covariance-based approach. *Current Science (Bangalore)*, 104, 67–75.
- Bouman, B., Peng, S., Castaneda, A. and Visperas, R. 2005. Yield and water use of irrigated tropical aerobic rice systems. *Agricultural Water Management*, 74, 87–105.
- Campbell, C.S., Heilman, J.L., McInnes, K.J., Wilson, L.T., Medley, J.C., Wu, G. and Cobos, D.R. 2001a. Diel and seasonal variation in CO<sub>2</sub> flux of irrigated rice. *Agricultural and Forest Meteorology*, 108, 15–27.
- Campbell, C.S., Heilman, J.L., McInnes, K.J., Wilson, L.T., Medley, J.C., Wu, G. and Cobos, D.R. 2001b. Seasonal variation in radiation use efficiency of irrigated rice. *Agricultural and Forest Meteorology*, 110, 45–54.

### Chapter 3 - Canopy gain, water use and yield in paddy and rainfed rice

- Cowan, I., 1982. Regulation of water use in relation to carbon gain in higher plants, *Physiological Plant Ecology II*. Springer, pp. 589–613.
- Davatgar, N., Neishabouri, M.R., Sepaskhah, A.R. and Soltani, A. 2009. Physiological and morphological responses of rice (*Oryza sativa* L.) to varying water stress management strategies. *International Journal of Plant Production*, 3, 19–32.
- Feng, Y.L. 2008. Nitrogen allocation and partitioning in invasive and native *Eupatorium* species. *Physiologia Plantarum*, 132, 350–358.
- Franks, P.J. 2004. Stomatal control and hydraulic conductance, with special reference to tall trees. *Tree Physiology*, 24, 865–878.
- Fukai, S. and Cooper, M. 1995. Development of drought-resistant cultivars using physiomorphological traits in rice. *Field Crops Research*, 40, 67–86.
- Gimenez, C., Connor, D.J. and Rueda, F. 1994. Canopy development, photosynthesis and radiation-use efficiency in sunflower in response to nitrogen. *Field Crops Research*, 38, 15–27.
- Gitelson, A.A. and Gamon, J.A. 2015. The need for a common basis for defining light-use efficiency: Implications for productivity estimation. *Remote Sensing of Environment*, 156, 196–201.
- Hacke, U.G. 2014. Variable plant hydraulic conductance. *Tree Physiology*, 34, 105–108.
- Harley, P., Tenhunen, J. and Lange, O. 1986. Use of an analytical model to study limitations on net photosynthesis in *Arbutus unedo* under field conditions. *Oecologia*, 70, 393–401.
- Hirel, B., Bertin, P., Quillere, I., Bourdoncle, W., Attagnant, C., Delley, C., Gouy, A., Cadiou, S., Retailliau, C., Falque, M. and Gallais, A. 2001. Towards a better understanding of the genetic and physiological basis for nitrogen use efficiency in maize. *Plant Physiology*, 125, 1258–1270.
- Intergovernmental Panel on Climate Change [IPCC], 2013. IPCC, 2013: Summary for Policymakers. In: *Climate Change 2013: The Physical Science Basis. Contribution of Working Group I to the Fifth Assessment Report of the Intergovernmental Panel on Climate Change*. Cambridge University Press, Cambridge, United Kingdom.
- International Rice Research Institute [IRRI], 2002. Water-wise rice production. *Proceedings*

### Chapter 3 - Canopy gain, water use and yield in paddy and rainfed rice

- of the International Workshop on Water-wise Rice Production, 8–11 April 2002. International Rice Research Institute [IRRI], Los Baños, the Philippines.
- Jearakongman, S., Rajatasereekul, S., Naklang, K., Romyen, P., Fukai, S., Skulkhu, E., Jumpaket, B. and Nathabutr, K. 1995. Growth and grain yield of contrasting rice cultivars grown under different conditions of water availability. *Field Crops Research*, 44, 139–150.
- Ju, C.X., Buresh, R.J., Wang, Z.Q., Zhang, H., Liu, L.J., Yang, J.C. and Zhang, J.H. 2015. Root and shoot traits for rice varieties with higher grain yield and higher nitrogen use efficiency at lower nitrogen rates application. *Field Crops Research*, 175, 47–55.
- Kato, Y., Kamoshita, A., Yamagishi, J. and Abe, J. 2006. Growth of three rice (*Oryza sativa* L.) cultivars under upland conditions with different levels of water supply 1. Nitrogen content and dry matter production. *Plant Production Science*, 9, 422–434.
- Katsura, K., Okami, M., Mizunuma, H. and Kato, Y. 2010. Radiation use efficiency, N accumulation and biomass production of high-yielding rice in aerobic culture. *Field Crops Research*, 117, 81–89.
- Kotula, L., Ranathunge, K. and Steudle, E. 2009. Apoplastic barriers effectively block oxygen permeability across outer cell layers of rice roots under deoxygenated conditions: roles of apoplastic pores and of respiration. *New Phytologist*, 184, 909–917.
- Ladha, J.K., Kirk, G.J.D., Bennett, J., Peng, S., Reddy, C.K., Reddy, P.M. and Singh, U. 1998. Opportunities for increased nitrogen-use efficiency from improved lowland rice germplasm. *Field Crops Research*, 56, 41–71.
- Li, Y.-L., Tenhunen, J., Owen, K., Schmitt, M., Bahn, M., Droesler, M., Otieno, D., Schmidt, M., Gruenwald, T., Hussain, M.Z., Mirzae, H. and Bernhofer, C. 2008. Patterns in CO<sub>2</sub> gas exchange capacity of grassland ecosystems in the Alps. *Agricultural and Forest Meteorology*, 148, 51–68.
- Limpus, S. 2009. Isohydric and anisohydric characterisation of vegetable crops. The classification of vegetables by their physiological responses to water stress. Project Report. The Department of Primary Industries and Fisheries. Queensland, pp. 11.
- Lindner, S., Otieno, D., Lee, B., Xue, W., Arnhold, S., Kwon, H., Huwe, B. and Tenhunen, J.

### Chapter 3 - Canopy gain, water use and yield in paddy and rainfed rice

2015. Carbon dioxide exchange and its regulation in the main agro–ecosystems of Haean catchment in South Korea. *Agriculture Ecosystems & Environment*, 199, 132–145.
- Lloyd, J. and Taylor, J.A. 1994. On the temperature–dependence of soil respiration. *Functional Ecology*, 8, 315–323.
- Locke, A.M. and Ort, D.R. 2015. Diurnal depression in leaf hydraulic conductance at ambient and elevated [CO<sub>2</sub>] reveals anisohydric water management in field–grown soybean and possible involvement of aquaporins. *Environmental and Experimental Botany*, 116, 39–46.
- Locke, A.M., Sack, L., Bernacchi, C.J. and Ort, D.R. 2013. Soybean leaf hydraulic conductance does not acclimate to growth at elevated [CO<sub>2</sub>] or temperature in growth chambers or in the field. *Annals of Botany*, 112, 911–918
- Makino, A., Mae, T. and Ohira, K. 1984. Relation between nitrogen and ribulose–1, 5–bisphosphate carboxylase in rice leaves from emergence through senescence. *Plant and Cell Physiology*, 25, 429–437.
- McMillan, A., Goulden, M.L. and Tyler, S.C. 2007. Stoichiometry of CH<sub>4</sub> and CO<sub>2</sub> flux in a California rice paddy. *Journal of Geophysical Research: Biogeosciences*, 112, G1, G01017.
- Murchie, E.H., Hubbart, S., Peng, S. and Horton, P. 2005. Acclimation of photosynthesis to high irradiance in rice: gene expression and interactions with leaf development. *Journal of Experimental Botany*, 56, 449–460.
- Niinemets, U. 2007. Photosynthesis and resource distribution through plant canopies. *Plant Cell & Environment*, 30, 1052–1071.
- Niinemets, U., Diaz–Espejo, A., Flexas, J., Galmes, J. and Warren, C.R. 2009. Importance of mesophyll diffusion conductance in estimation of plant photosynthesis in the field. *Journal of Experimental Botany*, 60, 2271–2282.
- Niinemets, U. and Keenan, T.F. 2012. Measures of light in studies on light–driven plant plasticity in artificial environments. *Frontiers in Plant Science*, 3, 156.
- Niinemets, U. and Tenhunen, J.D. 1997. A model separating leaf structural and physiological effects on carbon gain along light gradients for the shade–tolerant species *Acer*

### Chapter 3 - Canopy gain, water use and yield in paddy and rainfed rice

- saccharum*. Plant Cell & Environment, 20, 845–866.
- Niinemets, U. and Valladares, F. 2004. Photosynthetic acclimation to simultaneous and interacting environmental stresses along natural light gradients: Optimality and constraints. Plant Biology, 6, 254–268.
- Okami, M., Kato, Y. and Yamagishi, J. 2013. Grain Yield and leaf area growth of direct-seeded rice on flooded and aerobic soils in Japan. Plant Production Science, 16, 276–279.
- Osmont, K.S., Sibout, R. and Hardtke, C.S. 2007. Hidden branches: developments in root system architecture. Annual Review of Plant Biology, 58, 93–113.
- Otieno, D., Lindner, S., Muhr, J. and Borken, W. 2012. Sensitivity of peatland herbaceous vegetation to vapor pressure deficit Influences net ecosystem CO<sub>2</sub> exchange. Wetlands, 32, 895–905.
- Parent, B., Suard, B., Serraj, R. and Tardieu, F. 2010. Rice leaf growth and water potential are resilient to evaporative demand and soil water deficit once the effects of root system are neutralized. Plant, Cell & Environment, 33, 1256–1267.
- Rang, Z., Jagadish, S., Zhou, Q., Craufurd, P. and Heuer, S. 2011. Effect of high temperature and water stress on pollen germination and spikelet fertility in rice. Environmental and Experimental Botany, 70, 58–65.
- RDA, Rural Development Administration. 2008. Taxonomical classification of Korean soils. NIAST (National Institute of Agricultural Science and Technology), Suwon, Korea, pp. 4.
- Ruidisch, M. 2013. Flow and transport processes as affected by tillage management under monsoonal conditions in South Korea. Ph.D Thesis, Universität Bayreuth, pp. 196.
- Schaap, M.G., Leij, F.J. and van Genuchten, M.T. 1998. Neural network analysis for hierarchical prediction of soil hydraulic properties. Soil Science Society of America Journal, 62, 847–855.
- Sharkey, T.D., Bernacchi, C.J., Farquhar, G.D. and Singsaas, E.L. 2007. Fitting photosynthetic carbon dioxide response curves for C<sub>3</sub> leaves. Plant, Cell & Environment, 30, 1035–1040.
- Sinclair, T. and Horie, T. 1989. Leaf nitrogen, photosynthesis, and crop radiation use



### Chapter 3 - Canopy gain, water use and yield in paddy and rainfed rice

- efficiency: a review. *Crop Science*, 29, 90–98.
- Stiller, V., Lafitte, H.R. and Sperry, J.S. 2003. Hydraulic properties of rice and the response of gas exchange to water stress. *Plant Physiology*, 132, 1698–1706.
- Tanguilig, V., Yambao, E., O'toole, J. and De Datta, S. 1987. Water stress effects on leaf elongation, leaf water potential, transpiration, and nutrient uptake of rice, maize, and soybean. *Plant and Soil*, 103, 155–168.
- Tenhunen, J. 1987. Diurnal variations in leaf conductance and gas Exchange in natural environments. In: Tenhunen, J.D., Pearcy, R.W., and Lange, O.L. (eds.). *Stomatal function*, pp. 323.
- Thanawong, K., Perret, S. and Basset-Mens, C. 2014. Eco-efficiency of paddy rice production in Northeastern Thailand: a comparison of rain-fed and irrigated cropping systems. *Journal of Cleaner Production*, 73, 204–217.
- Vangenuchten, M.T. 1980. A closed-form equation for predicting the hydraulic conductance of unsaturated soils. *Soil Science Society of America Journal*, 44, 892–898.
- Wopereis, M.C.S., Kropff, M.J., Maligaya, A.R. and Tuong, T.P. 1996. Drought-stress responses of two lowland rice cultivars to soil water status. *Field Crops Research*, 46, 21–39.
- Yoshida, S., 1981. *Fundamentals of rice crop science*. The International Rice Research Institute, Manila, Philippines. pp. 130–146.
- Yoshida, S., Forno, D.A. and Cock, J.H. 1971. *Laboratory manual for physiological studies of rice*. International Rice Research Institute, Los Banos, Philippines, pp. 83.
- Yu, G.R., Nakayama, K., Matsuoka, N. and Kon, H. 1998. A combination model for estimating stomatal conductance of maize (*Zea mays* L.) leaves over a long term. *Agricultural and Forest Meteorology*, 92, 9–28.

### 3.9. Appendices

Appendix A. Seasonal performance of net primary production–incident PAR curve in paddy and rainfed rice

### Chapter 3 - Canopy gain, water use and yield in paddy and rainfed rice

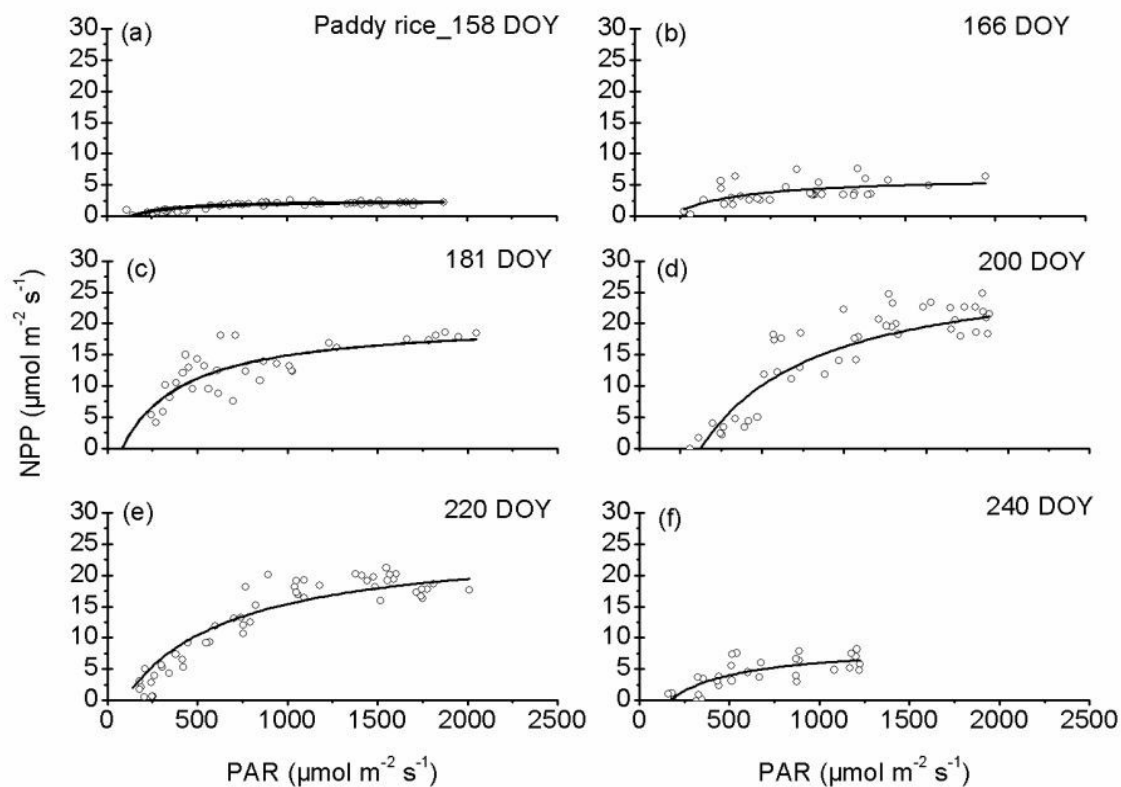


**Figure 3.10.A1** Light-net primary production response curve in paddy rice over growth stages.

### Chapter 3 - Canopy gain, water use and yield in paddy and rainfed rice

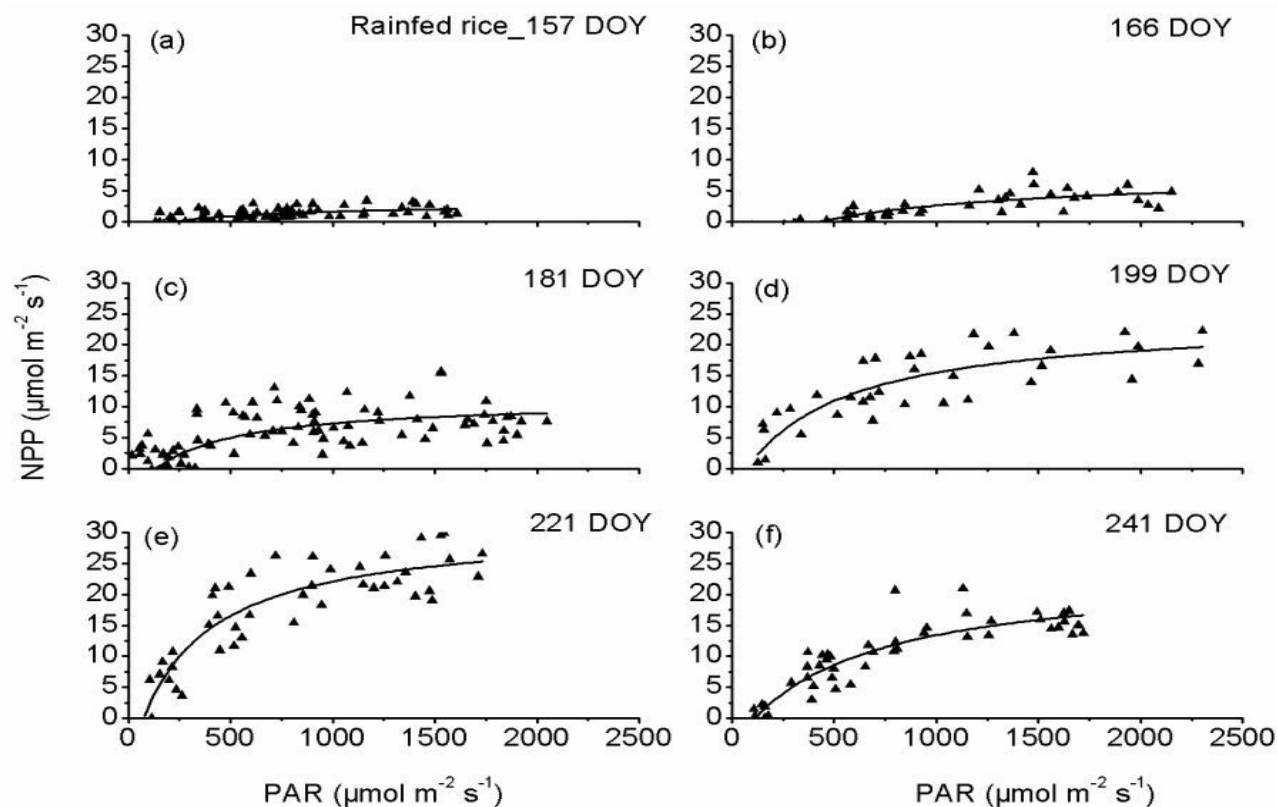


**Figure 3.11.A2** Light-net primary production response curve in rainfed rice over growth stages.

**Table 3.2.A1** Parameter estimation for instantaneous NPP–light response curve: initial slope ( $\alpha$ ) of response curve, saturating level ( $\beta$ ) of NPP at extremely high PAR, and y-axis intercept ( $\gamma$ ) when PAR is close to 0 in paddy and rainfed rice on different measuring dates.

DOY	Paddy rice			DOY	Rainfed rice		
	$\alpha$	$\beta$	$\gamma$		$\alpha$	$\beta$	$\gamma$
158	0.05 (0.004)	6.1 (0.29)	-3.4 (0.21)	157	0.01 (0.002)	4.6 (0.6)	-1.5 (0.2)
166	0.08 (0.01)	13.6 (2.0)	-7.1 (1.35)	166	0.02 (0.005)	12.3 (0.98)	-4.5 (0.7)
181	0.1 (0.008)	26.8 (1.97)	-6.2 (1.1)	181	0.05 (0.01)	15.7(1.4)	-4.7 (0.5)
200	0.06 (0.01)	36.0 (2.7)	-6.2 (1.1)	199	0.07 (0.01)	28.1 (3.5)	-4.1 (2.1)
220	0.07 (0.01)	32.0 (1.9)	-5.5 (2.45)	221	0.12 (0.02)	38.7 (4.2)	-7.9 (2.5)
240	0.06 (0.05)	15.2 (2.9)	-6.4 (3.5)	241	0.05 (0.004)	28.3 (1.9)	-4.7 (0.6)

### Chapter 3 - Canopy gain, water use and yield in paddy and rainfed rice

Appendix B. Characteristics of photosynthetic physiology in rainfed rice responding to leaf water potential and leaf temperature

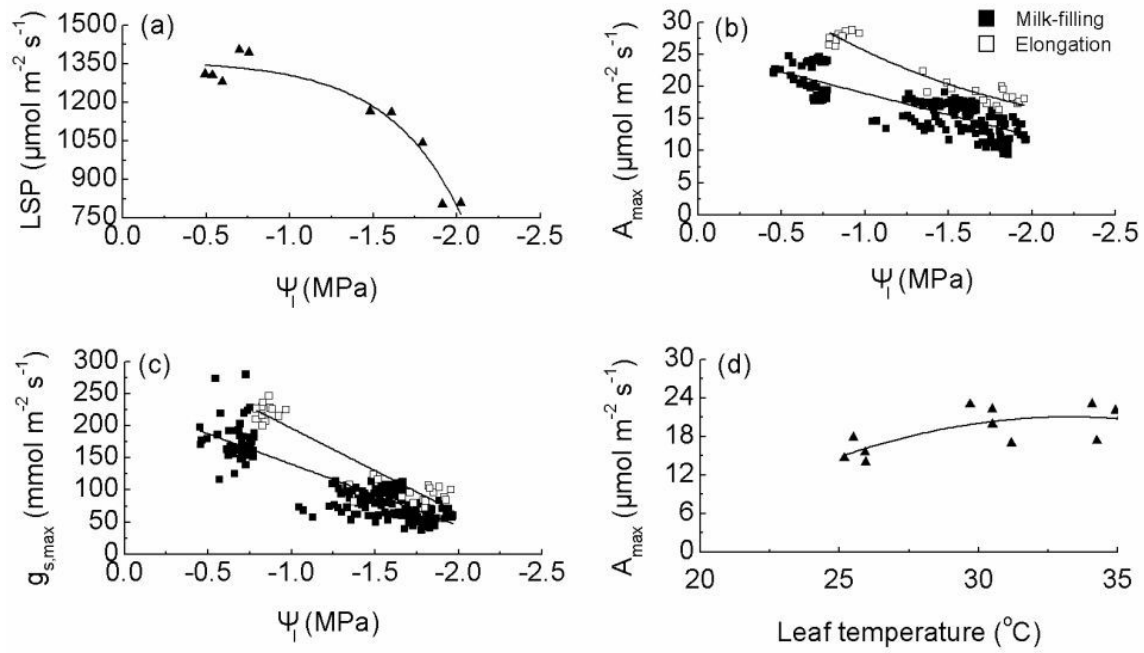


**Figure 3.12.B1** Dependence of light saturating point (LSP) on leaf water potential ( $\Psi_l$ ) (a); relationships between maximum photosynthetic capacity ( $A_{\max}$ ) and ( $\Psi_l$ ) (b), between maximum stomatal conductance ( $g_{s,\max}$ ) and ( $\Psi_l$ ) (c); and temperature response of  $A_{\max}$  in rainfed rice (d).

### Chapter 4

#### 4. Flux partitioning reveals trade-off between water and carbon loss of paddy and rainfed rice (*Oryza sativa* L.)

Bhone Nay-Htoon<sup>1</sup>, Wei Xue<sup>2</sup>, Steve Lindner<sup>2</sup>, Matthias Cuntz<sup>3</sup>, Jonghan Ko<sup>4</sup>, John Tenhunen<sup>2</sup>, Maren Dubbert<sup>1,5</sup>, Christiane Werner<sup>1,5</sup>

<sup>1</sup>Department of Agroecosystem Research, University of Bayreuth, 95447 Bayreuth, Germany

<sup>2</sup>Department of Plant Ecology, University of Bayreuth, 95447 Bayreuth, Germany

<sup>3</sup>Computation Hydrosystems, Helmholtz Center for Environmental Research (UFZ), 04318 Leipzig, Germany.

<sup>4</sup>Department of Applied Plant Science, Chonnam National University, 500757 Gwangju, South Korea

<sup>5</sup>Department of Ecosystem Physiology, University of Freiburg, 79085 Freiburg, Germany

#### 4.1. Abstract

Agricultural crops play an important role in the global carbon and water cycle. Global climate change scenarios predict enhanced water scarcity and altered precipitation pattern in many parts of the world and a mechanistic understanding of water fluxes, productivity and water use of cultivated crops is of major importance. We compared water and carbon fluxes of paddy and rainfed rice by canopy scale gas exchange measurements, crop growth, daily evapotranspiration, transpiration and carbon flux modeling. Throughout a monsoon rice growing season, soil evaporation in paddy rice contributed strongly to evapotranspiration (96.55% to 43.28% from initial growth (Day of year 140) to fully developed canopy (Day of year 200) and amounted to 57.93% of total water losses over the growing seasons. Evaporation of rainfed rice was much smaller (only 35.29% of growing season total evapotranspiration). Water use efficiency (WUE) was higher in rainfed rice both from an agronomic ( $WUE_{agro}$ , i.e. grain yield per evapotranspiration) and ecosystem ( $WUE_{eco}$ , i.e. gross primary production per evapotranspiration) perspective. However, rainfed rice also

## **Chapter 4 - Carbon and water fluxes between paddy and rainfed rice**

showed high ecosystem respiration losses and a slightly lower crop yield, demonstrating that higher WUE in rainfed rice comes at the expense of higher respiration losses and lower plant productivity, compared to paddy rice. Our results highlighted the need to partition water and carbon fluxes to improve our mechanistic understanding of carbon and water balance of rice ecosystems and environmental impact of different agricultural practices.

**Keywords:** Evapotranspiration, Flux partitioning, Net ecosystem CO<sub>2</sub> exchange, Paddy rice, Rainfed rice, Water use Efficiency

## Chapter 4 - Carbon and water fluxes between paddy and rainfed rice

### 4.2. Introduction

Water scarcity and extreme droughts are increasing in many regions of the world due to the changes in precipitation pattern, intensity and temperature (Intergovernmental panel on climate change [IPCC], 2013). Agricultural production accounts for 70% of global freshwater withdrawals while being the most sensitive sector to water scarcity (Food and Agriculture organization [FAO], 2012). According to recent projections, reduced crop productivity due to heat and drought stress is highly expected (Blanco et al., 2014; Peng et al., 2004; Watanabe and Kume, 2009) and crop management adaptation due to climate variability are under debate.

Rice (*Oryza Sativa* L.) is an important food source for half of the current world's population and global demand for rice is projected to increase along with increasing global population (Alexandratos and Bruinsma, 2012; Khush, 2005; Muthayya et al., 2014; Ray et al., 2013; Seck et al., 2012). More than 80% of global rice production area is located in Asia (Kudo et al., 2014; Yan et al., 2003) and 80% of it is cultivated under conventional flooded conditions (Bhattacharyya et al., 2014; Nie et al., 2012). Rice grown under flooded conditions consumes 1000 to 5000 l of water to produce 1 kg of grain and is also reported for its high methane (CH<sub>4</sub>) emission (Hussain et al., 2014; Kudo et al., 2014; Smith et al., 2007). Therefore, several water saving rice production techniques are introduced, which also aim at mitigating CH<sub>4</sub> emission (Bouman et al., 2005; Pittelkow et al., 2013; Zou et al., 2005). On the other hand, decreased crop yields under water limited conditions are reported (Bouman and Tuong, 2001), although it is a crop which can be grown under different water regimes (International Rice Research Institute [IRRI], 2002).

Agricultural land–use–changes such as shifting conventional flooded paddy rice to dry–land rice farming further impacts carbon and water exchange of rice ecosystems (Alberto et al., 2013, 2009; Kudo et al., 2014; Nishimura et al., 2008; Sakai et al., 2004; Wassmann et al., 2000; Zou et al., 2005). Even in conventional paddy rice systems, intensity and timing of flooding and drainage regulation influences the seasonal carbon and water balance (Alberto et

## **Chapter 4 - Carbon and water fluxes between paddy and rainfed rice**

al., 2009; Kudo et al., 2014; Miyata et al., 2000; Nishimura et al., 2015; Thanawong et al., 2014). Although previous studies report on differences in ecosystem carbon and water balance of paddy and rainfed rice (Alberto et al., 2009; Thanawong et al., 2014), a quantification of the contribution and seasonal dynamics of the productive (plant transpiration and gross primary productivity) and unproductive (respiration and soil evaporation) components of ecosystem carbon and water exchange to estimate possible trade-offs from ecosystem and agronomic perspective under different environmental conditions is still lacking.

We studied carbon and water exchange of paddy (conventional flooded system) and rainfed rice (non-irrigated, water saving rice production system) over a whole growing season by combining classical chamber flux measurements, high resolution remote sensing by Unmanned Aerial Vehicle (UAV) and crop growth modeling. The main goal of this study was to analyze the carbon and water fluxes of conventional paddy rice and rainfed rice systems by partitioning unproductive water losses (Evaporation) from productive water use (Transpiration) and carbon losses (Respiration) from carbon gain (Net ecosystem carbon exchange) to see the trade-offs between paddy and rainfed rice in regard to evaporative water and respiratory carbon loss.

### **4.3. Materials and methods**

#### **4.3.1. Study Site**

The study was conducted in the Chonnam National University research farm, (35°10' N, 126°53' E, alt. 33m), Gwangju, Chonnam province, Republic of Korea (South Korea). Chonnam province is one of the major rice growing regions of South Korea, which has typical East Asian monsoon climate with an annual mean temperature of 13.8°C and annual mean precipitation of ~1391 mm during the past 30 years (1981–2010). More than 60% of precipitation events occurred during the monsoon season (May to October). Both paddy and rainfed rice fields have similar soil properties with loamy texture and pH 6.5. Detailed soil properties are indicated in the supplementary material (1), Table 4.1.S1.



## Chapter 4 - Carbon and water fluxes between paddy and rainfed rice

Rice (*Oryza sativa* L. subsp. japonica cv. unkwang) was cultivated as rainfed dryland crop and flooded paddy crop. In both rainfed and paddy rice fields, N: P: K fertilizer (11:5:6) were applied at a rate of N = 115 kg ha<sup>-1</sup> (80% as basal dosage and 20% during the tillering stage). P fertilizer (62 kg ha<sup>-1</sup>) was applied as a 100% basal dosage. K fertilizer (60 kg ha<sup>-1</sup>) was applied as 65% basal dosage and 35% during tillering). All field management practices of paddy rice and fertilizer dosages reflected the practices of farmers in the region. Under rainfed conditions, rice was directly seeded and no additional irrigation was applied to natural precipitation. The experiment was conducted in a randomized complete block design with three replications.

### 4.3.2. Environmental variables

Weather data (global radiation, precipitation, air temperature, relative humidity and wind speed) were continuously collected at 2 m height with an automatic weather station every five minutes (Automated Weather Station, WS-GP1, Delta-T Devices Ltd., UK) and half hourly mean values were logged. Photosynthetic photon flux density (PPFD, LI-190, LI-COR, USA) was measured directly above the crop canopy (~20 cm above the canopy and inside the chamber). Air temperature ( $T_{\text{air}}$ ) (at ~20 cm above the canopy) inside the chamber was also measured by custom built temperature sensor. Soil temperature at root zone was manually measured along with gas exchange measurements using temperature probes (Conrad, Hirschau, Germany). Soil temperature and volumetric water content (5TE and 10HS, respectively, Decagon, Washington, USA) were measured at 5, 10, 20, 30 and 60 cm depth in each experiment plot. 15 min averaged data from 5TE sensors were stored in a datalogger (Em 50, Decagon, Washington, USA) and 30 min averaged data from 10HS sensors were stored in a datalogger (CR1000, Campbell Scientific, Logan, UT, USA).

On the days of flux measurements, above ground biomass of plants adjacent to vegetation plots were harvested. Leaf area (LA) was determined with a Leaf Area Meter (LI-3000A, LI-COR, USA) and leaf area index (LAI) was calculated as leaf area per ground area. Total

## Chapter 4 - Carbon and water fluxes between paddy and rainfed rice

aboveground biomass was collected, dried (60°C, 48 hours) and weighed. Plant height of representative plants was manually measured every month.

### 4.3.3. Canopy carbon and water flux measurement

Canopy fluxes were measured on canopy vegetation plots (3 replications per treatment) where soil collars were permanently installed soon after seeding of rainfed and planting of paddy rice. CO<sub>2</sub> and H<sub>2</sub>O fluxes of rainfed rice were measured by a custom built open chamber constructed according to Pape et al. (2009) and successfully tested by Dubbert et al. (2013). H<sub>2</sub>O fluxes were measured by a Cavity Ring-Down Spectrometer (CRDS, Picarro, Santa Clara, USA) and CO<sub>2</sub> fluxes were measured by a portable Infra-Red Gas Analyzer (LI-820, LI-COR, USA). Both carbon and water fluxes were calculated as differential CO<sub>2</sub> or H<sub>2</sub>O concentration (i.e. the CO<sub>2</sub> or H<sub>2</sub>O concentration difference between the air samples taken from the chamber inlet and outlet). Air inlet to the chamber was stabilized by a buffer bottle (200 L). Outlet air from the chamber was pumped to the analyzers via tubes heated up to 38°C to avoid condensation.

As the heavy weight of the open chamber was hard to handle in paddy soil conditions, CO<sub>2</sub> fluxes of paddy rice were measured by custom built closed chambers described by Li et al. (2008) and Otieno et al. (2012). CO<sub>2</sub> fluxes from both chambers did not differ significantly (t-test; n.s.). Ecosystem respiration ( $R_{eco}$ ) was measured by insulated opaque PVC dark chambers on crop canopy. Soil respiration ( $R_{soil}$ ) was measured from bare soil plots next to the vegetation plots. Data were collected from 6:00 hr to 18:00 hr in one and a half hour interval. Fluxes were recorded within 10 minutes of placing the chambers on soil collar. Diurnal courses of canopy fluxes were recorded during four important crop growth stages, namely; seedling (DOY 140 to 170); tillering (DOY 170 to 180); heading (DOY 200 to 210); maturity (DOY 210 to 220).

Gross Primary Production was calculated as:

$$GPP = -NEE + R_{eco} \quad (4.1)$$

## Chapter 4 - Carbon and water fluxes between paddy and rainfed rice

where GPP is gross primary production, NEE is net ecosystem CO<sub>2</sub> exchange and R<sub>eco</sub> is ecosystem respiration. Total daytime fluxes were calculated by summing up hourly carbon and water fluxes from 6:00 to 20:00 hr.

### 4.3.4. UAV remote sensing, modeling daily NDVI

An Unmanned Aerial Vehicle (UAV) equipped with Miniature Multiple Camera Array (Mini MCA) (Tetracam, Inc., USA) with 450, 550, 650, 800, 830, and 880 nm bands and 10 cm ground resolution at 300 m altitude was used. For radiometric calibration of MCA images, calibration targets (black, white and gray) were set up next to the paddy field. A cropsan instrument (MSR, Cropsan Inc., USA.) was used to calibrate and evaluate the reflectance data obtained by the UAV system.

Remote sensing images were analyzed by ENVI software (Exelis Visual Information Solutions, Inc., USA.). Three sampling points for each treatment plots of both rainfed and paddy rice were used to calculate normalized difference vegetation index (NDVI) as:

$$NDVI = \frac{\rho_{nir} - \rho_{red}}{\rho_{nir} + \rho_{red}} \quad (4.2)$$

Remote sensing campaigns were carried out at noon of DOY 172, 192, 206, 220 and 233. For daily crop ET and GPP modeling, daily NDVI was modeled by GRAMI crop growth model (for details see Ko et al., 2006; Stephan J Maas, 1993a; Stephan J. Maas, 1993b). Briefly, it simulates daily crop growth based on growing degree-day, radiation use, daily carbohydrate production by crop canopy, conversion from carbohydrate to leaf development and relationship between LAI and NDVI. Simulated crop growth, particularly, LAI and NDVI were validated by measured LAI by leaf area meter (LAI 2000, LI-COR, USA) and measured NDVI by crop scan (Figure 4.5.A3).

### 4.3.5. Modeling and partitioning crop evapotranspiration

Crop evapotranspiration was calculated based on FAO 56 dual crop coefficient model, which is a modified version of Penman Monteith (1965) ET model (Allen et al., 1998):

## Chapter 4 - Carbon and water fluxes between paddy and rainfed rice

$$\lambda(ET_o) = (\Delta(R_n - G) + (\rho C_p (e_s - e_a) / r_a)) / (\Delta + r(1 + (r_c / r_a))) \quad (4.3)$$

where  $\lambda$  is the latent heat of vaporization of water vapor,  $\Delta$  is the slope of the saturation vapor pressure temperature relationship,  $R_n$  is the net radiation,  $G$  is the soil heat flux,  $e_s - e_a$  is the vapor pressure deficit of the air,  $\rho$  is the mean air density at constant pressure,  $C_p$  is the specific heat of the air,  $r_a$  is aerodynamic resistance,  $r_c$  is the canopy resistance and  $r$  is the psychrometric constant.

The model estimates crop ET based on the reference crop evapotranspiration ( $ET_o$ ) multiplied to the sum of the transpiration coefficient ( $K_{cb}$ ) and the evaporation coefficient ( $K_e$ ) (Alberto et al., 2011, 2014; Allen et al., 1998; Payero and Irmak, 2013).

$$ET = (K_{cb} + K_e) \times ET_o \quad (4.4)$$

where ET is the crop evapotranspiration,  $K_{cb}$  is the transpiration coefficient equivalent to the ratio of transpiration to potential evapotranspiration,  $K_e$  is the evaporation coefficient equivalent to the ratio of soil evaporation to potential evapotranspiration,  $ET_o$  is the reference evapotranspiration of a well-watered and healthy grass layer.

In our case, instead of hypothetical parameters for grass canopy provided by FAO 56 dual crop coefficient model, we used the measured crop physiological parameters (leaf resistance to water vapor transfer, leaf transpiration, and daily canopy aerodynamic resistance) for well irrigated and healthy rice in the field. Therefore, our  $ET_o$  was reference crop evapotranspiration of rice under standard crop management.

We calculated canopy transpiration (T) by equation (3) but used the net radiation intercepted by crop canopy ( $Q_{int}$ ) instead of net solar radiation ( $R_n$ ). To estimate  $Q_{int}$ , we partitioned incoming net radiation ( $R_n$ ) to  $Q_{int}$  and  $Q_{res}$  (residual net radiation reaching the soil surface).  $Q_{int}$  was calculated according to Beer's law (Zhou et al., 2006):

$$Q_{int} = Q_o (1 - \exp(-K_l \cdot LAI)) \quad (4.5)$$

where  $K_l$  is the extinction coefficient of the vegetation for net radiation and is in the range of

## Chapter 4 - Carbon and water fluxes between paddy and rainfed rice

0.5 to 0.7; 0.6 was applied in our case (Kelliher et al., 1995; Mo et al., 2004). Simulated daily ET of rainfed rice was verified by chamber measured ET. The paddy rice ET model was validated by applying measured ET and NDVI of monsoon 2012 paddy rice, at Haeon, South Korea (Lee, et al., unpublished).

### 4.3.6. Calculation of $K_{cb}$

In the FAO 56 dual crop coefficient approach of Allen et al. (1998), the basal crop coefficient or transpiration coefficient ( $K_{cb}$ ) is calculated based on seasonal change in vegetation ground cover. Estimates of  $K_{cb}$  for several crops including rice is provided as a  $K_{cb}$  curve with four growth stages (initial, development, mid-season, and late season) and it is recommended to use the estimated  $K_{cb}$  values after specific climatic adjustment.

Instead of applying theoretical dual crop coefficient  $K_{cb}$  values of original FAO 56 model, we developed a daily basal crop coefficient ( $K_{cb}$ ) curve representing the actual crop growth and development. Following Choudhury (1994) we derived the daily  $K_{cb}$  based on the daily and high resolution NDVI of the whole field:

$$K_{cb} = 1 - \left( \frac{NDVI_{max} - NDVI}{NDVI_{max} - NDVI_{min}} \right)^{k/k^*} \quad (4.6)$$

where  $NDVI_{max}$ ,  $NDVI_{min}$  and  $NDVI$  are vegetation indices for dense canopy, bare soil and normal vegetation respectively,  $k$  is a damping coefficient derived from the correlation of LAI and the ratio of canopy transpiration to potential evapotranspiration,  $k^*$  is a damping coefficient derived from correlation of LAI and NDVI. The relationships between the ratio of unstressed transpiration ( $T$ ) to reference crop evapotranspiration ( $ET_o$ ) and leaf area index (LAI), relationships between LAI and vegetation indexes has been shown (Choudhury, 1994; Duchemin et al., 2006; Sellers, 1985). Damping coefficient  $k$  is the coefficient derived by exponential correlation of the ratio of calculated daily  $T$  to reference  $ET_o$  and LAI while damping coefficient  $k^*$  is the coefficient derived by exponential correlation of LAI and NDVI (Annex 1 and 2).

## Chapter 4 - Carbon and water fluxes between paddy and rainfed rice

### 4.3.7. Calculation of $K_e$

Evaporation coefficient ( $K_e$ ) was calculated according to Allen et al. (1998).  $K_e$  is maximal when the topsoil is wet or flooded and  $K_e$  is minimal to zero when the topsoil is dry. The upper limit of  $K_e$  ( $K_{cmax}$ ) which is an upper limit of evaporation and transpiration from cropped surfaces need to be defined before calculating  $K_e$  since the evaporation rate never reached to evapotranspiration and  $K_e$  needs to be limited by  $K_{cmax}$ .

$$K_{cmax} = \max \left\{ 1.2 + (0.04(u_2 - 2) - 0.004(rh_{min} - 45)) \left( \frac{h}{3} \right)^{0.2}, K_{cb} + 0.05 \right\} \quad (4.7)$$

where  $K_{cmax}$  is the upper limit of evaporation and transpiration from cropped surface,  $u_2$  is wind speed ( $m\ s^{-1}$ ),  $rh_{min}$  is the minimum relative humidity and  $K_{cb}$  is the transpiration coefficient derived by equation (4.6).

Soil evaporation process is assumed to be controlled by stages: Stage 1: an energy limiting stage and Stage 2: a falling-rate stage (Ritchie, 1972; Monteith, 1981; Allen, 1998). Soil evaporation reduction coefficient ( $K_r$ ) is 1 when the soil surface is wet;  $K_r$  decreases when water content in the topsoil is limiting, and  $K_r$  becomes zero when total evaporable water (TEW= maximum amount of water that can be evaporated) in the topsoil is depleted. TEW for a complete drying cycle was estimated as:

$$TEW = 1000(\theta_{FC} - 0.5\theta_{WP}) \times Z_e \quad (4.8)$$

where TEW is maximum depth of water that can evaporated from the soil when topsoil is completely wetted (mm),  $\theta_{FC}$  is soil water content at field capacity ( $m^3\ m^{-3}$ ),  $\theta_{WP}$  is soil water content at wilting point ( $m^3\ m^{-3}$ ) and  $Z_e$  is depth of surface soil layer (0.1 m).  $K_r$  for paddy rice is fixed at 1 since soil surface is flooded most of the time and soil surface is wet even during the drainage period.  $K_r$  of rainfed rice was calculated as:

$$K_r = \frac{TEW - D_{e,i-1}}{TEW - REW} \quad (4.9)$$

where  $K_r$  is the soil evaporation reduction coefficient dependent on soil water depletion,  $D_{e,i-1}$  is the cumulative depth of evaporation depletion from topsoil at the end of the day (i-1), TEW is the total evaporable water (mm) calculated by equation (8) and REW is the readily evaporable water which is cumulative depth of depletion of evaporable water from the soil

## Chapter 4 - Carbon and water fluxes between paddy and rainfed rice

surface layer at the end of stage one. During stage one drying,  $K_r$  is 1 and during stage two drying,  $K_r$  is 1 when  $D_{e, i-1} \leq REW$ ).

Finally, the evaporation coefficient ( $K_e$ ) is calculated as:

$$K_e = K_r (K_{c \max} - K_{cb}) \leq FEW \times K_{c \max} \quad (4.10)$$

where  $K_e$  is the soil evaporation coefficient,  $K_r$  is the evaporation reduction coefficient,  $K_{c \max}$  is the maximum value of  $K_c$ , FEW is the fraction of soil surface exposed and wetted.

### 4.3.8. Modeling and partitioning daily carbon fluxes

Gross primary production was simulated based on the chamber measured canopy light use efficiency, daily NDVI and PAR and estimation is based on Monteith (1972):

$$GPP = LUE \times fPAR \times PAR \quad (4.11)$$

where GPP is the gross primary production, LUE is the canopy light use efficiency, PAR is the photosynthetic active radiation (Glenn et al., 2008; Running et al., 2004) and fPAR is the fraction of incident to absorbed PAR. fPAR was calculated by NDVI-fPAR model, following Choudhury (1987) and Goward and Huemmrich (1992):

$$fPAR = \frac{(NDVI - NDVI_{\min}) \times (fPAR_{\max} - fPAR_{\min})}{NDVI_{\max} - NDVI_{\min}} \quad (4.12)$$

where, fPAR is the fraction of incident to absorbed PAR, NDVI is the normalized vegetation index of rice field,  $NDVI_{\min}$  and  $NDVI_{\max}$  are minimum and maximum NDVI,  $fPAR_{\max}$  is 0.95 while  $fPAR_{\min}$  is 0.001.

Light use efficiency (LUE) is the ratio of gross primary production to absorbed PAR (Gitelson et al., 2014; Glenn et al., 2008; Monteith, 1972; Running et al., 2004) and thus LUE was calculated based on chamber measured GPP and absorbed PAR. Absorbed PAR (aPAR) was calculated as the product of NDVI derived fPAR (see equation 4.12) and incident PAR.

Daily ecosystem respiration of rainfed and paddy rice was calculated following (Reichstein et al., 2002) as:

$$R_{eco} = R_{ecoref} \times f(T_{soil}) \times g(SWC) \quad (4.13)$$

## Chapter 4 - Carbon and water fluxes between paddy and rainfed rice

where  $g(\text{SWC})$  is the saturation function (Bunnell et al., 1977a; 1977b; Reichstein et al., 2002);  $R_{\text{ecoref}}$  is reference ecosystem respiration,  $f(T_{\text{soil}})$  is the function developed by (Lloyd and Taylor, 1994) as:

$$R_{\text{soil}} = R_{\text{soilref}} e^{E_0 \left( \frac{1}{T_{\text{ref}} - T_0} - \frac{1}{T_{\text{soil}} - T_0} \right)} \quad (4.14)$$

where  $T_{\text{ref}}$  and  $T_0$  are fixed to 15 and  $-46^\circ\text{C}$ , respectively,  $T_{\text{soil}}$  is the soil temperature at 5 cm depth,  $E_0$  is the activation energy and was considered to be a free parameter. Simulated  $\text{CO}_2$  fluxes were verified by measured  $\text{CO}_2$  fluxes.

The productivity of paddy and rainfed rice system was assessed by calculating agronomic and ecosystem water use efficiency (WUE). Agronomic WUE ( $\text{WUE}_{\text{agro}}$ ) is defined as the ratio of biomass production (grain yield) per amount of evapotranspiration (ET):

$$\text{WUE}_{\text{agro}} = \frac{\text{grain}}{\text{ET}} \quad (4.15)$$

Ecosystem water use efficiency ( $\text{WUE}_{\text{eco}}$ ) is defined as the ratio of gross primary production (GPP) to evapotranspiration (ET):

$$\text{WUE}_{\text{GPP}} = \frac{\text{GPP}}{\text{ET}} \quad (4.16)$$

Including both respiratory carbon fluxes ( $R_{\text{eco}}$ ) and ecosystem productivity (GPP), ecosystem WUE can also be defined as the ratio of net ecosystem carbon exchange (NEE) to ET:

$$\text{WUE}_{\text{NEE}} = \frac{\text{NEE}}{\text{ET}} \quad (4.17)$$

To exclude day to day effects of changing vapor pressure deficit and highlight the impact of seasonal changes in water availability on WUE, VPD is often included in the equation (Beer et al., 2009; Dubbert et al., 2014), however we did not find any significant VPD effects on the calculations of WUE during our monsoon 2013 field study in S. Korea.

To quantify the impact of unproductive water loss (E) and respiratory carbon loss ( $R_{\text{eco}}$ ), we



## Chapter 4 - Carbon and water fluxes between paddy and rainfed rice

also calculated productive  $WUE_{agro}$  (the ratio of yield to transpiration (T)) and productive  $WUE_{eco}$  by excluding evaporative losses (the ratio of GPP to T). We also calculated  $WUE_{eco}$  as the ratio of  $NEE/T$  to highlight the influence of evaporation on  $WUE_{eco}$  of paddy rice.

### 4.3.9. Statistical analysis

Two statistical tests were used to evaluate the model performance of daily NDVI, LAI, ET, GPP and  $R_{eco}$  simulation: i) root mean square error (RMSE) and ii) model efficiency (ME) (Nash and Sutcliffe, 1970). To test for a relationships between daily average environmental variables (Radiation,  $T_{air}$ ,  $T_{soil}$ , VPD, SWC) and measured canopy fluxes (sum of day time NEE, GPP,  $R_{eco}$ , ET), a Spearman rank order correlation was performed. To compare the water use efficiencies of the rainfed rice and paddy rice, the normality of all of WUEs and WUE component data were tested by Shapiro–Wilk test. When the data is normally distributed, t-test was performed and otherwise, Wilcoxon–Mann–Whitney Rank Sum test (a non-parametric ANOVA) was performed. All statistical analysis were performed using R statistical software version 3.1.2 (R Core Team, 2014).

## 4.4. Results

### 4.4.1. Climate and rice growth

The weather conditions of the study area generally followed the typical East Asian temperate monsoon climate system. Annual total rainfall of 1332 mm in 2013 was slightly less compared to 30 years annual average of 1391 mm (1981–2010). There was a dry period with almost no rainfall between DOY 190 and 235, which gave a very low ( $0.18 \text{ m}^3 \text{ m}^{-3}$ ) volumetric soil water content. However, because of the high intensity of some rain events, the total precipitation amounted to 973 mm during the rice growing season (i.e., May to September) was above long-term average of 799 mm. Daily solar radiation was up to  $26.9 \text{ MJ m}^{-2} \text{ s}^{-1}$  in May but declined from the end of June to a low of  $2.0 \text{ MJ m}^{-2} \text{ s}^{-1}$  in July with  $5 \pm 1.8$  sunshine hours per day. Daily mean, air temperature ( $T_{air}$ ) during the rice growing season were  $23.4^\circ\text{C}$ .  $T_{air}$  measured over the crop canopy was  $5.27 \pm 2.20^\circ\text{C}$  lower in paddy rice than

## Chapter 4 - Carbon and water fluxes between paddy and rainfed rice

in rainfed rice. The highest midday mean relative humidity (rh) was 98.31%, occurring in August and the lowest midday mean rh, 51.73% in May (Figure 4.1a, b, c).

Both rainfed and paddy rice had similar trends of LAI although rainfed rice reached slightly lower LAI from the end of June onwards (Figure 4.1d). The peak growth for both rainfed and paddy rice was reached in August with a maximum plant height of  $0.80 \pm 0.97$  m and  $0.89 \pm 0.66$  m (not shown), and LAI of  $2.69 \pm 1.21$  m<sup>2</sup> m<sup>-2</sup> and  $3.78 \pm 0.51$  m<sup>2</sup> m<sup>-2</sup>, respectively. Paddy rice yielded  $6612 \pm 218$  kg grains ha<sup>-1</sup> while the grain yield of rainfed rice was 9.53% lower ( $5989 \pm 683$  kg grains ha<sup>-1</sup>) but differences between paddy and rainfed were not statistically significant ( $W = 26.00$ ,  $p > 0.05$ ).

## Chapter 4 - Carbon and water fluxes between paddy and rainfed rice

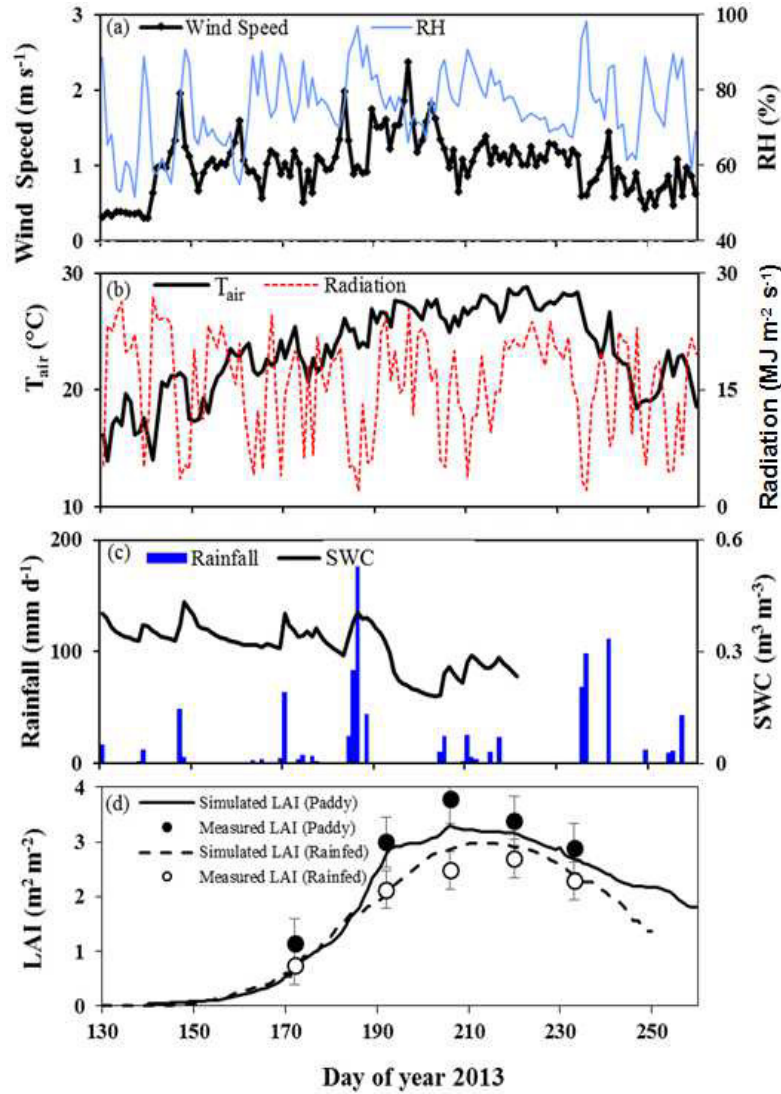


**Figure 4.1** Climate conditions and rice growth during the monsoon 2013. (a) Daily averages of windspeed ( $\text{m s}^{-1}$ ) and relative humidity (%); (b) daily averages of air temperature ( $^{\circ}\text{C}$ ) and radiation ( $\text{MJ m}^{-2} \text{s}^{-1}$ ); (c) daily total rainfall ( $\text{mm d}^{-1}$ ) and daily average volumetric soil water content at 5 cm depth ( $\text{m}^3 \text{m}^{-3}$ ); (d) daily LAI of paddy (solid line) and rainfed (dashed line); lines represent simulated LAI and circles represent measured LAI (Black circle = measured LAI of paddy, white circle measured LAI of rainfed rice,  $n = 9$ , mean values  $\pm$  SD).

### 4.4.2. Carbon and water fluxes of paddy and rainfed rice

To investigate the role of carbon and water exchange on  $\text{WUE}_{\text{eco}}$  we measured canopy gas exchange (NEE, GPP,  $R_{\text{eco}}$  and ET) at different growth stages. For the seasonal trend, we simulated daily NEE, GPP,  $R_{\text{eco}}$  and ET. Our simulated values were validated against the chamber measured fluxes, showing a good agreement between measured and

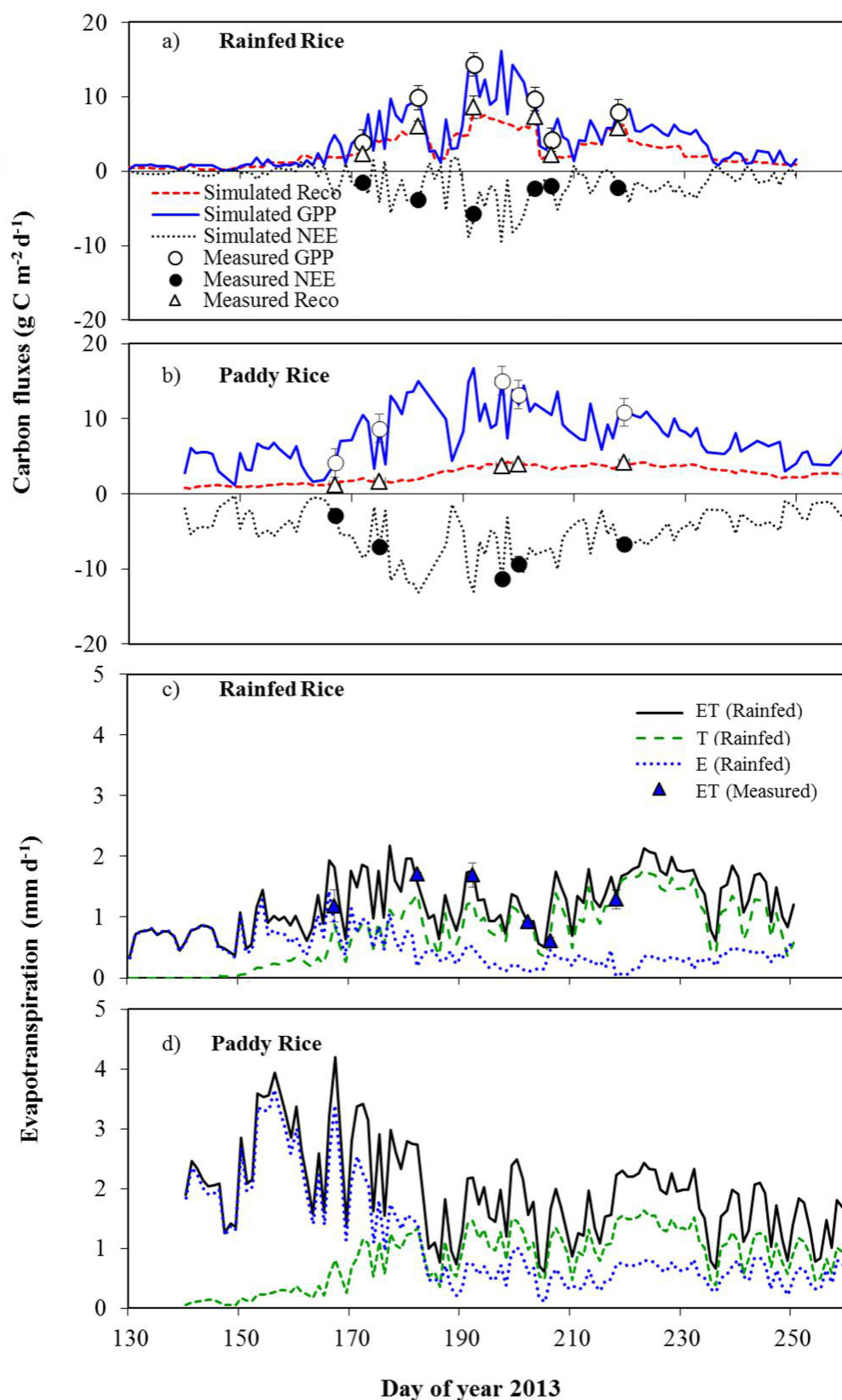


Figure 4.2

## Chapter 4 - Carbon and water fluxes between paddy and rainfed rice

**Figure 4.2** Seasonal carbon and water fluxes of paddy and rainfed rice: daily carbon fluxes of (a) paddy rice; (b) rainfed rice (simulated gross primary production, black line; measured gross primary production, black circle; simulated ecosystem respiration, red dashed line; measured ecosystem respiration, red triangle; simulated net ecosystem exchange, black dotted line; chamber measured net ecosystem exchange, white circle); daily water fluxes of (c) paddy rice and (d) rainfed rice. Simulated daily evapotranspiration, black line; chamber measured evapotranspiration, blue triangle, simulated transpiration, green dashed line; evaporation, blue dotted line) ( $n = 3$ , mean value  $\pm$  SD for measured fluxes).

modeled data (NEE: ME = 0.86, RMSE = 0.58,  $R^2 = 0.86$ ; GPP: ME = 0.95, RMSE = 0.63,  $R^2 = 0.99$ ;  $R_{eco}$ : ME = 0.72, RMSE = 0.51,  $R^2 = 0.75$ ; ET: ME = 0.82, RMSE = 0.13,  $R^2 = 0.97$ ) (Figure 4.2). Rainfed and paddy rice systems showed significantly different water and carbon fluxes ( $n = 12$ ,  $W = 54.00$ ,  $p \leq 0.01$ ). Growing season total evapotranspiration (ET) of paddy rice was 42.16% higher than that of rainfed rice. However, there was no significant difference between growing season total canopy transpiration (T) although T of paddy rice was 11.02% higher than that of rainfed rice.

Although we studied both rice systems adjacent to each other under the same environmental conditions, canopy microclimate differences between paddy and rainfed rice were observed. Canopy air temperature ( $T_{air}$ ) of paddy was always lower than that of rainfed rice (by  $5.27 \pm 2.20^\circ\text{C}$ ). Soil temperature ( $T_{soil}$ ) of paddy rice was lower than that of rainfed rice except during the maturity stage (DOY 230 onward) when the flooded water was drained from paddy field. Evapotranspiration of rainfed rice was mainly driven by  $T_{air}$ ,  $T_{soil}$  and VPD (Spearman's  $P = 0.65, 0.57, 0.47$ , respectively,  $p \leq 0.01$ ) while that of paddy rice was driven by radiation and VPD (Spearman's  $P = 0.87, 0.67$ , respectively,  $p \leq 0.01$ ).

Daily contribution of transpiration to evapotranspiration (T/ET) of paddy and rainfed rice was calculated based on simulated daily T and ET. T/ET of paddy rice steadily increased with the increasing canopy density (LAI) while T/ET of rainfed rice fluctuated with changes in soil water content (SWC) and the highest T/ET was found at SWC of  $0.34 \text{ m}^3 \text{ m}^{-3}$  during seedling stage (on DOY 162, data not shown).  $\text{H}_2\text{O}$  fluxes from rainfed rice was mainly dominated by transpiration (T/ET = 0.65) while that of paddy rice was mainly driven by evaporation (T/ET

## Chapter 4 - Carbon and water fluxes between paddy and rainfed rice

= 0.42). When soil water content (SWC) declined below field capacity, T contributed 80 to 90% of H<sub>2</sub>O flux in rainfed rice. Evaporative water loss (E) was dominant in the early vegetative stages (until DOY 200) in both paddy and rainfed rice. At the end of active tillering stage, along with the increasing canopy density, canopy T became the dominant water flux in both paddy and rainfed rice. Nevertheless, E of paddy was significantly higher than that of rainfed rice ( $W = 20.14$ ,  $p \leq 0.05$ ).

Growing season total gross primary production (GPP = sum of simulated daily GPP during monsoon rice growing season 2013) of paddy and rainfed rice were not significantly different. However, paddy rice had significantly lower ecosystem respiration ( $R_{eco}$ ) in both, chamber measured and simulated daily  $R_{eco}$ , hence net ecosystem exchange (NEE) was higher in paddy rice (Figure 4.2, 4.4). Growing season total ecosystem respiratory carbon loss in rainfed rice was 48.65% of net carbon fluxes while paddy rice ecosystem respiratory carbon loss was only 33.77% of net fluxes. Both measured and simulated  $R_{eco}$  of rainfed and paddy rice was strongly correlated to  $T_{air}$  and  $T_{soil}$  (Spearman's  $P = 0.74$ ,  $0.80$ , respectively for paddy; Spearman's  $P = 0.74$ ,  $0.80$ , respectively for rainfed,  $p \leq 0.01$ ) while that of paddy rice correlated to  $T_{air}$  and  $T_{soil}$  (Spearman's  $P = 0.90$ ,  $0.78$ , respectively,  $p \leq 0.01$ ). According to dark chamber measured soil and plant respiration,  $R_{eco}$  of paddy rice was dominated by plant respiration ( $R_{plant}$ ) while  $R_{eco}$  of rainfed rice was mainly dominated by soil respiration ( $R_{soil}$ ) (data not shown). Therefore, higher respiratory carbon loss of rainfed rice system was clearly due to its higher soil respiration.

### 4.4.3. Tradeoff between evaporative and respiratory losses in paddy and rainfed rice

Rainfed rice had higher water use in both Yield/ET and GPP/ET than paddy rice (Figure 4.3a). Interestingly, after excluding the differences in evaporative water loss, there was no significant difference between productive water use (GPP/T and yield/T, Figure 4.3b, c) of paddy and rainfed rice ( $W = 44.00$ ,  $p = 0.39$ ). These results highlighted that lower Yield/ET of paddy was mainly due to its higher evaporative water losses, rather than differences in crop yield or transpiration. Lower GPP/ET of paddy rice also resulted mainly from higher

## Chapter 4 - Carbon and water fluxes between paddy and rainfed rice

evaporative losses (Figure 4.3c), while interestingly, no significant differences in water use were found between paddy and rainfed rice when calculated based on the transpiration water use ( $GPP/T$ ) ( $W = 44.00$ ,  $p = 0.39$ ). When we consider the differences in ecosystem respiratory carbon losses of paddy and rainfed rice, i.e., ecosystem water use efficiency as the balance of net ecosystem carbon and water fluxes ( $NEE/ET$ ),  $NEE/ET$  of both paddy and rainfed were not different from each other ( $W = 62.58$ ,  $p = 0.58$ ), which revealed the dominant role of higher respiratory carbon losses in rainfed rice ecosystem carbon exchange and ecosystem water use efficiency. However, when we exclude the effect of  $E$  on  $NEE/ET$  (i.e.,  $NEE/T$ ), paddy significantly had higher water use (Figure 4.3c), pointing the dominant impacts of evaporative losses over  $NEE/ET$ . These results clearly show that ecosystem water use efficiency was not simply a ratio of  $GPP$  to  $ET$  but the effects of respiratory carbon loss and evaporative water loss over  $WUE_{eco}$  should also be considered in the calculation of  $WUE_{eco}$ .

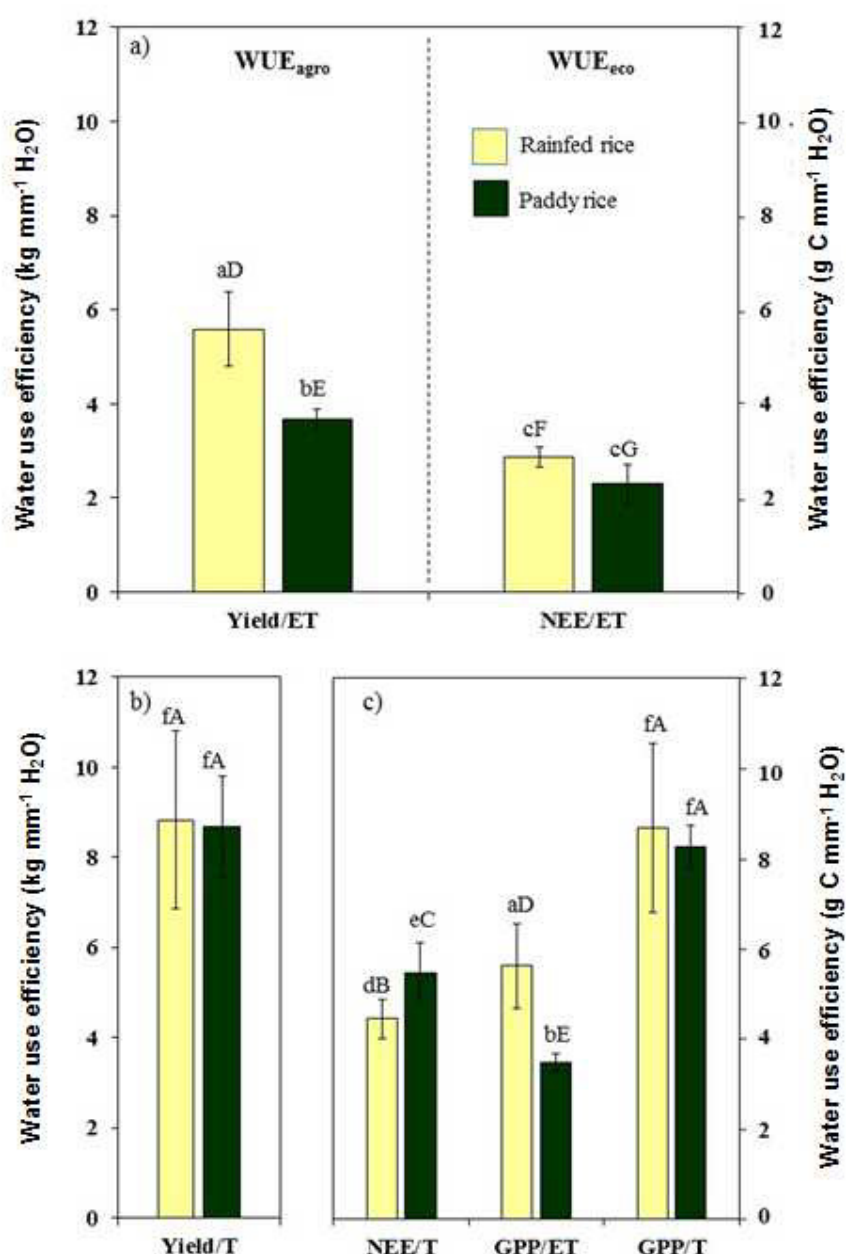


**Figure 4.3** Effects of respiratory carbon loss and evaporative water loss over water use efficiency: (a) Yield/ET of rainfed rice (light yellow) was higher than paddy rice (dark green) ( $W = 36.00$ ,  $p \leq 0.05$ ) but NEE/ET were not significantly different, (b) Yield/T was not significantly different between paddy and rainfed rice ( $W = 23.00$ ,  $p = 0.48$ ), highlighting the higher evaporative loss in paddy rice; (c) Lower GPP/ET of paddy rice due to its higher evaporative water loss ( $W = 119.00$ ,  $p \leq 0.05$ ); and higher GPP/ET of rainfed rice due to its higher respiratory carbon loss ( $W = 126.00$ ,  $p \leq 0.05$ ). (Wilcoxon-Mann-Whitney Rank Sum test (a non-parametric ANOVA) was performed to access WUE differences between paddy and rainfed ( $n = 3$  to  $12$ , mean value  $\pm$  SD); different small letters denote significant differences among paddy and rainfed rice within each panel (a to f) while different capital letters denote significant differences among different water use efficiencies (A to G).



### 4.5. Discussion

Agricultural production worldwide is highly sensitive to water scarcity and at the same time accounting for 70% of freshwater withdrawals. Increasing heat and drought stress predicted by climate change scenarios may thus strongly impact on carbon cycling and, hence, crop productivity, and strongly alter the hydrological cycle threatening sustainability of current production methods (FAO, 2012; Blanco et al., 2014). Rice production is one of the most water consuming crops and globally rice production has huge impacts on carbon and water cycling (Adekoya et al., 2014; Kim et al., 2013; Lindner et al., 2015). The main goal of this study was to compare carbon and water fluxes between conventional paddy and rainfed rice farming analyzing the distinct contributions of unproductive water losses from soil evaporation and respiratory carbon losses to net ecosystem carbon and water exchange. Quantifying the impact of these distinct irrigation treatments is specifically important to find an optimal balance between low evaporative and respiratory losses for a sustainable rice production.

Comparing paddy and rainfed system under the same climate condition revealed different carbon exchange process of water saving dryland rice and conventional paddy rice clearly (Figure 4.4).

## Chapter 4 - Carbon and water fluxes between paddy and rainfed rice

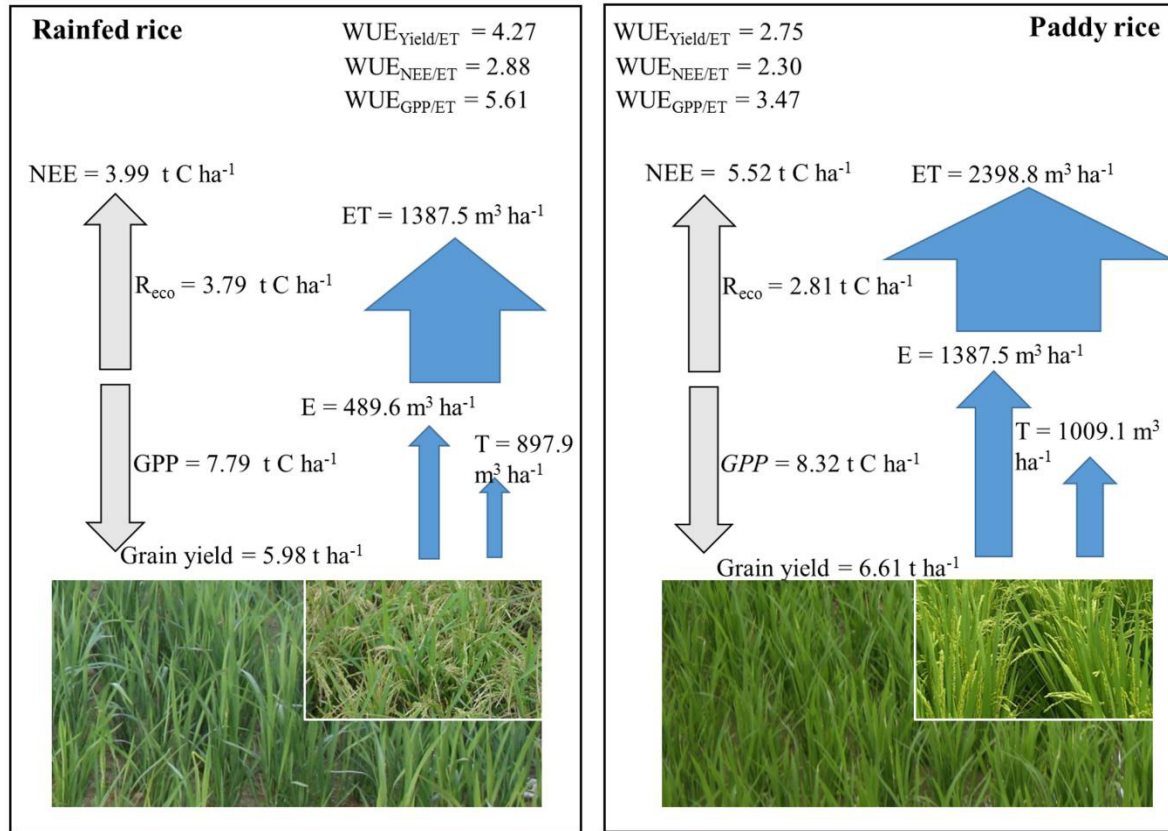


**Figure 4.4** Seasonal carbon and water balance of paddy and rainfed rice. Measured and simulated daily gross primary production (GPP), net ecosystem exchange (NEE), ecosystem respiration (Reco), evapotranspiration (ET), transpiration (T) and grain yields were used in this schematic representation. All flux data and grain yield are mean values (flux data:  $n = 3 \pm \text{SD}$ ; grain yield:  $n = 6 \pm \text{SD}$ ). Crop growing season was 120 days (sowing to harvest).

Rainfed rice production had higher  $R_{\text{eco}}$  (34.88% higher than paddy) due to its higher soil respiration (see also Miyata et al., 2000, Alberto et al., 2009; Thanawong et al., 2014). On the other hand, paddy rice has significantly higher evaporative water loss during the growth period, increasing the overall water loss of the ecosystem by 42.17%, compared to rainfed rice. Since the paddy rice system is the conventional rice production system which can be found in most of the global rice production area (International Rice Research Institute [IRRI], 2002; Seck et al., 2012; Tuong et al., 2005), significantly reduced evaporation per unit production area can raise a question on possible global or regional water cycle changes if most of paddy system were converted to water saving production systems (Fitzjarrald et al., 2008; Sakai et al., 2004; Wang et al., 2014; Zhao et al., 2008). Since global water and carbon fluxes are coupled by vegetation, impacts on water cycle could lead to impacts on the carbon

## Chapter 4 - Carbon and water fluxes between paddy and rainfed rice

balance (Hu et al., 2008; Istanbuluoglu et al., 2012; Tian et al., 2011; Williams and Albertson, 2005; Wolf et al., 2011).

As expected, we clearly found higher  $WUE_{eco}$  and  $WUE_{agro}$  (GPP and Yield/ET) in rainfed compared to paddy rice (Adekoya et al., 2014; Alberto et al., 2009; Thanawong et al., 2014; Figure 4.3). However, a different picture emerged when considering the productive water use and respiratory losses. Generally,  $WUE_{eco}$  defined as the ratio of gross primary production to evapotranspiration ( $WUE_{eco} = GPP/ET$ ) has been estimated for different ecosystems ranging from grasslands to cultivated vegetation without considering the influence of respiratory carbon losses ( $R_{eco}$ ) (Beer et al., 2009; Reichstein et al., 2002). Although, this yields information on the water use efficiency of plants to fix carbon at the stand level, considering ecosystem respiration into WUE assessments is crucial to gain an ecosystem perspective (Dubbert et al., 2014; Huang et al., 2010; Scott et al., 2006; Tallec et al., 2013; Zeri et al., 2013). Partitioning carbon and water fluxes in paddy and rainfed rice revealed the strong influence of  $R_{eco}$  over  $WUE_{eco}$ . Accordingly, higher GPP/ET in rainfed rice ecosystem was due to higher  $R_{eco}$  since rainfed rice had similar GPP to paddy rice but lower net ecosystem fluxes (NEE). Thus, accounting for this difference by considering net ecosystem exchange (NEE/ET) yielded comparable water use efficiencies of both rice production systems.

Along with respiratory carbon loss, unproductive water loss (evaporation; E) considerably affects the water use of rice production. Evaporation (E) influences T by influencing canopy microclimate (canopy temperature and VPD) which indirectly influences T/ET, water use, crop growth and yield (Alberto et al., 2009; Balwinder-Singh et al., 2014; Leuning et al., 1994). As a result of maximization of carbon gain per water use along with available water, productive water use efficiency (GPP/T and Yield/T) of paddy and rainfed rice were almost equal. However, T/ET was significantly different between paddy and rainfed rice (Figure 4.3; Blum, 2009) and increased along with crop growth. By contrast, the contribution of evaporation to H<sub>2</sub>O fluxes was relatively similar in both production types from the end of tillering stage onwards (DOY 200) when the crop canopy was dense, as major differences in

## Chapter 4 - Carbon and water fluxes between paddy and rainfed rice

unproductive water loss occurred before canopy closure. Overall, the higher  $WUE_{agro}$  of rainfed was in concert with significantly reduced evaporation but also a slightly decreased grain yield compared to paddy (Figure 4.3).

According to water scarcity projections based on socioeconomic assumptions, population density per capita income, climate change scenarios and mitigation options, the frequency of extreme droughts may increase in many regions (Eastern China, India, Western Europe and Middle East) (Arnell and Lloyd-Hughes, 2013; Hejazi et al., 2014), highlighting the change in regional specific hydrologic cycle. Moreover, global annual yield increase rate (current rate = 2.4%) of major agricultural crops (especially, rice, maize, wheat, soybean) should be doubled to meet the projected food demand by 2050 (Alexandratos and Bruinsma, 2012; Ray et al., 2013; Mutayya, et al., 2014). Hence, a choice between the trade-off of paddy rice production with high evaporative losses and methane emissions and rainfed rice with increased respiratory losses and possible impact on grain yield (though this was not significant in this study; Nay-Htoon et al., 2013; Tuong and Bouman, 2003, Figure 4.3), depends largely on the regional water availability and precipitation regime. Moreover, the greenhouse gas balance of conventional flooded rice system is still unclear since  $CH_4$  and  $N_2O$  emission not only depend on the amount of flooding but also on other factors such as climatic conditions, crop growth, atmospheric  $CO_2$  concentration (Alberto et al., 2014; Wassmann et al., 2000; Groenigen et al., 2011, 2012; Dijkstra et al., 2012), source and rate of fertilizer applied (Berger et al., 2013), inorganic and organic carbon substrate availability for denitrifying bacteria, oxygen availability and bacterial activity (Seo et al., 2013). Traditional flooded paddy rice has high  $CH_4$  and low  $N_2O$  emissions while non-flooded rainfed rice shows low  $CH_4$  but high  $N_2O$  emissions (Weller et al., 2014) together with high respiratory  $CO_2$  release, all being relevant greenhouse gases (Xiao et al., 2005).

Under the environmental conditions at the present study location, with abundant monsoon rainfall, the high water consumption of paddy rice presents much less of concern than high respiratory losses of rainfed rice. However, in different climates, such as the Mediterranean,

## Chapter 4 - Carbon and water fluxes between paddy and rainfed rice

Africa or Middle East, producing rice in a more sustainable management regime considering its impact on the regional hydrological cycle may well outweigh slight impacts on grain yield and higher respiratory losses.

### 4.6. Conclusion

We cultivated the same rice variety under the same environmental conditions except water available and observed significant differences in ecosystem carbon and water balance. Significantly high  $WUE_{agro}$  (yield/ET) was found in rainfed compared to paddy rice, as expected. However, this difference vanished when  $WUE_{agro}$  was calculated excluding the differences in unproductive water loss (evaporation). Moreover,  $WUE_{eco}$  of rainfed rice was only higher when calculated based on gross primary production. If we consider the ecosystem productivity by excluding respiratory losses,  $WUE_{eco}$  of rainfed and paddy rice were not significantly different. After excluding evaporative losses which is highly amounted to the whole water budget of paddy rice, neither  $WUE_{eco}$  nor  $WUE_{agro}$  of paddy and rainfed rice were significantly different. Therefore, given its higher WUEs in concert with significantly higher respiratory carbon loss and slightly reduced grain yield, altering conventional paddy rice system to water saving rice production such as rainfed rice should be based on careful analysis of the regional hydrological cycle and ecosystem and socioeconomic tradeoffs. Since unproductive carbon and water losses play an important role in vegetation carbon and water balance, they should be considered in  $WUE_{eco}$  studies.

### 4.7. Acknowledgments

This study was funded by the Deutsche Forschungsgemeinschaft (DFG) as part of the International Research and Training Group: TERRECO (GRK 1565/1) at the University of Bayreuth, Germany and Korean Research Foundation (KRF) at Kangwon National University, Chuncheon, S. Korea. We do acknowledge the help in the field by Seung Hyun Jo, Seungtaek Jeong, Fu Toncheng, Mijeong Kim, Jinsil Choi, Fabian Fischer, Nikolas Lichtenwald and Yannic Sigge. We especially thank Ilse Thaufelder and Margarete Wartinger for all of their

## Chapter 4 - Carbon and water fluxes between paddy and rainfed rice

technical supports in the laboratory.

### 4.8. References

- Adekoya, M., Liu, Z., Vered, E., Zhou, L., Kong, D., Qin, J., Ma, R., Yu, X., Liu, G., Chen, L. and Luo, L. 2014. Agronomic and Ecological Evaluation on Growing Water-Saving and Drought-Resistant Rice (*Oryza sativa* L.) Through Drip Irrigation. *Journal of Agriculture Science*, 6, 110–119.
- Alberto, M.C.R., Buresh, R.J., Hirano, T., Miyata, A., Wassmann, R., Quilty, J.R., Correa, T.Q. and Sandro, J. 2013. Carbon uptake and water productivity for dry-seeded rice and hybrid maize grown with overhead sprinkler irrigation. *Field Crop Research*, 146, 51–65.
- Alberto, M.C.R., Quilty, J.R., Buresh, R.J., Wassmann, R., Haidar, S., Correa, T.Q. and Sandro, J.M. 2014. Actual evapotranspiration and dual crop coefficients for dry-seeded rice and hybrid maize grown with overhead sprinkler irrigation. *Agricultural Water Management*, 136, 1–12.
- Alberto, M.C.R., Wassmann, R., Hirano, T., Miyata, A., Hatano, R., Kumar, A., Padre, A. and Amante, M. 2011. Comparisons of energy balance and evapotranspiration between flooded and aerobic rice fields in the Philippines. *Agricultural Water Management*, 98, 1417–1430.
- Alberto, M.C.R., Wassmann, R., Hirano, T., Miyata, A., Kumar, A., Padre, A., Amante, M., 2009. CO<sub>2</sub>/heat fluxes in rice fields: Comparative assessment of flooded and non-flooded fields in the Philippines. *Agriculture and Forest Meteorology*, 149, 1737–1750.
- Alexandratos, N. and Bruinsma, J. 2012. World agriculture towards 2030/2050: the 2012 revision. *ESA Work. Pap. No. 12–03*.
- Allen, R.G., Pereira, L.S., Raes, D., Smith, M., W, A.B. 1998. Crop evapotranspiration – Guidelines for computing crop water requirements – FAO Irrigation and drainage paper 56. *Irrig. Drain.* 1–15.
- Arnell, N.W. and Lloyd-Hughes, B. 2013. The global-scale impacts of climate change on water resources and flooding under new climate and socio-economic scenarios. *Climate Change*, 122, 127–140.

#### Chapter 4 - Carbon and water fluxes between paddy and rainfed rice

- Balwinder–Singh, Eberbach, P.L. and Humphreys, E. 2014. Simulation of the evaporation of soil water beneath a wheat crop canopy. *Agricultural Water Management*, 135, 19–26.
- Beer, C., Ciais, P., Reichstein, M., Baldocchi, D., Law, B.E., Papale, D., Soussana, J.–F., Ammann, C., Buchmann, N., Frank, D., Gianelle, D., Janssens, I. a., Knohl, A., Köstner, B., Moors, E., Rouspard, O., Verbeeck, H., Vesala, T., Williams, C. and Wohlfahrt, G. 2009. Temporal and among–site variability of inherent water use efficiency at the ecosystem level. *Global Biogeochemical Cycles*, 23, n/a–n/a.
- Berger, S., Jang, I., Seo, J., Kang, H. and Gebauer, G. 2013. A record of N<sub>2</sub>O and CH<sub>4</sub> emissions and underlying soil processes of Korean rice paddies as affected by different water management practices. *Biogeochemistry*, 115, 317–332.
- Bhattacharyya, P., Neogi, S., Roy, K.S., Dash, P.K., Nayak, K. and Mohapatra, T. 2014. Tropical low land rice ecosystem is a net carbon sink. *Agriculture, Ecosystem and Environment*, 189, 127–135.
- Blanco, G., Gerlagh, R., Suh, S., Barrett, J., de Coninck, H.C., Diaz Morejon, C.F., Mathur, R., Nakicenovic, N., Ofosu Ahenkora, A., Pan, J., Pathak, H., Rice, J., Richels, R., Smith, S.J., Stern, D.I., Toth, F.L. and Zhou, P. 2014. Drivers, Trends and Mitigation, in: Edenhofer, O., Pichs–Madrugá, R., Sokona, Y., Farahani, E., Kadner, S., Seyboth, K., Adler, A., Baum, I., Brunner, S., Eickemeier, P., Kriemann, B., Savolainen, J., Schlömer, S., von Stechow, C., Zwickel, T., Minx, J.C. (eds.), *Climate Change 2014: Mitigation of Climate Change. Contribution of Working Group III to the Fifth Assessment Report of the Intergovernmental Panel on Climate Change*. Cambridge University Press, Cambridge, United Kingdom, Rome, pp. 351–412.
- Bouman, B. and Tuong, T. 2001. Field water management to save water and increase its productivity in irrigated lowland rice. *Agricultural Water Management*, 49, 11–30.
- Bouman, B.A.M., Peng, S., Castañeda, A.R. and Visperas, R.M. 2005. Yield and water use of irrigated tropical aerobic rice systems. *Agricultural Water Management*, 74, 87–105.
- Bunnell, F.L., Tait, D.E.N. and Flanagan, P.W. 1977a. Microbial respiration and substrate weight loss. II. A model of the influences of chemical composition. *Soil Biology and Biochemistry*, 9, 41–47.

#### **Chapter 4 - Carbon and water fluxes between paddy and rainfed rice**

- Bunnell, F.L., Tait, D.E.N., Flanagan, P.W. and Van Clever, K. 1977b. Microbial respiration and substrate weight loss—I. *Soil Biology and Biochemistry*, 9, 33–40.
- Choudhury, B.J. 1994. Synergism of multispectral satellite observations for estimating regional land surface evaporation. *Remote Sensing of Environment*, 49, 264–274.
- Choudhury B.J. 1987. Relationship between Vegetation Indices, Radiation Absorption, and Net Photosynthesis Evaluated by a Sensitivity Analysis. *Remote Sensing of Environment*, 22, 209–233.
- Dubbert, M., Cuntz, M., Piayda, A., Maguás, C. and Werner, C. 2013. Partitioning evapotranspiration – Testing the Craig and Gordon model with field measurements of oxygen isotope ratios of evaporative fluxes. *Journal of Hydrology*, 496, 142–153.
- Dubbert, M., Piayda, A., Cuntz, M., Correia, A.C., Costa E Silva, F., Pereira, J.S. and Werner, C. 2014. Stable oxygen isotope and flux partitioning demonstrates understory of an oak savanna contributes up to half of ecosystem carbon and water exchange. *Frontier in Plant Science*, 5, 530.
- Duchemin, B., Hadria, R., Erraki, S., Boulet, G., Maisongrande, P., Chehbouni, a., Escadafal, R., Ezzahar, J., Hoedjes, J.C.B., Kharrou, M.H., Khabba, S., Mougenot, B., Olioso, a., Rodriguez, J.–C. and Simonneaux, V. 2006. Monitoring wheat phenology and irrigation in Central Morocco: On the use of relationships between evapotranspiration, crops coefficients, leaf area index and remotely–sensed vegetation indices. *Agricultural Water Management*, 79, 1–27.
- Fitzjarrald, D.R., Sakai, R.K., Moraes, O.L.L., Cosme de Oliveira, R., Acevedo, O.C., Czikowsky, M.J. and Beldini, T. 2008. Spatial and temporal rainfall variability near the Amazon–Tapajós confluence. *Journal of Geophysical Research*, 113, G00B11.
- Food and Agriculture Organization [FAO], 2012. Coping with water scarcity: An action framework for agriculture and food security, FAO Water . ed. FAO, Rome.
- Gitelson, A.A., Peng, Y. and Huemmrich, K.F. 2014. Relationship between fraction of radiation absorbed by photosynthesizing maize and soybean canopies and NDVI from remotely sensed data taken at close range and from MODIS 250m resolution data. *Remote Sensing of Environment*, 147, 108–120.



## **Chapter 4 - Carbon and water fluxes between paddy and rainfed rice**

- Goward, S.N. and Huemmrich, K.F. 1992. Vegetation canopy PAR absorbance and the normalized difference vegetation index: an assessment using the SAIL model. *Remote Sensing of Environment*, 39, 119–140.
- Glenn, E.P., Huete, A.R., Nagler, P.L. and Nelson, S.G. 2008. Relationship between remotely-sensed vegetation indices, canopy attributes and plant physiological processes: what vegetation indices can and cannot tell us about the landscape. *Sensors*, 8, 2136–2160.
- Hejazi, M.I., Edmonds, J., Clarke, L., Kyle, P., Davies, E., Chaturvedi, V., Wise, M., Patel, P., Eom, J. and Calvin, K. 2014. Integrated assessment of global water scarcity over the 21st century under multiple climate change mitigation policies. *Hydrology and Earth System Sciences*, 18, 2859–2883.
- Hu, Z., Yu, G., Fu, Y., Sun, X., Li, Y., Shi, P., Wang, Y. and Zheng, Z. 2008. Effects of vegetation control on ecosystem water use efficiency within and among four grassland ecosystems in China. *Global Change Biology*, 14, 1609–1619.
- Huang, X., Hao, Y., Wang, Y., Cui, X., Mo, X. and Zhou, X. 2010. Partitioning of evapotranspiration and its relation to carbon dioxide fluxes in Inner Mongolia steppe. *Journal of Arid Environment*, 74, 1616–1623.
- Hussain, S., Peng, S., Fahad, S., Khaliq, A., Huang, J., Cui, K. and Nie, L. 2014. Rice management interventions to mitigate greenhouse gas emissions: a review. *Environmental Science and Pollution Research*, 22, 3342–3360.
- Intergovernmental Panel on Climate Change [IPCC], 2013. IPCC, 2013: Summary for Policymakers. In: *Climate Change 2013: The Physical Science Basis. Contribution of Working Group I to the Fifth Assessment Report of the Intergovernmental Panel on Climate Change*. Cambridge University Press, Cambridge, United Kingdom.
- International Rice Research Institute [IRRI], 2002. Water-wise rice production. *Proceedings of the International Workshop on Water-wise Rice Production*, 8–11 April 2002. International Rice Research Institute [IRRI], Los Baños, the Philippines.
- Istanbulluoglu, E., Wang, T. and Wedin, D.A. 2012. Evaluation of ecohydrologic model parsimony at local and regional scales in a semiarid grassland ecosystem. *Ecohydrology*,

## Chapter 4 - Carbon and water fluxes between paddy and rainfed rice

142, 121–142.

- Kelliher, F.M., Leuning, R., Raupach, M.R. and Schulze, E.-D. 1995. Maximum conductances for evaporation from global vegetation types. *Agricultural and Forest Meteorology*, 73, 1–16.
- Khush, G.S. 2005. What it will take to feed 5.0 billion rice consumers in 2030. *Plant Molecular Biology*, 59, 1–6.
- Ko, J., Maas, S.J., Mauget, S., Piccinni, G. and Wanjura, D. 2006. Modeling water-stressed cotton growth using within-season remote sensing data. *Agronomy Journal*, 98, 1600–1609.
- Kudo, Y., Noborio, K., Shimoozono, N. and Kurihara, R. 2014. The effective water management practice for mitigating greenhouse gas emissions and maintaining rice yield in central Japan. *Agriculture, Ecosystem & Environment*, 186, 77–85.
- Leuning, R., Condon, A.G., Dunin, F.X., Zegelin, S. and Denmead, O.T. 1994. Rainfall interception and evaporation from soil below a wheat canopy. *Agricultural and Forest Meteorology*, 67, 221–238.
- Li, Y.-L., Tenhunen, J., Mirzaei, H., Hussain, M.Z., Siebicke, L., Foken, T., Otieno, D., Schmidt, M., Ribeiro, N., Aires, L., Pio, C., Banza, J. and Pereira, J. 2008. Assessment and up-scaling of CO<sub>2</sub> exchange by patches of the herbaceous vegetation mosaic in a Portuguese cork oak woodland. *Agricultural and Forest Meteorology*, 148, 1318–1331.
- Lindner, S., Otieno, D., Lee, B., Xue, W., Arnhold, S., Kwon, H., Huwe, B. and Tenhunen, J. 2015. Carbon dioxide exchange and its regulation in the main agro-ecosystems of Haeen catchment in South Korea. *Agriculture, Ecosystem & Environment*, 199, 132–145.
- Lloyd, J. and Taylor, J. 1994. On the temperature dependence of soil respiration. *Functional Ecology*, 8, 315.
- Maas, S.J. 1993. Parameterized model of Gramineous crop growth: I. leaf area and dry mass Simulation. *Agronomy Journal*, 85, 348.
- Maas, S.J. 1993b. Parameterized model of Gramineous crop growth: II. within-season simulation calibration. *Agronomy Journal* 85, 354.
- Miyata, A., Leuning, R., Denmead, O.T., Kim, J. and Harazono, Y. 2000. Carbon dioxide and

## Chapter 4 - Carbon and water fluxes between paddy and rainfed rice

- methane fluxes from an intermittently flooded paddy field. *Agricultural and Forest Meteorology*, 102, 287–303.
- Mo, X., Liu, S., Lin, Z. and Zhao, W. 2004. Simulating temporal and spatial variation of evapotranspiration over the Lushi basin. *Journal of Hydrology*, 285, 125–142.
- Monteith, J.L. 1972. Solar radiation and productivity in tropical ecosystems. *Journal of Applied Ecology*, 9, 747–766.
- Muthayya, S., Sugimoto, J.D., Montgomery, S. and Mabery, G.F. 2014. An overview of global rice production, supply, trade, and consumption. *Annals of the New York Academy of Sciences*, 1324, 7–14.
- Nash, J.E. and Sutcliffe, J.V. 1970. River flow forecasting through conceptual models part I – A discussion of principles. *Journal of Hydrology*, 10, 282–290.
- Nay-Htoon, B., Tung Phong, N., Schlüter, S. and Janaiah, A. 2013. A water productive and economically profitable paddy rice production method to adapt water scarcity in the Vu Gia–Thu Bon river basin, Vietnam. *Journal of Natural Resources and Development*, 3, 58–65.
- Nie, L., Peng, S., Chen, M., Shah, F., Huang, J., Cui, K. and Xiang, J., 2012. Aerobic rice for water-saving agriculture. A review. *Agronomy for Sustainable Development*, 32, 2, 411–418.
- Nishimura, S., Yonemura, S., Minamikawa, K. and Yagi, K. 2015. Seasonal and diurnal variations in net carbon dioxide flux throughout the year from soil in paddy field. *Journal of Geophysical Research, Biogeoscience*, n/a–n/a. doi:10.1002/2014JG002746
- Nishimura, S., Yonemura, S., Sawamoto, T., Shirato, Y., Akiyama, H., Sudo, S. and Yagi, K. 2008. Effect of land use change from paddy rice cultivation to upland crop cultivation on soil carbon budget of a cropland in Japan. *Agriculture, Ecosystem & Environment*, 125, 9–20.
- Otieno, D., Lindner, S., Muhr, J. and Borken, W. 2012. Sensitivity of peatland herbaceous vegetation to vapor pressure deficit influences net ecosystem CO<sub>2</sub> exchange. *Wetlands*, 32, 895–905.
- Owen, K.E., Tenhunen, J., Reichstein, M., Wang, Q., Falge, E., Geyer, R., Xiao, X., Stoy, P.,

## Chapter 4 - Carbon and water fluxes between paddy and rainfed rice

- Ammann, C., Arain, A., Aubinet, M., Aurela, M., Bernhofer, C., Chojnicki, B.H., Granier, A., Gruenwald, T., Hadley, J., Heinesch, B., Hollinger, D., Knohl, A., Kutsch, W., Lohila, A., Meyers, T., Moors, E., Moureaux, C., Pilegaard, K., Saigusa, N., Verma, S., Vesala, T. and Vogel, C. 2007. Linking flux network measurements to continental scale simulations: ecosystem carbon dioxide exchange capacity under non-water-stressed conditions. *Global Change Biology*, 13, 734–760.
- Pape, L., Ammann, C., Nyfeler-Brunner, Spirig, C., Hens, K. and Meixner, F.X. 2009. An automated dynamic chamber system for surface exchange measurement of non-reactive and reactive trace gases of grassland ecosystems. *Biogeoscience*, 6, 405–429.
- Payero, J.O. and Irmak, S. 2013. Daily energy fluxes, evapotranspiration and crop coefficient of soybean. *Agriculture Water Management*, 129, 31–43.
- Peng, S., Huang, J., Sheehy, J.E., Laza, R.C., Visperas, R.M., Zhong, X., Centeno, G.S., Khush, G.S. and Cassman, K.G. 2004. Rice yields decline with higher night temperature from global warming. *Proceedings of the National Academy of Sciences of the United States of America*, 101, 9971–9975.
- Pittelkow, C.M., Adviento-Borbe, M., Hill, J.E., Six, J., van Kessel, C. and Linquist, B. 2013. Yield-scaled global warming potential of annual nitrous oxide and methane emissions from continuously flooded rice in response to nitrogen input. *Agriculture, Ecosystem and Environment*, 177, 10–20.
- R Core Team, 2014. R: A language and environment for statistical computing. R Found. Stat. Comput. Vienna, Austria URL <http://www.R-project.org/>.
- Ray, D.K., Mueller, N.D., West, P.C. and Foley, J. 2013. Yield Trends Are Insufficient to Double Global Crop Production by 2050. *PLoS One*, 8, e66428.
- Reichstein, M., Tenhunen, J.D., Rouspard, O., Ourcival, J.-M., Rambal, S., Dore, S. and Valentini, R. 2002. Ecosystem respiration in two Mediterranean evergreen Holm Oak forests: drought effects and decomposition dynamics. *Functional Ecology*, 16, 27–39.
- Running, S.W., Nemani, R.R., Heinsch, F.A., Zhao, M., Reeves, M. and Hashimoto, H. 2004. A continuous satellite-derived measure of global terrestrial primary production. *Bioscience*, 54, 547.

#### **Chapter 4 - Carbon and water fluxes between paddy and rainfed rice**

- Sakai, R.K., Fitzjarrald, D.R., Moraes, O.L.L., Staebler, R.M., Acevedo, O.C., Czikowsky, M.J., Silva, R. Da, Brait, E. and Miranda, V. 2004. Land–use change effects on local energy, water, and carbon balances in an Amazonian agricultural field. *Global Change Biology*, 10, 895–907.
- Scott, R.L., Huxman, T.E., Cable, W.L. and Emmerich, W.E. 2006. Partitioning of evapotranspiration and its relation to carbon dioxide exchange in a Chihuahuan Desert shrubland. *Hydrological Process*, 20, 3227–3243.
- Seck, P.A., Diagne, A., Mohanty, S. and Wopereis, M.C.S. 2012. Crops that feed the world 7: Rice. *Food Security*, 4, 7–24.
- Sellers, P.J. 1985. Canopy reflectance, photosynthesis and transpiration. *International Journal of Remote Sensing*, 6, 1335–1372.
- Seo, J., Jang, I., Gebauer, G. and Kang, H. 2013. Abundance of methanogens, methanotrophic bacteria, and denitrifiers in rice paddy soils. *Wetlands*, 34, 213–223.
- Smith, P., Martino, D., Cai, Z., Gwary, D., Janzen, H., Kumar, P., McCarl, B., Ogle, S., O'Mara, F., Rice, C., Scholes, B. and Sirotenko, O. 2007. Agriculture, in: Metz, B., Davidson, O.R., Bosch, P.R., Dave, R., Meyer, L.A. (eds.), *Climate Change 2007: Mitigation. Contribution of Working Group III to the Fourth Assessment Report of the Intergovernmental Panel on Climate Change*. Cambridge University Press, Cambridge, United Kingdom and New York, NY, USA.
- Talleg, T., Béziat, P., Jarosz, N., Rivalland, V. and Ceschia, E. 2013. Crops' water use efficiencies in temperate climate: Comparison of stand, ecosystem and agronomical approaches. *Agricultural and Forest Meteorology*, 168, 69–81.
- Thanawong, K., Perret, S.R. and Basset–Mens, C. 2014. Eco–efficiency of paddy rice production in Northeastern Thailand: a comparison of rain–fed and irrigated cropping systems. *Journal of Cleaner Production*, 73, 204–217.
- Tian, H., Lu, C., Chen, G., Xu, X., Liu, M., Ren, W., Tao, B., Sun, G., Pan, S. and Liu, J. 2011. Climate and land use controls over terrestrial water use efficiency in monsoon Asia. *Ecohydrology*, 4, 322–340.
- Tuong, T.P., Bouman, B. a. M. and Mortimer, M. 2005. More rice, less water–integrated

## **Chapter 4 - Carbon and water fluxes between paddy and rainfed rice**

- approaches for increasing water productivity in irrigated rice-based systems in Asia. *Plant Production Science*, 8, 231–241.
- Tuong, T.P. and Bouman, B.A.M. 2003. Rice production in water-scarce environments, in: J.W. Kijne; R. Barker and D. Molden (eds.), *Water Productivity in Agriculture: Limits and Opportunities for Improvement*. pp. 53–67.
- Wang, L., Good, S.P. and Caylor, K.K. 2014. Global synthesis of vegetation control on evapotranspiration partitioning. *Geophysical Research Letter*, 41, 6753–6757.
- Wassmann, R., Lantin, R.S., Neue, H.U., Buendia, L. V, Corton, T.M. and Lu, Y. 2000. Characterization of methane emissions from rice fields in Asia. III. Mitigation options and future research needs. *Nutrient Cycling in Agroecosystems*, 58, 23–36.
- Watanabe, T. and Kume, T. 2009. A general adaptation strategy for climate change impacts on paddy cultivation: special reference to the Japanese context. *Paddy Water Environment*, 7, 313–320.
- Weller, S., Kraus, D., Ayag, K.R.P., Wassmann, R., Alberto, M.C.R., Butterbach-Bahl, K. and Kiese, R. 2014. Methane and nitrous oxide emissions from rice and maize production in diversified rice cropping systems. *Nutrient Cycling in Agroecosystems*, doi:10.1007/s10705-014-9658-1.
- Williams, C.A. and Albertson, J.D. 2005. Contrasting short- and long-timescale effects of vegetation dynamics on water and carbon fluxes in water-limited ecosystems. *Water Resource Research*, 41. doi:10.1029/2004WR003750
- Wolf, S., Eugster, W., Potvin, C. and Buchmann, N. 2011. Strong seasonal variations in net ecosystem CO<sub>2</sub> exchange of a tropical pasture and afforestation in Panama. *Agriculture and Forest Meteorology*, 151, 1139–1151.
- Xiao, Y., Xie, G., Lu, C., Ding, X. and Lu, Y. 2005. The value of gas exchange as a service by rice paddies in suburban Shanghai, PR China. *Agriculture, Ecosystem and Environment*, 109, 273–283.
- Yan, X., Ohara, T. and Akimoto, H. 2003. Development of region-specific emission factors and estimation of methane emission from rice fields in the East , Southeast and South Asian countries. *Global Change Biology*, 9, 237–254.

## Chapter 4 - Carbon and water fluxes between paddy and rainfed rice

- Zeri, M., Hussain, M.Z., Anderson-Teixeira, K.J., DeLucia, E. and Bernacchi, C.J. 2013. Water use efficiency of perennial and annual bioenergy crops in central Illinois. *Journal of Geophysical Research: Biogeosciences*, 118, 581–589.
- Zhao, X., Huang, Y., Jia, Z., Liu, H., Song, T., Wang, Y., Shi, L., Song, C. and Wang, Y. 2008. Effects of the conversion of marshland to cropland on water and energy exchanges in northeastern China. *Journal of Hydrology*, 355, 181–191.
- Zhou, M.C., Ishidaira, H., Hapuarachchi, H.P., Magome, J., Kiem, A.S. and Takeuchi, K. 2006. Estimating potential evapotranspiration using Shuttleworth Wallace model and NOAA-AVHRR NDVI data to feed a distributed hydrological model over the Mekong River basin. *Journal of Hydrology*, 327, 151–173.
- Zou, J., Huang, Y., Jiang, J., Zheng, X. and Sass, R.L. 2005. A 3-year field measurement of methane and nitrous oxide emissions from rice paddies in China: Effects of water regime, crop residue, and fertilizer application. *Global Biogeochemical Cycles*, 19, n/a–n/a.

### 4.9. Annex 1

LAI and  $T/ET_0$  relationship

Damping coefficient  $k$  (relationship of transpiration to potential evapotranspiration ratio to LAI) was derived from the figure A1.  $k$  of paddy rice = 0.49 and rainfed rice is 0.48.

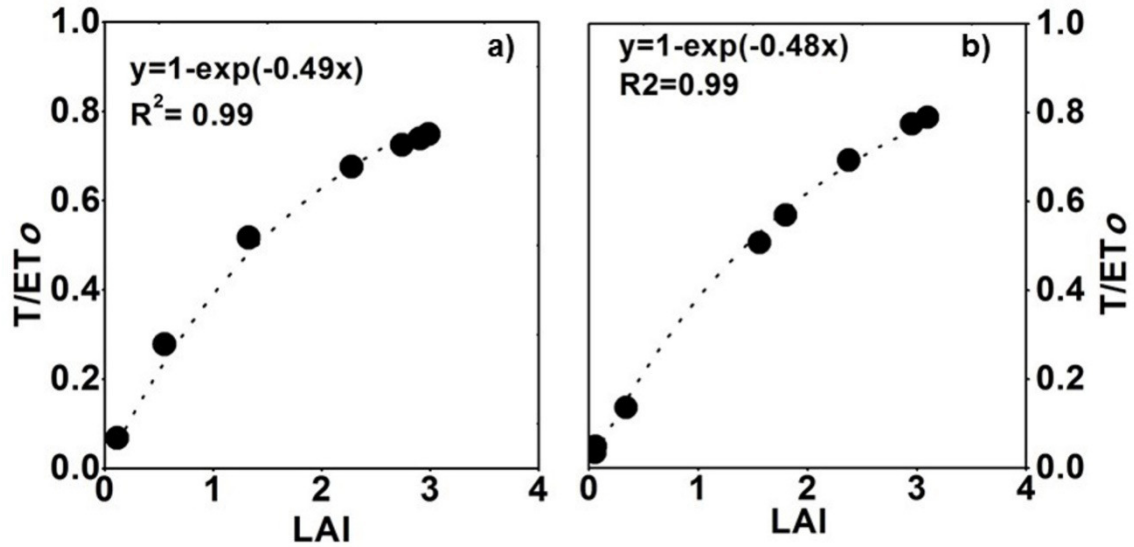


**Figure 4.5.A1** Relationship between T/ETo and LAI of (a) paddy and (b) rainfed rice. LAI was calculated as leaf area per ground area where Leaf area (LA) was determined with a Leaf Area Meter (LI-3000A, LI-COR, USA). T/ETo was calculated as the ratio of estimate daily transpiration of the LAI measurement date (equation 4.3 and 4.6) to estimated reference evapotranspiration (equation 4.3).

## Annex 2

### LAI and NDVI relationship

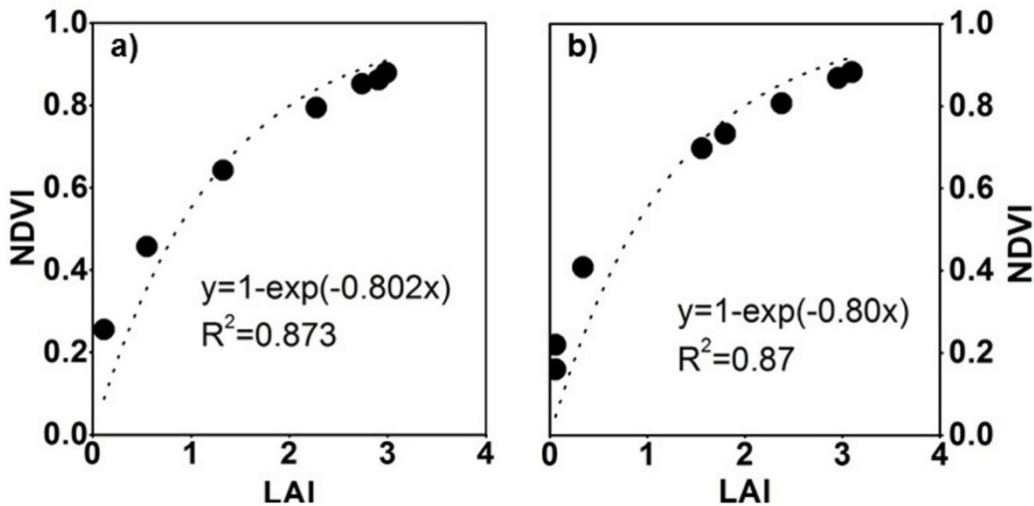


**Figure 4.6.A2** Relationship between NDVI and LAI of (a) paddy rice and (b) rainfed rice. LAI was calculated as leaf area per ground area where Leaf area (LA) was determined with a Leaf Area Meter (LI-3000A, LI-COR, USA). NDVI was measured by CropScan (CropScan Inc., USA). Damping coefficient  $k^*$  (relationship between NDVI and LAI) was derived from figure 4.6A2.  $k^*$  for both paddy and rainfed rice = 0.8.



## Chapter 4 - Carbon and water fluxes between paddy and rainfed rice

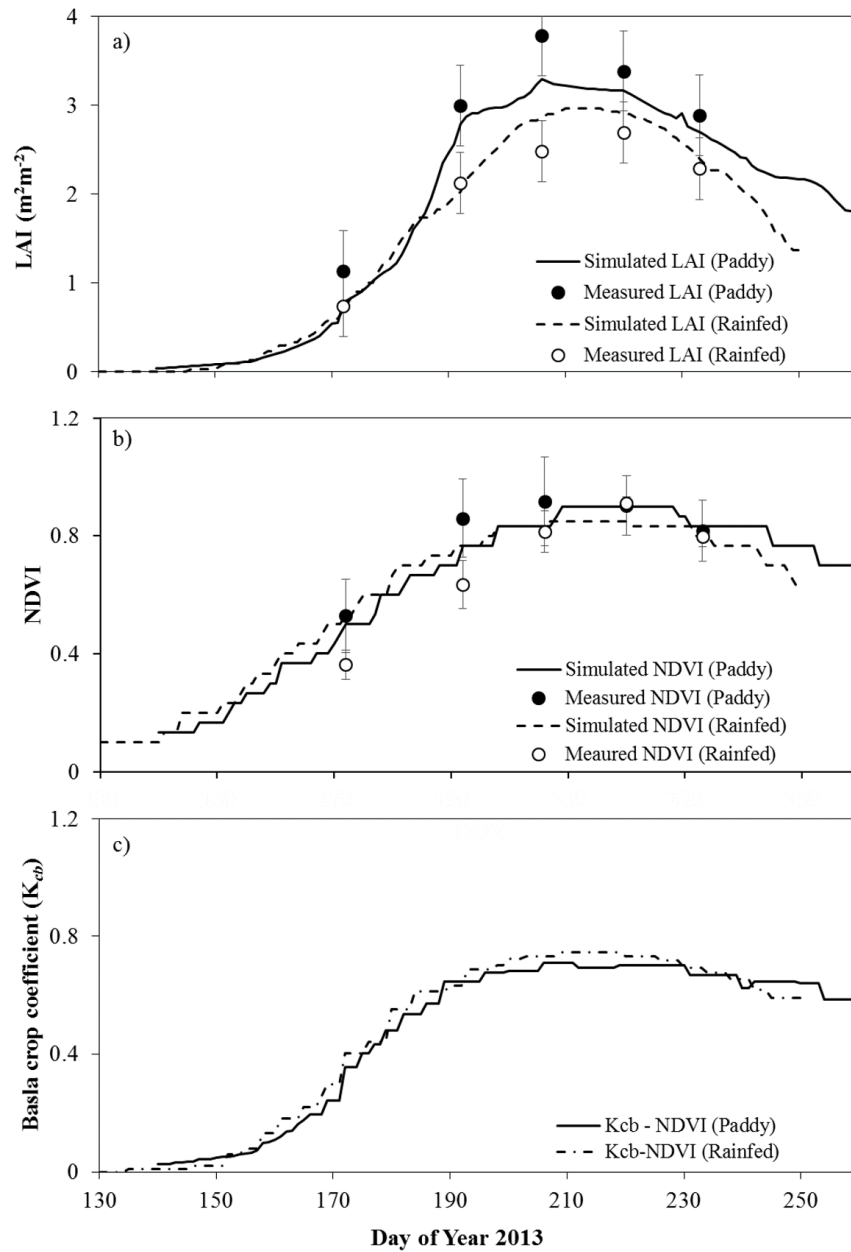


**Figure 4.7.A3** Simulated daily crop growth of paddy and rainfed rice a) LAI, b) NDVI, c) Dual crop coefficient ( $K_{cb}$ ). Daily  $K_{cb}$  was simulated based on daily NDVI, after following Choudhury (1994).

## Chapter 4 - Carbon and water fluxes between paddy and rainfed rice

### 4.10. Supplementary

**Table 4.1.S1** Soil chemical and physical properties of study area, Chonnam National University research farm, Gwangju, S. Korea.

Parameters	Values
pH (1:5)*	6.5 (0.1)
Total organic carbon (g C kg <sup>-1</sup> )	12.3 (0.5)
Total N (g K g <sup>-1</sup> )	1.0 (0.2)
Available P (mg P <sub>2</sub> O <sub>5</sub> kg <sup>-1</sup> )	13.1(0.7)
CEC (com kg <sup>-1</sup> )	14.4 (0.4)
Texture	Loam (Sand: Silt: Clay= 40: 37: 23)

Values were mean values of six replicates and standard errors in Parentheses.

\*the ratio of soil: water

## Chapter 4 - Carbon and water fluxes between paddy and rainfed rice

**Table 4.2.S2** Water and carbon fluxes, grain yield and water use efficiency of paddy and rainfed rice. Net Ecosystem Exchange (NEE,  $-NEE = GPP + R_{eco}$ ) is the balance between photosynthetic uptake and release of carbon dioxide by autotrophic and heterotrophic respiration. Gross primary production (GPP) is photosynthetic uptake. Ecosystem respiration ( $R_{eco}$ ) is respiration from soil and plant. Ecosystem water use efficiency was calculated as the ratio of NEE to evapotranspiration (ET); the ratio of NEE to transpiration (T) and the ratio of GPP to T. Agronomic water use efficiency was calculated as the ratio of grain yield to ET. Differences between paddy and rainfed were tested by one way ANOVA: Carbon, water fluxes, Grain yield and water use efficiency were compared not only as crop seasonal sum but also as growth stage specific.

Crop	DOY	GS	Measured daily carbon and water fluxes					Grain yield (kg ha <sup>-1</sup> )	Water Use Efficiency				
			GPP (gCm <sup>-2</sup> d <sup>-1</sup> )	NEE (gCm <sup>-2</sup> d <sup>-1</sup> )	$R_{eco}$ (gCm <sup>-2</sup> d <sup>-1</sup> )	ET (mmm <sup>-2</sup> d <sup>-1</sup> )	T (mmm <sup>-2</sup> d <sup>-1</sup> )		$NEE/ET$	$NEE/T$	$GPP/ET$	$GPP/T$	WUE <i>agro</i>
			(n=3)	(n=3)	(n=3)	(n=3)	(n=3)		(n=3)	(n=3)	(n=3)	(n=3)	(n=6)
R	172	S	3.96 ± 0.27	-1.57 ± 0.13 *	2.35 ± 1.5 *	1.23 ± 0.26 **	0.89 ± 0.11	n/a	1.28 ± 0.19	1.76 ± 0.15 *	3.22 ± 0.51 *	4.45 ± 0.21	n/a
R	182	T	12.02 ± 1.53	-3.86 ± 0.81 *	6.01 ± 0.73 *	1.74 ± 0.01 **	1.38 ± 0.08	n/a	2.22 ± 1.38	2.80 ± 1.12 **	6.91 ± 0.87 **	8.71 ± 0.37	n/a
R	206	H	9.45 ± 0.70 **	-1.99 ± 0.21 *	2.19 ± 0.08 *	0.96 ± 0.04 **	0.87 ± 0.01	n/a	2.08 ± 0.87	2.28 ± 0.66 **	9.84 ± 0.24 **	10.86 ± 0.42	n/a
R	218	M	8.87 ± 0.70	-2.24 ± 0.48 *	5.74 ± 0.39 *	1.39 ± 0.12 **	1.37 ± 0.01	n/a	1.61 ± 1.37 *	1.64 ± 0.87 *	6.38 ± 0.80	6.47 ± 0.47	n/a
P	167	S	4.12 ± 0.18	-2.92 ± 0.13 *	1.20 ± 0.06 *	2.27 ± 0.21 **	0.79 ± 0.09	n/a	1.26 ± 0.06	3.70 ± 0.17 **	1.81 ± 0.08 *	5.15 ± 0.06	n/a
P	175	T	8.68 ± 0.51	-7.08 ± 0.42 *	1.59 ± 0.11 *	3.61 ± 0.38 **	1.11 ± 0.16	n/a	1.96 ± 0.12	6.38 ± 0.22 **	2.41 ± 0.14 **	7.82 ± 0.11	n/a
P	200	H	13.19 ± 1.12 **	-9.31 ± 0.98 *	3.88 ± 0.20 *	3.99 ± 0.51 **	1.46 ± 0.24	n/a	2.33 ± 0.25	6.38 ± 0.17 **	3.29 ± 0.28 **	9.01 ± 0.28	n/a
P	219	M	10.84 ± 0.03	-6.65 ± 0.27 *	4.19 ± 0.26 *	1.66 ± 0.28 **	1.55 ± 0.18	n/a	4.01 ± 0.16 *	4.29 ± 0.11 **	6.53 ± 0.02	6.99 ± 0.02	n/a
R	crop season total		779.08 ± 265.43	399.25 ± 147.32 **	379.53 ± 242.48 **	138.75 ± 68.43 **	89.79 ± 57.35	5989 ± 683	2.88 ± 0.22	4.44 ± 0.63 **	5.61 ± 0.94 *	8.68 ± 1.87	5.58 ± 0.79 **
P	crop season total		832.43 ± 189.78	552.13 ± 211.54 **	281.30 ± 161.32 **	239.88 ± 87.45 **	100.91 ± 34.32	6612 ± 218	2.30 ± 0.41	5.47 ± 0.17 **	3.47 ± 0.19 *	8.25 ± 0.48	3.68 ± 0.21 **

\* one way ANOVA between RF-PD followed by TukeyHSD test (significant at  $p < 0.05$ )

\*\* one way ANOVA between RF-PD followed by TukeyHSD test (significant at  $p < 0.01$ )

Note: GS= growth stages, R= Rainfed, P= Paddy, S= seedling, T= Tillering, H = Heading, M= Maturity. Numbers followed the ± sign is SD.

## Chapter 4 - Carbon and water fluxes between paddy and rainfed rice

**Table 4.3.S3** Correlation matrix of carbon and water fluxes and environmental variables of paddy rice

	GPP	NEE	Reco	ET	T	Radiation	Tair	Tsoil	VPD	SWC	Windspeed
GPP											
Spearman's ( $\rho$ )		-0.96	0.57	0.46	0.84	0.52	0.57	0.71	0.43	-0.41	0.46
P		0.00	0.00	0.00	0.00	0.00	0.00	0.00	0.00	0.00	0.00
NEE											
Spearman's ( $\rho$ )	-0.96		-0.37	-0.60	-0.76	-0.62	-0.39	-0.59	-0.47	0.26	-0.39
P	0.00		0.00	0.00	0.00	0.00	0.00	0.00	0.00	0.00	0.00
Reco											
Spearman's ( $\rho$ )	0.57	-0.37		-0.15	0.70	0.04	0.90	0.78	0.20	-0.80	0.42
P	0.00	0.00		0.11	0.00	0.67	0.00	0.00	0.03	0.00	0.00
ET											
Spearman's ( $\rho$ )	0.46	-0.60	-0.15		0.36	0.87	0.00	0.26	0.67	0.07	0.20
P	0.00	0.00	0.11		0.00	0.00	0.96	0.00	0.00	0.45	0.03
T											
Spearman's ( $\rho$ )	0.84	-0.76	0.70	0.36		0.48	0.63	0.70	0.44	-0.62	0.25
P	0.00	0.00	0.00	0.00		0.00	0.00	0.00	0.00	0.00	0.01
Radiation											
Spearman's ( $\rho$ )	0.52	-0.62	0.04	0.87	0.48		0.06	0.30	0.78	-0.18	0.24
P	0.00	0.00	0.67	0.00	0.00		0.51	0.00	0.00	0.05	0.01
Tair											
Spearman's ( $\rho$ )	0.57	-0.39	0.90	0.00	0.63	0.06		0.86	0.29	-0.70	0.55
P	0.00	0.00	0.00	0.96	0.00	0.51		0.00	0.00	0.00	0.00
Tsoil											
Spearman's ( $\rho$ )	0.71	-0.59	0.78	0.26	0.70	0.30	0.86		0.38	-0.67	0.48
P	0.00	0.00	0.00	0.00	0.00	0.00	0.00		0.00	0.00	0.00
VPD											
Spearman's ( $\rho$ )	0.43	-0.47	0.20	0.67	0.44	0.78	0.29	0.38		-0.34	0.39
P	0.00	0.00	0.03	0.00	0.00	0.00	0.00	0.00		0.00	0.00
SWC											
Spearman's ( $\rho$ )	-0.41	0.26	-0.80	0.07	-0.62	-0.18	-0.70	-0.67	-0.34		-0.17
P	0.00	0.00	0.00	0.45	0.00	0.05	0.00	0.00	0.00		0.06
Windspeed											
Spearman's ( $\rho$ )	0.46	-0.39	0.42	0.20	0.25	0.24	0.55	0.48	0.39	-0.17	
P	0.00	0.00	0.00	0.03	0.01	0.01	0.00	0.00	0.00	0.06	

## Chapter 4 - Carbon and water fluxes between paddy and rainfed rice

**Table 4.4.S4** Correlation matrix of carbon and water fluxes and environmental variables of rainfed rice

	GPP	NEE	Reco	ET	T	Radiation	Tair	Tsoil	VPD	SWC	Windspeed
GPP											
Spearman's ( $\rho$ )		-0.81	0.89	0.71	0.79	0.25	0.72	0.80	0.20	-0.42	0.56
P		0.00	0.00	0.00	0.00	0.01	0.00	0.00	0.03	0.00	0.00
NEE											
Spearman's ( $\rho$ )	-0.81		-0.50	-0.66	-0.67	-0.53	-0.46	-0.58	-0.43	0.36	-0.43
P	0.00		0.00	0.00	0.00	0.00	0.00	0.00	0.00	0.00	0.00
Reco											
Spearman's ( $\rho$ )	0.89	-0.50		0.55	0.65	-0.01	0.74	0.80	0.00	-0.35	0.55
P	0.00	0.00		0.00	0.00	0.90	0.00	0.00	0.97	0.00	0.00
ET											
Spearman's ( $\rho$ )	0.71	-0.66	0.55			0.43	0.65	0.57	0.47	-0.36	0.43
P	0.00	0.00	0.00			0.00	0.00	0.00	0.00	0.00	0.00
T											
Spearman's ( $\rho$ )	0.79	-0.67	0.65	0.89		0.23	0.76	0.59	0.28	-0.56	0.39
P	0.00	0.00	0.00	0.00		0.01	0.00	0.00	0.00	0.00	0.00
Radiation											
Spearman's ( $\rho$ )	0.25	-0.53	-0.01	0.43	0.23		-0.02	0.10	0.81	-0.04	0.12
P	0.01	0.00	0.90	0.00	0.01		0.86	0.27	0.00	0.65	0.21
Tair											
Spearman's ( $\rho$ )	0.72	-0.46	0.74	0.65	0.76	-0.02		0.82	0.19	-0.58	0.62
P	0.00	0.00	0.00	0.00	0.00	0.86		0.00	0.03	0.00	0.00
Tsoil											
Spearman's ( $\rho$ )	0.80	-0.58	0.80	0.57	0.59	0.10	0.82		0.22	-0.38	0.72
P	0.00	0.00	0.00	0.00	0.00	0.27	0.00		0.01	0.00	0.00
VPD											
Spearman's ( $\rho$ )	0.20	-0.43	0.00	0.47	0.28	0.81	0.19	0.22		-0.25	0.24
P	0.03	0.00	0.97	0.00	0.00	0.00	0.03	0.01		0.01	0.01
SWC											
Spearman's ( $\rho$ )	-0.42	0.36	-0.35	-0.36	-0.56	-0.04	-0.58	-0.38	-0.25		-0.26
P	0.00	0.00	0.00	0.00	0.00	0.65	0.00	0.00	0.01		0.00
Windspeed											
Spearman's ( $\rho$ )	0.56	-0.43	0.55	0.43	0.39	0.12	0.62	0.72	0.24	-0.26	
P	0.00	0.00	0.00	0.00	0.00	0.21	0.00	0.00	0.01	0.00	

### Chapter 5

#### 5. Nutritional and developmental influences on components of rice crop light use efficiency

Wei Xue<sup>1,2</sup>; Steve Lindner<sup>1</sup>; Bhone Nay-Htoon<sup>3</sup>; Maren Dubbert<sup>3,6</sup>; Dennis Otieno<sup>1</sup>, Jonghan Ko<sup>4</sup>; Hiroyuki Muraoka<sup>5</sup>; Christiane Werner<sup>3,6</sup>; John Tenhunen<sup>1</sup>; Peter Harley<sup>1</sup>

<sup>1</sup>Department of Plant Ecology, BayCEER, University of Bayreuth, 95440 Bayreuth, Germany

<sup>2</sup>State Key Laboratory of Desert and Oasis Ecology, Xinjiang Institute of Ecology and Geography, Chinese Academy of Sciences, 830011 Urumqi, China

<sup>3</sup>Department of Agroecosystem Research, BayCEER, University of Bayreuth, 95440 Bayreuth, Germany

<sup>4</sup>Department of Applied Plant Science, Chonnam National University, 500757 Gwangju, South Korea

<sup>5</sup>River Basin Research Center, Gifu University, 1-1 Yanagido, Gifu, 501-1193 Japan

<sup>6</sup>Department of Ecosystem Physiology, University of Freiburg, 79085 Freiburg, Germany

#### 5.1. Abstract

Light use efficiency (LUE) plays a vital role in determination of crop biomass and yield. Important components of LUE, i.e. canopy structure, nitrogen distribution, photosynthetic capacity and CO<sub>2</sub> diffusion conductance were investigated in paddy rice grown under low, normal and high supplemental nitrogen (0, 115, and 180 kg N ha<sup>-1</sup>). Photosynthetic characteristics varied linearly with leaf nitrogen content (N<sub>a</sub>), independent of treatment and canopy position, so differences in photosynthesis were due to differences in N allocation. CO<sub>2</sub> diffusion resistances were significant and constrained LUE (more during late season), but there were no differences between treatments. Early in the season (tillering stage) leaves in the fertilized treatments had higher photosynthetic rates due to higher leaf N content leading to larger amounts of rate-limiting photosynthetic proteins, which gave them an early head start and boost in productivity and leaf area index, bringing increases in canopy light absorption. Later during the growth season, differences in leaf N<sub>a</sub> and photosynthetic characteristics between treatments were slight. Enhanced LAI in fertilized plots throughout the growing season was related to greater leaf number and leaf area per planted bundle and a

## **Chapter 5 - Nutritional and developmental influences on carbon gain capacity**

larger leaf area in the upper canopy (LAUC). Fertilized treatments had a higher LAUC with high leaf nitrogen concentration and reduced mesophyll diffusion limitation but greater exposure to full sunlight that led to improved nitrogen use efficiency and efficient carbon gain. In conclusion, differences in carbon gain and biomass accumulation under differing N fertilization were associated primarily with resource allocation associated with canopy leaf area development rather than leaf morphological or physiological properties. The results provide new insights with respect to the multi-dimensional coordinated structural and physiological adjustments governing LUE over the course of rice crop development.

**Keywords:** canopy structure; CO<sub>2</sub> diffusion conductance; light use efficiency; nitrogen; photosynthesis; rice crop

### 5.2. Introduction

As proposed by Monteith (1972, 1977) ecosystem or crop productivity is largely determined by the amount of solar radiation intercepted and the efficiency with which that absorbed energy is converted to carbohydrates in the process of photosynthesis. The percentage of incident photosynthetically active radiation that is absorbed by a plant canopy (APAR) is largely determined by canopy architecture (leaf area index, leaf angle distribution) and leaf pigments, while the efficiency of energy conversion is a function of leaf physiological processes. Although light use efficiency (LUE) has been equated with quantum use efficiency in the plant physiology literature (Ehleringer and Pearcy, 1983), in the remote sensing and crop production communities, LUE is defined as total carbon uptake (Gitelson and Gamon, 2015), integrated over some period of time divided by the total irradiance incident on or absorbed by the vegetation.

LUE of developing crops therefore depends on canopy leaf area and leaf angle distribution which determine light interception, on the distribution of nitrogen in the canopy as it relates to the profile of photosynthetic capacity, and on diffusional limitations which restrict delivery of CO<sub>2</sub> to the site of fixation (Parry et al., 2011). Until recently, the only diffusional limitations considered were boundary layer and stomatal conductances. Recent progress in the analysis of leaf gas exchange, however, has elucidated an additional component of leaf structure and function that significantly affects crop photosynthesis, namely the mesophyll conductance of the leaves,  $g_m$  (Ethier and Livingston, 2004; Niinemets et al., 2009a).

Depending on the magnitude of  $g_m$ , the CO<sub>2</sub> gradient between substomatal cavities and the chloroplast stroma varies, which impacts the physiology of photosynthesis and, over the long-term, influences natural selection along ecological gradients (Muir et al. 2014; Flexas et al., 2012; Niinemets et al., 2009b), and  $g_m$  has been identified as an important factor in regulation of crop primary production (Adachi et al., 2013; Parry et al., 2011). Mesophyll conductance is positively correlated with and essentially linearly related to photosynthetic capacity (Bernacchi et al., 2002; Evans and Loreto, 2000) when considering a broad spectrum of leaf types with varying leaf density (Niinemets, 2009b). However, based on existing data from herbaceous species, the relationship is relatively scattered (Flexas et al., 2012; Niinemets et al., 2009b; Warren and Adams, 2006), indicating that additional factors influence carbon uptake of crop species to a different degree and in different ways. For



## Chapter 5 - Nutritional and developmental influences on carbon gain capacity

example, nitrogen allocation rather than leaf structural modifications may primarily mediate changes in  $g_m$  and  $A_{max}$  (the maximum net photosynthesis rate at saturating light, optimal temperature and normal atmospheric  $CO_2$  concentration) in species with herbaceous-type leaves (Niinemets, 2007).

While mesophyll conductance has gained much attention recently, comprehensive studies of nutritional influences on leaf area index development and allocation, canopy nitrogen distribution, stomatal conductance ( $g_s$ ) limitations, time-dependent changes in  $A_{max}$  and canopy GPP, and the ecophysiological regulation of  $g_m$  are lacking (Niinemets, 2009b) and needed as they are fundamental physiological concepts in sustainable crop production (Foulkes and Reynolds, 2015). To gain greater insight, several studies concerning the relationships among leaf N,  $g_m$ ,  $g_s$  and photosynthesis in crops have been implemented, but these have been carried out in controlled environments or over short time periods. Longer-term studies of crop production over the seasonal cycle and in natural field environments are needed in order to better understand the multiple influences that regulate LUE and production.

In this study, gas exchange and chlorophyll fluorescence measurements were made on leaves of rice to determine  $CO_2$  uptake, transpiration,  $g_s$  and  $g_m$ . These measurements were carried out simultaneously with observations of crop development and canopy  $CO_2$  exchange in experimental fields of Chonnam National University, Gwangju, South Korea under three nutrient treatment levels. We examine the extent to which increased nutrient supply leads to increases in canopy leaf area, altered nitrogen investments, as well as changes in leaf gas exchange and biomass production (Yoshida, 1981). We address the following hypotheses:

1. Seasonal development of rice is characterized by a LUE optimization-oriented coordination in LAI, canopy N distribution, and leaf conductance ( $g_s$  and  $g_m$ ) limitations on carbon gain.
2. Increasing nutrient supply to the rice crop leads to an acceleration in the rate of canopy development (rate of increase in LAI) and overall carbon gain, but not to the basic way in which coordination of the process relevant to LUE occurs.
3. Variation in leaf function in rice grown with different nutrient supply and under varying light environments within the crop canopy is largely explained by variations in leaf nitrogen allocation and nitrogen-driven gas exchange.

### 5.3. Materials and methods

#### 5.3.1. Study site

The experimental site is located at the agricultural fields of Chonnam National University, Gwangju, South Korea (126°53' E, 35°10' N, altitude 33 m). Rice (*Oryza sativa* L. cv. Unkwang) seedlings cultivated in a nursery were transplanted to a flooded field using a four-row rice transplanting machine on May 20th, 2013 (day of year–DOY–140), with a row-line spacing of 12 × 30 cm. On average, each planted bundle contained five seedlings. A mass ratio of N:P:K of 11:5:6 was used in the paddy rice plots for three fertilization treatments: 0 kg N ha<sup>-1</sup> (no supplemental fertilization as a control referred to as low; plot size ~511 m<sup>2</sup>), 115 kg N ha<sup>-1</sup> (the agricultural agency recommended amount, referred to as normal, plot size ~1387 m<sup>2</sup>) and 180 kg N ha<sup>-1</sup> (referred to as high, plot size ~511 m<sup>2</sup>). Nitrogen was applied in two dosages, 80% as basal dosage two days prior to transplanting and 20% during the tillering stage, 19 Days After Transplanting (DAT). P fertilizer (62 kg ha<sup>-1</sup>) was applied as a 100% basal dosage, and K fertilizer (60 kg ha<sup>-1</sup>) was applied as 65% basal dosage and 35% during tillering. All field management practices of paddy rice and fertilizer dosages reflected the practices of farmers in the region. Fertilizer migration between nutrient treatments and potential losses via runoff were minimized by cement walls 35 cm wide, inserted to a depth of one meter in the soil. Excess water drained out of the field during the summer monsoon in July and August when heavy rainfall occurred. The time periods during which rice under these field conditions grew in different agronomic developmental stages after transplanting were unaffected by fertilization treatment, and are shown in Table 5.1.

**Table 5.1** Time periods during which paddy rice cultivar Unkwang grew in different agronomic stages.

Growth stage	Day After Transplanting	Day Of Year
Recovery from transplanting	0 – 10	142 - 152
Active tillering	10 – 30	152 - 172
Elongation	30 – 64	172 - 206
Flowering	64 – 70	206 - 212
Grain-filling	71 – 120	212 - 162

To underpin several physiological assumptions, the same rice variety was planted in September 2014 in a greenhouse at the University of Bayreuth, Germany (11°34' E, 49°56'

## Chapter 5 - Nutritional and developmental influences on carbon gain capacity

N). Seedlings were transplanted at 10 cm height into plastic containers (top diameter 25.4 cm and height 25 cm) with similar plant spacing as in the 2013 field experiment. The equivalent to the 115 kg N ha<sup>-1</sup> field treatment was applied again two times, before transplanting and at the tillering stage as nutrient liquid from 100g N/l Wuxal super (Agrarvers and Oberland Inc., Schongau, Germany). For gas exchange experiments, the plants were then acclimated in a growth chamber to daytime air temperature 30°C, relative humidity 60% and light intensity of 900  $\mu\text{mol m}^{-2} \text{s}^{-1}$ . Air temperature during nighttime was constant at 25°C.

### 5.3.2. Field measurements of diurnal courses of canopy and leaf CO<sub>2</sub> exchange

Four plots were established in the middle of the paddy fields for each nutrient treatment to monitor diurnal canopy CO<sub>2</sub> gas exchange, using a custom-built set of one transparent and one opaque chamber (L 39.5 × W 39.5 × H 50.5 cm; detailed information on chamber construction and measurement protocols are given in Li et al. (2008) and Lindner et al. (2015). Three frames, each enclosing three bundles of healthy plants, and a fourth frame without plants were deployed. Diurnal gas exchange courses of net ecosystem CO<sub>2</sub> exchange (NEE – with transparent chamber) and ecosystem respiration (R<sub>eco</sub> – with opaque darkened chamber) per square meter ground surface were monitored at hourly intervals from sunrise to sunset. Incident PAR in the transparent chamber was measured with a quantum sensor (LI-190, LI-COR, Lincoln, Nebraska, USA). A hyperbolic light response model was fit to estimate gross primary production (GPP; sum of NEE and R<sub>eco</sub>) as a function of incident PAR, generating instantaneous canopy light use efficiency (LUE<sub>ins</sub>) defined as the initial slope of the response, and an estimate of potential maximum GPP rate at PAR of 1500  $\mu\text{mol m}^{-2} \text{s}^{-1}$  (GPP<sub>max</sub>) (Li et al., 2008; Lindner et al., 2015). Canopy LUE<sub>inc</sub>, defined as daytime integrated GPP divided by daytime total incident above-canopy PAR, was calculated for each day of measurement.

Diurnal gas exchange and chlorophyll fluorescence measurements in the sunlit (uppermost), second, third and fourth mature leaves of the high fertilization group were conducted using a portable gas-exchange and chlorophyll fluorescence system (GFS-3000 and PAM Fluorometer 3050-F, Heinz Walz GmbH, Effeltrich, Germany) on 57 and 73 DAT to track ambient environmental conditions external to leaf cuvette. The measurement dates of diurnal courses of the sunlit (uppermost) leaves in the low and normal groups were 31 and 72 DAT, and 25 and 77 DAT, respectively. Middle parts of two or three intact and healthy leaves were

## **Chapter 5 - Nutritional and developmental influences on carbon gain capacity**

enclosed from sunrise to sunset. Microenvironmental factors such as incident light intensity, air/leaf temperature, air humidity, and CO<sub>2</sub> concentration were recorded simultaneously. Leaf-level light use efficiency was determined from a linear estimation of photosynthesis response to light when incident PAR was less than 200  $\mu\text{mol m}^{-2} \text{s}^{-1}$ .

### **5.3.3. Measurements of CO<sub>2</sub> response curves of net assimilation rate**

The Walz GFS-3000 was used to measure net assimilation CO<sub>2</sub> response curves at different leaf temperatures. CO<sub>2</sub> response curves of uppermost canopy leaves were measured twice for the low and normal fertilization treatments, on around 28 DAT (tillering stage) and around 74 DAT (beginning of grain-filling stage: subsequently termed grain-filling). CO<sub>2</sub> curves were commenced after leaves had acclimated to the cuvette microenvironment (CO<sub>2</sub> concentration of 400  $\mu\text{mol mol}^{-1}$  and saturating PAR of 1500  $\mu\text{mol m}^{-2} \text{s}^{-1}$ ) after which CO<sub>2</sub> concentration was changed progressively according to the sequence 1500, 900, 600, 400, 200, 100 to 50  $\mu\text{mol mol}^{-1}$ . Relative humidity was controlled to ca. 60%. Assimilation rate and stomatal conductance data were recorded after new steady-state readings were obtained. At least three replicate CO<sub>2</sub> curves were obtained at each leaf temperature, which was varied in 5°C steps from 20 to 35°C at the tillering stage and from 25 to 35°C at the grain-filling stage. For each CO<sub>2</sub> response curve, the protocol described by Sharkey et al. (2007) was used to estimate values for the parameters  $V_{\text{cmax}}$  and  $J_{\text{max}}$ .

$A_{\text{max}}$  (photosynthesis rate at 400  $\mu\text{mol CO}_2 \text{mol}^{-1}$ , saturating PAR of 1500  $\mu\text{mol m}^{-2} \text{s}^{-1}$  and 30°C) in leaves at different depths in the canopy were measured on around 54 DAT (low, normal and high fertilization treatments) and around 72 DAT (low and high fertilization treatments) using the GFS-3000. On 90 DAT similar photosynthetic capacity determinations were conducted, but only on the uppermost leaves in the canopy.

### **5.3.4. Measurement of canopy reflectance**

Radiometric measurements were carried out intensively in three nutrient groups over growth season by a portable instrument equipped by multispectral radiometers (MSR, Cropscan Inc, MN, USA). The MRS-5 was positioned facing vertically downward at 2 m above crop canopies, and measurements were taken at solar noon to minimize the effect of diurnal changes in solar zenith angle. 6 replications surrounding plots for canopy gas exchange

## Chapter 5 - Nutritional and developmental influences on carbon gain capacity

measurements were conducted, and reflectance measurements were then averaged. Normalized difference vegetation indices (NDVI) was calculated from the spectral bands obtained in the channel 3 and 4 of the MSR5, corresponding to the red (630-690 nm) and near infra red wavelength (760-900 nm) respectively by following formula,

$$NDVI = \frac{\rho_{nir} - \rho_{red}}{\rho_{nir} + \rho_{red}} \quad (5.1)$$

To get the NDVI on those days when measurements of canopy gas exchange were implemented and on other days that were clear and sunny at solar noon, the time series function was fit to measured NDVI,

$$NDVI = a \cdot t^b \cdot e^{c \cdot t} \quad (5.2)$$

where a, b and c are coefficient and t is time (day after transplanting)

### 5.3.5. Characterization of leaf nitrogen content, leaf area, leaf angle, and biomass

After conducting gas exchange measurements, leaf samples were collected to estimate leaf area, dry mass and nitrogen content. On 26, 33, 54, 72 and 86 DAT, three planted bundles consisting of fifteen plants (five seedlings comprising one planted bundle) from each treatment were harvested, and total plant area (leaf and stem) of each was determined with an LI-3100 leaf area meter (LI-COR Inc, Lincoln, Nebraska, USA). On 54 and 72 DAT a portion of the standing canopy in each fertilization treatment was stratified into vertical layers, each layer 15 cm in thickness. Leaf and stem area and biomass in each stratified layer were measured. After chamber gas exchange measurement, the green biomass overlying one half square meter of ground in each nutrient group was harvested. All samples were dried at 60°C in a ventilated oven for at least 48 hours before determination of dry mass. Leaf nitrogen content was measured by C:N analyzer (Model 1500, Carlo Erba Instruments, Milan, Italy). On 43 DAT, three typical bundles from each treatment were randomly selected to record individual leaf laminar area. Grain yield determinations were obtained at four sampling plots (0.5 × 0.5 m) at the end of the growing season at 113 DAT (253 DOY), and were weighed after air-drying. Seasonal changes of leaf area index were measured using a plant canopy analyzer (LAI-2000, LI-COR, Lincoln, Nebraska, USA). Measurements were taken across

## Chapter 5 - Nutritional and developmental influences on carbon gain capacity

the rows and above the water surface using a cover with small view of 45° at early growth stages and one with large view of 270° at later growth stages. All measurements were made when there was no direct beam of sunlight, either in the late afternoon or during periods of uniform cloudiness.

### 5.3.6. Characterization of canopy light and nitrogen distribution profiles

Vertical profiles of incident light were determined either the day before or on the day of plant sampling with light data loggers (HOBO, Onset Computer Corporation, Bourne, MA) mounted on thin rods with vertical spacing of 15 cm from base 0 cm to top of the canopy, and where multiple rods were placed along a transect diagonal to the planted rows. Data was logged every 15 min on two consecutive days when the measurements of stratified leaf area were made for nutrient groups. The HOBO logger light values were periodically compared to PAR measured with a LI-COR quantum sensor to develop a calibration curve and to estimate the PAR profiles. A trapezoidal integration was conducted to obtain daily integrated PAR. Close correspondence between daily integrated PAR from the quantum sensor of the GFS-3000 and those from HOBO loggers indicated that the computation method was reliable. PAR was assumed to be attenuated through the canopy according to the Lambert-Beer law, where  $Q$ , the daily integrated PAR at a given canopy height is calculated as:

$$Q = Q_o \exp (- K_l f) \quad (5.3)$$

where  $Q_o$  is the daily integrated PAR above the canopy,  $K_l$  the canopy light attenuation coefficient, and  $f$  is the plant area index (PAI) from the top of canopy to the measurement level. There were few leaves in the 15–30 cm layer and no leaves in the 0–15 cm layer during late growth stages. Substantial presence of stems at lower layers, nevertheless, caused light attenuation, and plant area index showed a better correlation with measured light intensity at each layer than LAI. An exponential equation analogous to Eq. 5.3, substituting an N extinction coefficient  $K_N$  for  $K_l$ , was used to describe leaf nitrogen distribution. When  $K_l$  or  $K_N$  is equal to 0, uniform distributions of light or N resources occur in the profiles. Increasing coefficients indicate a steeper gradient in resource distribution.

## Chapter 5 - Nutritional and developmental influences on carbon gain capacity

Light use efficiency based on absorbed PAR ( $LUE_{abs}$ ) was defined as the ratio of daily integrated canopy GPP at each measuring date to integrated PAR intercepted by the canopy. Intercepted radiation,  $Q_{int}$ , was estimated by two methods, one using Eq. 5.4, derived from Eq. 5.3 (Hui et al., 2001).

$$Q_{int} = Q_o(1 - \exp(-K_l \cdot f)) \quad (5.4)$$

The other is from NDVI-fPAR correlation (fPAR is fraction of incident to  $Q_{int}$ ). The relationship between vegetation index NDVI and fPAR is generally found to be curvilinear (Choudhury, 1987; Goward and Huemmrich, 1992; Inoue et al., 2008; Gitelson et al., 2014). Linear correlation between those two biophysical variants in paddy rice before ripening stage was structured by Inoue (2008), while their data integrated with those in cereal crops grown under different ecological conditions from Choudhury (1987) actually followed exponential trend which is formulated by,

$$fPAR = fPAR_{max} \left[ 1 - \left( \frac{NDVI_{max} - NDVI}{NDVI_{max} - NDVI_{min}} \right)^\epsilon \right] \quad (5.5)$$

For determination of fPAR two types of variant need to be priori quantified based on field grown rice at specific nutrient manipulation condition: canopy geometry property ( $\epsilon$ ) which is the ratio of dampening factor  $K_p$  and factor  $K_{vi}$ , maximum and minimum NDVI values.  $K_p$  is coefficient controlling correlation between canopy light interception and LAI,  $K_{vi}$  being coefficient controlling relationship between NDVI and LAI.  $fPAR_{max}$  in rice is 0.95 recommended by Atwell et al. (1999). Max. NDVI in fertilization group and low group were 0.92 and 0.84 which were field observations, respectively.  $K_p$  and  $K_{vi}$  at 0.48 and 0.8 in rice suggested by Nay-Htoon (2015) were adopted, generating  $\epsilon$  of 0.6, which compares favorably to modeling outputted  $\epsilon$  of 0.58 via apply Eq. 5.5 to integrated data group in Figure 5.1a. Min. NDVI (x-intercept) is 0.11 when fPAR is zero. The model simulation was tested against field observations at three nutrient groups. Striking correspondence between prediction by Eq. 5.5 and field observations (calculated from Eq. 5.4) documented that values of independent variants in Eq. 5.5 are representative proxy reflecting rice growth and development and can be used for estimation of fPAR and thereby  $LUE_{abs}$  at the days when canopy gas exchange were collected.

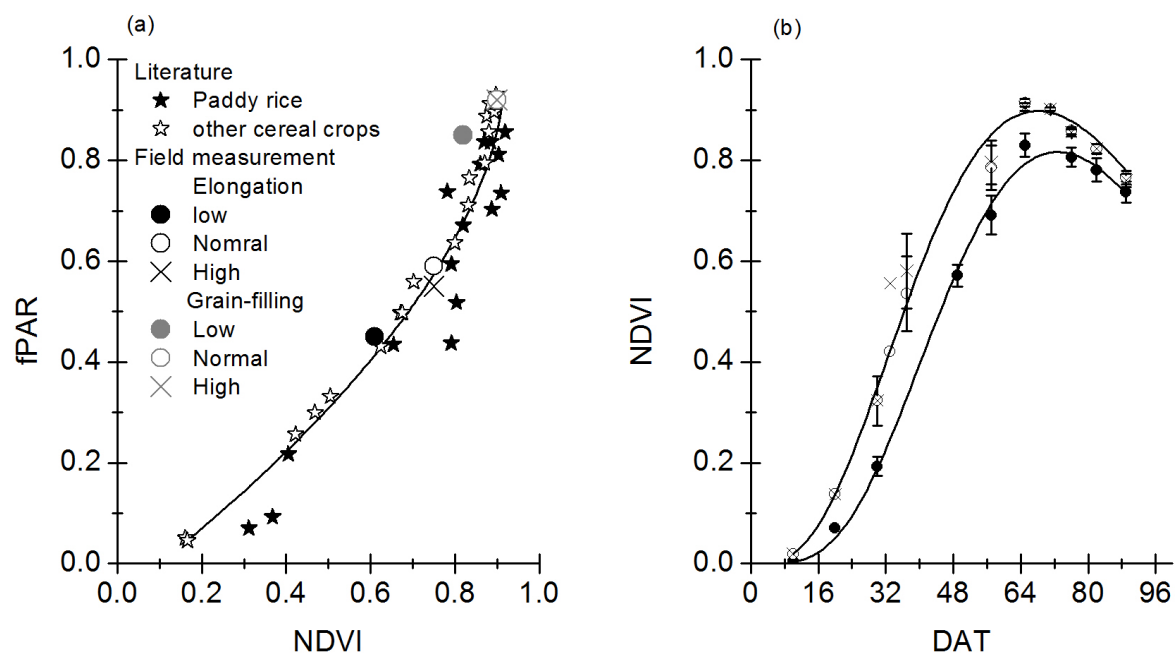


**Figure 5.1** (a) Exponential correlation between normalized difference vegetation indices (NDVI) and fraction of incident PAR to absorbed PAR in cereal crops. Filled stars represent data in paddy rice from Inoue et al. (2008) and open stars in other cereal crops from Choudhury (1987). (b) Seasonal development of NDVI in paddy rice grown under three nutrient treatments: low (filled circles, 0 kg N ha<sup>-1</sup>), normal (open circles, 115 kg N ha<sup>-1</sup>) and high (cross symbols, 180 kg N ha<sup>-1</sup>).

The amount of sunlit leaf area (leaves exposed to full sunlight) in each canopy layer at the low and normal groups during grain-filling stage was estimated based on the classical gap probability function in canopies (see Caldwell et al. (1986) for detailed description), in which sunlit leaf area is a function of solar position in the sky and the surface area and leaf geometry of each layer. For these calculations, a weighted average method considering the proportion of individual leaf area to total leaf area at each layer was used to generate average leaf angle of each layer. Leaf absorptance of PAR was assumed to be 0.84, and the leaf clumping factor used was 0.8, representative values for grain crops. Tight correlation between predications in light intensity at each layer by radiation transfer model and measurements  $y=0.82x+1.2$  ( $R^2 = 0.90$ ,  $p < 0.01$ ) meant the pragmatic implementation of classical gap probability function to mimic canopy dynamics with respect to light distribution and sunlit leaf area.



## Chapter 5 - Nutritional and developmental influences on carbon gain capacity

### 5.3.7. Estimation of the mesophyll diffusion conductance ( $g_m$ )

The variable  $J_p$  method of Harley et al. (1992) for estimating mesophyll conductance was applied to data on the ETR-limited portions of  $CO_2$  response curves. The proportion of generated electron transport rate that is used by  $CO_2$  fixation process was quantified (Appendix A, Figure 5.A1a). In general, ETR, inferred from fluorescence measurements, became stable when  $C_i$  was higher than ca.  $240 \mu\text{mol mol}^{-1}$ . Assimilation rate and ETR in the region from 240 to  $600 \mu\text{mol mol}^{-1}$  were used, because i)  $g_m$  estimates over this range of  $C_i$  values are reliable, since photosynthesis is limited by regeneration of RuBP and limitations by triose phosphate utilization usually occur only at higher  $CO_2$  concentrations (Flexas et al., 2007; Harley et al., 1992; Sharkey et al., 2007); and ii) the determinations are appropriate for the values observed for  $C_i$  under natural field conditions (ca.  $250 \mu\text{mol mol}^{-1}$ ). Thus,

$$g_m = A / (C_i - ((\Gamma^* (J_p + 8A + 8R_{day})) / (J_p - 4A - 4R_{day}))) \quad (5.6)$$

where  $A$ ,  $C_i$  and  $J_p$  are measured directly. Chloroplast  $CO_2$  compensation point ( $\Gamma^*$ ), the intercellular  $CO_2$  concentration at which carboxylation rate equals photorespiration rate in the light was determined for our rice cultivars to be  $44.4 \pm 1.3 \mu\text{mol mol}^{-1}$  (Appendix A, Figure 5A1b), which is consistent with values reported for cultivars as tobacco (Bernacchi et al., 2002).  $R_{day}$ , non-photorespiratory  $CO_2$  evolution in the light, was approximately 60% of dark respiration as measured by gas exchange.

Using values of  $V_{cmax}$  and  $J_{max}$  determined from  $CO_2$  response measurements, rates of net assimilation were predicted assuming different values of  $C_c$ , the  $CO_2$  partial pressure at the site of fixation, which is jointly determined by fixation rate, stomatal and mesophyll conductances. The limitations on photosynthetic capacity resulting from finite stomatal and mesophyll conductance were evaluated by comparing measured  $A_{400}$  at  $C_a = 400$  with rates predicted assuming infinite stomatal and/or mesophyll conductance by Eq. 7-9 (Harley et al., 1986; Monteith, 1972):

$$L_{gm} = 100 \frac{A_{cc=ci} - A_{400}}{A_{cc=ci}} \quad (5.7)$$

$$L_{gs} = 100 \frac{A_{ci=400} - A_{400}}{A_{ci=400}} \quad (5.8)$$

$$L_{total} = 100 \frac{A_{cc=400} - A_{400}}{A_{cc=400}} \quad (5.9)$$

where  $L_{gm}$  is the percent limitation due to mesophyll conductance,  $L_{gs}$  that due to stomatal

## Chapter 5 - Nutritional and developmental influences on carbon gain capacity

conductance, and  $L_{\text{total}}$  the total percent limitation of the conductance pathway on photosynthesis.

### 5.4. Results

#### 5.4.1. Seasonal changes in canopy reflectance, biomass production, canopy LUE, and leaf area in response to fertilizer treatments

Time series functions connecting measured NDVI at solar noon during sunny days were indicated in Figure 5.1 that NDVI value at fertilization group during vegetative growth stage before flowering and ripening stage were significantly higher than control group (Friedman ANOVA,  $p = 0.045$ ). Green biomass accumulation in all three nutrient groups exhibited similar seasonal trends. Biomass increased rapidly after ca. 30 DAT, reached a maximum on ca. 64 DAT, and subsequently declined (Figure 5.2a). Peak aboveground biomass was significantly higher in the normal and high fertilization treatment groups by 62% and 56%, respectively, compared to the low group. Similar to biomass production, grain yields in normal and high fertilization treatments were similar but markedly higher than in the control group by 58% and 73%. The seasonal change in measured rates of  $GPP_{\text{max}}$  is shown in Figure 5.2b. During tillering (16 DAT)  $GPP_{\text{max}}$  was low in all treatments (ca.  $2 \mu\text{mol m}^{-2} \text{s}^{-1}$ ; no significant difference,  $p > 0.05$ ) and increased rapidly with increasing LAI.  $GPP_{\text{max}}$  increased throughout the elongation period, but plants in the normal and high fertilization treatments showed increased carbon gain relative to the low fertilization after 30 DAT ( $p = 0.05$ ). The highest  $GPP_{\text{max}}$  ( $\sim 28 \mu\text{mol m}^{-2} \text{s}^{-1}$ ) occurred in fertilized plots at approx. 60 DAT, just before commencement of the grain-filling stage, at which time  $GPP_{\text{max}}$  in unfertilized plots averaged  $\sim 21 \mu\text{mol m}^{-2} \text{s}^{-1}$ . Subsequently,  $GPP_{\text{max}}$  in low N plots leveled off and  $GPP_{\text{max}}$  in fertilized treatments declined to  $\sim 23 \mu\text{mol m}^{-2} \text{s}^{-1}$ , so that 20 days later, during grain-filling (78 DAT),  $GPP_{\text{max}}$  in fertilized groups was only 10% higher.  $GPP_{\text{int}}$  exhibited similar seasonal trends across the three groups, reaching a maximum of  $11.3 \text{ g C d}^{-1}$  in the fertilized group and  $9.4 \text{ g C d}^{-1}$  in the plots receiving no additional nitrogen (Figure 5.2b).

Seasonal time courses for daily  $LUE_{\text{inc}}$  (Figure 5.2c) based on incident light were similar to those for  $GPP_{\text{max}}$  and  $GPP_{\text{int}}$ . On an incident radiation basis, differences among treatments were found as expected with higher  $LUE_{\text{inc}}$  in fertilized plots after 16 DAT, and the difference increasing over time. At approx. 60 DAT, the differences were statistically significant ( $p =$

## Chapter 5 - Nutritional and developmental influences on carbon gain capacity

0.039).

LAI in all treatments increased rapidly through the elongation stage, and substantial differences in LAI among treatments occurred after 34 DAT ( $p < 0.01$ ; Figure 5.2d) as LAI increased much more rapidly in the fertilized plots. These differences in LAI between treatments had multiple causes. Early in the elongation stage at 43 DAT, both leaf number and leaf mass per planted bundle were much higher in the normal and high plots than in the low treatment (Table 5.2). There were no significant differences in leaf biomass per bundle between the normal and high treatments, but the differences between non-fertilized and fertilized plots increased dramatically throughout the elongation stage ( $p < 0.05$ ). Furthermore, plants in the fertilized treatments exhibited significantly greater amounts of leaf area in the upper levels of the growing canopy. At 43 DAT, early in the elongation stage, the mean area of individual leaves whose height of petiolar insertion was more than 20 cm above ground surface was significantly greater in the fertilized treatments than in the low N plots (the normal and high treatments greater by 33% and 22%, respectively; Table 5.2). Similar differences were found later in the elongation stage, at 53 DAT, with fertilized plots accumulating a greater amount of leaf area in leaves originating in upper portions of the canopy, between 45 and 60 cm and between 60 and 75 cm above ground. By the grain-filling stage, however, leaf area in the upper levels of the canopy (above 60 cm insertion height) were 21.6, 23.0, and 23.0 cm<sup>2</sup> in the low, normal and high nutrient groups, and were no longer significantly different (Table 5.2).

## Chapter 5 - Nutritional and developmental influences on carbon gain capacity

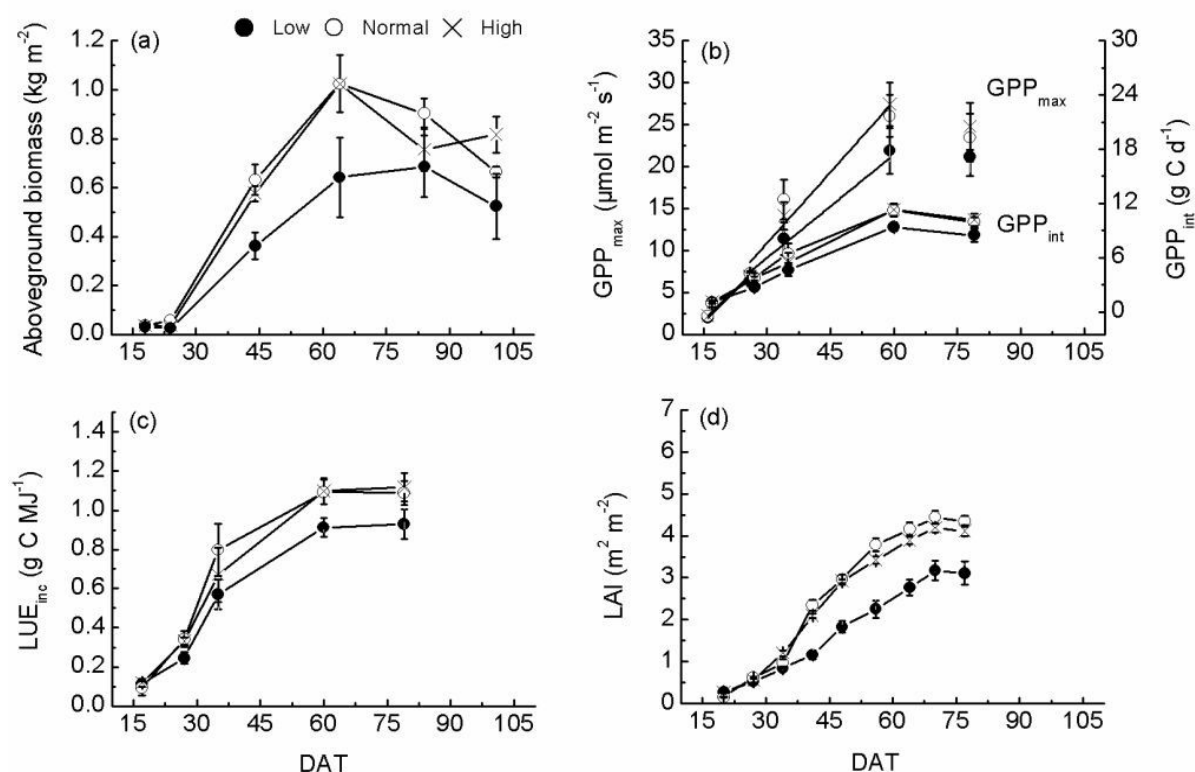


**Figure 5.2** Seasonal courses for aboveground biomass production, observed maximum rates in gross primary production ( $\text{GPP}_{\text{max}}$ ) during daily measurement cycles, integral daytime GPP ( $\text{GPP}_{\text{int}}$ ), canopy light use efficiency ( $\text{LUE}_{\text{inc}}$ ), and leaf area index for paddy rice grown at three levels of fertilization. Low = no fertilizer addition; normal =  $115 \text{ kg N ha}^{-1}$ ; high =  $180 \text{ kg N ha}^{-1}$  as described in the methods. Bars indicate S.E.;  $n = 2$  to  $12$ .

**Table 5.2** Leaf dry mass per planted bundle (g) and mean leaf laminar area ( $\text{cm}^2$ ) at different developmental stages and in different canopy layers in paddy rice grown at low ( $0 \text{ kg N ha}^{-1}$ ), normal ( $115 \text{ kg N ha}^{-1}$ ) and high ( $180 \text{ kg N ha}^{-1}$ ) fertilizer levels. S.E. is given in parentheses.

Growth stage	Nutrient treatment	Leaf dry mass per bundle (g)	Number of leaves per bundle	Mean leaf area in a given canopy height range ( $\text{cm}^2$ )			
Canopy height above ground				> 20 cm	45-60 cm	60-75 cm	75-90 cm
Early-elongation 43 DAT (184 DOY)	Low	2.1	57 (4)	22.1 (2.2)			
	Normal	3.1	101 (4)	29.4 (1.1)			
	High	3.4		26.9 (1.3)			
Mid-elongation 53 DAT (194 DOY)	Low	4.6 (0.5)			9.3 (0.6)	3.7 (0.9)	
	Normal	7.2 (1.1)			13.10 (0.8)	7.2 (0.8)	
	High	6.8 (0.4)			12.0 (0.8)	4.2 (1.0)	
Grain-filling 73 DAT (214 DOY)	Low	4.2 (0.4)			9.9 (1.0)	12.8 (1.4)	8.9 (1.0)
	Normal	8.7 (0.7)			13.8 (0.7)	13.4 (1.0)	9.6 (1.2)
	High	9.6 (1.1)			13.0 (0.6)	12.2 (0.9)	10.8 (1.4)

#### 5.4.2. Seasonal changes in leaf morphology and physiology in response to fertilizer treatments and canopy position

During the course of development, average SLA of top of canopy leaves decreased by approx. 33% (Figure 5.3a) but SLA values for sunlit leaves in the three fertilization groups were not significantly different ( $p > 0.05$ ). Despite this presumed increase in leaf thickness over the growing season, leaf nitrogen per unit area ( $N_a$ ) decreased strongly, by approx. 40% in all treatments (Figure 5.3a). The decrease occurred more rapidly during the elongation stage when the crop canopy was closing rapidly, than during the flowering and grain-filling stages. Although no significant differences in  $N_a$  between leaves of the normal and high fertilization treatments were observed over the entire growing season, leaf nitrogen in both was significantly greater than in the low fertilizer treatment during leaf elongation. No significant differences in  $N_a$  were observed between the three groups at grain-filling stage (after 60 DAT,  $p < 0.05$ ).

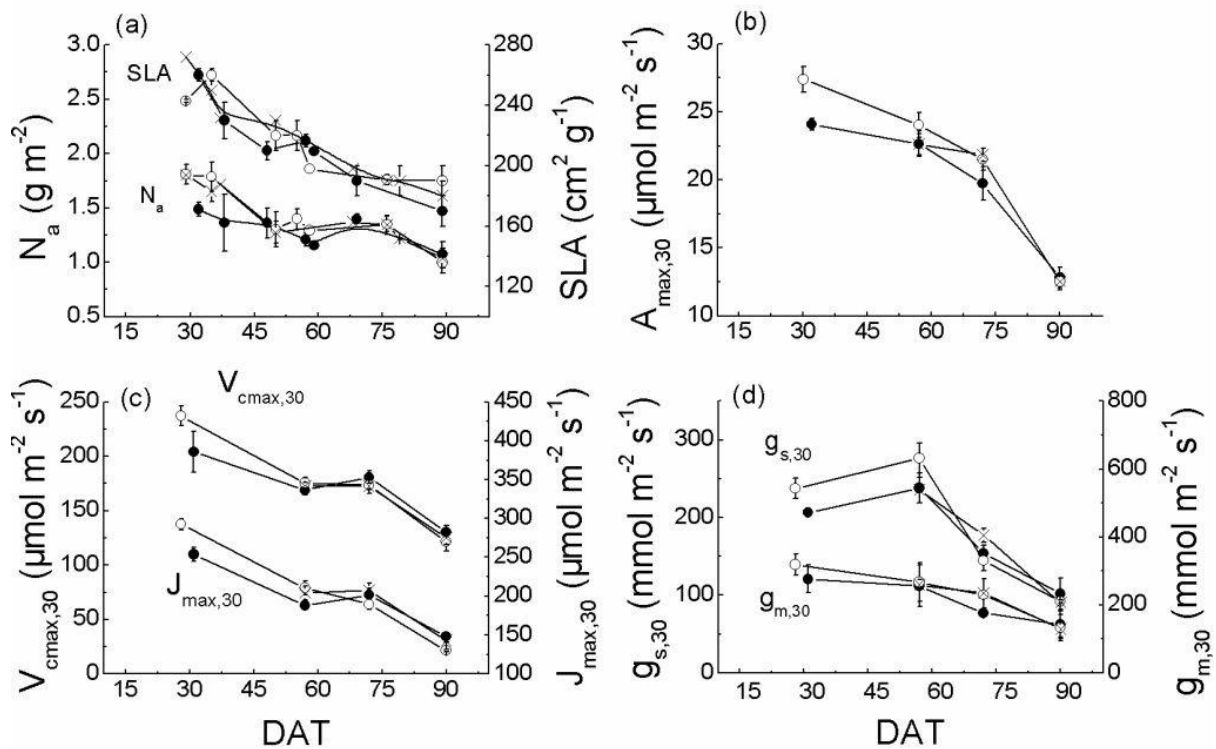


**Figure 5.3** Seasonal changes in sunlit mature leaves at top of canopy for leaf nitrogen content ( $N_a$ ), specific leaf area (SLA), photosynthesis capacity ( $A_{\text{max},30}$ ), and maximum Rubisco carboxylation rate ( $V_{\text{cmax},30}$ ), maximum electron transport rate ( $J_{\text{max},30}$ ), stomatal conductance ( $g_{\text{s},30}$ ), and mesophyll conductance ( $g_{\text{m},30}$ ) under the same environmental conditions. Bars indicate S.E.,  $n = 3$  to 6.

## Chapter 5 - Nutritional and developmental influences on carbon gain capacity

The seasonal decreases and differences among treatments in  $N_a$  were reflected in concurrent changes in photosynthetic activity, measured at saturating PAR and 30°C ( $A_{\max,30}$ ). Thus,  $A_{\max,30}$  was 14% lower in the low fertilization treatment during early growth ( $p = 0.02$ ; Figure 5.3b), but the differences were relatively small (~7%) during the grain-filling stage (ca. DAT 72). Carboxylation ( $V_{\max,30}$ ) and electron transport ( $J_{\max,30}$ ) capacities (Figure 5.3c) were greater in the normal and high fertilization treatments at tillering stage (prior to 60 DAT;  $p = 0.05$  and  $p = 0.04$ , respectively), consistent with observed differences in  $A_{\max}$  and  $N_a$ . Parallel decreases in mesophyll and stomatal conductance also occurred over the course of the season (Figure 5.3d), but differences among treatments were not apparent. The limitations on carbon gain due to mesophyll conductance ( $L_{gm}$ ) and stomatal conductance ( $L_{gs}$ ) were of similar magnitude in all treatments and did not differ significantly at comparable phenological stages (Table 5.3). As conductances decreased from the elongation stage to grain-filling stage, however, the limitations by both  $g_m$  and  $g_s$  increased dramatically, by between 22 and 49%. The total limitation of carbon gain due to transport from the external air to the site of fixation was substantial, ranging from 28 to 37%, with the highest value occurring in the low fertilization plants at the grain-filling stage, when the lowest leaf  $N_a$  was also observed.

Changes in leaf physiological function with depth in the canopy were investigated during the elongation and grain-filling stages (Figure 5.4). Leaf  $N_a$  decreased with depth in the canopy for all treatments during the elongation phase, but the decline was particularly pronounced in the low fertilization treatment (Figure 5.4a). Thus, significantly higher levels of  $N_a$  were observed in second and third leaves in the higher nitrogen treatments at the elongation stage (Figure 5.4a;  $p = 0.003$ ), which may be related to initial N investments during tillering (ca. 30 DAT) (cf. Figure 5.3a). During grain-filling, when canopy closure was more complete,  $N_a$  declined even more rapidly with depth in canopy, but the  $N_a$  profiles were similar ( $p > 0.05$ ) for all treatments (Figure 5.4b). In general, leaf nitrogen profiles were reflected in similar declines in physiological variables related to photosynthetic activity, such as  $A_{\max,30}$ ,  $V_{\max,30}$ ,  $J_{\max,30}$ ,  $g_{m,30}$ , and  $g_{s,30}$  (Figure 5.4c–f). Despite observed differences in  $N_a$  profiles during the elongation phase, canopy profiles of these physiological variables showed no striking treatment differences during either period of growth ( $p > 0.05$ ).

## Chapter 5 - Nutritional and developmental influences on carbon gain capacity

**Table 5.3** Comparisons among nutrient treatments in plant area index (PAI,  $\text{m}^2 \text{m}^{-2}$ ), leaf area index (LAI,  $\text{m}^2 \text{m}^{-2}$ ), daytime integral GPP ( $\text{GPP}_{\text{int}}$ ,  $\text{g C d}^{-1}$ ), average overall  $\text{CO}_2$  diffusive limitation ( $L_{\text{total}}$ , %), stomatal limitation ( $L_{\text{gs}}$ , %) and mesophyll limitation ( $L_{\text{gm}}$ , %), canopy light attenuation coefficient ( $K_l$ ), and canopy nitrogen attenuation coefficient at elongation (ca. 54) and grain-filling stages (ca. 73) at low ( $0 \text{ kg N ha}^{-1}$ ), normal ( $115 \text{ kg N ha}^{-1}$ ) and high ( $180 \text{ kg N ha}^{-1}$ ) fertilizer levels. Grain yields ( $\text{g m}^{-2}$ ) in three groups is indicated. S.E. is given in parentheses,  $n = 3$  to 6.

	Low		Normal		High	
	Elongation	Grain-filling	Elongation	Grain-filling	Elongation	Grain-filling
PAI	3.54 (0.66)	4.45 (0.53)	5.56 (0.50)	6.38 (0.51)	5.30 (0.55)	6.40 (0.69)
LAI	2.04 (0.17)	3.2 (0.23)	3.36 (0.13)	4.53 (0.16)	3.15 (0.07)	4.29 (0.13)
$\text{GPP}_{\text{int}}$	9.39 (0.48)	8.67 (0.70)	11.25 (0.25)	9.94 (0.55)	11.31 (0.68)	10.20 (0.65)
$L_{\text{total}}$	29.6 (4.1)	37.1 (5.1)	29.1 (5.5)	--	27.6 (3.2)	35.3 (4.8)
$L_{\text{gm}}$	16.9 (4.0)	24.3 (2.1)	15.6 (1.24)	--	16.1 (1.51)	24.2 (2.4)
$L_{\text{gs}}$	18.3 (1.16)	23.7 (3.7)	20.6 (5.4)	--	21.6 (1.31)	26.4 (2.6)
$K_l$	0.19 (0.04)	0.42 (0.04)	0.18 (0.03)	0.40 (0.05)	0.16 (0.04)	0.39 (0.04)
$K_N$	0.14 (0.02)	0.28 (0.02)	0.06 (0.005)	0.14 (0.01)	0.06 (0.01)	0.12 (0.01)
Yield	717 (110.5)		1135 (131.2)		1243 (22.94)	

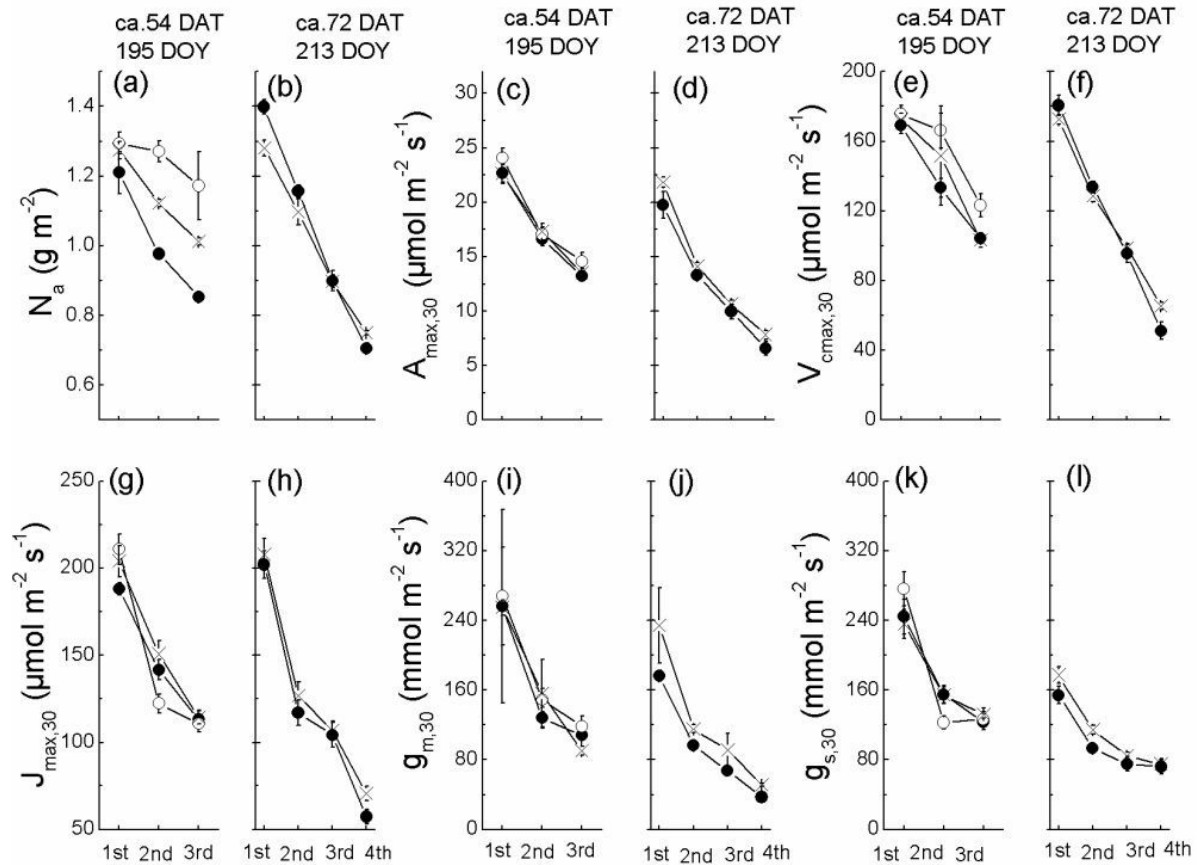


**Figure 5.4**

## Chapter 5 - Nutritional and developmental influences on carbon gain capacity

**Figure 5.4** Dependence on leaf position in crop canopy of paddy rice for leaf nitrogen content  $N_a$  (a, b), photosynthetic capacity  $A_{\max,30}$  (c, d), maximum Rubisco carboxylation rate  $V_{\max,30}$  (e, f), maximum electron transport rate  $J_{\max,30}$  (g, h), mesophyll conductance  $g_{m,30}$  (i, j), and stomatal conductance  $g_{s,30}$  (k, l) at elongation and grain-filling stages. Bars indicate S.E.,  $n = 3$  to 6.

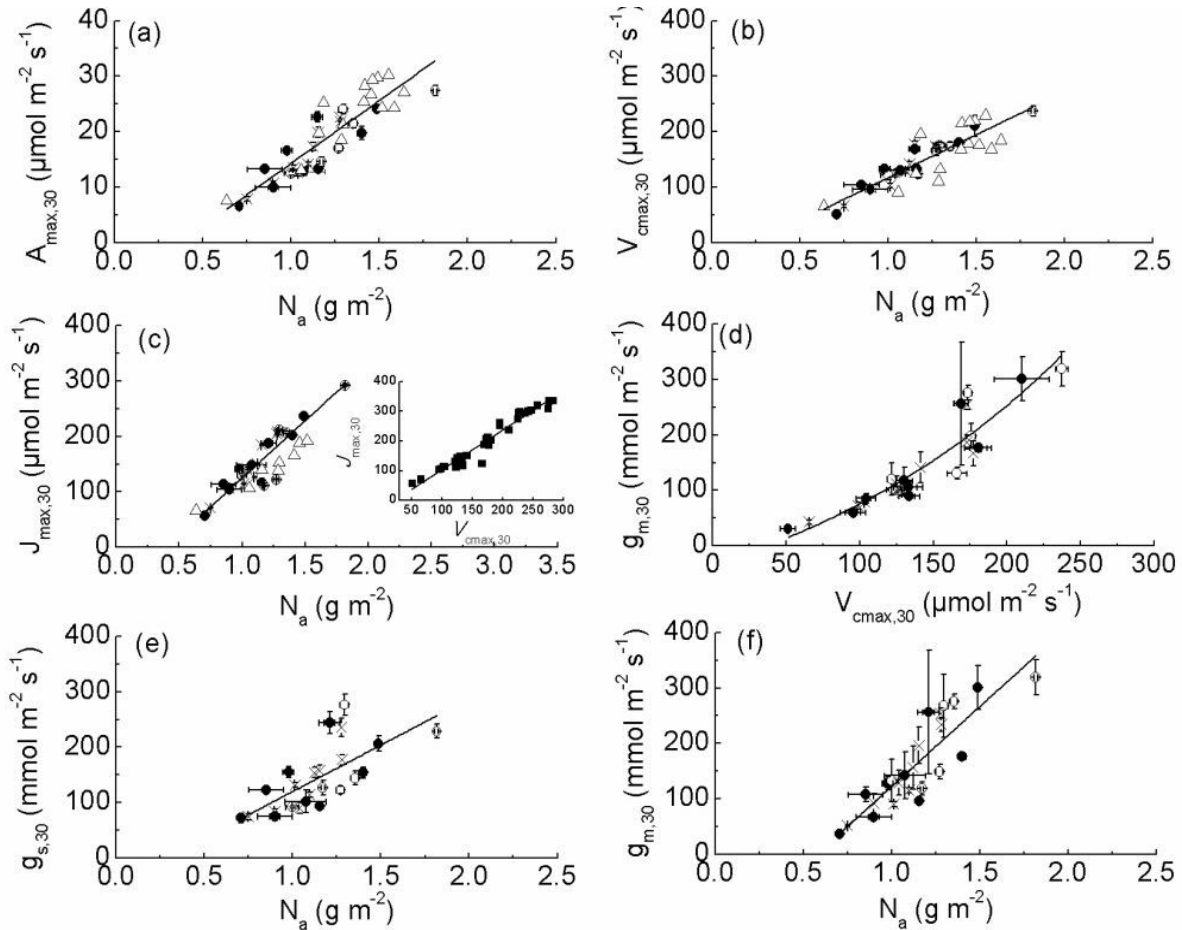


**Figure 5.5** (a) Dependence of photosynthetic capacity ( $A_{\max,30}$ ) on leaf nitrogen content ( $N_a$ ); (b) relationship of maximum carboxylation rate ( $V_{\max,30}$ ) to  $N_a$ ; (c) correlation between maximum electron transport rate ( $J_{\max,30}$ ) and  $N_a$ ; (d) correlation of mesophyll conductance ( $g_{m,30}$ ) and  $V_{\max,30}$ ; (e) stomatal conductance ( $g_{s,30}$ ) and  $N_a$ , and (f)  $g_{m,30}$  and  $N_a$  pooling data from both sunlit and within-canopy leaves grown in the field and from growth chamber experiments (open triangle). Inset in plot c indicated correlation between  $J_{\max,30}$  and  $V_{\max,30}$ .

The conservative nature of leaf function in dependence on  $N_a$  is shown in Figure 5.5. When measured data on leaf gas exchange traits were pooled across all treatments, a tight linear correlation between  $N_a$  and  $A_{\max,30}$  is evident ( $R^2 = 0.78$ ,  $p < 0.01$ ; Figure 5.5a). Reflecting the dependence of  $A_{\max}$  on Rubisco capacity and light harvesting, strong linear correlations between  $V_{\max,30}$  and  $N_a$ , and between  $J_{\max,30}$  and  $N_a$  were also found across all treatments ( $R^2$



## Chapter 5 - Nutritional and developmental influences on carbon gain capacity

$> 0.80$ ,  $p < 0.01$ ; Figure 5.5b, c).  $V_{\text{cmax},30}$  linearly scaled to  $J_{\text{max},30}$  with a constant ratio of 1.3, independent of growth environment (inset in Figure 5.5c). A strong but curvilinear relationship was observed between  $V_{\text{cmax},30}$  and  $g_{\text{m},30}$  ( $R^2 = 0.76$ ,  $p < 0.01$ ).  $V_{\text{cmax}}$  appears to be an important determinant of mesophyll conductance, although the curvilinearity suggests that some additional physiological factors play a role. Both  $g_{\text{m},30}$  ( $R^2 = 0.78$ ,  $p < 0.01$ ) and  $g_{\text{s},30}$  ( $R^2 = 0.47$ ,  $p < 0.01$ ) increased linearly with  $N_a$ , but the slope was significantly higher for  $g_{\text{m},30}$  (Figure 5.5e, f). As a result, we observed a negative correlation between  $N_a$  and ratio of  $g_{\text{s},30}$  to  $g_{\text{m},30}$  ( $R^2 = 0.61$ ,  $p < 0.001$ ) (Figure 5.6d).

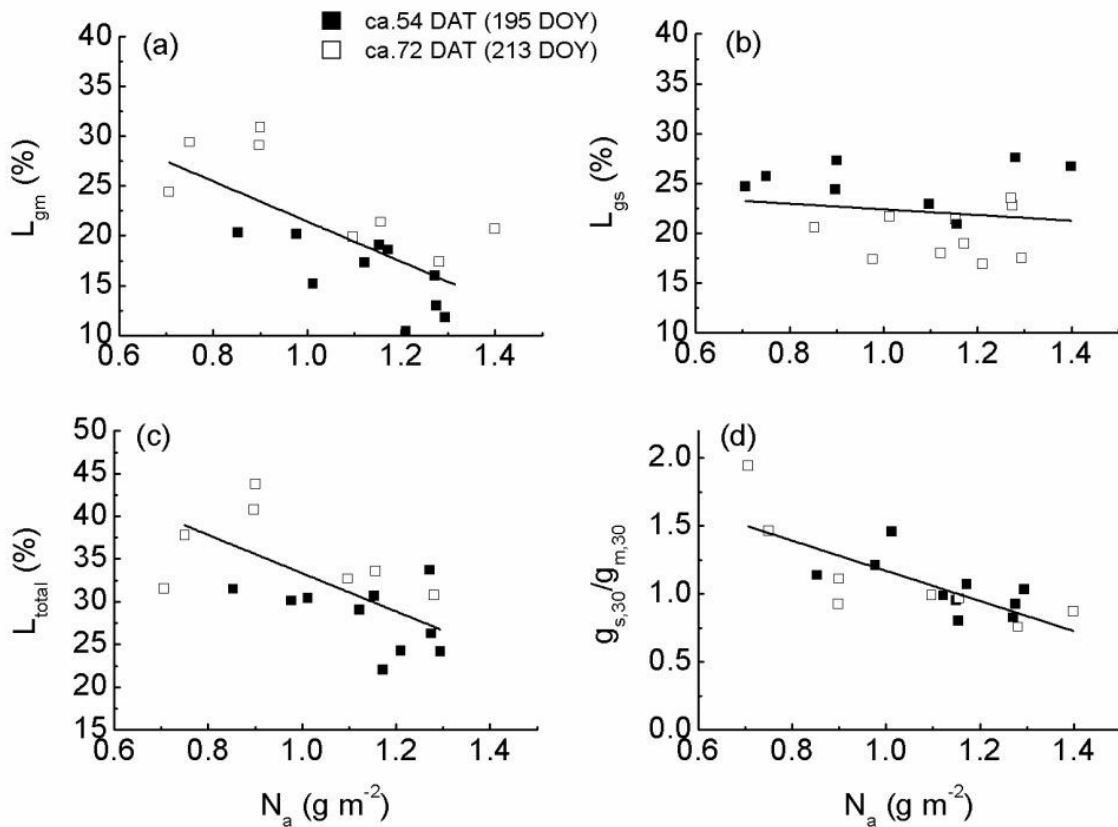


**Figure 5.6** Photosynthetic limitation by mesophyll conductance ( $L_{\text{gm}}$ ) and by stomatal limitation ( $L_{\text{gs}}$ ) in canopy profiles against leaf nitrogen content ( $N_a$ ) at the low, normal and high fertilization treatments in sunlit leaves during elongation and grain-filling stages.

There was a strong negative correlation between  $L_{\text{gm}}$  and  $N_a$  in canopy profiles (Figure 5.6a) ( $R^2 = 0.50$ ,  $p = 0.014$ ), but only a slight, non-significant ( $R^2 = 0.04$ ,  $p = 0.51$ ) decline in  $L_{\text{gs}}$  with increasing  $N_a$  (Figure 5.6b). Due to the  $N_a$  dependency of  $L_{\text{gm}}$ ,  $L_{\text{total}}$  also declined with increasing  $N_a$  ( $R^2 = 0.50$ ,  $p = 0.006$ ) (Figure 5.6c). The varying trend for mesophyll and stomatal limitation respectively corresponded to the  $\text{CO}_2$  drawdown i.e. concentration

## Chapter 5 - Nutritional and developmental influences on carbon gain capacity

gradient between leaf surface and intercellular airspace, between intercellular airspace and chloroplast carboxylation site, respectively (not shown).

### 5.4.3. Seasonal changes in canopy structure in responses to nutrient additions and effects on canopy LUE

$LUE_{inc}$  increases with increasing canopy LAI (Figure 5.7a) and the relationship applies to all fertilization treatments, but as canopy closure increases, the effect of additional increases in LAI lessens. The result is a hyperbolic response of  $LUE_{inc}$  to developing LAI which approaches a saturation value of ca.  $1.1 \text{ g C MJ}^{-1}$  at LAI values above  $3 \text{ m}^2 \text{ m}^{-2}$ . Differences among nutrient groups in light use efficiency on an absorbed radiation basis ( $LUE_{abs}$ ) during the active tillering ( $p = 0.46$  between low and normal group) and grain-filling stages ( $p = 0.49$  between low and normal group) were not statistically significant (Figure 5.7b). Overall,  $LUE_{abs}$  in all treatments increased after seedlings transplanting and approached observed maximum level  $3.2 \text{ g C MJ}^{-1}$  at the low group at the end of active tillering stage, after that decreased, which changes in parallel with leaf nitrogen content (Figure 5.3a).

Total LAI differed between treatments (Figure 5.2d) but there were also treatment differences in the vertical distribution of leaf area within the canopy. When leaf area in each of five canopy layers (each 15 cm thick) is expressed as a percentage of the total canopy leaf area (Figure 5.7c, d), it is clear that during both elongation and grain-filling stages, an increasing percentage of total leaf area is allocated to upper levels of the canopy as N fertilization is increased. A tight correlation between  $LUE_{inc}$  and total leaf N ( $N_{total}$ ) during both elongation and grain-filling stages were achieved. Fertilized plots had high  $LUE_{inc}$  accompanied by higher  $N_{total}$ . These differences must be related to enhanced LAI since leaf N values were similar or higher in the unfertilized group (Figure 5.4a, b). Thus, it seems that canopy leaf area development and allocation were important determinants of canopy carbon gain.

When  $LUE_{inc}$  for all treatments is plotted against the percentage of total leaf area which is found above 45 cm (termed as leaf area of upper canopy, LAUC), a linear relationship is

## Chapter 5 - Nutritional and developmental influences on carbon gain capacity

obtained at both elongation ( $R^2 = 0.84$ ,  $p = 0.056$ ) (Figure 5.7e) and grain-filling stages ( $R^2 = 0.99$ ,  $p = 0.002$ ) (Figure 5.7f). At elongation stage, enlargement of LAUC by 75% promoted  $LUE_{inc}$  up to 21%, and enhancement of  $LUE_{inc}$  during grain-filling stage was 23.1% compared to 32% enlargement of LAUC (Figure 5.7f). Similar linear relationship between  $LUE_{ins}$  and LAUC at elongation and grain-filling phases was evidenced, giving increment of  $LUE_{ins}$  by 19.5% and 25.7%, respectively for a 75% and 32% increase in LAUC (Figure 5.7e). At both development stages, increasing LAUC could be one growth strategy for the plant canopy to improve carbon gain, since there was a tight correlation between leaf nitrogen content on a mass basis and leaf LUE ( $R^2 = 0.62$ ;  $p < 0.01$ , data not shown). Another advantage due to enlargement of the upper canopy was that a higher proportion of leaf area was exposed to full sunlight, especially during midday (Figure 5.8c, d). Compared to the low nutrient group, over the course of the day, the total amount of sunlit leaf area of the upper canopy in the normal group was significantly larger, by 44%. To examine the effect of changing the vertical distribution of leaf area, we reversed the vertical distribution patterns found in the two fertilization treatments and recalculated sunlit leaf area (gray lines in Figure 5.8c, d) (i.e., the vertical distribution of leaf area in the low treatment (Figure 5.7d) was used to recalculate sunlit leaf area in the high nutrient treatment and vice versa.). This had the effect of reducing the difference in sunlit leaf area in the upper canopy between treatments to 20%. Likewise, increasing LAUC in the low fertilization treatment increased the amount of sunlit leaf area in the upper canopy by 22% (Figure 5.8d, grey lines). Importantly, allocating more leaf area to positions higher in the canopy where leaves contain more nitrogen (Figure 5.4a, b) would have the effect of allocating additional leaf nitrogen to canopy positions experiencing high light conditions and enhancing photosynthetic nitrogen use efficiency (Figure 5.8a).

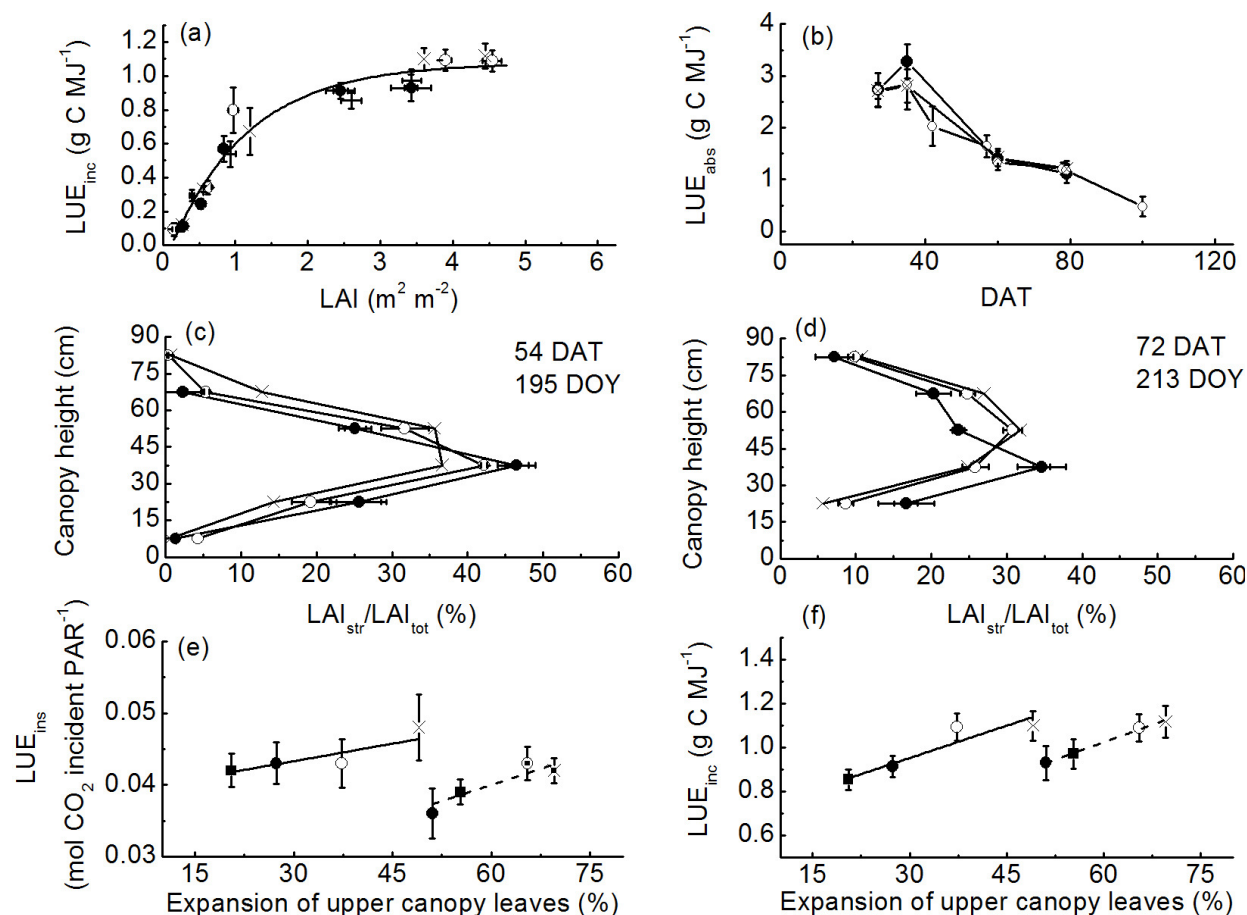


**Figure 5.7** Correlation between canopy light use efficiency ( $LUE_{inc}$ ) and leaf area index (a), seasonal development of  $LUE_{abs}$  (b), proportion of stratified leaf area height > 45 cm to total canopy area (c and d). Instantaneous canopy light use efficiency ( $LUE_{ins}$ ) and expansion of upper canopy leaves (based on plot c and d) (e), and  $LUE_{inc}$  and expansion of upper canopy leaves (f) during elongation (solid line) and grain-filling stage (dot line). Bars indicated S.E.,  $n = 3$  to 6.

## Chapter 5 - Nutritional and developmental influences on carbon gain capacity

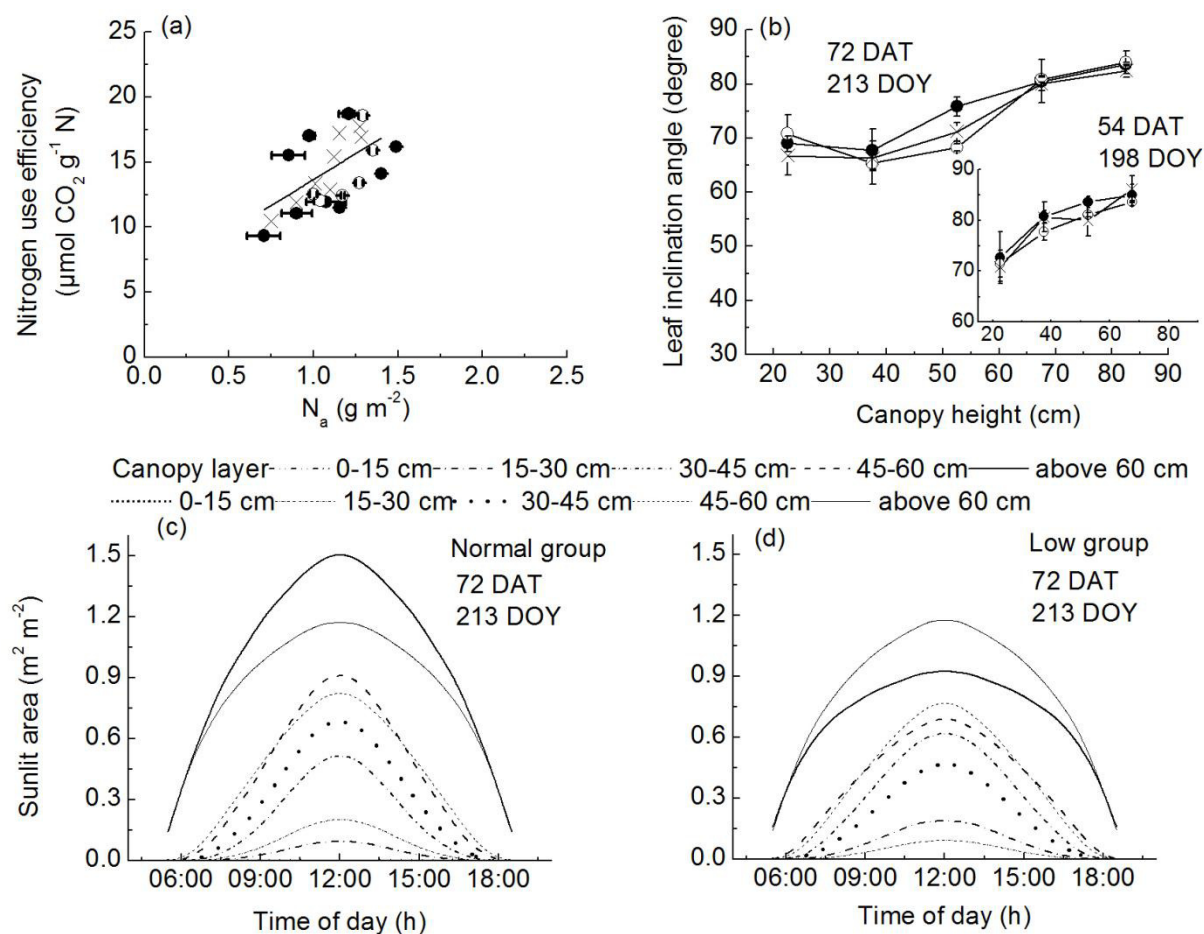


**Figure 5.8** (a) Correlation between nitrogen use efficiency and leaf nitrogen content per leaf area, and (b) leaf inclination angle comparisons in canopy positions at elongation and grain-filling stages. (c) and (d) Changes of sunlit leaf area at canopy layers from sunrise to sunset during grain-filling stage for low and normal groups using actual measured vertical leaf distributions (black lines) or using reversed leaf distributions (grey lines). Bars indicate S.E.,  $n = 3$  to 6.

### 5.5. Discussion

In this study, carried out in South Korea in the summer of 2013, paddy rice plants (*Oryza sativa* L. cv. Unkwang) were grown under three levels of nitrogen fertilization, and the effects of fertilization on biomass accumulation were investigated. Not surprisingly and corresponding to previous research (Yang et al., 2015), aboveground biomass accumulation in paddy rice fields responded positively to increased levels of fertilization, although the positive effects of increased nitrogen seemed to be saturated at levels of  $115 \text{ kg N ha}^{-1}$ , since addition of  $180 \text{ kg N ha}^{-1}$  led to no further increase in production (Figure 5.2a). 80% of the total fertilizer addition was applied two days prior to transplanting and the remaining 20%

## Chapter 5 - Nutritional and developmental influences on carbon gain capacity

was applied 19 DAT. Only slight aboveground biomass differences between treatments were observed throughout the tillering phase, which lasted until approximately 30 DAT. With the onset of the elongation growth phase following 30 DAT, however, aboveground biomass in the two treatments receiving supplemental N was greatly accelerated relative to the unfertilized plots. The productivity gap between fertilized and unfertilized plots continued to widen until peak biomass was reached at the end of the elongation stage (~64 DAT), at which time aboveground biomass in the two fertilized treatments was approximately 60% greater than in the plots receiving no supplemental nitrogen. Following peak biomass, aboveground biomass in the fertilized plots declined more rapidly through flowering and grain-filling stages than in the unfertilized plots, and at 100 DAT the advantage in the fertilized plots had fallen to approximately 40%. Similar to biomass accumulation, there was only a small discrepancy in grain yield between the normal and high groups, but they produced 58% and 73% more grain, respectively, than the low fertilization treatment.

In general, during tillering, plots in all nutrient treatments exhibited low  $GPP_{max}$  and  $GPP_{int}$ , both of which rapidly increased after ~32 DAT, reaching a peak at the end of the reproductive stage and then declining until the end of ripening stage or at harvest (Figure 5.2b). Following tillering (after 32 DAT) ample fertilization management significantly promoted  $GPP_{max}$  and biomass production relative to unfertilized plots, and the  $GPP_{max}$  advantage of fertilized plots continued to increase throughout the elongation stage. Observed  $GPP_{max}$  values in our research (21.4 to 27.4  $\mu\text{mol m}^{-2} \text{s}^{-1}$ ) were compatible with reports of  $21.8 \pm 3.7 \mu\text{mol m}^{-2} \text{s}^{-1}$  in South Korea (Lindner et al., 2015). The integrated GPP ( $GPP_{int}$ ) under normal field management in our study (9.9 to 11.3  $\text{g m}^{-2} \text{d}^{-1}$ ; Table 5.3) fell within the reported range of Asia traditional paddy system 10.36 to 15.2  $\text{g m}^{-2} \text{d}^{-1}$  (Alberto et al., 2012; Miyata et al., 2000; Lee, 2015). Reported variability in carbon gain capacity of paddy rice can probably be ascribed to ecological conditions where rice was planted such as field management practice and fertilizer application rate, and also to endogenous variations in the rice genotypes selected.

## Chapter 5 - Nutritional and developmental influences on carbon gain capacity

We sought to determine the mechanistic basis for the observed productivity enhancement with supplemental fertilization. Crop productivity is largely determined by the amount of solar radiation intercepted by the canopy and the efficiency with which that absorbed energy is converted to carbohydrates in the process of photosynthesis (Monteith, 1972; Goward and Huemmrich, 1992; Inoue et al., 2008). This notion has been formalized in the concept of light utilization efficiency, which in the context of crop production, has been defined as carbon uptake divided by irradiance, both integrated over some period of time. As pointed out by Gitelson and Gamon (2015), carbon uptake can be variously defined as net photosynthesis, gross or net primary production, and irradiance as incident or absorbed PAR.  $LUE_{inc}$  is defined here as daily GPP ( $g\ C\ m^{-2}\ ground$ ) integrated over the daylight hours, divided by incident PAR (MJ), integrated over the same period.

$LUE_{inc}$  was measured five times during the growing season (Figure 5.2c) and increased rapidly in all treatments as canopy leaf area increased during the tillering and elongation stages of development, then leveled off as the canopy approached full closure. Beginning during tillering,  $LUE_{inc}$  in the fertilized plots exceeded that in the unfertilized treatment by 20-30%, a differential that persisted into the flowering and grain-filling stages. Research in soybean reported maximum  $LUE_{inc}$  of  $1.2\ g\ C\ MJ^{-1}$  (Gitelson and Gamon, 2015) and approximately  $1.0\ g\ C\ MJ^{-1}$  in rice (Atwell et al., 1999), which are similar to our values in this rice study ( $1.12\ g\ C\ MJ^{-1}$  for fertilized and  $0.92\ g\ C\ MJ^{-1}$  for unfertilized plots).

$LUE_{inc}$  is a representative reflection of crop ecophysiology responding to varying growth environment, and is influenced by multiple factors such as leaf area development, canopy light interception, light conversion efficiency, and leaf photosynthetic physiology associated with nitrogen investment in leaves and diffusional limitations. We will examine each of these factors that contribute to  $LUE_{inc}$  to better understand how fertilized rice plants utilize supplemental N to enhance their growth rates and biomass accumulation.

## Chapter 5 - Nutritional and developmental influences on carbon gain capacity

### 5.5.1. The role of leaf photosynthetic capacity in determining $LUE_{inc}$

Enhanced nitrogen supplied through supplemental fertilization, if allocated to individual leaves, might be expected to increase net photosynthetic rates by increasing the amounts of rate limiting enzymes. The importance of  $N_a$  in establishing photosynthetic performance is highlighted by data in Figure 5.5.  $A_{max}$ , across all fertilization treatments and over the course of the season, is a linear function of  $N_a$  (Figure 5.5a) as often reported previously (Yoshida 1981; Campbell et al., 2001a; Niinemets, 2007). Furthermore, as reported by Evans and Loreto (2000) and Bernacchi et al. (2002) the primary determinants of photosynthetic competence,  $V_{cmax}$  and  $J_{max}$ , are also linearly related by  $N_a$  (Figure 5.5b, c), resulting in a strong linear relationship between the two (Figure 5.5c, inset) with a slope 1.3 that falls within the range reported for a variety of  $C_3$  species (Niinemets et al., 2009a; Wullschlegel, 1993). This linear relationship between  $N_a$  and photosynthetic components is explained by the importance of nitrogen in determining amounts of rate-limiting enzymes in the Calvin cycle (especially Rubisco) and the electron transport chain. Both stomatal and mesophyll conductances also increase linearly with  $N_a$  (Figure 5.5e, f) but a mechanistic basis for this dependency is less obvious; however, it reveals the high degree of coordination between leaf biochemistry and diffusional limitations, which forms the basis of, for example, the empirical model of stomatal conductance developed by Ball et al. (1987). One of the consequences of this coordination between  $g_s$  and  $A_{max}$  is to maintain values of  $C_i$  across all treatment within a fairly narrow range (240 to 260  $\mu\text{mol mol}^{-1}$ ).

Clear treatment differences are apparent in the allocation of available nitrogen to photosynthetic processes early in the growing season. During tillering stage,  $N_a$  in the normal and high fertilization treatment was approx. 32% higher than in the low treatment (Figure 5.3a).  $N_a$  subsequently declined in all treatments, but the decline was particularly pronounced in fertilized plots, such that treatment differences in  $N_a$  narrowed, and by 47 DAT, midway through the elongation phase, significant differences were no longer apparent.

These differences in leaf nitrogen were reflected in photosynthetic performance at the



## Chapter 5 - Nutritional and developmental influences on carbon gain capacity

individual leaf level. Light-saturated net photosynthesis at 30°C ( $A_{\max,30}$ ) of upper canopy leaves was approximately 16% greater in fertilized plots during tillering, but as  $N_a$  declined through the growing season, treatment differences in  $A_{\max,30}$  were greatly reduced (Figure 5.3b). Similarly, higher rates of both  $V_{\max,30}$  and  $J_{\max,30}$  (Figure 5.3c) observed in fertilized treatments during tillering were largely eliminated during later growth stages as  $N_a$  declined more rapidly in fertilized than unfertilized plots.

Figure 5.4 illustrates profiles through the canopy of  $N_a$  and photosynthetic parameters during the elongation and grain-filling developmental stages. During elongation, plants in fertilized plots clearly allocated more nitrogen to within canopy leaves than plants in the unfertilized treatment (Figure 5.4a) but, surprisingly, these differences were not reflected in parallel changes in  $A_{\max,30}$  (Figure 5.4c) with depth in the canopy.  $V_{\max,30}$  values of lower canopy leaves were less in plants without supplemental fertilizer, reflecting lower  $N_a$ , but  $J_{\max,30}$  values did not differ at this stage between treatments. The absence of a nitrogen effect on  $A_{\max,30}$  may therefore reflect the fact that within-canopy leaves were operating on the RuBP-regeneration portion of the A-C<sub>i</sub> response curve (Bernacchi et al., 2002; Yamori et al., 2011), where reductions in  $V_{\max,30}$  would not be reflected in the photosynthesis measurement. Lower canopy leaves, in which photosynthesis is often light-limited, would benefit from preferentially allocating limiting nitrogen to light-harvesting proteins (i.e.,  $J_{\max,30}$ ) at the expense of Rubisco ( $V_{\max,30}$ ). Later in the season, during grain-filling, canopy profiles of  $N_a$  and photosynthetic parameters were largely indistinguishable across treatments (Figure 5.4b, d, f, h, j).

Canopy area development and the total amount of free nitrogen content have been considered limiting factors in mediating canopy carbon gain (Leuning et al., 1995). Establishing a dynamic balance between reduced canopy area and sufficiently high nitrogen invested in leaves is a survival strategy under limited nitrogen conditions (Anten, 1995; Niinemets, 2007). Consistent with this, rice plants in the low fertilization group were able to maintain leaf nitrogen levels, especially in uppermost leaves, comparable to leaves in plants with

## Chapter 5 - Nutritional and developmental influences on carbon gain capacity

supplemental nitrogen (Figure 5.3a; Figure 5.4a, b), but only by limiting the development of total canopy leaf area (Figure 5.2d). This nitrogen allocation strategy explains the narrowed difference in leaf N among nutrient groups in the elongation and grain-filling stages.

Independent of leaf biochemistry, CO<sub>2</sub> diffusion resistance in leaves, both stomatal and in the mesophyll, can significantly constrain carbon fixation by reducing the CO<sub>2</sub> partial pressure at the site of fixation. As mentioned above, as photosynthetic capacity increased with increasing N<sub>a</sub>, the total limitation imposed by diffusional constraints declines (Figure 5.6c). A comparison of Figs. 5e and 5f indicates that g<sub>m</sub> increases more rapidly with increasing N<sub>a</sub> than does g<sub>s</sub>, such that the ratio of the two (g<sub>s,30</sub>:g<sub>m,30</sub>) declines (Figure 5.6d). Thus, the relative importance of g<sub>m</sub> in limiting net photosynthesis declines with increasing nitrogen and stomatal limitations becomes increasingly significant. The percent limitation imposed by stomata is somewhat scattered, varying between 17 and 27%, but shows no clear dependence on N<sub>a</sub> (Figure 5.6b), while mesophyll limitations clearly become less pronounced as N<sub>a</sub> increase (Fig 6a), which was also previously reported (Monti et al., 2009; Tosens et al., 2012). Thus, diffusional limitations, particularly those imposed by the mesophyll, became more important as the growing season advanced and leaf nitrogen declined. Although diffusional limitations increased through the growing season, and represented a significant limitation (up to almost 45%) during grain-filling, there were no clear treatment differences in either mesophyll or stomatal limitations (Table 5.3).

In summary, large treatment differences in leaf photosynthetic physiology were apparent only in the early stages of development. Plants in the unfertilized paddies were generally able to maintain leaf nitrogen levels and photosynthetic capacities comparable to fertilized plants, but only at the expense of reduced canopy leaf area, discussed below.

### 5.5.2. Differences in seasonal canopy development between fertilization treatments

In addition to leaf photosynthetic properties that help determine LUE<sub>inc</sub> through their role in controlling GPP<sub>max</sub> and GPP<sub>int</sub>, LUE<sub>inc</sub> also depends strongly on the amount of light absorbed

## Chapter 5 - Nutritional and developmental influences on carbon gain capacity

by the canopy, which depends on LAI (Leuning et al., 1995) and to a lesser extent, leaf angle distribution and leaf clumping.

In the first few weeks after transplanting, canopy development was slow, but by the beginning of the leaf elongation stage of development (ca. 30 DAT) canopy leaf area in the fertilized treatment had clearly accelerated relative to that in unfertilized plots, and this LAI advantage was maintained through flowering and grain-filling (Figure 5.2d). As a result, on any given day, fertilized canopies were able to absorb significantly more above-canopy PAR than unfertilized plots throughout the leaf elongation, flowering and grain-filling stages. Since GPP is strongly influenced by absorbed PAR, seasonal changes in both  $GPP_{max}$  and  $GPP_{int}$  (Figure 5.2b) paralleled changes in LAI (Figure 5.2b), increasing rapidly through the elongation phase and then leveling off during flowering and grain-filling. Inasmuch as  $LUE_{inc}$  is driven primarily by  $GPP_{int}$ , it is not surprising that  $LUE_{inc}$  differences between fertilization treatments also persisted throughout the growing season (Figure 5.2c).

Treatment differences in LAI, PAI and light absorption coefficients at two different growth stages are apparent in Figure 5.1 and Figure 5.7. During elongation (ca. 54 DAT)  $K_L$  values were similar across all treatments, while both LAI and PAI were approximately 50% greater in the fertilized plots than in the unfertilized treatment. The percentage of incoming PAR absorbed by canopies in each treatment was calculated using Eq. 4 and PAI and  $K_L$  values from Table 5.3, and the unfertilized plots absorbed 44% of incoming PAR, significantly less than the normal or high nutrient plots (59% and 55%, respectively). High canopy light interception in fertilization group was directly documented by canopy reflectance NDVI which exponentially correlates to absorption of PAR by canopy (Figure 5.1a). Field measurement of light interception across three nutrient groups corresponded well to canopy level spectrum reflectance, meaning NDVI could be one powerful biophysical index to reflect variation of canopy light interception due to soil nutrient availability. The observed lower canopy light interception ratio in the low treatment was actually ascribed primarily to lower canopy leaf area. Three weeks later, in the grain-filling stage (ca. 74 DAT), when all canopies

## Chapter 5 - Nutritional and developmental influences on carbon gain capacity

were further developed,  $K_L$  values were much larger, and  $K_L$  in the unfertilized plots was comparable to the normal or high nutrient treatments, perhaps reflected in similarities in leaf angle distributions (Figure 5.8b).  $K_L$  measured during grain-filling stage fell in the range of 0.2–0.3 for erect canopy and 0.6–0.8 for prostrate canopy in rice (Sheehy and Mitchell, 2013), and favorably conformed to reports in two cultivars Nipponbare and Chugoku 117 with 0.24 and 0.5 at elongation and grain-filling stage, respectively (Saitoh et al., 2002) and 0.4 at end of elongation stage (Lee et al., 2006). Research in crops indicates that leaves in the upper part of the canopy tend to be more erect, with high leaf inclination angle, while lower positioned leaves tend to be displayed more horizontally in order to intercept transmitted light more efficiently (Anten et al., 1995). During the measuring seasons, averaged leaf angle distributions at each layer were similar among nutrient groups (Figure 5.8b), which might relate to similar light attenuation coefficient (Table 5.3), since variation in  $K_L$  value is commonly associated with leaf angle (Atwell et al., 1999; Sheehy and Mitchell, 2013). Compared to elongation stage, plants during grain-filling had significantly higher LAI, PAI and light extinction coefficients and thus absorbed a much higher fraction of incident PAR than earlier. Although PAR absorption by fertilized plots (92% and 91% in normal and high treatments, respectively) remained higher than in the unfertilized paddies (85%), treatment differences had clearly narrowed compared to earlier growth phases. The greatest benefit arising from increased nitrogen availability is the burst in productivity early in the elongation stage that stimulates rapid canopy development and increasing LAI (Figure 5.2d). Thus, development of aboveground biomass is accelerated in fertilized plots, enabling them to maintain their LAI advantage throughout development. This leads to greater PAR absorption in fertilized plots, enhancing both  $GPP_{int}$  and  $LUE_{inc}$ . Thus,  $GPP_{max}$  increased rapidly between DAT 30–60 (Figure 5.2b) despite the fact that  $A_{max}$  (net assimilation at the leaf scale) and  $LUE_{abs}$  both were already declining (Figure 5.3b; Figure 5.7b), implying that the observed increase in GPP is not a result of improved photosynthesis at the leaf level, but rather it is due to increased PAR absorption.

Light use efficiency based on absorbed light by canopy ( $LUE_{abs}$ ) across three nutrient groups

## Chapter 5 - Nutritional and developmental influences on carbon gain capacity

were not constant over growing season, with higher level at active tillering phase and lowering level going on after that stage. Light use efficiency might not be constant and change as crop species develop (Alberto et al., 2013; Gimenez et al., 1994), with a maximum existing during vegetative stage and lower at early and late seasons in crops (Hall et al., 1995). Our reports favorably compared to theirs.  $LUE_{abs}$  of post-anthesis of spikelet fluctuated in a range from 0.73 to 1.22 g C MJ<sup>-1</sup> and that of elongation growth between 1.52 and 2.1 g C MJ<sup>-1</sup> (Campbell et al., 2001b). Similar seasonal tendency was also reported in paddy rice by Inoue et al. (2008).  $LUE_{abs}$  of grain-filling plants in our research ranged within their reports, while relatively high levels at elongation stage in our research were observed. Large fluctuations in seasonal  $LUE_{abs}$  in fast-growing rice crop are within our anticipation, since crop physiology and resource use strategy change significantly within short time period especially growth stage transit from active tillering to elongation and flowering stage (Figure 5.2). Variations in GPP (product of  $LUE_{abs}$  and intercepted PAR) can not be solely interpreted by either  $LUE_{abs}$  or intercepted light. Decline in  $LUE_{abs}$  partially interpret phenomena of GPP saturation at higher LAI that decline of  $LUE_{abs}$  might counteract benefits gained from increasing canopy light interception.

In addition to allocating more resources to leaf area development, plants in the fertilized treatments also produced a higher percentage of the leaves in the upper layers of the canopy during both elongation and grain-filling stages (Figure 5.7c, d). Recent research reported potential enhancement of carbon gain capacity arising from the enlargement of mid-upper canopy leaves in cucumber (Chen et al., 2014). In our study, in all treatments at the elongation stage, the canopy layer with the highest amount of leaf area was the 15-cm thick layer centered at 37.5 cm height. In the low nutrient treatment, leaf area distribution was symmetrical, with approximately 26.9% of leaf area displayed in lower canopy layers, below 30 cm height, and 27.2% in layers above 45 cm. In fertilized plots, leaf area distribution was skewed towards upper layers, with 38.9% above 45 cm and only 15.0% below 30 cm in the normal nutrient plots, while in the high fertilization treatment the values were 37.2% and 23.4% in the upper and lower portions of the canopy, respectively. Later, during grain-filling,

## Chapter 5 - Nutritional and developmental influences on carbon gain capacity

as canopy height increases, differences were maintained as only 27.4% of leaf area in low N plots was found above 60 cm height while 50.2% occurred below 45 cm. Corresponding numbers for the normal treatment were 34.7% and 30.4% and for the high fertilization treatment, 37.6% and 33.4%.

Positioning a higher percentage of leaf area in upper layers of the canopy exposes a greater amount of leaf area in fertilized plants to full sunlight conditions. This effect can be seen in Figure 5.8c, d which presents modeling results using the multi-layer light interception model of Caldwell et al. (1986) comparing the amount of sunlit leaf area in low and normal fertilization plots during grain-filling, and examines the effect of vertical leaf distribution. Total light absorption by the fertilized canopies was about 7% higher (92% in normal vs. 85% in low) but it is clear that far more leaf area is potentially exposed to sunlit conditions in the normal fertilization plots. Most of this difference is clearly the result of higher total leaf area, but we used the model to investigate the effect of altering the vertical leaf distribution. When the sunlit leaf area of the normal fertilization canopy was re-calculated using the vertical leaf distribution associated with the low nutrient canopy, the total amount of sunlit leaf area was unchanged, but more of the sunlit area was located in the lower canopy layers. When the leaf distribution of the normal canopy was used to re-calculate sunlit leaf area in the low fertilization canopy, the reverse was true. Depending on the vertical distribution of leaf nitrogen, discussed below, these shifts in the vertical distribution of sunlit leaves could have implications for canopy carbon uptake. Since there is a steep gradient in  $N_a$  (and photosynthetic capacity) within rice canopies (Figure 5.4) the ability of fertilized rice plants to display more sunlit leaves in upper canopy layers, where leaves have higher leaf nitrogen and photosynthetic capacity, should provide an additional advantage to rice in fertilized paddies. Because there is a significant amount of residual nitrogen (i.e., nitrogen allocated to non-photosynthetic processes, x-intercept in Figure 5.5a) leaf nitrogen use efficiency ( $\mu\text{mol CO}_2 \text{ g}^{-1} \text{ N}$ ) increases with increasing  $N_a$  (Figure 5.8a) particularly when incident PAR is high, as in upper canopy leaves. Similarly, leaf LUE also increases with increasing leaf nitrogen (data not shown), providing an additional advantage to displaying more leaf area in upper

## Chapter 5 - Nutritional and developmental influences on carbon gain capacity

layers of the canopy. The linear correlations found between the percentage of leaf area in the upper canopy and both  $LUE_{ins}$  (Figure 5.7e), and  $LUE_{inc}$  (Figure 5.7f) supported promising role of deployment of leaf area allocation in crop canopies to optimally adjust gross carbon fixation.

### 5.5.3. Promoted canopy leaf area by fertilization depends on leaf number per bundle and relates to nitrogen-facilitated photosynthesis occurring initially

Differences in the rate of canopy leaf area development appear to be a key component in determining treatment differences in GPP and  $LUE_{inc}$ . It appears that supplemental nitrogen supplied during tillering enhances leaf nitrogen concentrations in early emerging leaves (Figure 5.3a), which manifests itself in higher amounts of photosynthetic enzymes (Figure 5.3c) and higher rates of light-saturated photosynthesis (Figure 5.3b). It appears that the initial photosynthetic advantage enjoyed by fertilized plants provides an initial burst of biomass production that is allocated to rapid production of new leaves. As shown in Table 5.2, relatively early in the elongation phase (DAT 43), the mean number of leaves per planted bundle (five plants) in the normal fertilization treatment (101) is 75% greater than in unfertilized paddies (57). This difference is also reflected in the mean leaf biomass per bundle, which was 50% higher in the normally fertilized treatment than in the unfertilized plots, and 60% higher in the high nitrogen treatment. A comparative study in the first year of growth of eight perennial grasses observed that plants under nutrient-rich habitat had higher SLA (Elberse and Berendse, 1993), which increases the above ground LAI significantly (Knops and Reinhart, 2000). In our study there were no clear differences in leaf SLA among the three nutrient treatments (Figure 5.3a) or in canopy level SLA (not shown). Higher leaf area in fertilized paddies therefore mainly resulted from increased leaf numbers per planted bundle (Table 5.2), dramatically promoted by fertilization, rather than treatment differences in leaf thickness or morphology. This early advantage in leaf number and canopy leaf area development stimulated  $GPP_{int}$  and  $LUE_{inc}$  (Figure 5.7b) and allowed the fertilized plots to maintain their LAI advantage for the remainder of the growing season, despite having leaf photosynthetic characteristics similar to unfertilized paddies.

## Chapter 5 - Nutritional and developmental influences on carbon gain capacity

Very large gradients of light intensity exist within plant canopies, with light attenuation as large as 90% in bottom layers especially in dense canopies (Rosenberg et al., 1983). In our study, maximum light attenuation of 92% was observed late in the season, during grain-filling, in the normal fertilization plots. Research in several crop species has demonstrated that light distribution is commonly coupled to nitrogen patterns within canopies (Hirose and Werger, 1987), and that nitrogen extinction coefficients are higher under conditions of low N supply (Milroy et al., 2001; Moreau et al., 2012). In our study, higher values of  $K_N$  in the low nutrient group at both elongation and grain-filling stages were evident (Table 5.3), in agreement with previous reports. Leaf nitrogen distribution at the grain-filling stage was less uniform (i.e., higher  $K_N$ ) than during leaf elongation in all nutrient treatments, which parallels seasonal changes in light extinction ( $K_l$ ). Thus, nitrogen allocation patterns as the canopy developed reflected increasing light gradients.

### 5.6. Conclusion

Sustainable rice production system is treated as capable of producing high yield production with less nitrogen and water resource consumption and minimized impacts on environment sustainability. A sustainable rice production system is currently challenging by critical global environmental problems caused by surplus fertilizer application and greenhouse gas emission. Harvest high biomass production from this fast-growing crop coincident with environmental protection needs a priori establishment of fundamental knowledge with respect to plant growth, regulation and adaption to anthropogenic intervention. Biomass accumulation by plant is a direct result of photosynthesis which could be stimulated by soil nitrogen addition. Disentangling ecophysiological mechanisms influencing regulations of rice plant growth and carbon fluxes is still open area need to fill in. In this research, we attempt to understand ecophysiological traits that relate to plant efficient carbon gain, and to determine important factors need to be concerned in sustainable rice production system.

During active tillering stage, fertilization manipulations enhanced leaf N content and



## **Chapter 5 - Nutritional and developmental influences on carbon gain capacity**

consequently contributed to higher photosynthesis rates, presumably due to significantly higher rate-limiting photosynthetic proteins. An important consequence of greater assimilation rates was the more rapid production of new leaves, resulting in higher leaf number per planted bundle and head start in canopy area size which is a promising resource use strategy to maximize canopy light interception and thereby plant carbon gain capacity and biomass accumulation. Rapid increase in GPP dismissed and approached saturation when canopy was closing intensively, even though more light could be intercepted. DPP saturation at higher LAI could be partially explained by continuous decline of light use efficiency after active tillering stage. Whereas, allocate more leaves at upper part of canopy is seeming to be promising growth strategy to enhance carbon gain, since more leaves are exposed to full sunlight environment and those leaves assemble more nitrogen concentration with lowering CO<sub>2</sub> diffusion resistance. We suggest that basic knowledge of coordinated adjustments between structure and leaf physiology should be in concert in sustainable rice production system.

### **5.7. Acknowledgments**

This study was carried out as part of the International Research Training Group TERRECO (GRK 1565/1) funded by the Deutsche Forschungsgemeinschaft (DFG) at the University of Bayreuth, Germany and the Korean Research Foundation (KRF) at Kangwon National University, Chuncheon, S. Korea. We thank the agricultural logistics group of CNU for the field management and for the rice seedling cultivation in the nursery. W. Xue thanks financial support from the program of China Scholarships Council (CSC No. 201204910156). We do acknowledge the helps in the field by Seung Hyun Jo, Toncheng Fu, Fabian Fischer, Nikolas Lichtenwald and Yannic Ege. We gratefully acknowledge the technical assistance of Ms. Margarete Wartinger and Ms. Ilse Thaufelder for all their support in the field and laboratory.

### **5.8. References**

Adachi, S., Nakae, T., Uchida, M., Soda, K., Takai, T., Oi, T., Yamamoto, T., Ookawa,

## Chapter 5 - Nutritional and developmental influences on carbon gain capacity

- T., Miyake H., Yano M., and Hirasawa T. 2013. The mesophyll anatomy enhancing CO<sub>2</sub> diffusion is a key trait for improving rice photosynthesis. *Journal of Experimental Botany*, 64, 1061–1072.
- Alberto, M.C.R., Hirano, T., Miyata, A., Wassmann, R., Kumar, A., Padre, A. and Amante, M. 2012. Influence of climate variability on seasonal and interannual variations of ecosystem CO<sub>2</sub> exchange in flooded and non-flooded rice fields in the Philippines. *Field Crops Research*, 134, 80–94.
- Alberto, M.C.R., Buresh, R.J., Hirano, T., Miyata, A., Wassmann, R., Quilty, J.R., Correa, T.Q. and Sandro, J. 2013. Carbon uptake and water productivity for dry-seeded rice and hybrid maize grown with overhead sprinkler irrigation. *Field Crops Research*, 146, 51–65.
- Anten, N.P.R., Schieving, F. and Werger, M.J.A. 1995. Patterns of light and nitrogen distribution in relation to whole canopy carbon gain in C<sub>3</sub> and C<sub>4</sub> mono- and dicotyledonous species. *Oecologia*, 101, 504–513.
- Atwell, B.J., Kriedemann, P.E., Turnbull, C.G.N. 1999. Sunlight: an all pervasive source of energy–light use efficiency. In *Plants in Action: Adaption in nature, performance in cultivation*. Macmillan Education Australia Pty Ltd, Melbourne, Australia.
- Bernacchi, C.J., Portis, A.R., Nakano, H., von Caemmerer, S. and Long, S.P. 2002. Temperature response of mesophyll conductance. Implications for the determination of Rubisco enzyme kinetics and for limitations to photosynthesis in vivo. *Plant Physiology*, 130, 1992–1998.
- Caldwell, M.M., Meister, H.P., Tenhunen, J.D., Lange, O.L. 1986. Canopy structure, light microclimate and leaf gas exchange of *Quercus coccifera* L. in a Portuguese macchia: measurements in different canopy layers and simulations with a canopy model. *Trees–Structure and Function*, 1, 25–41.
- Campbell, C.S., Heilman, J.L., McInnes, K.J., Wilson, L.T., Medley, J.C., Wu, G. and Cobos, D.R. 2001a. Seasonal variation in radiation use efficiency of irrigated rice. *Agricultural and Forest Meteorology*, 110, 45–54.
- Campbell, C.S., Heilman, J.L., McInnes, K.J., Wilson, L.T., Medley, J.C., Wu, G. and Cobos, D.R. 2001b. Seasonal variation in radiation use efficiency of irrigated rice. *Agricultural*

## Chapter 5 - Nutritional and developmental influences on carbon gain capacity

- and Forest Meteorology, 110, 45–54.
- Chen, T.-W., Henke, M., de Visser, P.H.B., Buck-Sorlin, G., Wiechers, D., Kahlen, K. and Stuetzel, H. 2014. What is the most prominent factor limiting photosynthesis in different layers of a greenhouse cucumber canopy? *Annals of Botany*, 114, 677–688.
- Choudhury, B.J. 1987. Relationships between vegetation indices, radiation absorption, and net photosynthesis evaluated by a sensitivity analysis. *Remote Sensing of Environment*, 22, 209–233.
- Ehleringer, J. and Pearcy, R.W. 1983. Variations in quantum yield for CO<sub>2</sub> uptake among C<sub>3</sub> and C<sub>4</sub> plants. *Plant Physiology*, 73, 555–559.
- Elberse, W.T. and Berendse, F. 1993. A comparative study of the growth and morphology of eight grass species from habitats with different nutrient availabilities. *Functional Ecology*, 7, 223–229.
- Ethier, G.J. and Livingston, N.J. 2004. On the need to incorporate sensitivity to CO<sub>2</sub> transfer conductance into the Farquhar–von Caemmerer–Berry leaf photosynthesis model. *Plant Cell and Environment*, 27, 137–153.
- Flexas, J., Diaz–Espejo, A., Galmes, J., Kaldenhoff, R., Medrano, H. and Ribas–Carbo, M. 2007. Rapid variations of mesophyll conductance in response to changes in CO<sub>2</sub> concentration around leaves. *Plant Cell and Environment*, 30, 1284–1298.
- Flexas, J., Ribas–Carbó, M., Diaz–Espejo, A., Galmés, J. and Medrano, H. 2008. Mesophyll conductance to CO<sub>2</sub>: current knowledge and future prospects. *Plant Cell and Environment*, 31, 602–621.
- Flexas, J., Barbour, M.M., Brendel, O., Cabrera, H.M., Carriquí, M., Diaz–Espejo, A., Douthe, C., Dreyer, E., Ferrio, J.P., Gago, J., Gallé, A., Galmés, J., Kodama, N., Medrano, H., Niinemets, Ü., Peguero–Pina, J.J., Pou, A., Ribas–Carbó, M., Tomás, M., Tosens, T. and Warren, C.R. 2012. Mesophyll diffusion conductance to CO<sub>2</sub>: an unappreciated central player in photosynthesis. *Plant Science*, 193, 70–84.
- Foulkes, M.J. and Reynolds, M.P., 2015. Breeding challenge: improving yield potential. *Crop Physiology: Applications for Genetic Improvement and Agronomy*, 2nd Edition, 397–421 pp.

## Chapter 5 - Nutritional and developmental influences on carbon gain capacity

- Genty, B., Briantais, J.M. and Baker, N.R. 1989. The relationship between the quantum yield of photosynthetic electron transport and quenching of chlorophyll fluorescence. *Biochimica Et Biophysica Acta*, 990, 87–92.
- Gimenez, C., Connor, D. and Rueda, F. 1994. Canopy development, photosynthesis and radiation–use efficiency in sunflower in response to nitrogen. *Field Crops Research*, 38, 15–27.
- Gitelson, A.A., Peng Y. and Huemmrich K.F. 2014. Relationship between fraction of radiation absorbed by photosynthesizing maize and soybean canopies and NDVI from remotely sensed data taken at close range and from MODIS 250 m resolution data. *Remote Sensing of Environment*, 147, 108–120.
- Gitelson, A.A. and Gamon, J.A. 2015. The need for a common basis for defining light–use efficiency: Implications for productivity estimation. *Remote Sensing of Environment*, 156, 196–201.
- Goward, S.N. and Huemmrich, K.F. 1992. Vegetation canopy PAR absorptance and the normalized difference vegetation index: an assessment using the SAIL model. *Remote Sensing of Environment*, 39, 119–140.
- Hall, A., Connor, D. and Sadras, V. 1995. Radiation–use efficiency of sunflower crops: effects of specific leaf nitrogen and ontogeny. *Field Crops Research*, 41, 65–77.
- Harley, P.C., Loreto, F., Dimarco, G. and Sharkey, T.D. 1992. Theoretical considerations when estimating the mesophyll conductance to CO<sub>2</sub> flux by the analysis of the response of photosynthesis to CO<sub>2</sub>. *Plant Physiology*, 98, 1429–1436.
- Harley, P.C., Tenhunen, J.D. and Lange, O.L. 1986. Use of an analytical model to study limitation on net photosynthesis in *Arbutus unedo* under field conditions. *Oecologia*, 70, 393–401.
- Hirose, T. and Werger, M.J.A. 1987. Maximizing daily canopy photosynthesis with respect to the leaf nitrogen allocation pattern in the canopy. *Oecologia*, 72, 520–526.
- Hui, D.F., Luo, Y.Q., Cheng, W.X., Coleman, J.S., Johnson, D.W. and Sims, D.A. 2001. Canopy radiation– and water–use efficiencies as affected by elevated CO<sub>2</sub>. *Global Change Biology*, 7, 75–91.

## Chapter 5 - Nutritional and developmental influences on carbon gain capacity

- Inoue, Y., Peñuelas, J., Miyata, A. and Mano, M. 2008. Normalized difference spectral indices for estimating photosynthetic efficiency and capacity at a canopy scale derived from hyperspectral and CO<sub>2</sub> flux measurements in rice. *Remote Sensing of Environment*, 112, 156–172.
- Knops, J.M.H. and Reinhart, K. 2000. Specific leaf area along a nitrogen fertilization gradient. *American Midland Naturalist*, 144, 265–272.
- Laisk, A. and Loreto, F. 1996. Determining photosynthetic parameters from leaf CO<sub>2</sub> exchange and chlorophyll fluorescence–Ribulose–1,5–bisphosphate carboxylase oxygenase specificity factor, dark respiration in the light, excitation distribution between photosystems, alternative electron transport rate, and mesophyll diffusion resistance. *Plant Physiology*, 110, 903–912.
- Leuning, R., Kelliher, F.M., Depury, D.G.G. and Schulze, E.D. 1995. Leaf nitrogen, photosynthesis, conductance and transpiration: scaling from leaves to canopies. *Plant Cell and Environment*, 18, 1183–1200.
- Lee, B. 2015. Remote sensing–based assessment of gross primary production in agricultural ecosystems. Doctor degree dissertation, University of Bayreuth, pp. 41–62.
- Lee, D.Y., Kim, M.H., Lee, K.J. and Lee, B.W. 2006. Changes in radiation use efficiency of rice canopies under different nitrogen nutrition status. *Korean Journal of Agricultural and Forest Meteorology*, 8, 190–198.
- Loreto, F., Dimarco, G., Tricoli, D. and Sharkey, T.D. 1994. Measurements of mesophyll conductance, photosynthetic electron transport and alternative electron sinks of field grown wheat leaves. *Photosynthesis Research*, 41, 397–403.
- Milroy, S.P., Bange, M.P. and Sadras, V.O. 2001. Profiles of leaf nitrogen and light in reproductive canopies of cotton (*Gossypium hirsutum*). *Annals of Botany*, 87, 325–333.
- Miyata, A., Leuning, R., Denmead, O.T., Kim, J., Harazono, Y. 2000. Carbon dioxide and methane fluxes from an intermittently flooded paddy field. *Agriculture and Forest Meteorology*, 102, 287–303.
- Monteith, J.L. 1972. Solar radiation and productivity in tropical ecosystems. *Journal of Applied Ecology*, 9, 747–766.

## Chapter 5 - Nutritional and developmental influences on carbon gain capacity

- Monteith, J.L. 1977. Climate and the efficiency of crop production in Britain. *Philosophical Transactions of the Royal Society B: Biological Sciences*, 281, 277–294.
- Moreau, D., Allard, V., Gaju, O., Gouis, J.L., Foulkes, M.J. and Martre, P. 2012. Acclimation of leaf nitrogen to vertical light gradient at anthesis in wheat is a whole-plant process that scales with the size of the canopy. *Plant Physiology*, 160, 1479–1490.
- Monti, A., Bezzi, G. and Venturi, G. 2009. Internal conductance under different light conditions along the plant profile of Ethiopian mustard (*Brassica carinata* A. Brown.). *Journal of Experimental Botany*, 60, 2341–2350.
- Muir, C.D., Hangarter, R.P., Moyle, L.C. and Davis, P.A. 2014. Morphological and anatomical determinants of mesophyll conductance in wild relatives of tomato (*Solanum sect. Lycopersicon, sect. Lycopersicoides*; Solanaceae). *Plant Cell and Environment*, 37, 1415–1426.
- Nay-Htoon B. 2015. Water use efficiency of rainfed and paddy rice ecosystem. Ph.D dissertation, University of Bayreuth.
- Niinemets, U. 2007. Photosynthesis and resource distribution through plant canopies. *Plant Cell and Environment*, 30, 1052–1071.
- Niinemets, Ü., Díaz-Espejo, A., Flexas, J., Galmés, J. and Warren, C.R. 2009a. Importance of mesophyll diffusion conductance in estimation of plant photosynthesis in the field. *Journal of Experimental Botany*, 60, 2271–2282.
- Niinemets, Ü., Díaz-Espejo, A., Flexas, J., Galmés, J. and Warren, C.R. 2009b. Role of mesophyll diffusion conductance in constraining potential photosynthetic productivity in the field. *Journal of Experimental Botany*, 60, 2249–2270.
- Niinemets, Ü. and Keenan, T.F. 2012. Measures of light in studies on light-driven plant plasticity in artificial environments. *Frontiers in Plant Science*, 3, 1–21.
- Parry, M.A.J., Reynolds, M., Salvucci, M.E., Raines, C., Andralojc, P.J., Zhu, X.-G., Price, G.D., Condon, A.G. and Furbank, R.T. 2011. Raising yield potential of wheat. II. Increasing photosynthetic capacity and efficiency. *Journal of Experimental Botany*, 62, 453–467.
- Rosenberg, N.J., Blad, B.L. and Verma, S.B., 1983. Microclimate: the biological environment.

## Chapter 5 - Nutritional and developmental influences on carbon gain capacity

Microclimate: the biological environment., i–xxiii, 1–495 pp.

- Saitoh, K., Yonetani, K., Murota, T. and Kuroda, T. 2002. Effects of flag leaves and panicles on light interception and canopy photosynthesis in high-yielding rice cultivars. *Plant Production Science*, 5, 275–280.
- Sharkey, T.D., Bernacchi, C.J., Farquhar, G.D. and Singsaas, E.L. 2007. Fitting photosynthetic carbon dioxide response curves for  $C_3$  leaves. *Plant Cell and Environment*, 30, 1035–1040.
- Sheehy, J.E. and Mitchell, P.L. 2013. Designing rice for the 21st century: the three laws of maximum yield. Discussion Paper Series 48. Los Banos, International Rice Research Institute, p19.
- Tosens, T., Niinemets, U., Vislap, V., Eichelmann, H. and Castro Diez, P. 2012. Developmental changes in mesophyll diffusion conductance and photosynthetic capacity under different light and water availabilities in *Populus tremula*: how structure constrains function. *Plant Cell and Environment*, 35, 839–856.
- Warren, C.R. and Adams, M.A. 2006. Internal conductance does not scale with photosynthetic capacity: implications for carbon isotope discrimination and the economics of water and nitrogen use in photosynthesis. *Plant Cell and Environment*, 29, 192–201.
- Wullschlegel, S.D. 1993. Biochemical limitations to carbon assimilation in  $C_3$  plants—a retrospective analysis of the  $A/C_i$  curves from 109 species. *Journal of Experimental Botany*, 44, 907–920.
- Yamori, W., Nagai, T. and Makino, A. 2011. The rate-limiting step for  $CO_2$  assimilation at different temperatures is influenced by the leaf nitrogen content in several  $C_3$  crop species. *Plant Cell and Environment*, 34, 764–777.
- Yang, J., Gao, W., Ren, S.R. 2015. Long-term effects of combined application of chemical nitrogen with organic materials on crop yields, soil organic carbon and total nitrogen in fluvo-aquic soil. *Soil Tillage Research*, 151, 67–74.
- Yoshida, S., 1981. Fundamentals of rice crop science. The International Rice Research Institute, Manila, Philippines. pp. 130–146.

## Chapter 5 - Nutritional and developmental influences on carbon gain capacity

### 5.9. Appendices

#### Chloroplast CO<sub>2</sub> compensation point

CO<sub>2</sub> response curves at different measuring light intensities (PAR of 500, 200 and 100  $\mu\text{mol m}^{-2} \text{s}^{-1}$ ) and at leaf temperature of 30°C at tillering and grain-filling stage were obtained using growth chamber acclimated plants. CO<sub>2</sub> curves were commenced after leaves had acclimated to the cuvette microenvironment (CO<sub>2</sub> 400  $\mu\text{mol mol}^{-1}$  and measuring PAR 1500  $\mu\text{mol m}^{-2} \text{s}^{-1}$ ) after which CO<sub>2</sub> concentration was changed progressively in the sequence 400, 200, 150, 100 to 50  $\mu\text{mol mol}^{-1}$ . Relative humidity was controlled to ca. 60%. Assimilation rate and stomatal conductance data were recorded after new steady-state readings were obtained. At least three replicate CO<sub>2</sub> curves were obtained. Chlorophyll fluorescence was measured simultaneously. Fully expanded leaves in different age classes, distinguished by distinct differences in photosynthetic capacity, were selected for study. Leaf physiology was not altered by the experimental manipulations at different CO<sub>2</sub> concentrations as indicated by complete recovery afterward to the initial  $A_{\text{max}}$  at 400. Leaves adjacent to those used for CO<sub>2</sub> curve measurements were then enclosed in the leaf cuvette at O<sub>2</sub> concentration of ca. 1% provided by an external gas cylinder (99% N<sub>2</sub>) in stable flow rate identical to working frequency of pump of Walz GFS-3000 system, and CO<sub>2</sub> response determinations were repeated. Chloroplast CO<sub>2</sub> compensation point was defined as the intercellular CO<sub>2</sub> concentration where downward extension of linear phase of each photosynthesis-CO<sub>2</sub> response curve cross-transit (Figure 5.A1b).

#### Estimation of linear electron transport rate ( $J_p$ )

While measuring gas exchange, chlorophyll fluorescence was simultaneously assessed with a Walz PAM-Fluorometer 3050-F to monitor dynamics of the quantum yield of photosystem II ( $\Phi_{\text{PSII}}$ ) in response to varying CO<sub>2</sub> concentrations. Only those fluorescence data exhibiting a clear saturation plateau after application of a saturating actinic pulse were considered in the calculations described below. The electron transport rate (ETR) passing through photosystem II ( $J_F$ ) was calculated using the equation of Genty et al. (1989),

$$J_F = \Phi_{\text{PSII}} \cdot \alpha \cdot \beta \cdot Q \quad (5.A1)$$



## Chapter 5 - Nutritional and developmental influences on carbon gain capacity

where  $Q$  is incident PAR,  $\alpha$  is leaf absorptance (0.84 for rice adopted here from Agarie et al. (1996), and  $\beta$  is the fraction of excitation energy absorbed by PS II.

Partitioning  $J_F$  into component  $J_P$  with flow through PS II and I to support Rubisco carboxylation and oxygenation and an alternative component,  $J_A$ , which supports electron consumption by  $O_2$ -dependent acceptors (i.e., the Mehler reaction, nitrite reduction, and oxaloacetate reduction) and  $O_2$ -independent acceptors (i.e., cyclic electron transport around PS II) is physiologically meaningful under saturating light in cereals (Loreto et al., 1994). The electron transport rate calculated from chlorophyll fluorescence measurements,  $J_F$ , is the sum of  $J_P$  plus  $J_A$ . The component  $J_P$  which is required to calculate mesophyll conductance of the leaf can be expressed as:

$$J_p = J_F \cdot (1 - b_F) \quad (5.A2)$$

where  $b_F$  is the ratio of  $J_A$  to  $J_F$ . Rearranging,

$$b_F = 1 - J_p/J_F \quad (5.A3)$$

The value of  $b_F$  is assumed to be constant in unstressed plants at normal atmospheric  $CO_2$  and 21% or lower  $O_2$ . The value of  $b_F$ , and therefore the value for  $J_p$ , can be obtained in the following manner. Eq. 5.A1 can be re-expressed as follows:

$$J_F = \sigma \cdot \Phi_{CO_2} \cdot \alpha \cdot \beta \cdot Q \quad (5.A4)$$

where  $\sigma$  is the ratio of  $\Phi_{PSII}$  to  $\Phi_{CO_2}$ , the efficiency of  $CO_2$  fixation,  $\Phi_{CO_2}$  is defined as  $G/Q$  where  $G$ , gross photosynthesis. Substituting for  $\Phi_{CO_2}$ ,

$$J_F = \sigma \cdot G \cdot \beta \quad (5.A5)$$

Assuming a conservative value for the number of electrons required for NADPH synthesis and the amount of NADPH required for regeneration of one molecule of ribulose-1,5-bisphosphate (RuBP), i.e., 4 electrons consumed for one molecule of  $CO_2$  fixed in the absence of photorespiration,  $J_P = 4G$ . Substituting this value for  $J_P$  and the value for  $J_F$  from Eq. 5.A5 into Eq. 5.A3,

## Chapter 5 - Nutritional and developmental influences on carbon gain capacity

$$b_f = 1 - J_p / J_F = 1 - 4G / (G \cdot \sigma \cdot \beta) = 1 - 4 / (\sigma \cdot \beta) \quad (5.A6)$$

We estimated the value of  $\sigma$  by calculating  $\Phi_{PSII}$  and  $\Phi_{CO_2}$  over a range of varying ambient  $CO_2$  concentrations and light intensities under low  $O_2$  (to infer the alternative electron transport rate, ETR, occurring under normal atmosphere conditions) and then plotting them against one another (Figure 5.A1a). The slope of the relationship, i.e.,  $\sigma$  was found to be 8.5, which fell in the range reported in the herbaceous under relatively high light and normal air conditions (Flexas et al., 2007; Genty et al., 1989; Laisk and Loreto, 1996; Loreto et al., 1994) and parallel with the average (slope of black line) (Figure 5.A1a). The fraction of absorbed light used by PS II,  $\beta$ , varies between 0.45 and 0.6 in herbaceous and tree species (Laisk and Loreto, 1996), and similar values between 0.39 and 0.51 have been reported for several  $C_3$  species (Flexas, 2007). We assume that the absorbed radiation is equally distributed between PS I and PS II, i.e.,  $\beta = 0.5$ . With  $\sigma = 8.5$  and  $\beta = 0.5$ , the value of  $b_F$  for our data is 0.06, meaning that  $J_A$  is only a few percent of  $J_P$  to compensate variations in the NADPH synthesis as compare to the linear flow.

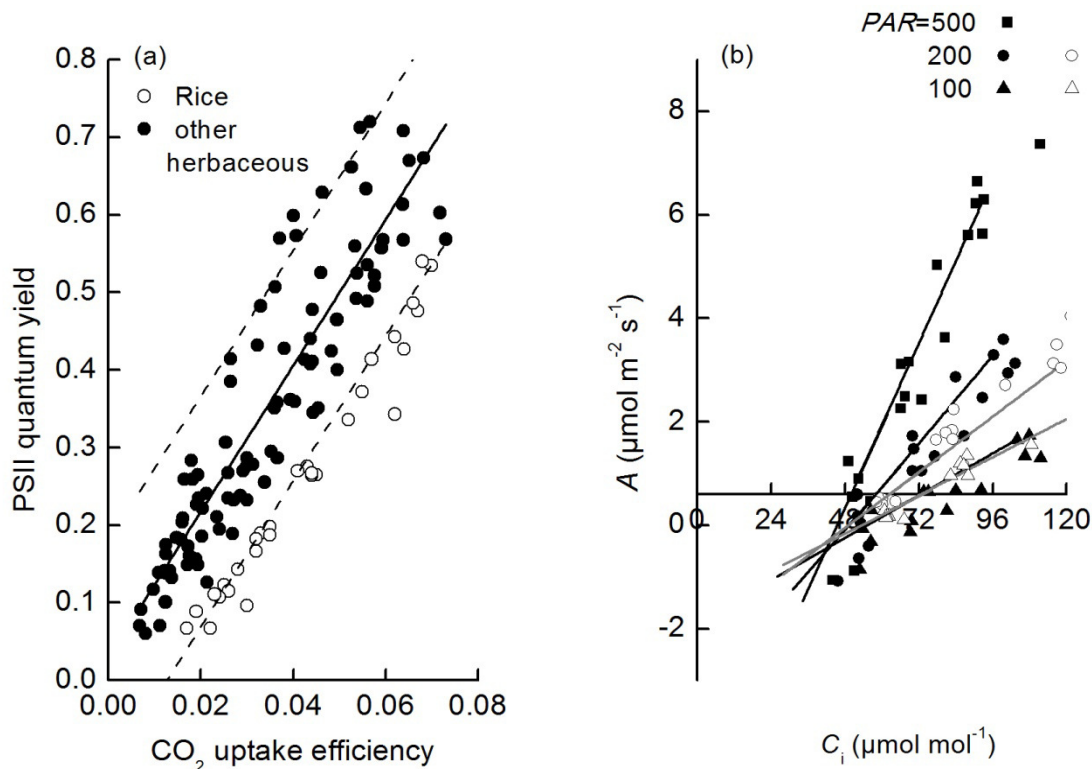


**Figure 5.9.A1**

## Chapter 5 - Nutritional and developmental influences on carbon gain capacity

**Figure 5.9.A1** (a) Relationship between quantum yield of PS II and efficiency of CO<sub>2</sub> fixation under varying ambient CO<sub>2</sub> concentration and light intensity with O<sub>2</sub> approximately 1% in rice (open circle) and other herbaceous (black circle). (b) CO<sub>2</sub> response curves at measuring light intensities of 500, 200, 100  $\mu\text{mol m}^{-2} \text{s}^{-1}$  and leaf temperature 30°C during tillering (filled symbols) and grain-filling stage (open symbols).  $n = 5$  to 6. Linear fits to each data set were made to estimate the C<sub>i</sub> value at which response curves intersect, indicative of  $\Gamma^*$  of  $44.4 \pm 1.3 \mu\text{mol mol}^{-1}$ .

## Appendix

### Appendix

#### List of other publications

Steve Lindner, Dennis Otieno, Bora Lee, Wei Xue, Sebastian Arnhold, Hyojung Kwon, Bernd Huwe, John Tenhunen. 2014. Carbon dioxide exchange and its regulation in the main agro–ecosystems of Haeen catchment in South Korea. *Agriculture, Ecosystems and Environment*, 199, 132–145.

Wei Xue, Bhone Nay–Htoon, Steve Lindner, Maren Dubbert, Jonghan Ko, Dennis Otieno, Christiane Werner, John Tenhunen. Soil water availability and nitrogen allocation strategy influence variations in components of intrinsic water use efficiency in rice. (going to submit to *Functional Plant Biology*)

Wei Xue, Steve Lindner, Bora Lee, Bhone Nay–Htoon, Christiane Werner, John Tenhunen. Evaluation of biophysical factors driving seasonal variations in carbon gain capacity in rice production systems. (under preparation)

## Declaration

### Declaration / Erklärung

#### (Eidesstattliche) Versicherungen und Erklärungen

(§ 8 S. 2 Nr. 6 PromO)

*Hiermit erkläre ich mich damit einverstanden, dass die elektronische Fassung meiner Dissertation unter Wahrung meiner Urheberrechte und des Datenschutzes einer gesonderten Überprüfung hinsichtlich der eigenständigen Anfertigung der Dissertation unterzogen werden kann.*

(§ 8 S. 2 Nr. 8 PromO)

*Hiermit erkläre ich eidesstattlich, dass ich die Dissertation selbständig verfasst und keine anderen als die von mir angegebenen Quellen und Hilfsmittel benutzt habe.*

(§ 8 S. 2 Nr. 9 PromO)

*Ich habe die Dissertation nicht bereits zur Erlangung eines akademischen Grades anderweitig eingereicht und habe auch nicht bereits diese oder eine gleichartige Doktorprüfung endgültig nicht bestanden.*

(§ 8 S. 2 Nr. 10 PromO)

*Hiermit erkläre ich, dass ich keine Hilfe von gewerblichen Promotionsberatern bzw. -vermittlern in Anspruch genommen habe und auch künftig nicht nehmen werde.*

.....  
Ort, Datum, Unterschrift